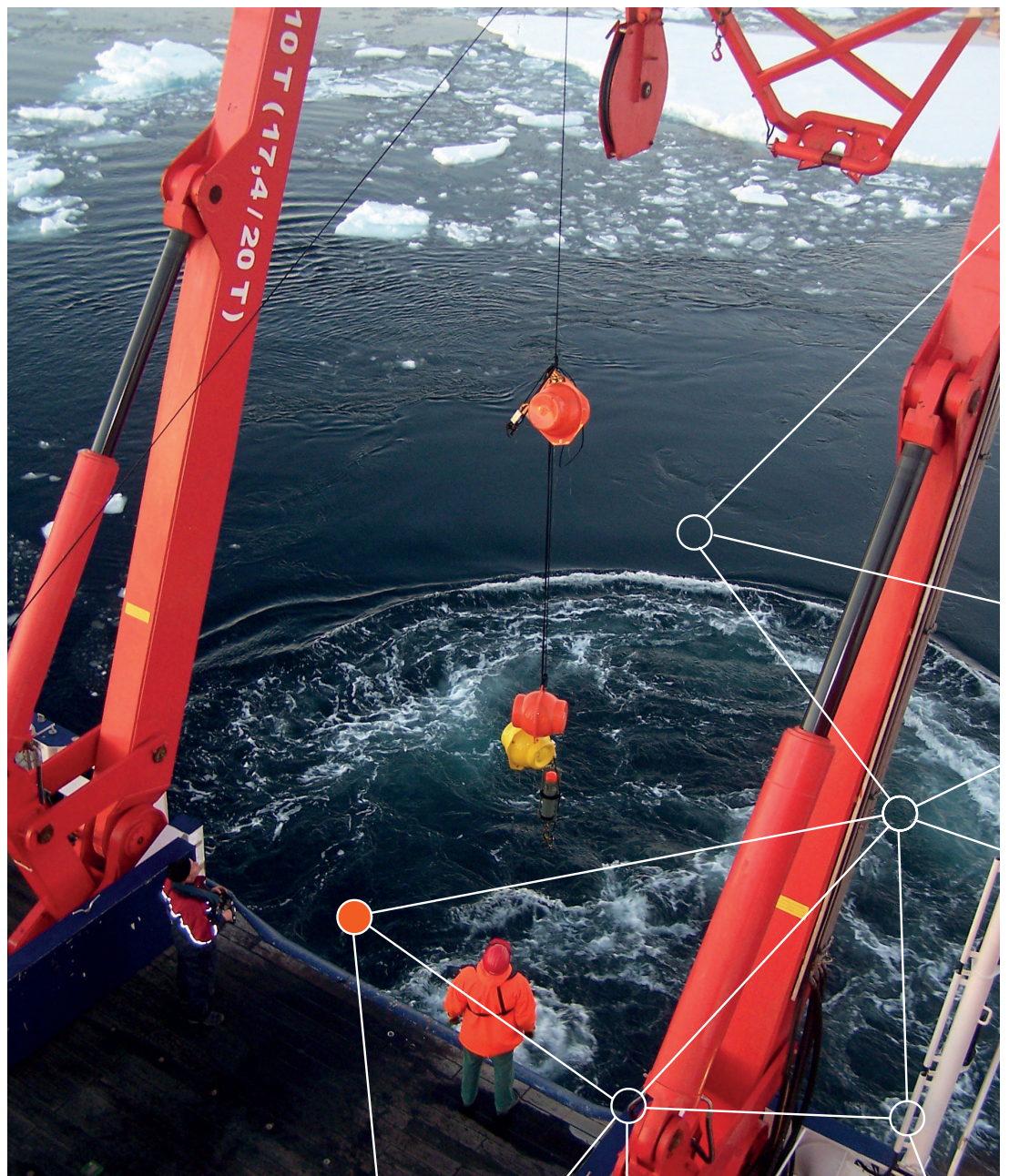


ICES REPORT ON OCEAN CLIMATE 2014

*Prepared by the Working Group
on Oceanic Hydrography*

ICES COOPERATIVE RESEARCH REPORT

RAPPORT
DES RECHERCHES
COLLECTIVES



ICES REPORT ON OCEAN CLIMATE 2014

ISBN: 978-87-7482-178-6

ISSN: 1017-6195

Published annually by
International Council for the Exploration of the Sea
Conseil International pour l'Exploration de la Mer

H. C. Andersens Boulevard 44-46
DK-1553 Copenhagen V
Denmark

T (+45) 33 38 67 00

F (+45) 33 93 42 15

www.ices.dk

Cover image courtesy of Agnieszka Beszczynska-Möller. Non-credited images are from ICES image bank.

EDITORS

Karin M. H. Larsen, Cesar Gonzalez-Pola, Paula Fratantoni,
Agnieszka Beszczynska - Möller, and Sarah L. Hughes

SERIES EDITOR

Emory D. Anderson

RECOMMENDED FORMAT FOR PURPOSES OF CITATION

Larsen, K. M. H., Gonzalez-Pola, C., Fratantoni, P., Beszczynska-Möller, A.,
and Hughes, S. L. (Eds.) 2016.

ICES Report on Ocean Climate 2014.

ICES Cooperative Research Report No. 329. 139 pp.

For permission to reproduce material from this publication,
please apply to the General Secretary.

This document is a report of an Expert Group under the auspices
of the International Council for the Exploration of the Sea and
does not necessarily represent the view of the Council.

CONTENTS

1. INTRODUCTION	4
1.1 Highlights of the North Atlantic for 2013	5
1.2 Highlights of the North Atlantic for 2014	5
1.3 Highlights of the North Atlantic atmosphere in winter 2012/2013	6
1.4 Highlights of the North Atlantic atmosphere in winter 2013/2014	6
1.5 Outlook for North Atlantic atmosphere in winter 2014/2015	6
2. SUMMARY OF UPPER OCEAN CONDITIONS IN 2014	10
2.1 <i>In situ</i> stations and sections	10
2.2 Sea surface temperature	14
2.3 Gridded temperature and salinity fields	16
3. THE NORTH ATLANTIC ATMOSPHERE	24
3.1 Sea level pressure	24
3.2 Surface air temperature	30
4. DETAILED AREA DESCRIPTIONS, PART I: THE UPPER OCEAN	32
4.1 Introduction	32
4.2 Area 1 - West Greenland	34
4.3 Area 2 - Northwest Atlantic: Scotian Shelf and Newfoundland-Labrador Shelf	37
4.4 Area 2b - Labrador Sea	47
4.5 Area 2c - Mid-Atlantic Bight	50
4.6 Area 3 - Icelandic waters	58
4.7 Area 4 - Bay of Biscay and eastern North Atlantic	64
4.8 Area 4b - Northwest European continental shelf	68
4.9 Area 5 - Rockall Trough to Iceland	72
4.10 Area 5b - Irminger Sea	76
4.11 Areas 6 and 7 - Faroese waters and Faroe-Shetland Channel	78
4.12 Areas 8 and 9 - Northern and southern North Sea	85
4.13 Area 9b - Skagerrak, Kattegat, and the Baltic	92
4.14 Area 10 - Norwegian Sea	99
4.15 Area 11 - Barents Sea	104
4.16 Area 12 - Greenland Sea and Fram Strait	108
5. DETAILED AREA DESCRIPTIONS, PART II: THE DEEP OCEAN	112
5.1 Introduction	112
5.2 Nordic Seas deep waters	114
5.3 North Atlantic deep waters	120
5.4 North Atlantic intermediate waters	127
6. CONTACT INFORMATION	136

1. INTRODUCTION

Long time-series of ocean properties are rare in the surface ocean and even rarer in the deep ocean. The North Atlantic region is unusual in having a relatively large number of locations at which oceanographic data have been collected repeatedly for many years or decades; the longest records go back more than a century.

In the ICES Report on Ocean Climate (IROC), these valuable data are collated to provide the very latest information from the ICES areas of the North Atlantic and the Nordic seas. A description of the status of sea temperature and salinity during 2013 and 2014 at locations where the ocean is regularly measured is offered, along with observed trends over the past decade and longer where possible.

In the first section of the report, information is compiled from the longest time-series to give the best possible overview of changes in the ICES Area. Although the focus of the report is on temperature and salinity measurements, additional complementary datasets are provided throughout the report, such as sea level pressure, air temperature, and ice cover.

The main focus of this report is the observed variability in the upper ocean (the upper 1000 m). The introductory section includes gridded fields constructed by optimal analysis of the Argo float data distributed by the Coriolis data centre in France. Later in the report, a short section summarizes the variability of the intermediate and deep waters of the North Atlantic.

The data presented here represent an accumulation of knowledge collected by many individuals and institutions through decades of observations. It would be impossible to list them all; the list of contacts for each dataset at the end of the report therefore includes e-mail addresses for the individuals who provided the information as well as the data centres at which the full archives of data are held. Much of the data included in this report are available for download via a web tool at <http://ocean.ices.dk/iroc>.

For those interested in a more detailed overview of a particular region, a full description of the datasets used to develop the time-series presented in this report can be found in the annual meeting reports of the ICES Working Group on Oceanic Hydrography at <http://www.ices.dk/community/groups/Pages/WGOH.aspx>.

1.1 HIGHLIGHTS OF THE NORTH ATLANTIC FOR 2013

- » Waters on the Newfoundland and Labrador shelves remain warmer and fresher than normal, but with a decreasing trend in temperature.
- » Wet weather ended the period of anomalously high salinity in the Bay of Biscay, and temperature and salinity returned to near-normal conditions.
- » Freshening was observed in the upper ocean from the Irminger Sea to Rockall Trough and northward into the southern Norwegian Sea, although salinities remain above the long-term mean.
- » Temperature and salinity of Atlantic water in the Norwegian Sea both decreased, although temperatures were still near normal and salinities above average.
- » The Barents Sea was considerably warmer than normal and sea ice extent was low, becoming ice-free during late summer.
- » Outflows from the Baltic Sea were large during 2013, and it was unusually cold during March.

1.2 HIGHLIGHTS OF THE NORTH ATLANTIC FOR 2014

- » Record-high air temperatures were observed across the eastern North Atlantic. This was reflected in some shelf sea regions, with record-high sea surface temperatures in the North Sea and mild ice conditions in the Baltic Sea.
- » The ice extent in the Barents Sea was close to or above average in the second half of 2014, although waters were warmer than normal throughout the year.
- » The upper layers of the open ocean remained warm in 2014, particularly east of Iceland where temperatures were close to the highest observed. However, sea surface temperature data reveal a substantial cold anomaly centred near 50°N in the central North Atlantic, away from the area of *in situ* sampling.
- » Despite colder-than-normal air temperatures over the North American continent, ocean temperatures remained above normal on the continental shelf of the northeastern USA.
- » The recent freshening trend continues in the upper layers of the Irminger Sea, Rockall Trough, and in the southern Norwegian Sea. Salinities were close to the long-term mean, although temperatures remained high. Freshening was observed in the upper central waters of the Biscay region for the first time in ten years.
- » A major inflow to the Baltic Sea took place in late 2014.
- » New time-series in the deep ocean offer valuable insight into variability in the North Atlantic and Iberian regions.

1.3 HIGHLIGHTS OF THE NORTH ATLANTIC ATMOSPHERE IN WINTER 2012/2013

- » The winter North Atlantic Oscillation (NAO) index was strongly negative (-1.97).
- » Air temperatures were lower than normal over much of northwestern Europe and higher than normal over the Labrador Sea.
- » Windspeeds were weaker than normal across the Nordic seas, Rockall Trough, North Sea, and the central subpolar gyre and stronger at the latitude of the Azores.

1.4 HIGHLIGHTS OF THE NORTH ATLANTIC ATMOSPHERE IN WINTER 2013/2014

- » The winter North Atlantic Oscillation (NAO) index was strongly positive ($+3.10$), and the sea level pressure pattern was typical, bringing stronger-than-normal winds and higher precipitation to some areas in southwestern Europe.
- » Winter air temperatures were higher than normal over much of northwestern Europe and lower than normal over the central subpolar region and North American continent.

1.5 OUTLOOK FOR NORTH ATLANTIC ATMOSPHERE IN WINTER 2014/2015

We include here an initial assessment of the North Atlantic atmosphere at the end of the IROC year. Atmospheric conditions during winter are a determining factor of oceanic conditions for the following year; therefore, this outlook offers some predictive capability for spring–autumn 2015.

Winter (December 2014–March 2015) exhibited conditions indicating that it was a NAO positive-index winter, with stronger-than-average windspeeds across the central subpolar gyre and Nordic seas and weaker-than-average winds between the Azores and Iberia. Air temperatures were cold over northeastern North America, the Labrador and Irminger seas, Iceland Basin, Rockall, and Iberia. Over the Nordic seas, Scandinavia, and eastern Europe air temperatures were warmer than average.

**WINTER (DECEMBER 2014-MARCH 2015)
EXHIBITED CONDITIONS
INDICATING THAT IT WAS A
NAO POSITIVE-INDEX WINTER**



FIGURE 1: OVERVIEW OF NORTH ATLANTIC UPPER OCEAN TEMPERATURE

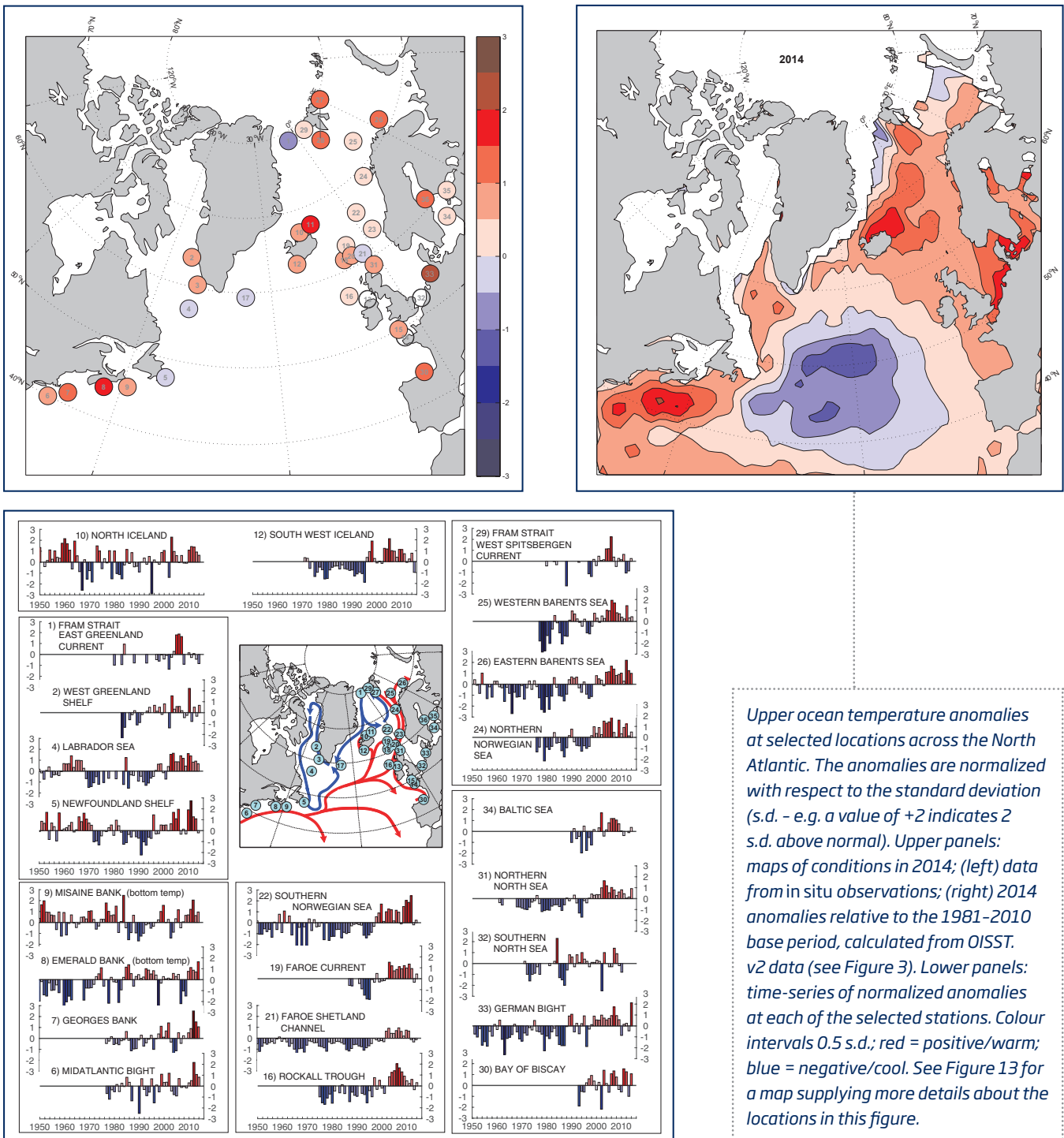
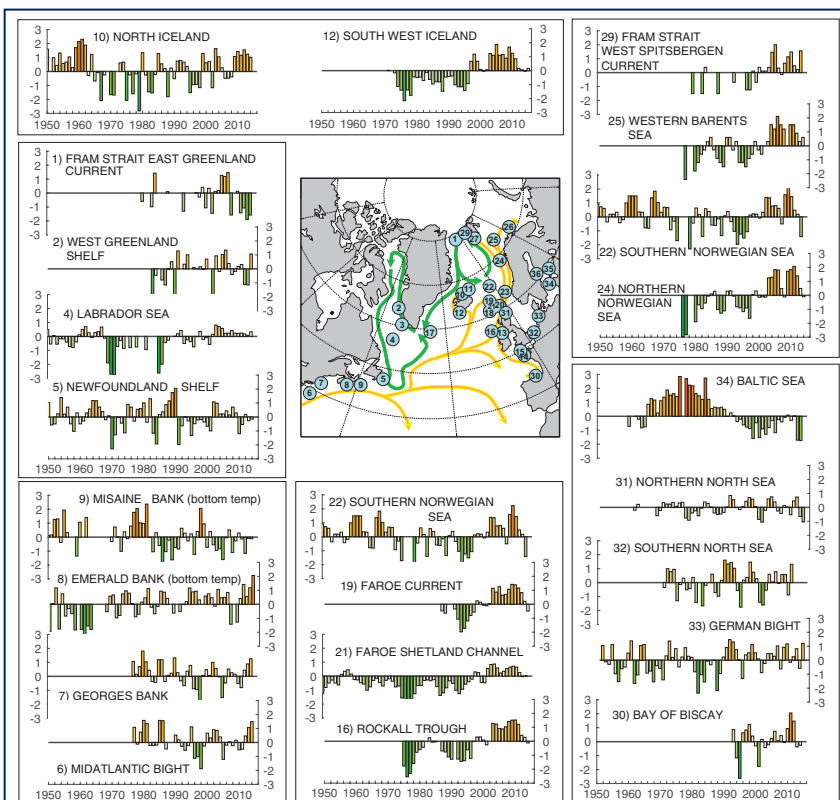
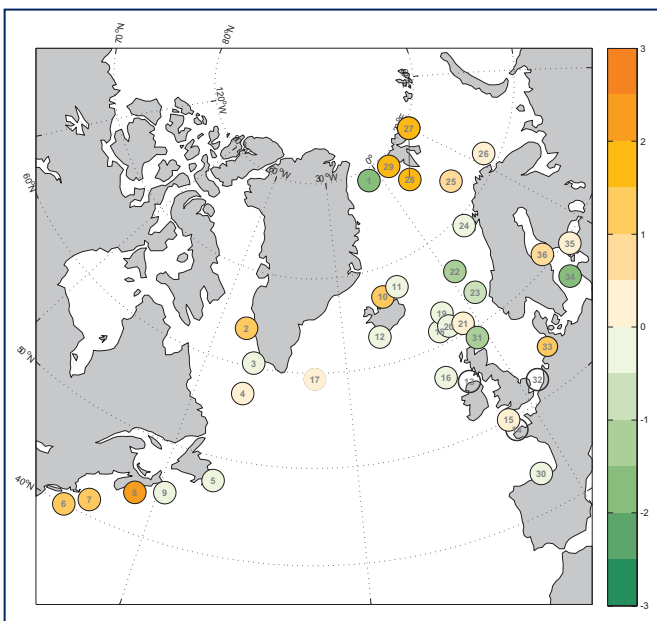


FIGURE 2: OVERVIEW OF NORTH ATLANTIC UPPER OCEAN SALINITY



Upper ocean salinity anomalies at selected locations across the North Atlantic. The anomalies are calculated relative to a long-term mean and normalized with respect to the s.d. (e.g. a value of +2 indicates 2 s.d. above normal). Upper panel: map of conditions in 2014. Lower panels: time-series of normalized anomalies at each of the selected stations. Colour intervals 0.5 s.d.; orange = positive/saline; green = negative/fresh. See Figure 13 for a map supplying more details about the locations in this figure.

2. SUMMARY OF UPPER OCEAN CONDITIONS IN 2014

This section summarizes the conditions in the upper layers of the North Atlantic during 2014 using data from (i) a selected set of sustained observations, (ii) gridded sea surface temperature (SST) data, and (iii) gridded vertical profiles of temperature and salinity from Argo floats.

2.1 *IN SITU* STATIONS AND SECTIONS

Where *in situ* section and station data are presented in the summary tables and figures, normalized anomalies have been provided to allow better comparison of trends in the data from different regions (Figures 1-3; Tables 1 and 2). The anomalies have been normalized by dividing the values by the standard deviation (s.d.) of the data during 1981-2010 (or the closest time period available). A value of +2 thus represents data (temperature or salinity) at 2 s.d. higher than normal.

“Sustained observations” or “time-series” are regular measurements of ocean temperature and salinity made over a long period (10-100 years). Most measurements are made 1-4 times a year, but some are made more frequently.

“Anomalies” are the mathematical differences between each individual measurement and the average values of temperature, salinity, or other variables at each location. Positive anomalies in temperature and salinity mean warm or saline conditions; negative anomalies mean cool or fresh conditions.

“Seasonal cycle” describes the short-term changes at the surface of the ocean brought about by the passing of the seasons; the ocean surface is cold in winter and warms through spring and summer. Temperature and salinity changes caused by the seasonal cycle are usually much greater than the prolonged year-to-year changes described here.



TABLE 1: TEMPERATURE

	2005	2006	2007	2008	2009	2010	2011	2012	2013	2014
1 (12)	1.79	1.87	1.64	-0.9		0.15	-0.28	0.08	-0.44	-0.84
2 (1)	0.56	0.57	0.18	-0.46	-0.25	2.22	-0.81	0.5	-0.33	0.67
3 (1)	0.49	-0.29	1.04	0.06	0.7	1.15	0.57	1.28	0.18	0.83
4 (2b)	0.81	0.84	0.14	0.26	-0.49	1.12	0.01	0.39	-0.1	-0.01
5(2)	1.09	1.96	-0.32	0.14	-0.3	1.91	2.74	1.27	1.09	-0.2
6 (2c)	-0.9	0.69	-0.12	-0.05	-0.17	0.3	0.51	2.17	1.07	0.82
7 (2c)	-1.13	0.52	-0.46	0.24		0.51	0.9	2.51	1.51	1.06
8 (2)	0.29	0.49	-2.2	-1.04	-1.5	0.76	1.12	0.87	0.71	1.64
9 (2)	0.34	1.16	-0.49	0.06	0.65	0.69	1.2	2.05	0.64	0.96
10 (3)	0.6	-0.02	0.61	-0.09	-0.1	1.1	1.43	1.38	0.93	0.63
11 (3)	-0.21	0.25	-0.65	0.64	0.46	0.3	1.03	0.64	0.79	1.89
12 (3)	2.1	1.01	0.96	0.4	1.12	1.11	0.73	-0.07	0.25	0.77
13 (4b)	1.67				1.53	0.7	1.21	0.15		
14 (4b)	-0.03	-1.22	1.88	0.2	-0.65	-2.04	0.2	0.54		
15 (4b)	0.21	-1.86	1.01	0.4	-0.66	0.02	0.05	0.59	-0.26	0.7
16 (5)	1.39	2.03	1.66	1.29	0.9	0.47	0.23	0.6	-0.34	0.3
17 (5b)	0.98	0.6	1.15	-0.57	-0.74	0.53	0.68	-0.27		
18 (6)	0.02	1	1.1	1.3	1.41	0.73	1.28	-0.03	0.04	0.55
19 (6)	0.72	0.85	1.1	0.92	1.2	0.98	1.34	0.93	-0.32	0.43
20 (7)	0.44	0.58	0.71	0.75	0.92	1.35	0.91	0.34	0.45	0.6
21 (7)	0.44	0.7	0.95	1.26	0.62	1.46	1.35	0.25		
22 (10)	0.17	1.14	0.96	-0.11	1.48	2.05	1.87	2.47	-0.19	0.23
23 (10)	0.35	1.28	1.89	0.19	1.71	0.86	1.12	0.44	0.55	0.33
24 (10)	1.42	2.08	0.45	0.03	1.58	0.33	0.91	1.23	0.14	0.49
25 (11)	0.97	1.93	1.69	0.79	0.7	0.38	0.22	1.44	0.31	0.43
26 (11)	1.15	1.66	1.39	0.81	0.9	1.02	0.28	2.2	1.25	1
27 (12)	1.03	2.17	1.08	-0.18	0.57	0.42	1.01	0.9	0.06	1.1
28 (10)	1.36	1.57	0.65	0.22	0.53	-0.01		0.6	-0.23	1.17
29 (12)	1.15	2.24	0.38	-0.48	0.26	0.14	0.63	-1.08	-0.89	0.25
30 (4)	-0.62	1.07	1.33	0.77	-0.37	-0.6	1.53	1.25	-1	1.07
31 (8&9)	0.54	1.02	0.79	0.28	0.61	0.81	0.45	0.04	0.15	0.92
32 (8&9)	-0.26	-0.13	0.7	0.06	0.24	-1.26				
33 (8&9)	0.69	0.94	1.74	0.94	0.57	-0.87	0.15	0.24	-0.45	2.12
34 (9b)	0.8	1.19	1.19	1.05	0.7	0.05	-0.38		-0.11	0.37
35 (9b)	0.4	1.14	0.68	1.17	1.36	0.42	-1.06	0.52	0.84	0.01
36 (9b)	-0.02	-0.02	1	1.26	1.33	-0.53	-0.97	-0.16	0.02	1.43

Changes in temperature at selected stations in the North Atlantic region during the past decade, 2003–2012. The index numbers on the left can be used to cross-reference each point with information in Figures 1 and 2 and in Table 3. Numbers in brackets refer to detailed area descriptions featured later in the report. Unless specified, these are upper-layer anomalies. The anomalies are normalized with respect to the s.d. (e.g. a value of +2 indicates that the data for that year were 2 s.d. above normal). Blank boxes indicate that data were unavailable for a particular year at the time of publication. Colour intervals 0.5 s.d.; red = warm; blue = cold.

TABLE 2: SALINITY

	2005	2006	2007	2008	2009	2010	2011	2012	2013	2014
1 (12)	1.27	1.19	1.46	-1.57		0.13	-1.42	-1.07	-1.89	-1.57
2 (1)	1.03	1.35	0.39	-0.40	-0.18	0.17	0.31	-1.12	-1.15	1.07
3 (1)	0.51	-0.34	0.29	0.11	1.24	0.07	1.20	-0.14	0.80	-0.47
4 (2b)	0.51	0.19	0.27	-0.28	0.17	0.03	-0.17	-0.31	-0.14	0.20
5(2)	0.22	0.44	0.16	0.71	0.29	-1.20	-0.54	0.18	-0.27	-0.15
6 (2c)	-1.21	-0.19	0.05	-0.23	0.16	-0.53	-0.49	0.47	1.07	1.49
7 (2c)	-1.52	-0.48	0.52	0.26	0.15	-0.52	-0.81	0.44	0.89	1.26
8 (2)	0.50	0.85	-1.43		-1.28	0.42	1.42	0.56	1.19	2.07
9 (2)	-1.61	-0.05	0.51	-1.11	-0.27	0.29	-0.13	-1.16	-0.09	-0.11
10 (3)	0.27	-0.49	-0.48	-0.39	1.07	1.43	1.16	1.55	1.24	1.02
11 (3)	-0.10	0.96	0.95	1.07	0.66	0.99	1.13	1.55	1.22	-0.04
12 (3)	1.88	1.10	1.16	0.90	1.69	1.24	0.85	0.16	0.06	-0.04
13 (4b)										
14 (4b)	1.08	0.54	1.19		-0.02	-0.18	0.85	1.42		
15 (4b)	1.12	0.86	1.09	0.39	0.75	0.46	1.31	0.76	0.79	0.46
16 (5)	0.92	0.88	1.04	1.42	1.51	1.52	1.22	0.43	0.29	-0.12
17 (5b)	1.10	0.78	0.97	0.00	0.13	1.39	0.84	0.46		
18 (6)	0.89	0.49	0.51	1.22	1.61	1.53	1.41	0.31	0.46	-0.08
19 (6)	1.26	0.66	0.70	1.08	1.43	1.39	1.17	0.83	0.22	-0.49
20 (7)	0.56	0.44	0.26	0.58	1.08	1.18	0.75	0.65	0.17	-0.35
21 (7)	0.59	0.23	0.35	1.13	1.27	1.36	1.27	0.98		
22 (10)	0.78	0.81	0.61	-0.51	1.59	2.23	1.45	0.48	0.18	-1.42
23 (10)	0.74	0.70	0.97	0.51	2.01	1.82	1.53	0.69	0.30	-0.63
24 (10)	1.85	1.81	0.48	-0.12	1.73	1.85	2.07	1.40	0.49	-0.10
25 (11)	1.20	2.11	1.51	1.20		1.51	1.51	0.90	0.30	0.60
26 (11)	0.88	0.88	1.42	0.16	0.52	0.88	1.60	0.34	-0.02	0.16
27 (12)	1.12	1.61	1.26	0.39	0.65	0.91	1.70	1.68	0.98	1.59
28 (10)	1.61	1.89	1.45	0.92	0.71	0.82		1.45	1.00	1.74
29 (12)	1.45	1.99	0.32	-0.14	0.67	1.13	1.48	0.48	0.22	1.56
30 (4)	0.23	0.75	0.07	0.43	-0.04	0.93	2.05	1.47	-0.38	-0.26
31 (8&9)	0.39	-0.26	-0.44	0.14	0.03	-0.53	0.47	0.74	-0.65	-1.05
32 (8&9)	0.23	0.76	0.01	0.77	0.56	-1.00	1.30	1.50		
33 (8&9)	0.29	1.02	-0.63	0.93	1.17	-0.15	0.25	0.82	-0.58	1.21
34 (9b)	-0.31	-1.18	-0.24	-0.40	-0.08	0.08	-0.29	0.03	-1.71	-1.74
35 (9b)	0.25	1.92	0.20	0.12	0.63	0.85	0.06	-1.00	0.85	0.11
36 (9b)	1.06	0.57	0.99	0.32	0.62	2.13	1.92	1.01	0.39	1.00

Changes in salinity at selected stations in the North Atlantic region during the past decade, 2003–2012. The index numbers on the left can be used to cross-reference each point with information in Figures 1 and 2 and in Table 3. Numbers in brackets refer to detailed area descriptions featured later in the report. Unless specified, these are upper-layer anomalies. The anomalies are normalized with respect to the s.d. (e.g. a value of +2 indicates that the data for that year were 2 s.d. above normal). Blank boxes indicate that data were unavailable for a particular year at the time of publication. Note that no salinity data are available for stations 5, 12, and 29. Colour intervals 0.5 s.d.; orange = saline; green = fresh.

TABLE 3

Index	Description	Area	Measurement depth	Long-term average	Lat	Lon	Mean T °C	Standard deviation T	Mean S	Standard deviation S
1	Fram Strait – East Greenland Current	12	50–500 m	1980–2010	78.83	6.00	0.84	0.64	34.702	0.126
2	Station 4 – Fylla Section – Greenland Shelf	1	0–50 m	1983–2010	63.88	–53.37	2.64	1.10	33.162	0.392
3	Cape Desolation Station 3	1	75–200 m	1983–2010	60.47	–50.00	5.72	0.66	34.923	0.062
4	Area2b – west – central AR7W stations	2b	0–150 m	1971–2000	56.70	–52.50	3.73	0.38	34.710	0.088
5	Station 27 – Newfoundland Shelf temperature – Canada	2	0–175 m	1981–2010	47.55	–52.59		0.35		0.233
6	Oleander Section (inshore of the 100 m isobath) Mid-Atlantic Bight – USA	2c	Surface	1980–2010	39.00	–71.50				
7	Northwest Georges Bank – Mid Atlantic Bight USA	2c	1–30 m	1981–2010	42.00	–70.00	9.98	0.79	32.600	0.28
8	Emerald Bank– Central Scotian Shelf– Canada	2	Near bottom	1981–2010	44.00	–63.00		0.83		0.151
9	Misaine Bank – Northeast Scotian Shelf – Canada	2	Near bottom	1981–2010	45.00	–59.00		0.63		0.134
10	Siglunes Station 2–4 – North Iceland – Irminger Current	3	50–150 m	1981–2010	67.00	–18.00	3.41	0.98	34.859	0.108
11	Langanes Station 2–6 – Northeast Iceland – East Icelandic Current	3	0–50 m	1981–2010	67.50	–13.50	1.22	0.61	34.729	0.067
12	Selvogsbanki Station 5 – Southwest Iceland – Irminger Current	3	0–200 m	1981–2010	63.00	–22.00	7.88	0.47	35.187	0.049
13	Malin Head Weather Station	4b	Surface	1981–2010	55.37	–7.34	10.18	0.55		
14	Point 33 – Astan	4b	5 m	1998–2010	48.78	–3.94	12.79	0.34	35.206	0.112
15	Western Channel Observatory (WCO) – E1 – UK	4b	Depth average 0–40 m	1981–2010	50.03	–4.37	12.26	0.41	35.212	0.094
16	Ellett Line – Rockall Trough – UK (Section average)	5	30–800 m	1981–2010	56.75	–11.00	9.44	0.33	35.351	0.040
17	Central Irminger Sea – Subpolar Mode Water	5b	200–400 m	1991–2010	59.40	–36.80	4.34	0.53	34.900	0.031
18	Faroe Bank Channel – West Faroe Islands	6	Upper layer, high salinity core	1988–2010	61.00	–8.00	8.80	0.36	35.302	0.043
19	Faroe Current – North Faroe Islands (Modified North Atlantic Water)	6	Upper layer, high salinity core	1988–2010	63.00	–6.00	8.13	0.40	35.250	0.042
20	Faroe Shetland Channel – Shetland Shelf (North Atlantic Water)	7	Upper layer, high salinity core	1981–2010	61.00	–3.00	9.68	0.31	35.382	0.034
21	Faroe Shetland Channel – Faroe Shelf (Modified North Atlantic Water)	7	Upper layer, high salinity core	1981–2010	61.50	–6.00	7.99	0.49	35.252	0.038
22	Ocean Weather Station Mike – 50m	10	50 m	1981–2010	66.00	–2.00	7.71	0.44	35.176	0.036
23	Southern Norwegian Sea – Svinøy section – Atlantic Water	10	50–200 m	1981–2010	63.00	3.00	8.10	0.39	35.245	0.039
24	Central Norwegian Sea – Gimsøy section – Atlantic Water	10	50–200 m	1981–2010	69.00	12.00	6.91	0.34	35.168	0.030
25	Fugloya – Bear Island section – Western Barents Sea – Atlantic Inflow	11	50–200 m	1981–2010	73.00	20.00	5.55	0.46	35.078	0.035
26	Kola section – Eastern Barents Sea	11	0–200 m	1981–2010	71.50	33.50	4.22	0.52	34.771	0.056
27	Greenland Sea section – West of Spitsbergen	12	200 m	1996–2010	76.50	10.50	3.19	0.61	35.058	0.045
28	Northern Norwegian Sea – Sørkapp section – Atlantic Water	10	50–200 m	1981–2010	76.33	10.00	4.08	0.60	35.073	0.038
29	Fram Strait – West Spitsbergen Current	12	50–500 m	1980–2010	78.83	7.00	3.08	0.72	35.023	0.038
30	Santander Station 6 (shelf break) – Bay of Biscay – Spain	4	5–200 m	1993–2010	43.70	–3.78	12.67	0.45	35.608	0.06
31	Fair Isle Current Water (waters entering North Sea from Atlantic)	8&9	0–100 m	1981–2010	59.00	–2.00	10.01	0.46	34.844	0.064
32	Section average – Felixstowe – Rotterdam	8&9	Surface	1981–2010	52.00	3.00		0.72		0.212
33	Helgoland Roads – Coastal waters – German Bight North Sea	8&9	Surface	1971–2000	54.19	7.90	10.10	0.72	32.110	0.544
34	Baltic Proper – East of Gotland – Baltic Sea	9b	Surface	1981–2010	57.50	19.50	9.27	1.03	7.172	0.196
35	Baltic – LL7 – Baltic Sea	9b	70 m	1991–2010	59.51	24.50	3.97	0.72	7.961	0.667
36	Baltic – SR5 – Baltic Sea	9b	110 m	1991–2010	61.05	19.35	3.27	0.58	6.428	0.141

Details of the datasets included in Figures 1 and 2 and in Tables 1 and 2. Blank boxes indicate that no information was available for the area at the time of publication. T = temperature, S = salinity. Some data are calculated from an average of more than one station; in such cases, the latitudes and longitudes presented here represent a nominal midpoint along that section.

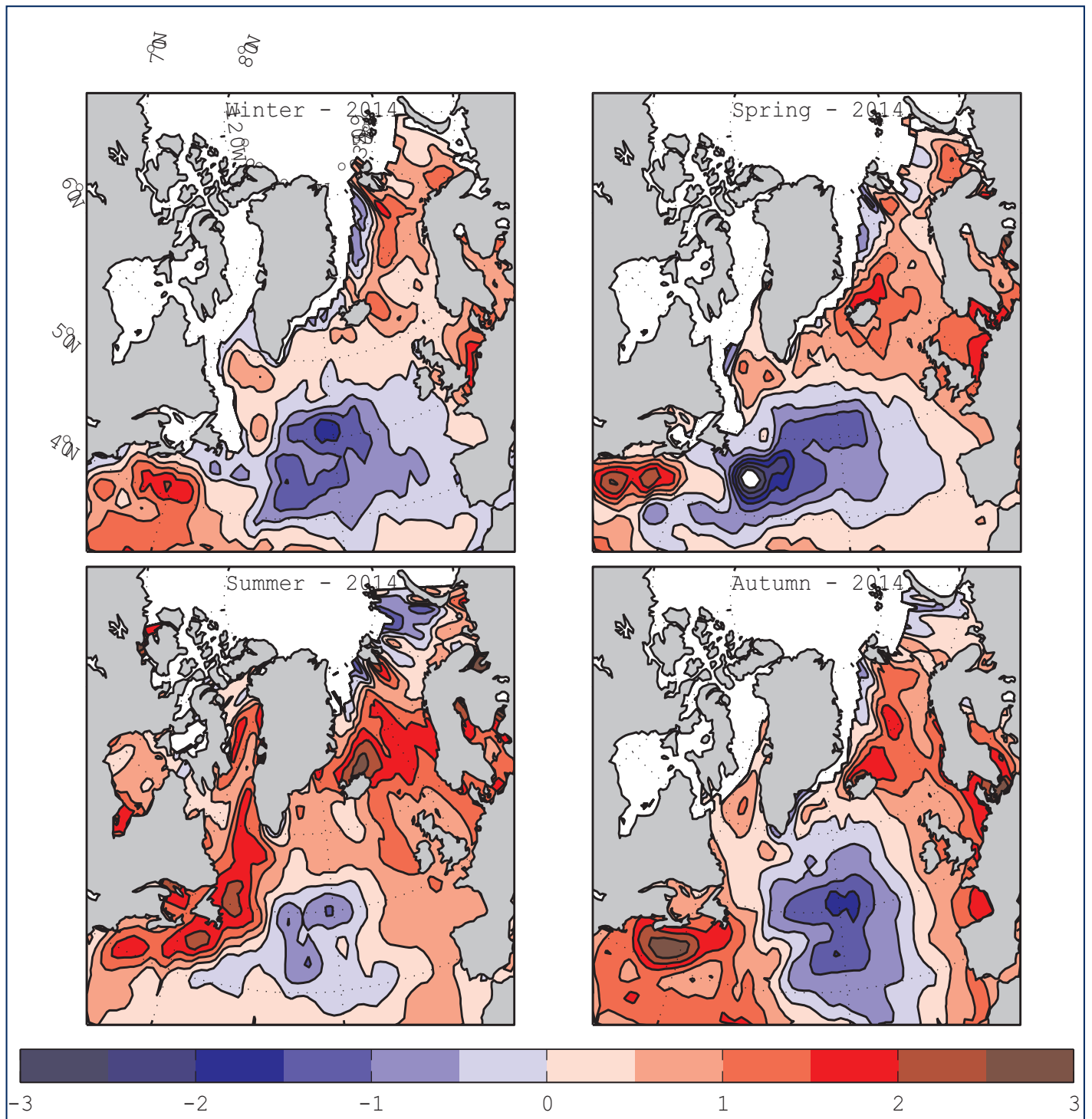
2.2 SEA SURFACE TEMPERATURE

Sea surface temperatures across the entire North Atlantic have also been obtained from a combined satellite and *in situ* gridded dataset. Figure 3 shows the seasonal SST anomalies for 2012 (relative to 1981–2010) extracted from the Optimum Interpolation SST dataset (OISST.v2) provided by the NOAA-CIRES Climate Diagnostics Center in the USA. The 1981–2010 climatology was prepared from a combination of ERSST and OISST data¹. At high latitudes, where *in situ* data are sparse and satellite data are hindered by cloud cover, the data may be less reliable. Regions with ice cover for >50% of the averaging period appear blank.



¹ http://www.cpc.ncep.noaa.gov/products/people/yxue/sstclim/Note_SST_Climatology_1981-2010.doc.

FIGURE 3



Maps of seasonal sea surface temperature anomalies ($^{\circ}\text{C}$) over the North Atlantic for 2014 from the NOAA Optimum Interpolation SSTv2 dataset provided by the NOAA-CIRES Climate Diagnostics Center, USA. The colour-coded temperature scale is the same in all panels. In this case, the anomaly is calculated with respect to normal conditions for 1981-2010. The data are produced on a 1° grid from a combination of satellite and in situ temperature data. Regions with ice cover for $>50\%$ of the averaging period are left blank.

2.3 GRIDDED TEMPERATURE AND SALINITY FIELDS

“Argo and the *In Situ* Analysis System”

The Argo² network of profiling floats has been established to monitor large-scale global ocean variability. Argo data are transmitted in real-time and quickly made available by the two Global Data Assembly Centres (Argo-GDAC). Delayed-mode data are also available; these datasets have undergone more detailed quality control and calibration. Depending on the timing of the analysis process, the most recent 1–2 years of data presented in this report may come from a near real-time dataset; older data will come from the higher quality delayed-mode datasets.

The dataset presented here was prepared at the Coriolis data centre³. Although the Argo dataset remains the main contribution in the open ocean, Coriolis assembles many types of data transmitted in real-time, merging the Argo dataset with data collected by the Global Telecommunications System (GTS) relating to mooring, marine animals, gliders, and conductivity temperature depth profilers (CTDs).

As the ISAS analysis was designed to produce monthly synthesis over the global ocean, the time and space scales have been adjusted to the most general data available; overall, this dataset is less suited to describe conditions in the shallower marginal seas.

In the North Atlantic, the Argo dataset has adequately described temperature and salinity conditions of the upper 2000 m since 2002. This dataset is thus suitable for an overview of the oceanographic conditions in the deeper and more central regions of the North Atlantic basin, and complements the data from the IROC repeat stations and sections which are collected mainly at the periphery of the basin.

Figures 4 and 5 show the 2014 seasonal mean fields of temperature and salinity at 10 m as anomalies from a reference climatology (Antonov *et al.*, 2006; Locarnini *et al.*, 2006). Annual mean anomalies of temperature and salinity for recent years at two selected depths, 10 and 1000 m, are presented in Figures 6 and 7. Finally, in Figure 8, the winter (February) mixed-layer depth is shown. Note that the mixed-layer depth (z) is defined as the depth where temperature has decreased by 0.5°C from the temperature measured at 10 m depth ($T(z) < T(10\text{ m}) - 0.5$). This criterion is not suitable for areas where effects of salinity are important (ice melting) or where basic stratification is weak. Therefore, results in the Labrador Sea, around Greenland, and in the Gulf of Lion are not significant.

Temperature and salinity fields are estimated on a regular half-degree (Mercator scale) grid using the Coriolis *In Situ* Analysis System (ISAS). For data between 2002 and 2012, the results presented here were produced with delayed-mode data from version 6 of ISAS (Gaillard, 2015). For 2013 and 2014, delayed-mode data are not yet available; therefore, near real-time data (NRTISAS, near real-time processing done by Coriolis) are presented. Temperature and salinity anomalies are calculated relative to monthly climatological averages prepared from the World Ocean Atlas (WOA05 - Antonov *et al.*, 2006; Locarnini *et al.*, 2006).

²<http://www.argo.ucsd.edu/>.

³<http://www.coriolis.eu.org>.

During winter 2014 (Figure 4 and 5), near-surface waters were cold and fresh in a large area of the northern North Atlantic centred on approximately 50°N. The pattern of surface temperature compared very well to that presented in the OISST.v2 dataset (Figure 3). ISAS gridded fields are based entirely on *in situ* products, whereas OISST is a combination of *in situ* and satellite sea surface temperatures; of course, the ISAS dataset has the advantage of including both temperature and salinity fields as well as subsurface data. The area of cold and freshwater persisted throughout the year, weakening a little in summer, but extending further northward by autumn 2014. South of 40°N, warm and salty conditions were observed throughout the year. It should be noted that this colder and fresher region is unlikely to have been sampled by the *in situ* datasets located around the margins of the basin where conditions have generally remained warmer and saltier than normal. The contrast between the cooler central regions and the warmer margins was particularly marked in autumn 2014 (Figures 3 and 4).

Along the eastern seaboard of the US and Canada, waters were anomalously warm and salty. This feature, suggesting a northward shift of the Gulf Stream, has persisted in this region since 2012 (Figure 6). Persistently warm and salty conditions have been observed east of Greenland in this dataset since at least 2005.

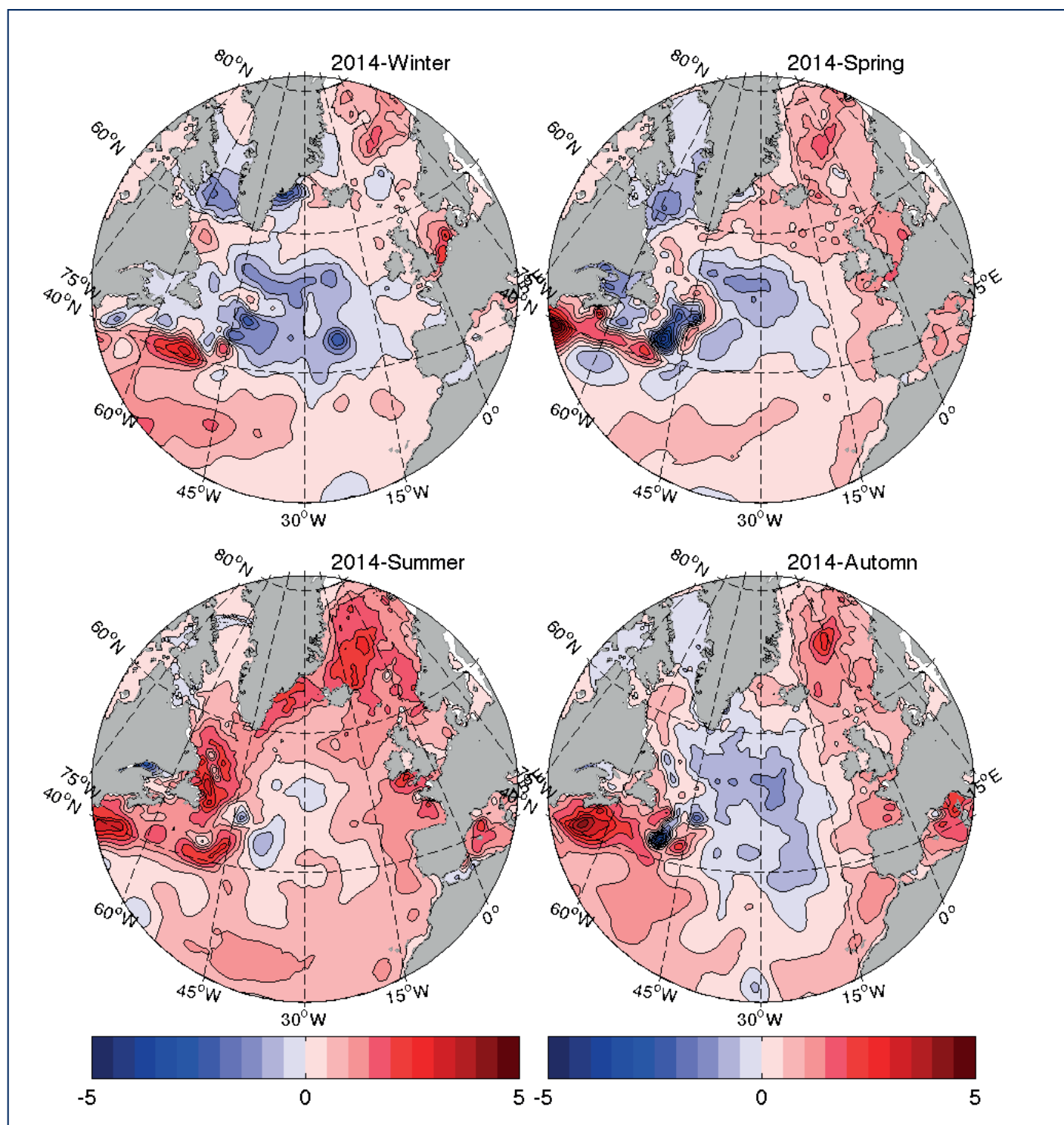
Annual mean anomalies for the ocean interior at a depth of 1000 m are shown in Figure 7. The Greenland, Labrador, and Irminger seas remained warmer than normal, a pattern that has persisted since at least 2009. In contrast, east of 30°W in the Iceland Basin and Rockall Trough, conditions have been persistently cooler and also fresher than normal over the same time-period.

Variations in the February mixed-layer depth (defined as the depth where temperature differs by more than 0.5°C from the 10 m value) are shown in Figure 8. During 2014, an area with a deep mixed layer (deeper than 600 m) was observed in the eastern North Atlantic, extending from the Porcupine Abyssal plain and centring at approximately 22.5°E. In the winters of 2009–2013, the mixed-layer depth in this same area was 200–300 m.



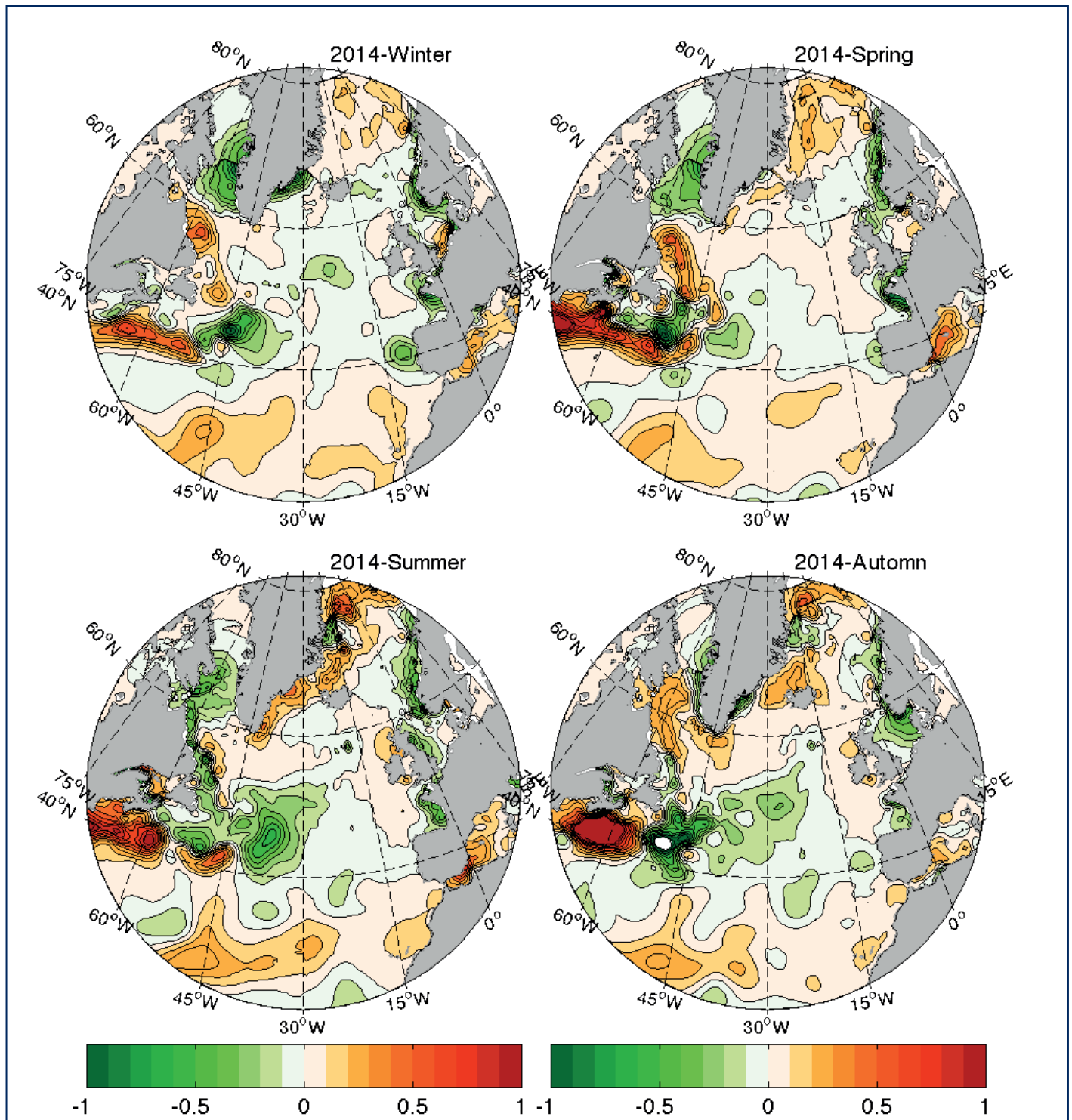
**PERSISTENTLY WARM AND
SALTY CONDITIONS HAVE BEEN
OBSERVED EAST OF GREENLAND
SINCE AT LEAST 2005.**

FIGURE 4



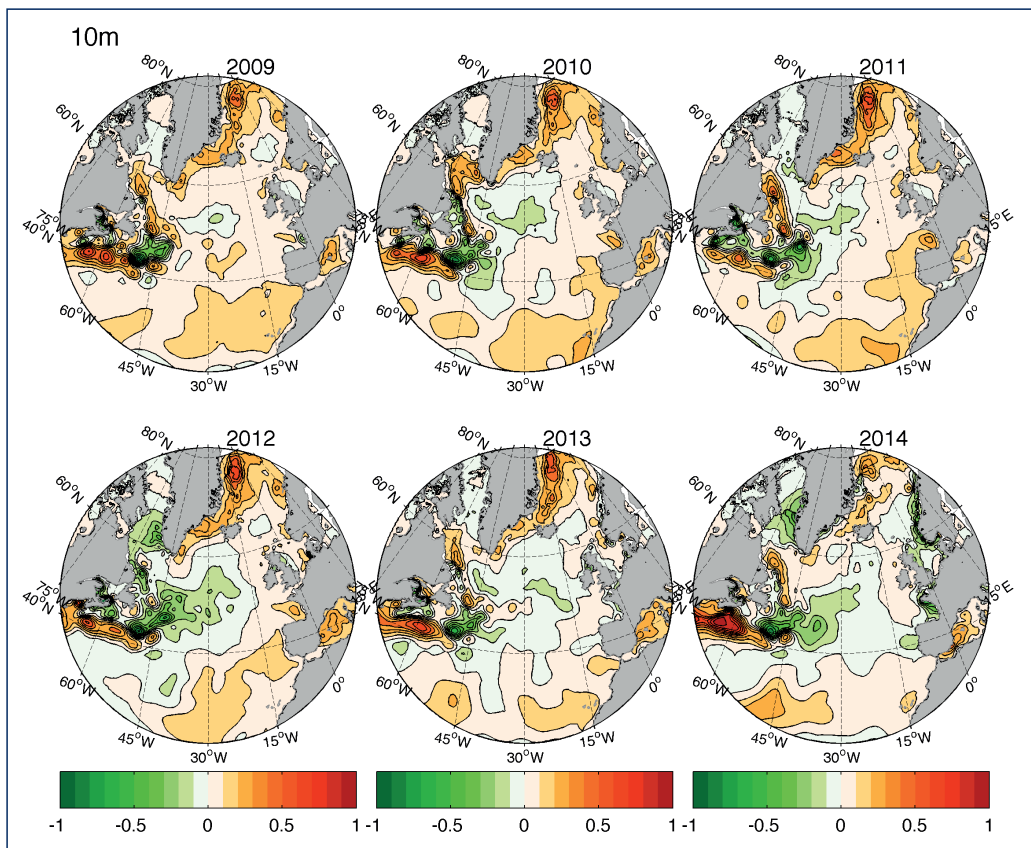
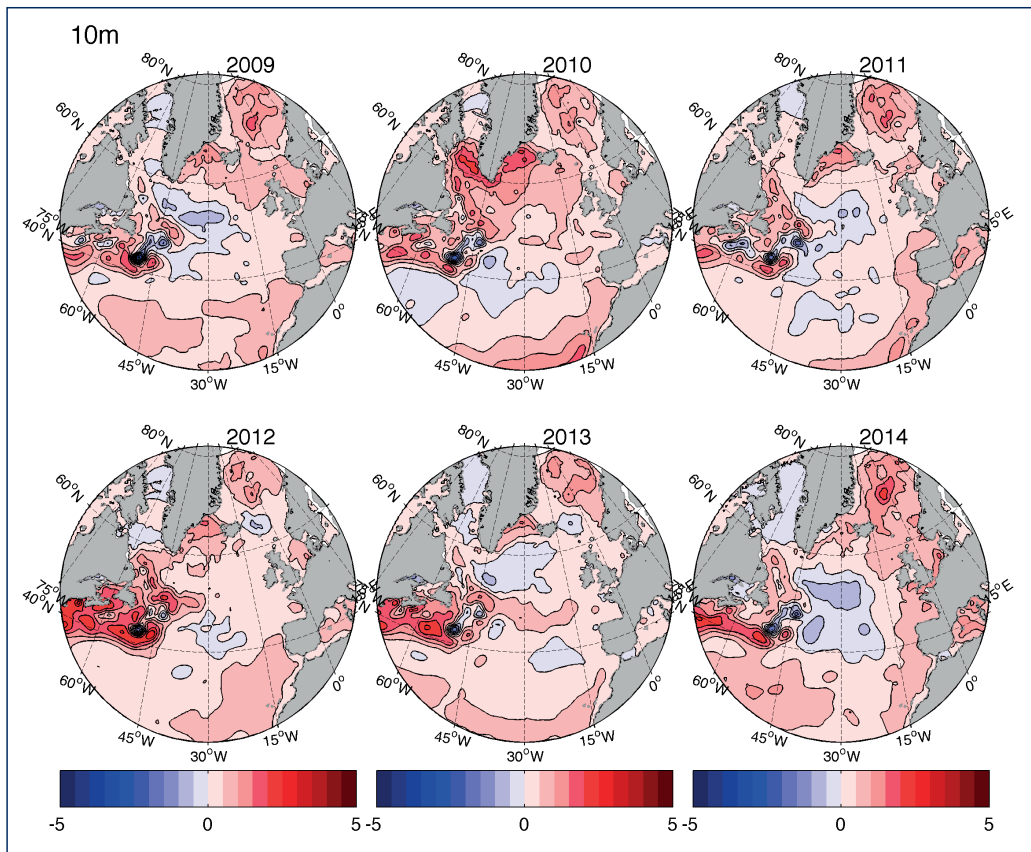
Maps of 2014 seasonal temperature anomalies at 10 m depth in the North Atlantic. Anomalies are the differences between the ISAS monthly mean values and the reference climatology WOA05 (Locarnini et al., 2006). The colour-coded temperature scale is the same in all panels. From the ISAS monthly analysis of Argo data.

FIGURE 5



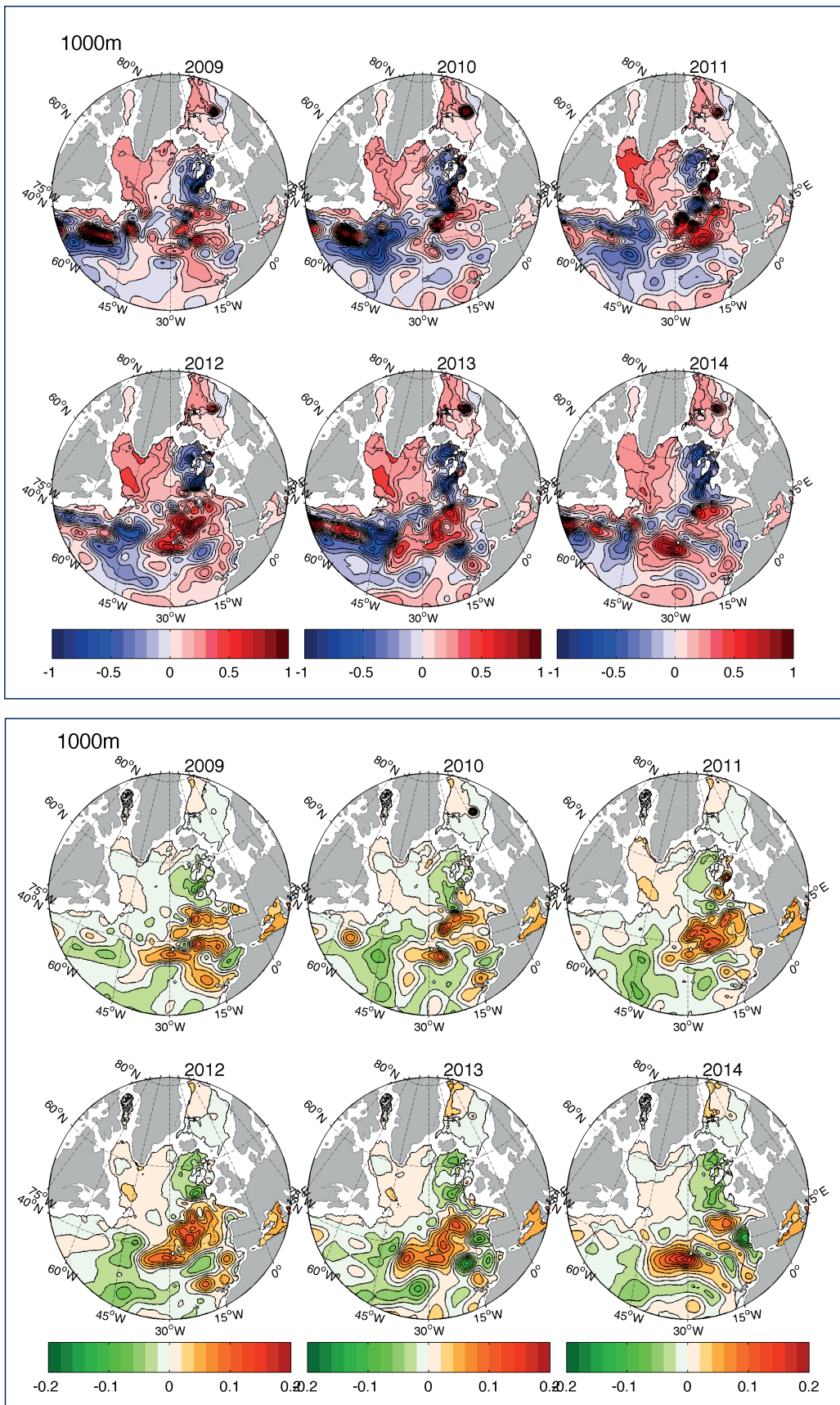
Maps of 2014 seasonal salinity anomalies at 10 m depth in the North Atlantic. Anomalies are the differences between the ISAS monthly mean values and the reference climatology WOA05 (Antonov et al., 2006). The colour-coded salinity scale is the same in all panels. From the ISAS monthly analysis of Argo data.

FIGURE 6



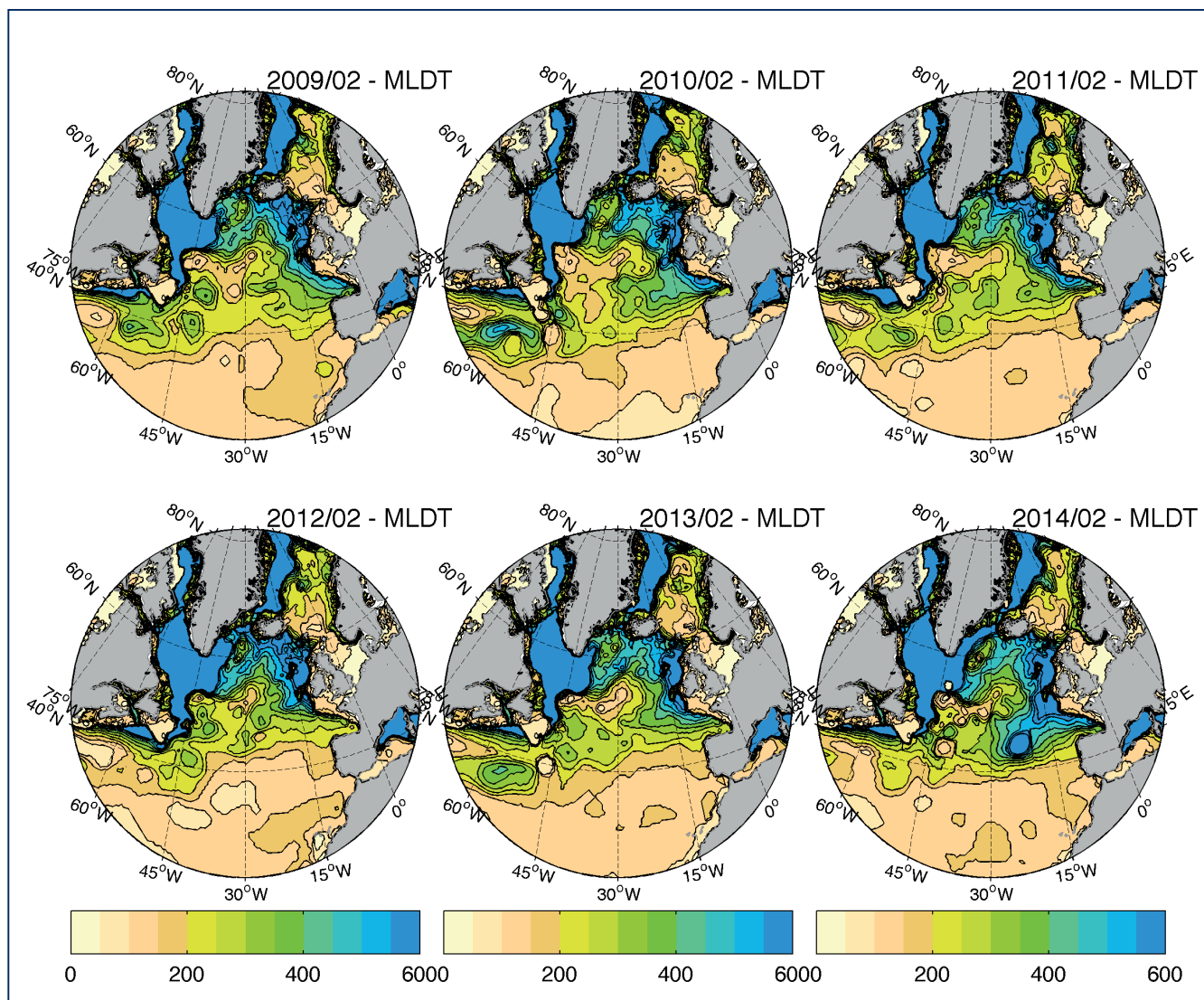
Maps of annual temperature (upper) and salinity (lower) anomalies at 10m for 2009–2014. From the ISAS monthly analysis of Argo data.

FIGURE 7

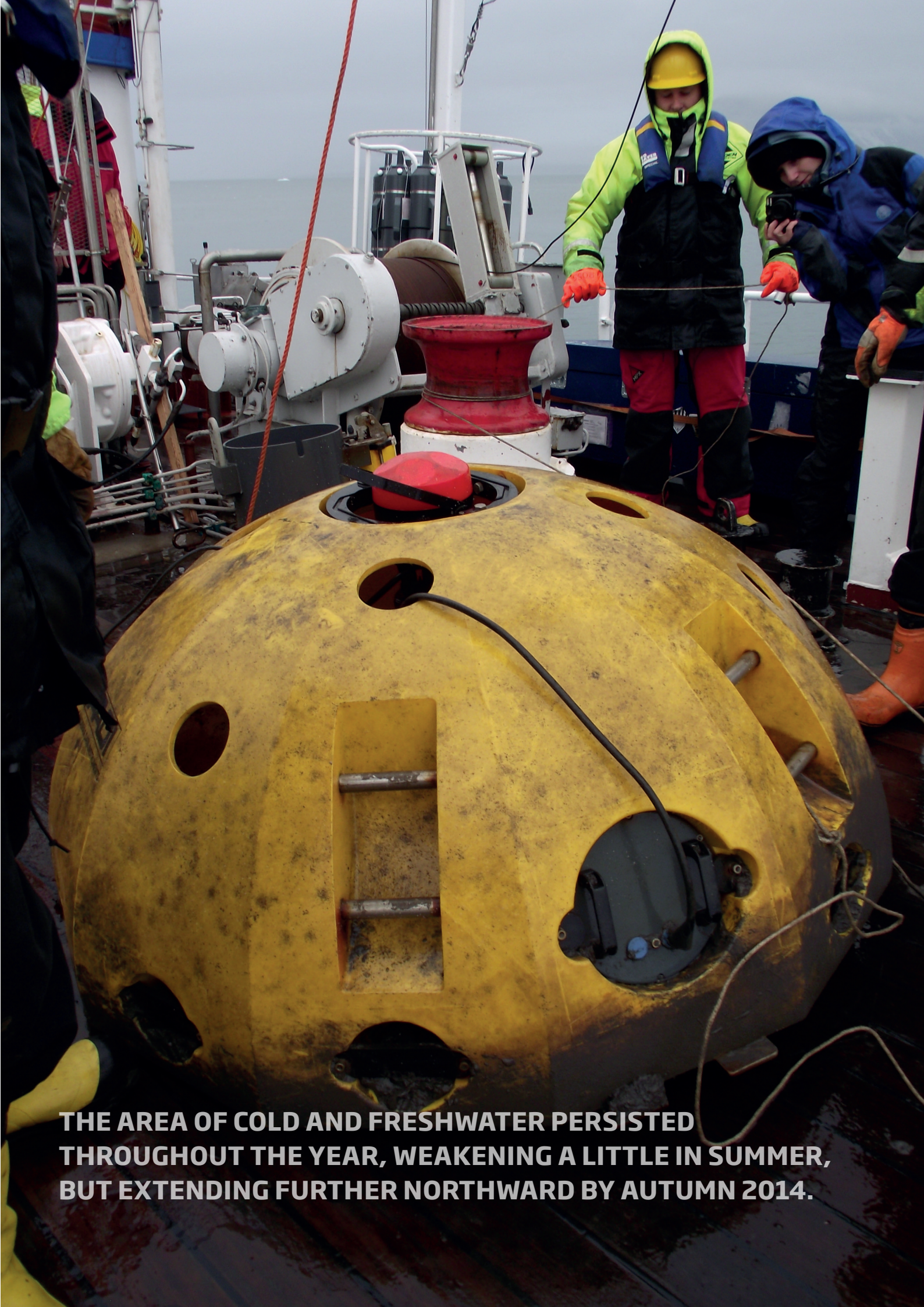


Maps of annual temperature (upper) and salinity (lower) anomalies at 1000 m for 2009-2014. From the ISAS monthly analysis of Argo data.

FIGURE 8



Maps of North Atlantic winter (February) mixed-layer depths for 2009-2014. From the ISAS monthly analysis of Argo data. Note that the mixed-layer depth is defined as the depth at which temperature has decreased by more than 0.5°C from the temperature at 10 m depth. This criterion is not suitable for areas where effects of salinity are important (ice melting) or where the basic stratification is weak. Therefore, results in the Labrador Sea, around Greenland, and in the Gulf of Lion are not significant.



THE AREA OF COLD AND FRESHWATER PERSISTED THROUGHOUT THE YEAR, WEAKENING A LITTLE IN SUMMER, BUT EXTENDING FURTHER NORTHWARD BY AUTUMN 2014.

3. THE NORTH ATLANTIC ATMOSPHERE

3.1 SEA LEVEL PRESSURE AND WINDSPEED

The North Atlantic Oscillation (NAO) is a pattern of atmospheric variability that has a significant impact on oceanic conditions. It affects windspeed, precipitation, evaporation, and the exchange of heat between ocean and atmosphere, and its effects are most strongly felt in winter. The NAO index is a simple device used to describe the state of the NAO. It is a measure of the strength of the sea level air pressure gradient between Iceland and Lisbon, Portugal. When the NAO index is positive, there is a strengthening of the Icelandic low-pressure system and the Azores high-pressure system. This produces stronger mid-latitude westerly winds, with colder and drier conditions over the western North Atlantic, and warmer and wetter conditions in the eastern North Atlantic. When the NAO index is negative, there is a reduced pressure gradient, and the effects tend to be reversed.

When the NAO is weak, two additional dominant atmospheric regimes have been recognized as useful descriptors: (i) the Atlantic Ridge mode, when a strong anticyclonic ridge develops off western Europe (similar to the East Atlantic pattern); and (ii) the Blocking regime, when the anticyclonic ridge develops over Scandinavia. The four regimes (positive NAO, negative NAO, Atlantic Ridge, and Blocking) have all been occurring at around the same frequency (20–30% of all winter days) since 1950. These modes of variability are revealed through cluster analysis of sea level pressure (SLP) rather than examining point-to-point SLP gradients.

There are several slightly different versions of the NAO index calculated by climate scientists. The Hurrell winter (December/January/February/March, or DJFM) NAO index is most commonly used and is particularly relevant to the eastern North Atlantic. Note that although winter is commonly thought of as coming at the end of the year, here the “winter season” spans an annual boundary and precedes the year of interest, so the winter of December 2012 – March 2013 sets up conditions for summer 2013.





Following a long period of increase, from an extreme and persistent negative phase in the 1960s to a most extreme and persistent positive phase during the late 1980s and early 1990s, the Hurrell NAO index underwent a large and rapid decrease during winter 1995/1996. In many of the years between 1996 and 2009, the Hurrell winter NAO index was both fairly weak and a less useful descriptor of atmospheric conditions, due mainly to the patterns of sea level pressure not following a typical NAO pattern.

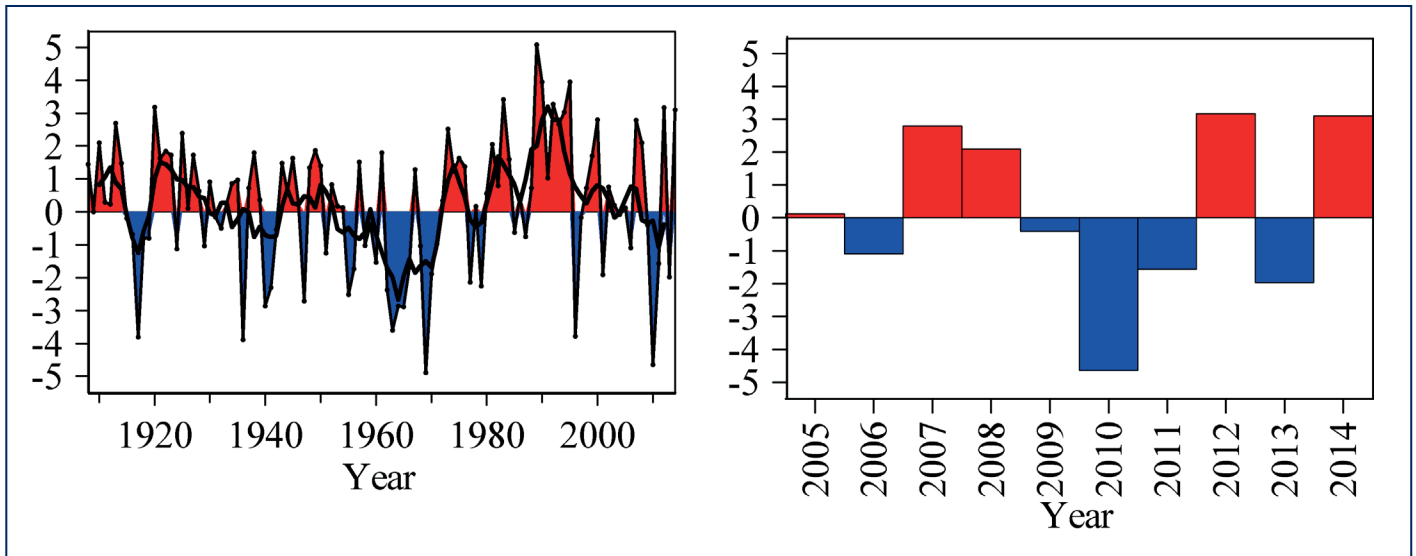
In winter 2010, the index was strongly negative (Figure 9), and its anomaly pattern exerted a dominant influence on atmospheric conditions. This was the strongest negative anomaly since 1969 and the second strongest negative value for the Hurrell winter NAO index on record (starting in 1864). In winter 2013/2014, the Hurrell winter NAO index was strongly positive (+3.10), almost as strong as seen in 2011/2012. In between, winter 2012/2013 was negative.

Atmospheric conditions indicated by the NAO index are often more clearly understandable when the anomaly fields are mapped. Ocean properties are particularly dominated by winter conditions; hence the inclusion of maps of sea level pressure for the winter period (Figure 10). Figure 10a shows the winter SLP averaged over 30 years (1981–2010). The dominant features (“action centres”) are the Iceland Low (the purple patch situated southwest of Iceland) and the Azores High (the orange patch west of Gibraltar).

Figure 10b shows the mean SLP for winter 2014 (December 2013, January–March 2014), and Figure 10c shows the 2014 winter SLP anomaly (i.e. the difference between Figures 10a and 10b). In winter 2014, the orientation of the centres of high and low pressure were typical of the average pattern. Both the Iceland Low and the Azores High were evident, with the main difference being that the Iceland low was stronger and extended farther south than normal, and the Azores high was stronger and farther west than normal. The resultant sea level pressure anomaly showed a strong negative centre over the Iceland Basin and Rockall Trough.

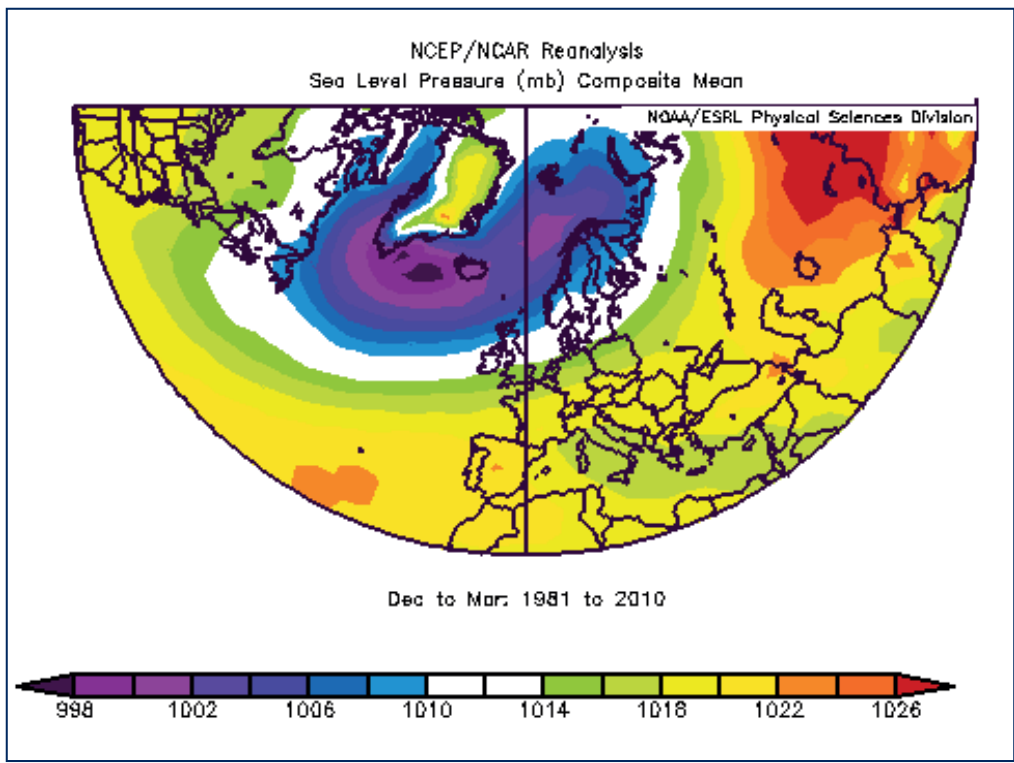
The pattern of sea level pressure is closely related to patterns of wind; the geostrophic (or “gradient”) wind blows parallel to the isobars, with lower pressure to the left, and the closer the isobars, the stronger the wind. Strength of the winter mean surface wind averaged over the 30-year period (1981–2010) is shown in Figure 11a, while Figure 11b shows the mean surface wind for winter 2014 and Figure 11c shows the anomaly in winter 2014. Stronger-than-normal winds associated with the strong northwest-southeast orientation of the isobars were observed over the eastern North Atlantic. These enhanced winds are likely linked to the deeper-than-normal mixed layer observed in the same area (Figure 8). Stronger-than-normal winds were also seen northwest of Iceland and in the northern North Sea.

FIGURE 9



The Hurrell winter (DJFM) NAO index for the past 100 years with a two-year running mean applied (left panel) and for the current decade (right panel). Data source: Hurrell et al. (2015).

FIGURE 10a



Winter (DJFM) sea level pressure (SLP) fields. Figure 10a: SLP averaged over 30 years (1981-2010). Figure 10b: mean SLP in winter 2014 (December 2013, January-March 2014). Figure 10c: winter 2014 SLP anomaly – the difference between Figures 10a and 10b. Images provided by the NOAA/ESRL Physical Sciences Division, Boulder, CO (available online at <http://www.cdc.noaa.gov/>).

FIGURE 10b

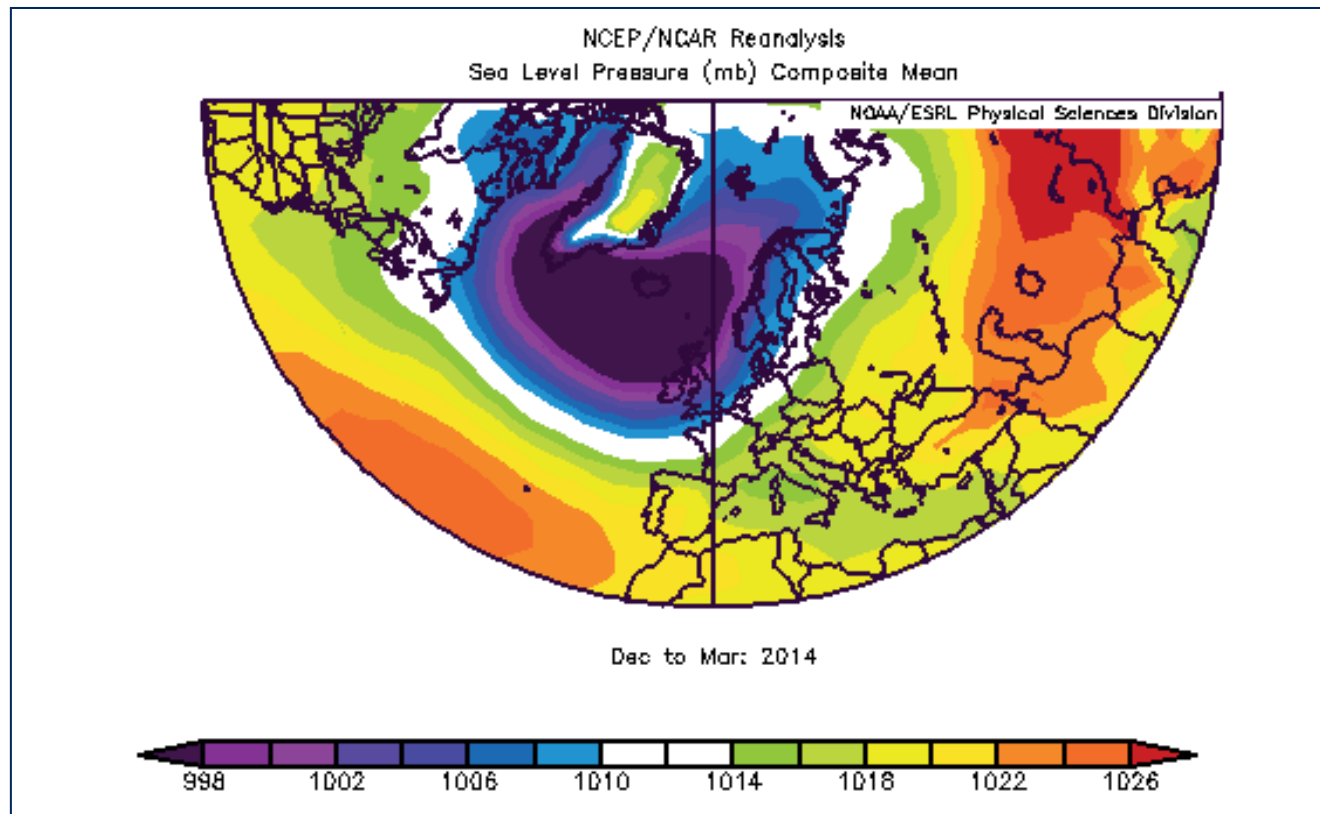


FIGURE 10c

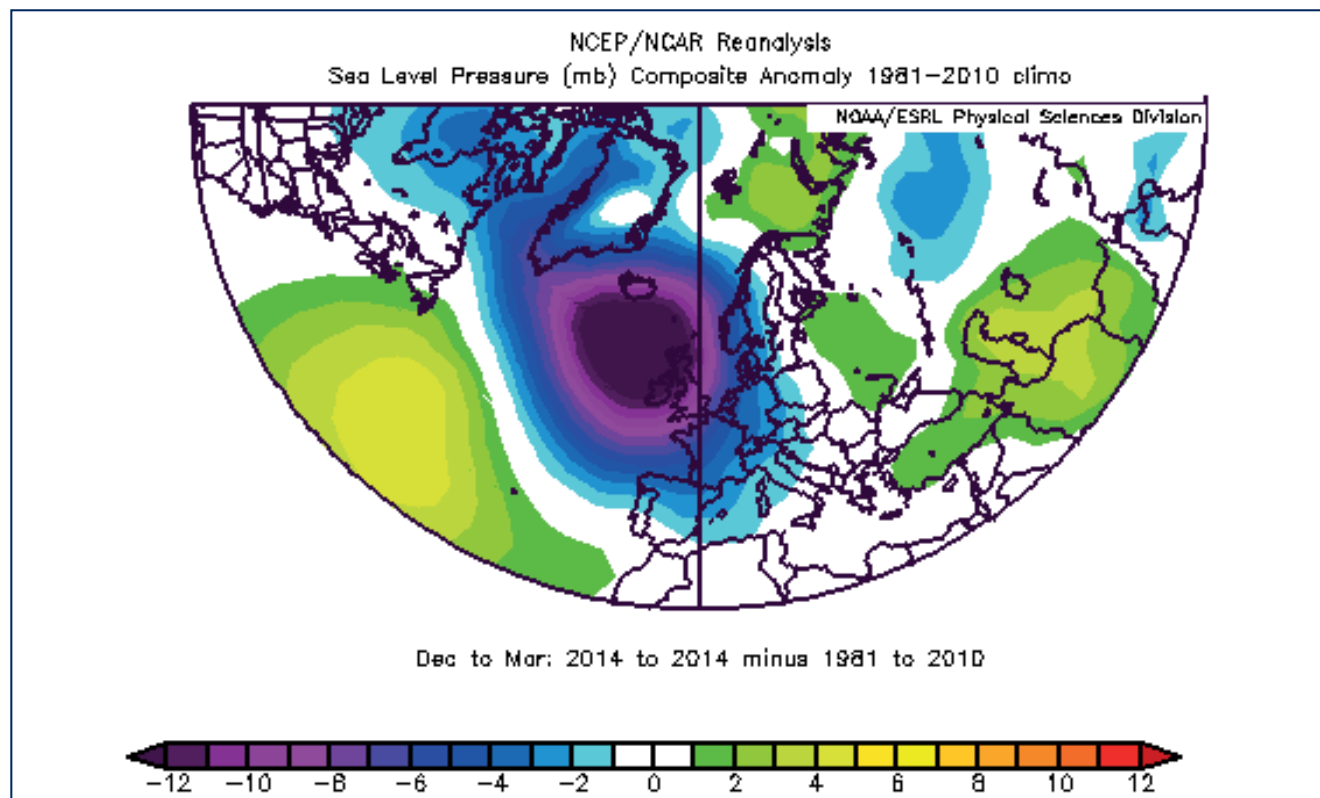
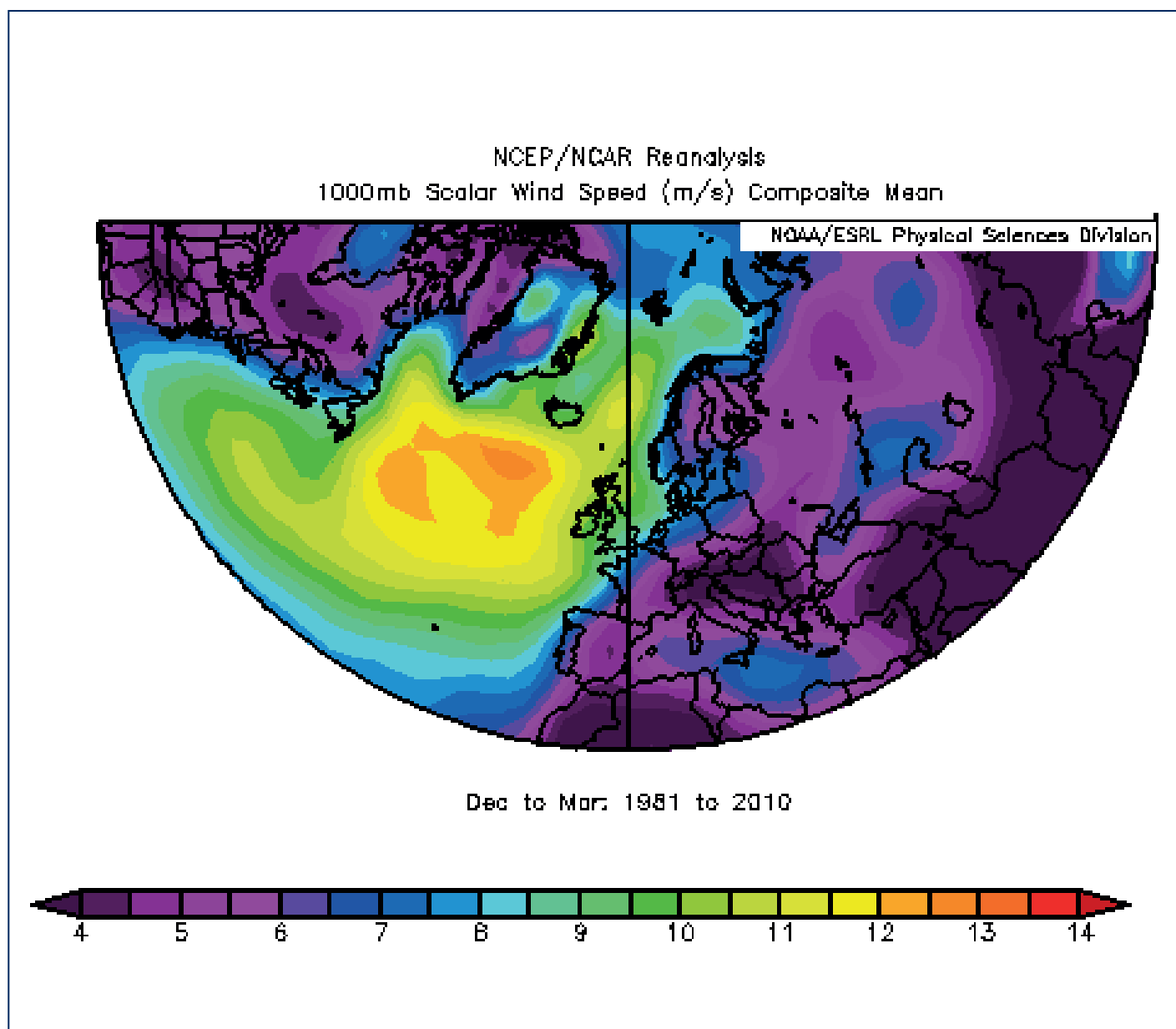


FIGURE 11a



Winter (DJFM) surface windspeed. Figure 11a: surface windspeed averaged over 30 years (1981-2010). Figure 11b: mean surface windspeed in winter 2014 (December 2013, January-March 2014). Figure 11c: winter 2014 surface windspeed anomaly – the difference between Figures 11a and b. Images provided by the NOAA/ESRL Physical Sciences Division, Boulder, CO (available online at <http://www.cdc.noaa.gov/>).

FIGURE 11b

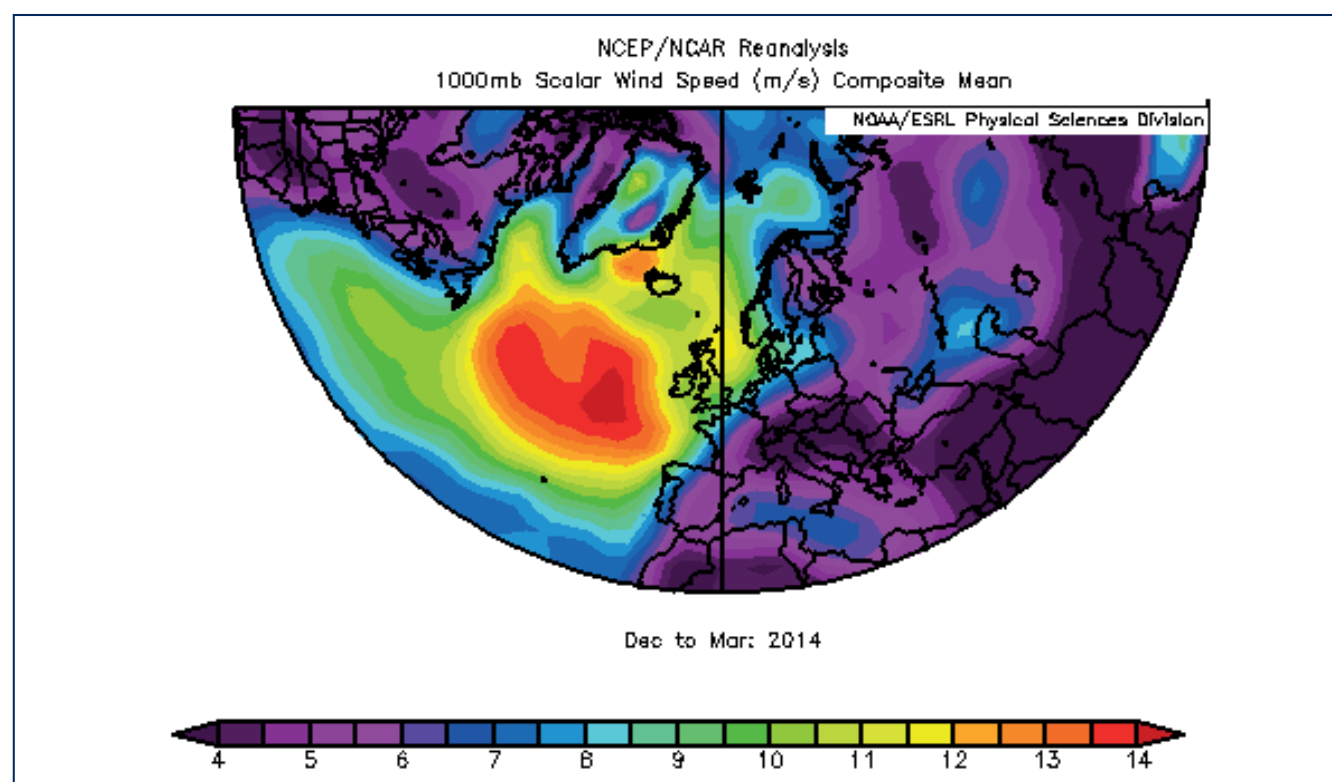
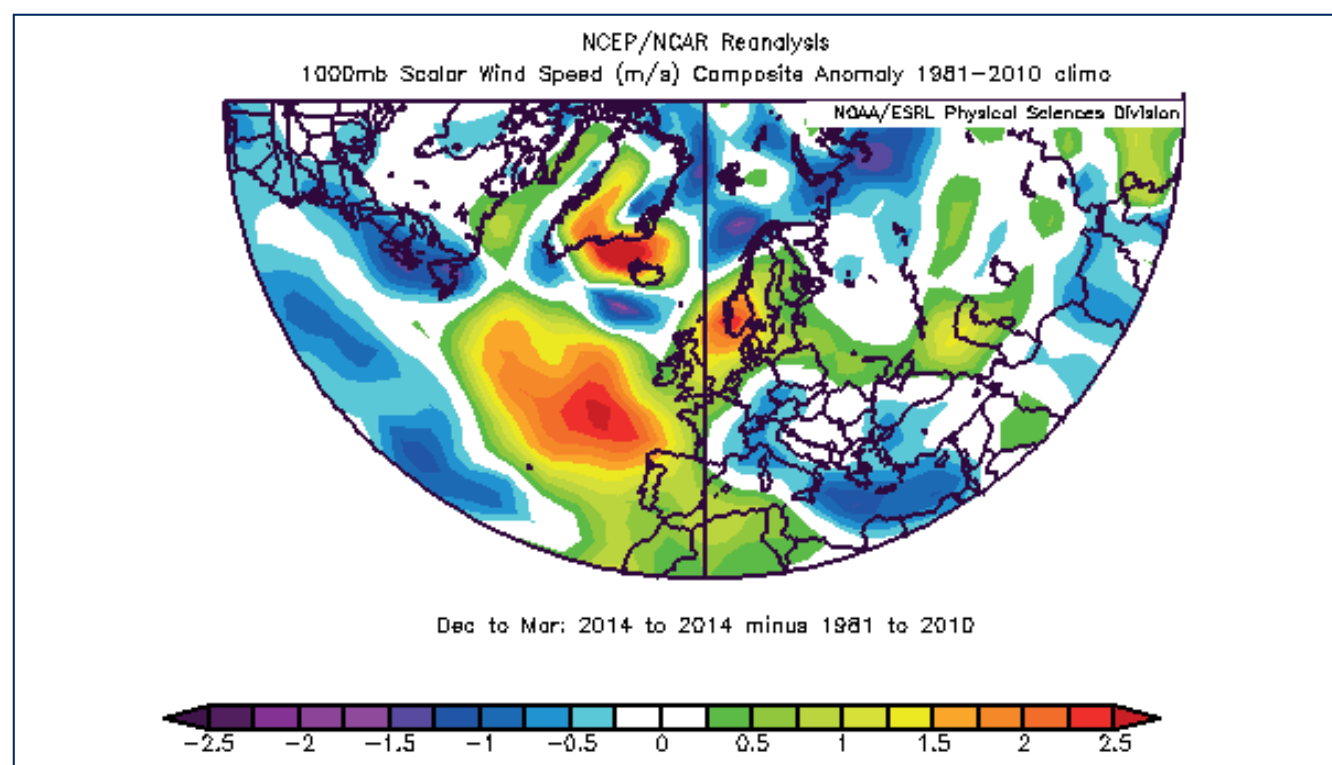


FIGURE 11c

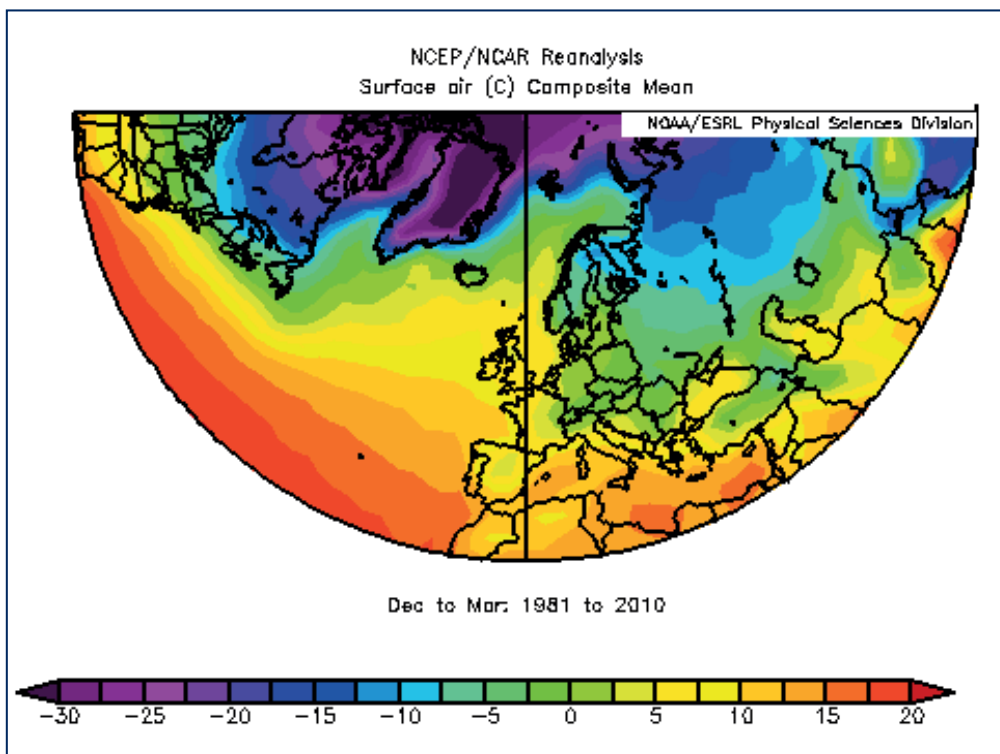


3.2 SURFACE AIR TEMPERATURE

North Atlantic winter mean surface air temperatures are shown in Figure 12. The 1981–2010 mean conditions (Figure 12a) show warm temperatures penetrating far to the north on the eastern side of the North Atlantic and the Nordic seas, caused by the northward movement of warm oceanic water. Figure 12b shows the conditions in winter (DJFM) 2013/2014, and Figure 12c shows the difference between the two.

Winter 2013/2014 was warmer than normal over the majority of the European continental area and across the Greenland and Norwegian seas. Over the continental area of the USA and Canada, however, winter was much colder than normal, and there was also a strong area of colder-than-normal air over the central North Atlantic, likely related to sea surface temperature anomalies observed in this region.

FIGURE 12a



Winter (DJFM) surface air temperature fields. Figure 12a: surface air temperature averaged over 30 years (1981–2010). Figure 12b: temperatures in winter 2014 (December 2013, January–March 2014). Figure 12c: winter 2014 surface air temperature anomaly – the difference between Figures 12a and 12 b. Images provided by the NOAA/ESRL Physical Sciences Division, Boulder, CO (available online at <http://www.cdc.noaa.gov/>).

FIGURE 12b

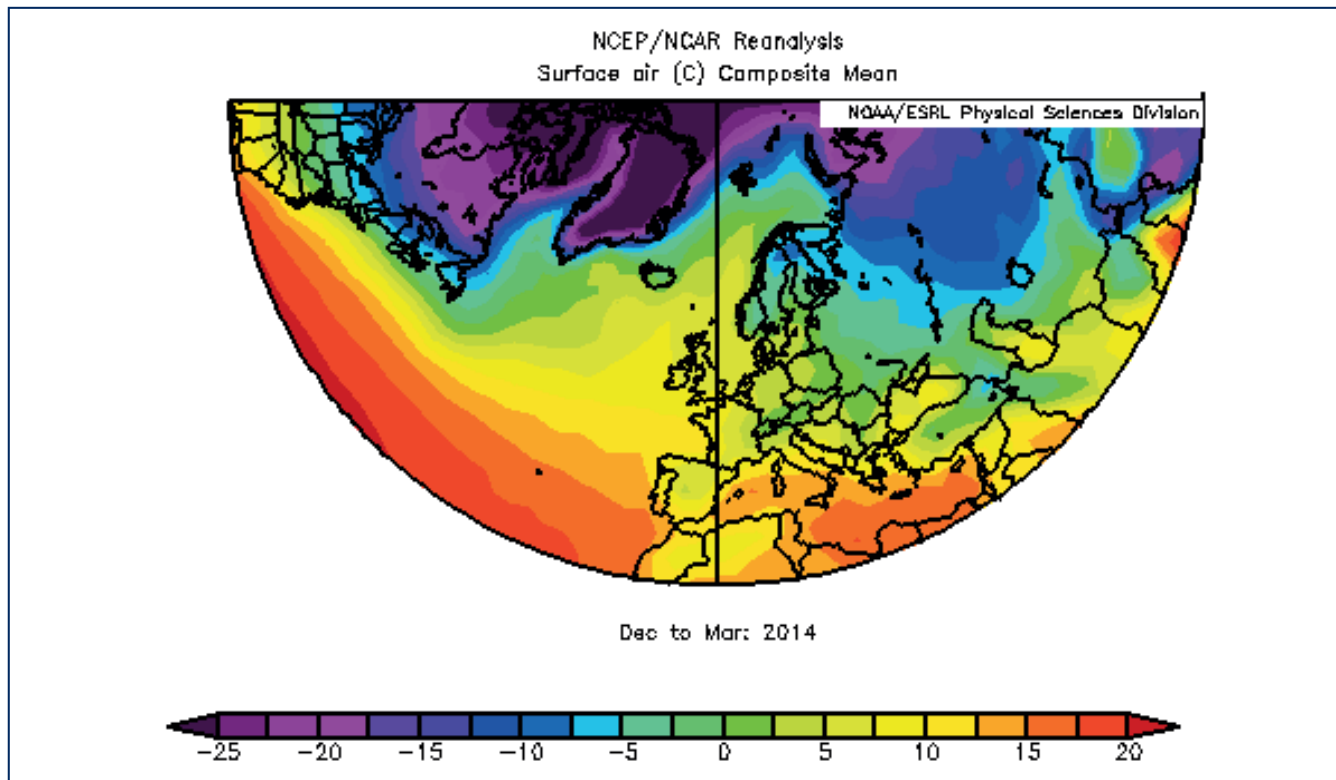
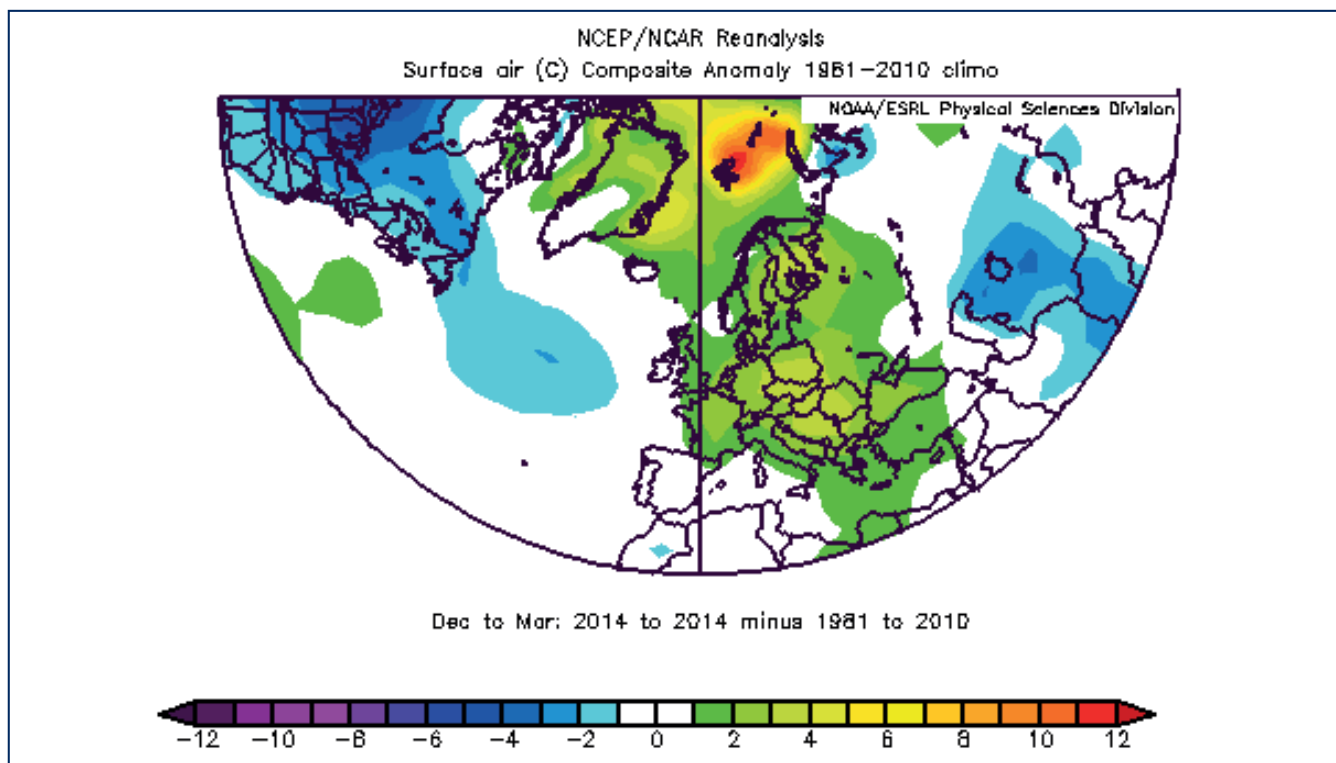


FIGURE 12c



4. DETAILED AREA DESCRIPTIONS, PART I: THE UPPER OCEAN

4.1 INTRODUCTION

This section presents time-series from many sustained observations in each of the ICES Areas. The general pattern of oceanic circulation in the upper layers of the North Atlantic, in relation to the areas described here, is given in Figure 13. In addition to temperature and salinity, other indices are presented where they are available, such as air-temperature and sea-ice indices. The text summarizes the regional context of the sections and stations, noting any significant recent events.

Most standard sections or stations are sampled annually or more frequently. Often, the time-series presented here have been extracted from larger datasets and chosen as indicators of conditions in a particular area. Where appropriate, data are presented as anomalies to demonstrate how the values compare with the average or “normal” conditions (usually the long-term mean of each parameter during 1981–2010). For datasets that do not extend as far back as 1981, average conditions have been calculated from the start of the dataset up to 2010.

In places, the seasonal cycle has been removed from a dataset either by calculating the average seasonal cycle during 1981–2010 or by drawing on other sources, such as regional climatology datasets. Smoothed versions of most time-series are included using a “Loess smoother”, a locally weighted regression with a two- or five-year window.

In some areas, data are sampled at sufficiently regular intervals to allow a good description of the seasonal cycle. Where possible, monthly data from 2012 are presented and compared with the average seasonal conditions and statistics.

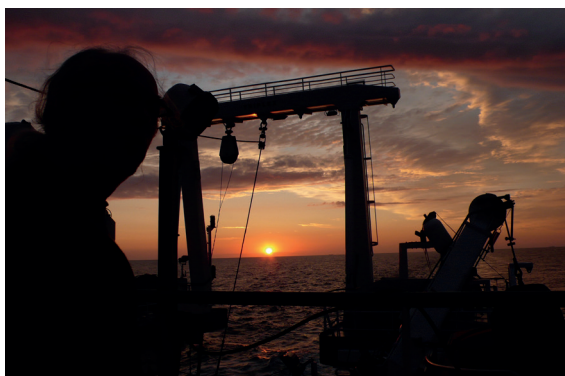
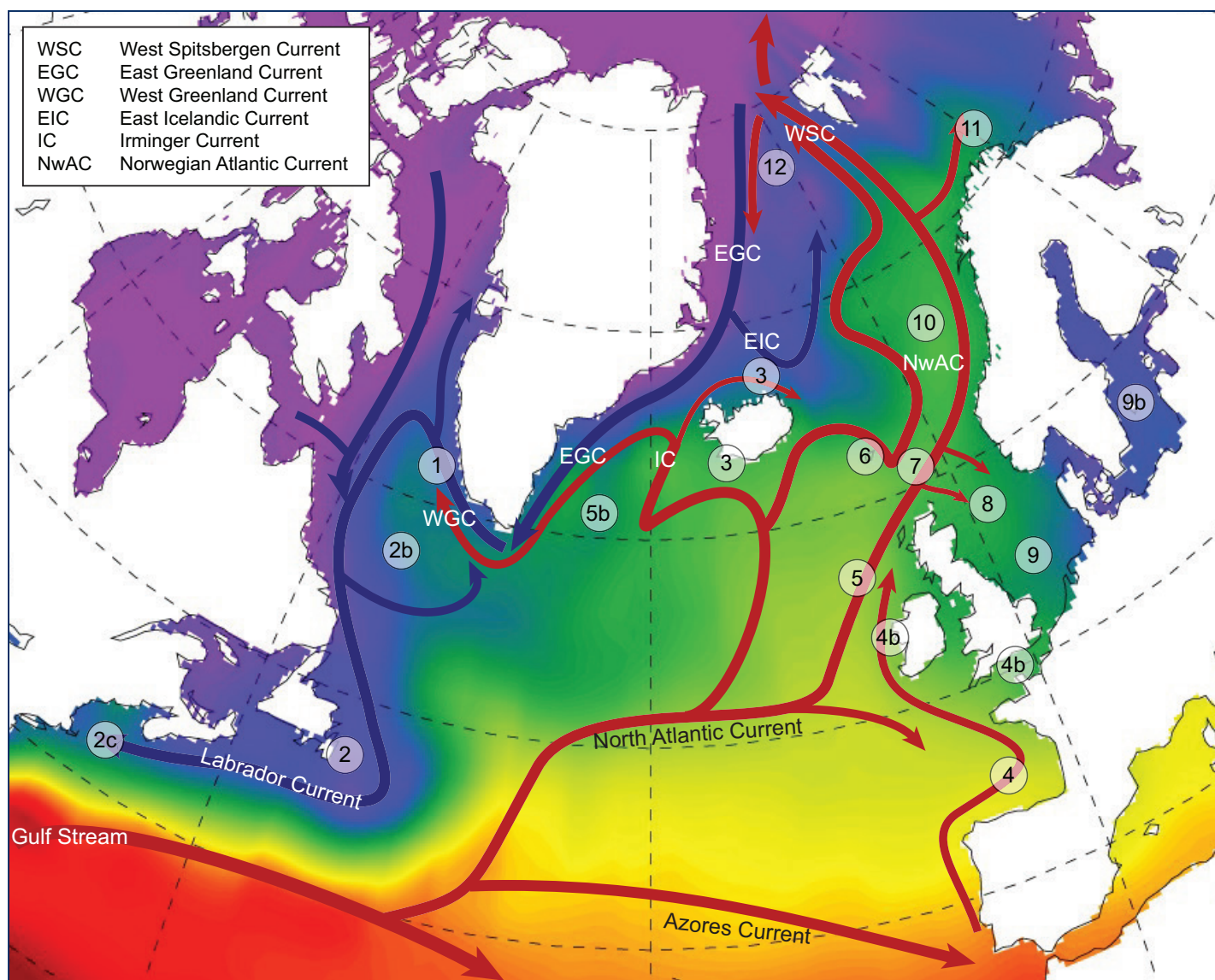


FIGURE 13



Schematic of the general circulation of the upper ocean (0-1000 m) in the North Atlantic in relation to the numbered areas presented below. Blue arrows = movement of cooler waters of the Subpolar Gyre; red arrows = movement of warmer waters of the Subtropical Gyre.

4.2 AREA 1 – WEST GREENLAND

The West Greenland Current (WGC) carries water northward along the west coast of Greenland and consists of two components: (i) a cold and fresh inshore component, which is a mixture of polar water and melt water, and (ii) a saltier and warmer Irminger Sea water component offshore. The WGC is part of the cyclonic Subpolar Gyre and thus subject to hydrographic variations at the different time-scales associated with gyre variability. Hydrographic conditions are monitored at two oceanographic sections across the continental slope of West Greenland. Two offshore stations at each section have been chosen to document changes in hydrographic conditions off West Greenland.

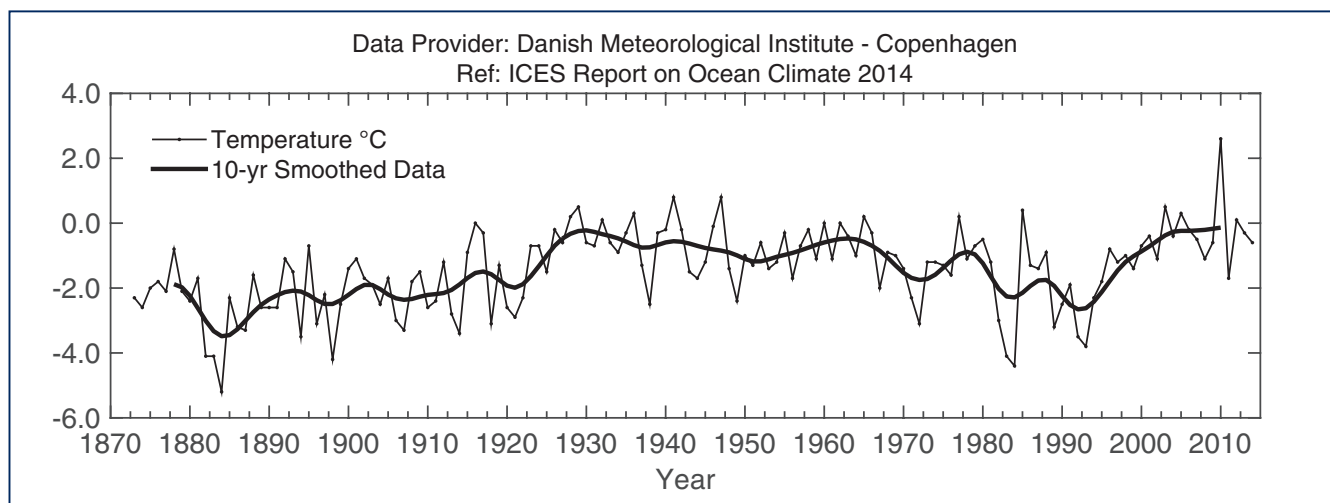
In 2014, the NAO index was positive (3.1) describing anomalous strong westerlies over the North Atlantic. The annual mean air temperature at Nuuk Weather Station in West Greenland was -0.6°C in 2014, 0.8°C above the long-term mean (1981-2010).

Water properties between depths of 0 and 50 m at Fyllas Bank Station 4 are used to monitor the variability of the fresh polar water component of the West Greenland Current. In 2014, the temperature of this water mass was 3.38°C , 0.74°C above its long-term mean (1983-2010). The salinity anomaly of the polar water was strongly negative between 2012 and 2013, while salinity increased in 2014 and was 0.42 above its long-term mean.

The temperature and salinity of the Irminger Sea water component of the West Greenland Current started to increase towards the end of the 1990s, coinciding with a slowing down of the Subpolar Gyre. In 2014, water temperature in the 75-200 m layer at Cape Desolation Station 3 was 6.27°C , 0.55°C above the long-term mean (1983-2010). In 2014, salinity in the 75-200 m layer at Cape Desolation Station 3 was 34.89, 0.03 below the long-term mean.

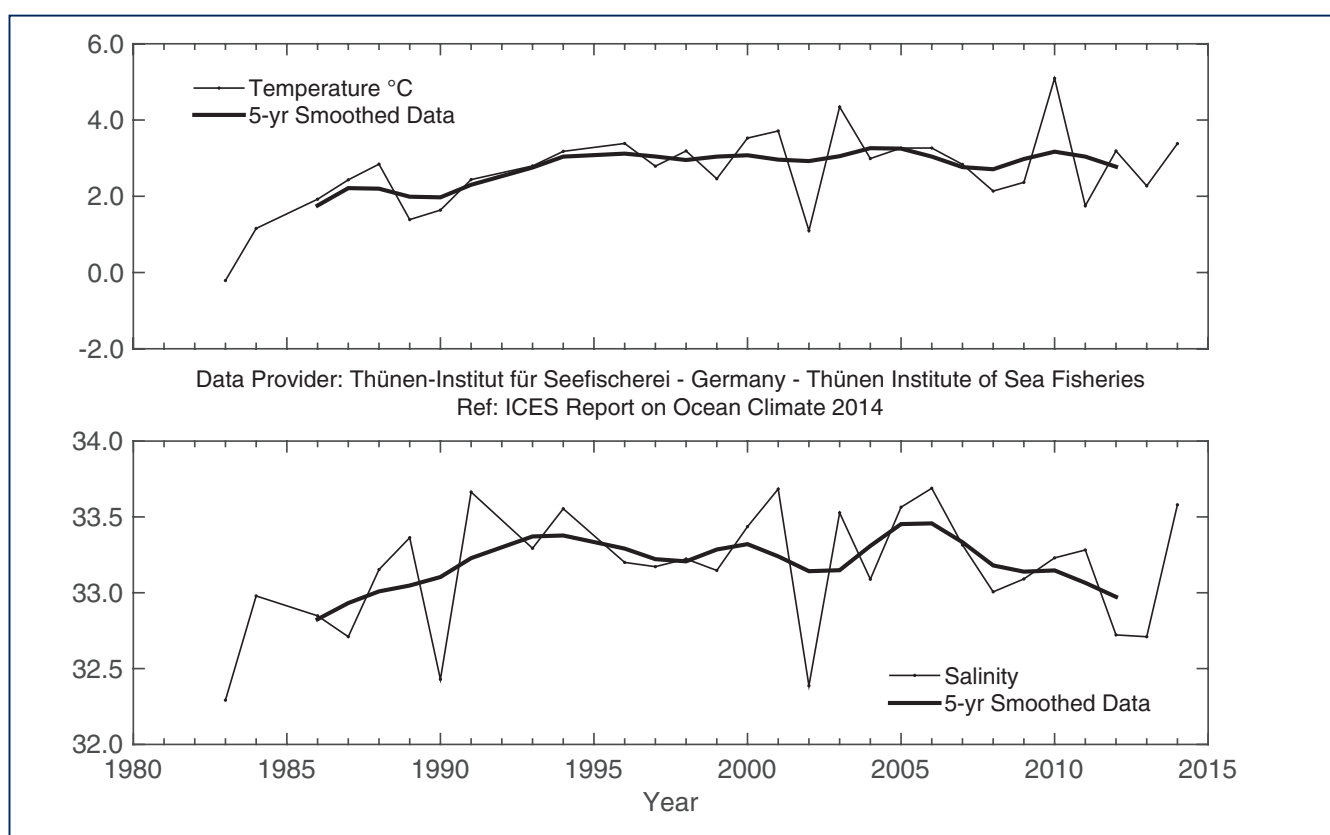


FIGURE 14



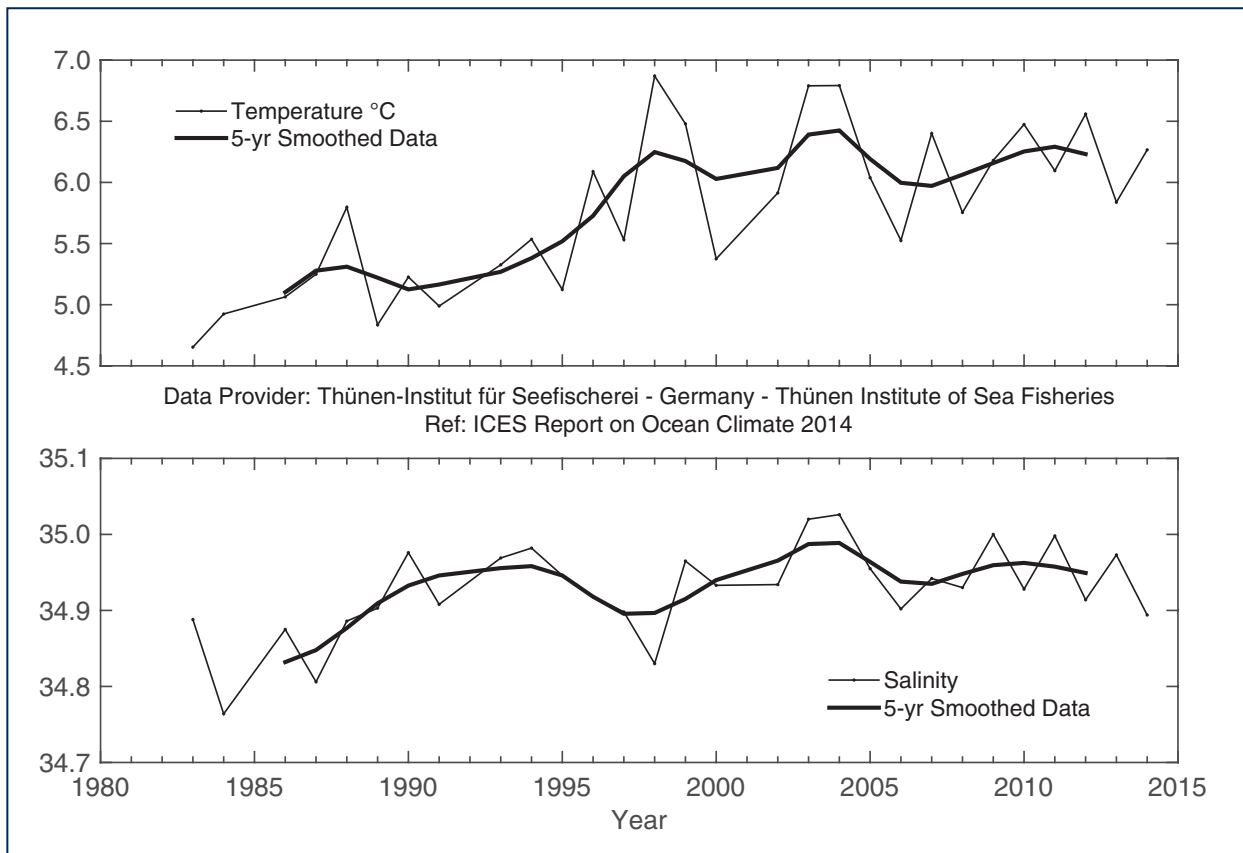
Area 1 - West Greenland. Annual mean air temperature at Nuuk station (64.16°N 51.75°W). Data source: Cappelen (2013).

FIGURE 15



Area 1 - West Greenland. Mean temperature (upper panel) and salinity (lower panel) between 0 and 50 m at Fyllas Bank Station 4 (63.88°N 53.37°W).

FIGURE 16



Area 1 - West Greenland. Temperature (upper panel) and salinity (lower panel) between 75 and 200 m at Cape Desolation Station 3 (60.47°N 50°W).



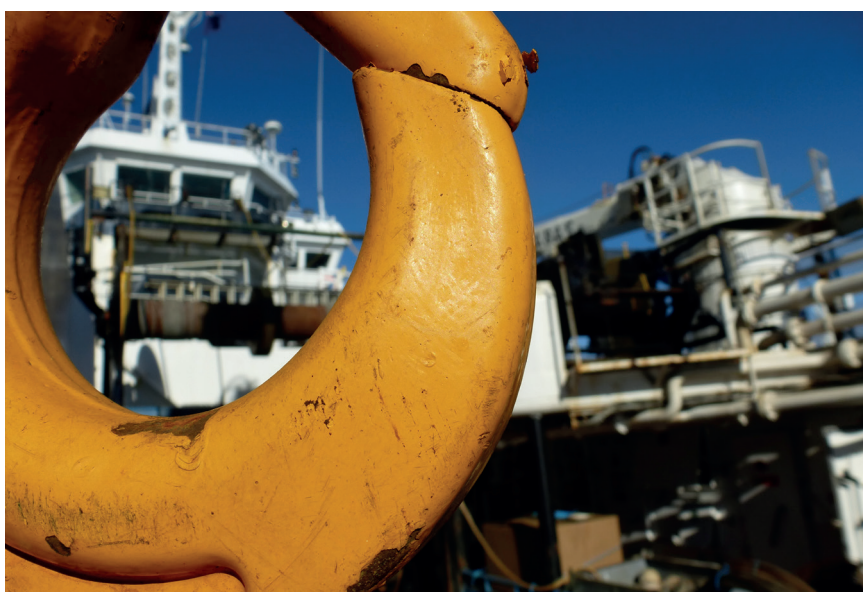
4.3 AREA 2 – NORTHWEST ATLANTIC: SCOTIAN SHELF AND NEWFOUNDLAND – LABRADOR SHELF

SCOTIAN SHELF

The continental shelf off the coast of Nova Scotia is characterized by complex topography consisting of many offshore shallow banks and deep mid-shelf basins. It is separated from the southern Newfoundland Shelf by the Laurentian Channel and borders the Gulf of Maine to the southwest. Surface circulation is dominated by a general flow towards the southwest, interrupted by clockwise movement around the banks and anticlockwise movement around the basins, with strengths varying seasonally.

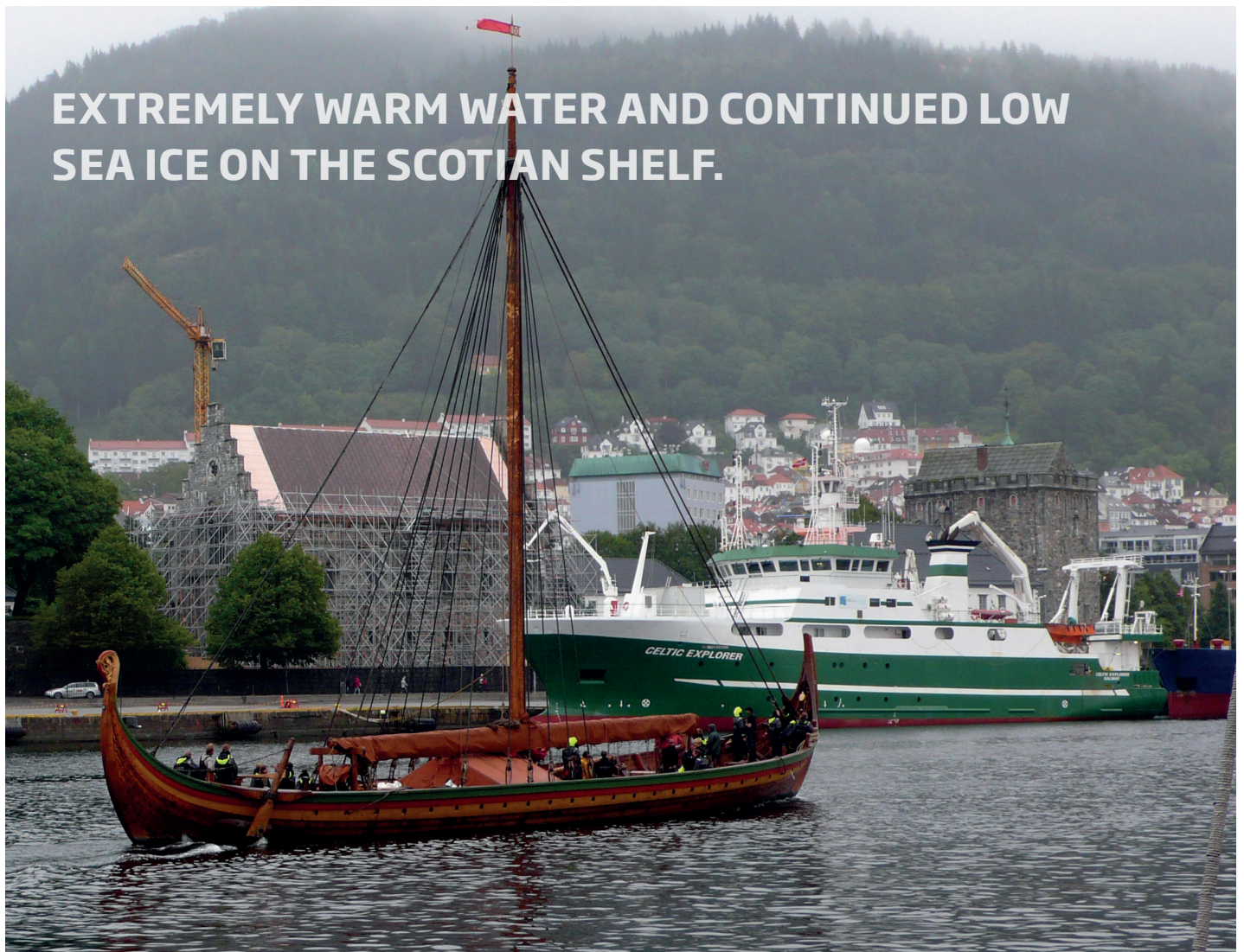
Hydrographic conditions on the Scotian Shelf are determined by heat transfer between ocean and atmosphere, inflow from the Gulf of St Lawrence and the Newfoundland Shelf, and exchange with offshore slope waters. Water properties have large seasonal cycles and are modified by freshwater runoff, precipitation, and melting of sea ice. Temperature and salinity exhibit strong horizontal and vertical gradients that are modified by diffusion, mixing, currents, and shelf topography.

In 2013, annual mean air temperature over the Scotian Shelf, represented by Sable Island observations, was $+0.8^{\circ}\text{C}$ (corresponding to $+1.1$ s.d.) above the long-term mean (1981-2010). In 2014, the annual temperature anomaly was $+1.4^{\circ}\text{C}$ ($+1.7$ s.d.) above the long-term mean. The amount of sea ice on the Scotian Shelf in 2013, as measured by the total area of ice seaward of Cabot Strait between Nova Scotia and Newfoundland in January-April, was 3900 km^2 , well below the long-term mean coverage of $32\ 000\text{ km}^2$. This is the seventh lowest coverage in the 53-year time-series. The years 2010, 2011, and 2012 had the second to fourth lowest ice coverage, respectively. In 2014, ice coverage returned to normal, rising to $34\ 400\text{ km}^2$.



Topography separates the northeast Scotian Shelf from the rest of the shelf. In the northeast, the bottom tends to be covered by relatively cold waters (1–4°C), whereas the basins in the central and southwest regions typically have bottom temperatures of 8–10°C. The origin of the latter is offshore slope waters, whereas water in the northeast comes principally from the Gulf of St Lawrence. Interannual variability of the two water masses differs.

Measurements of temperatures at 100 m at the Misaine Bank station capture changes in the northeast. They revealed average conditions in 2013 and 2014, with temperatures slightly above normal at +0.4°C (+0.6 s.d.) and +0.6°C (+1.0 s.d.) and salinities at -0.01 (-0.1 s.d.) and -0.02 (-0.2 s.d.) below normal, respectively. The deep Emerald Basin anomalies represent the slope water intrusions onto the shelf that are subsequently trapped in the inner basins. In 2013, the 250-m temperature and salinity anomalies were above normal by +0.6°C (+0.7 s.d.) and +0.18 (+1.2 s.d.), respectively. The temperature and salinity anomalies were much larger in 2014, +1.4°C (+1.7 s.d.) and +0.32 (+2.1 s.d.), respectively. Model simulations of the region showed a large flux of warm salty water from the slope region.



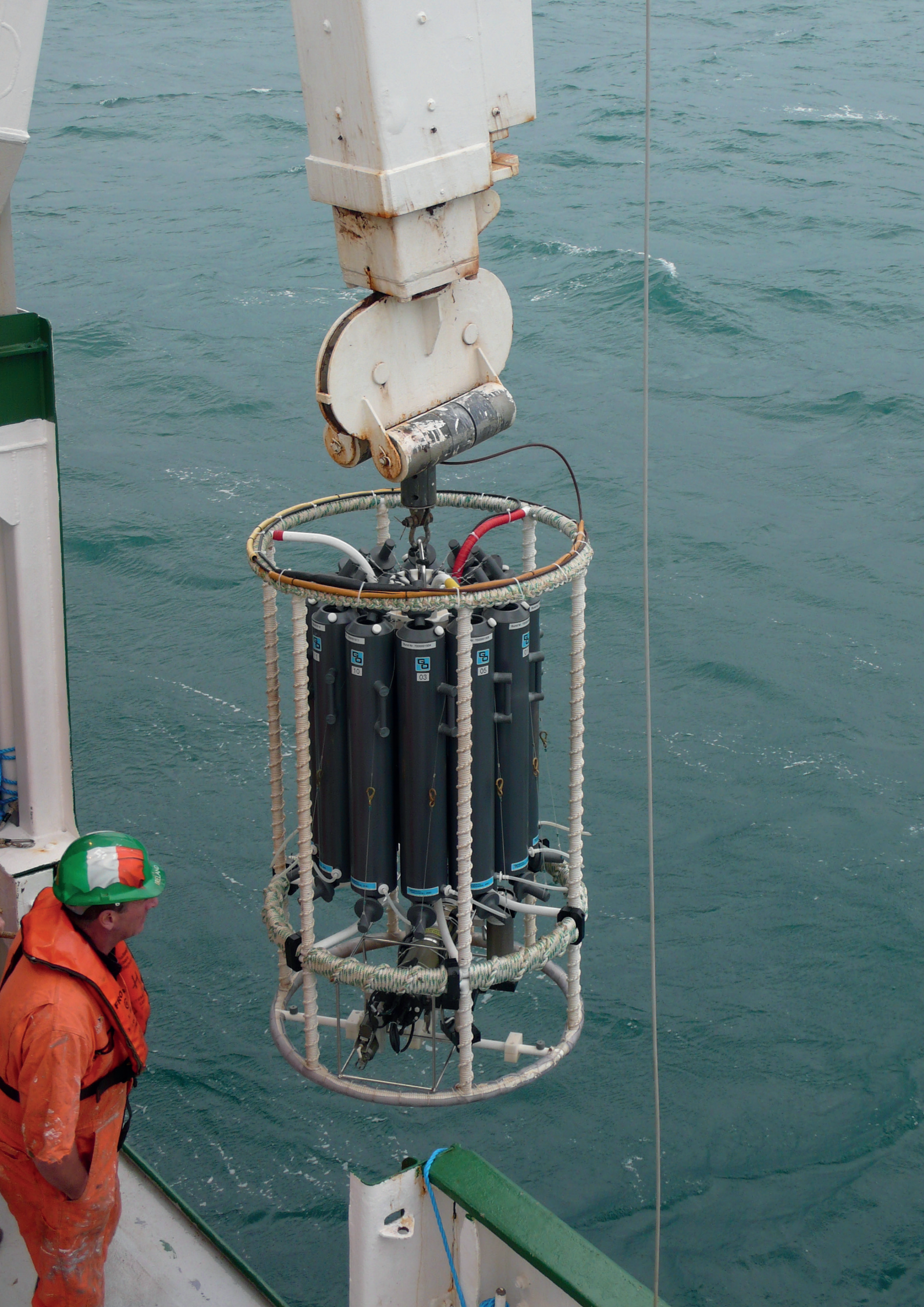
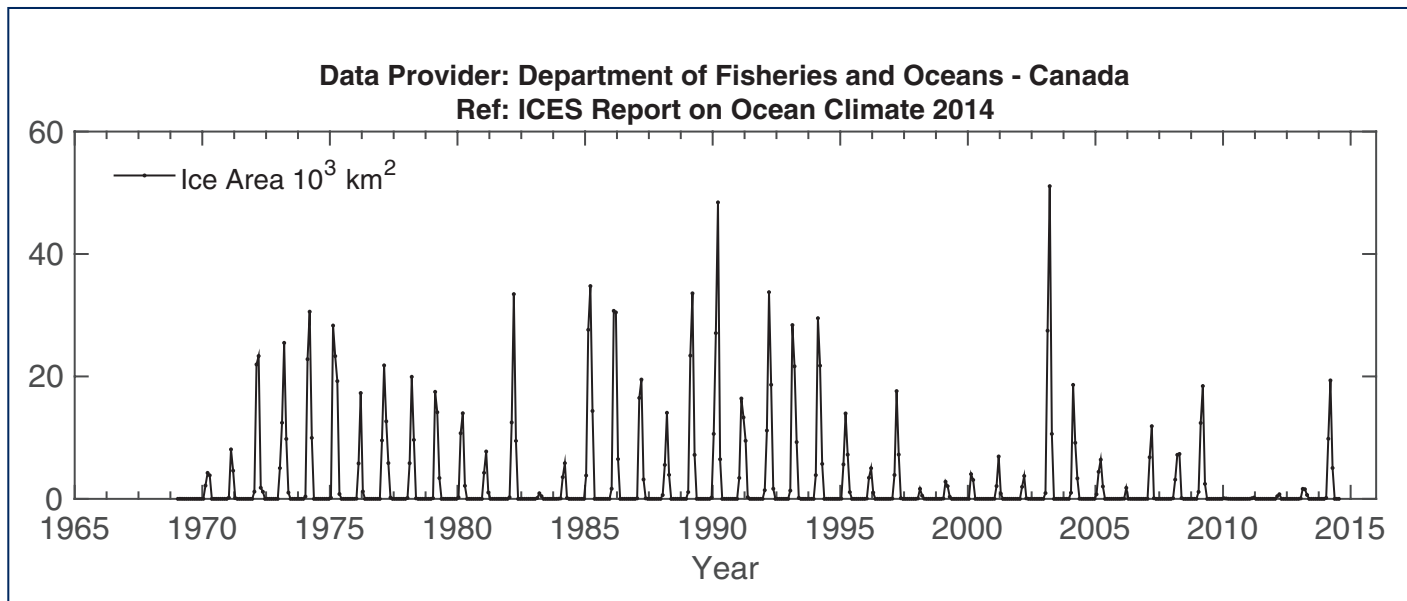


FIGURE 17



Area 2 - Northwest Atlantic: Scotian Shelf. Monthly means of ice area seaward of Cabot Strait (upper panel) and air temperature anomalies at Sable Island on the Scotian Shelf (lower panel).

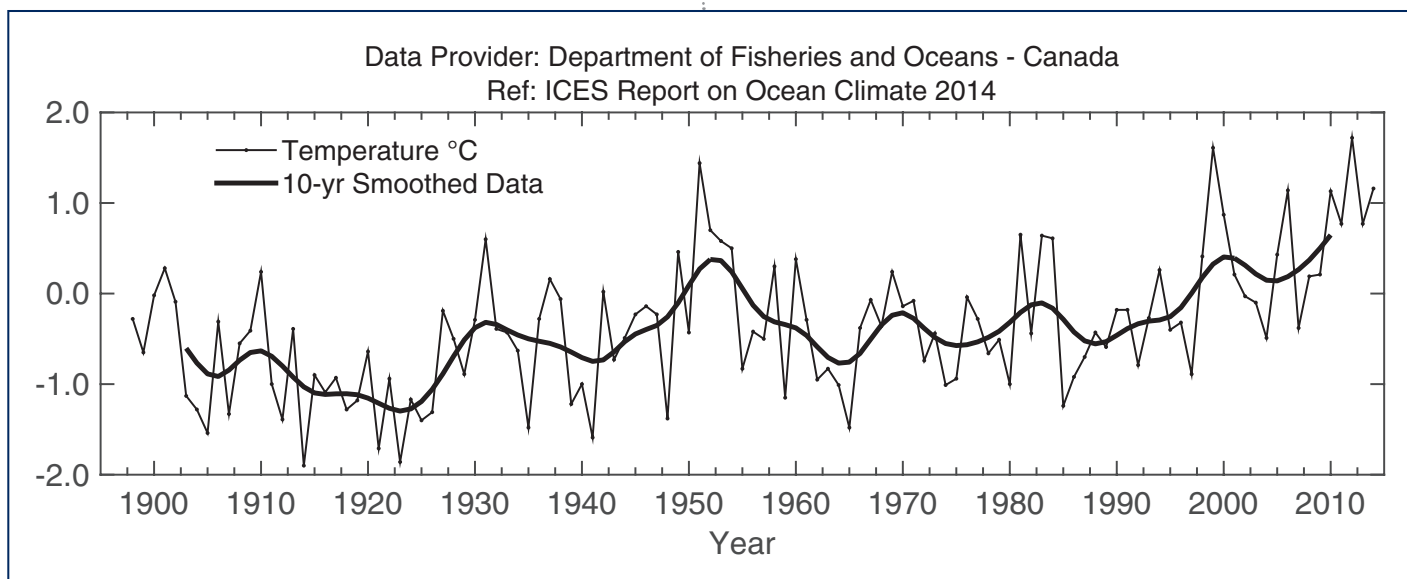
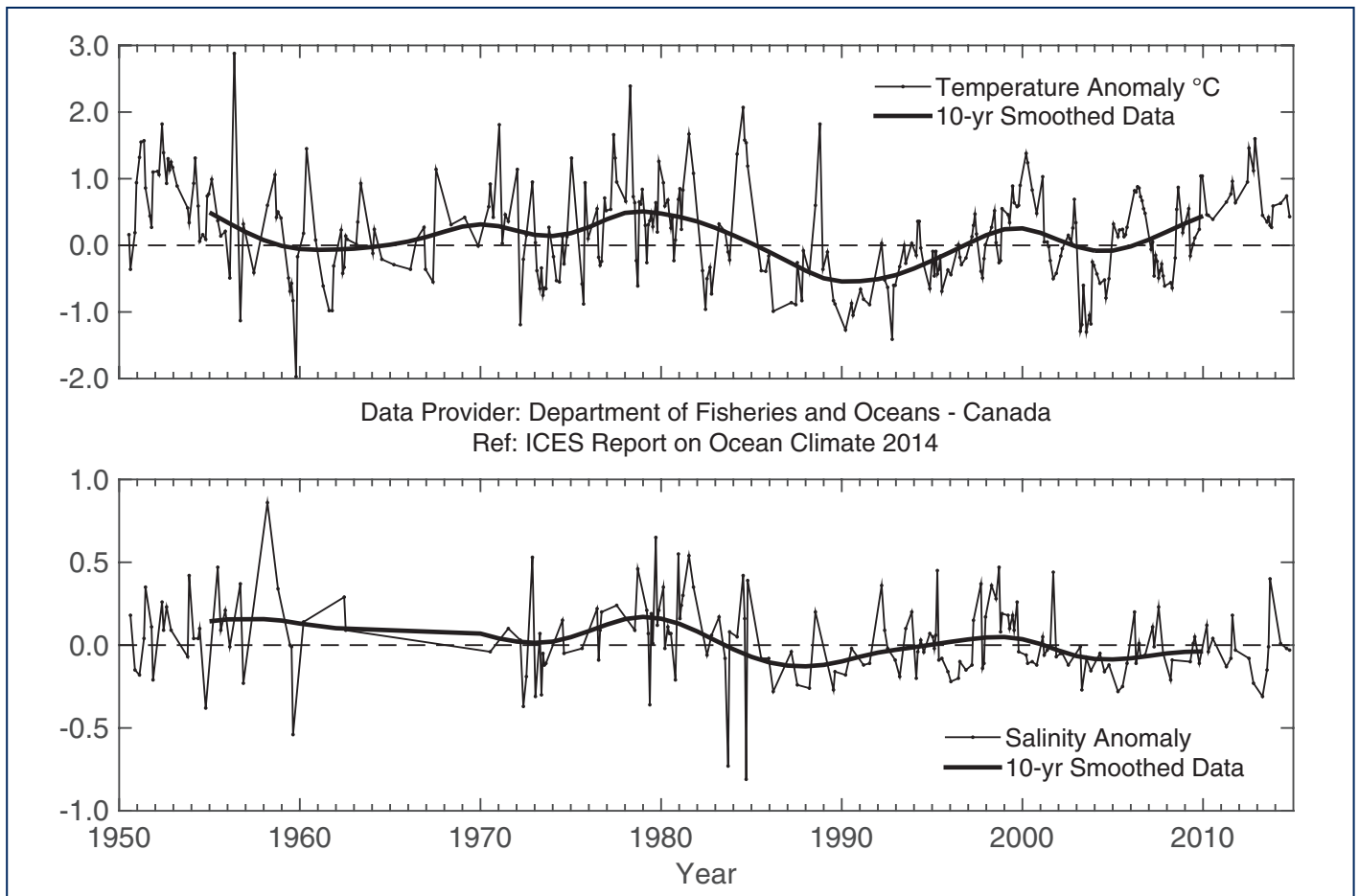


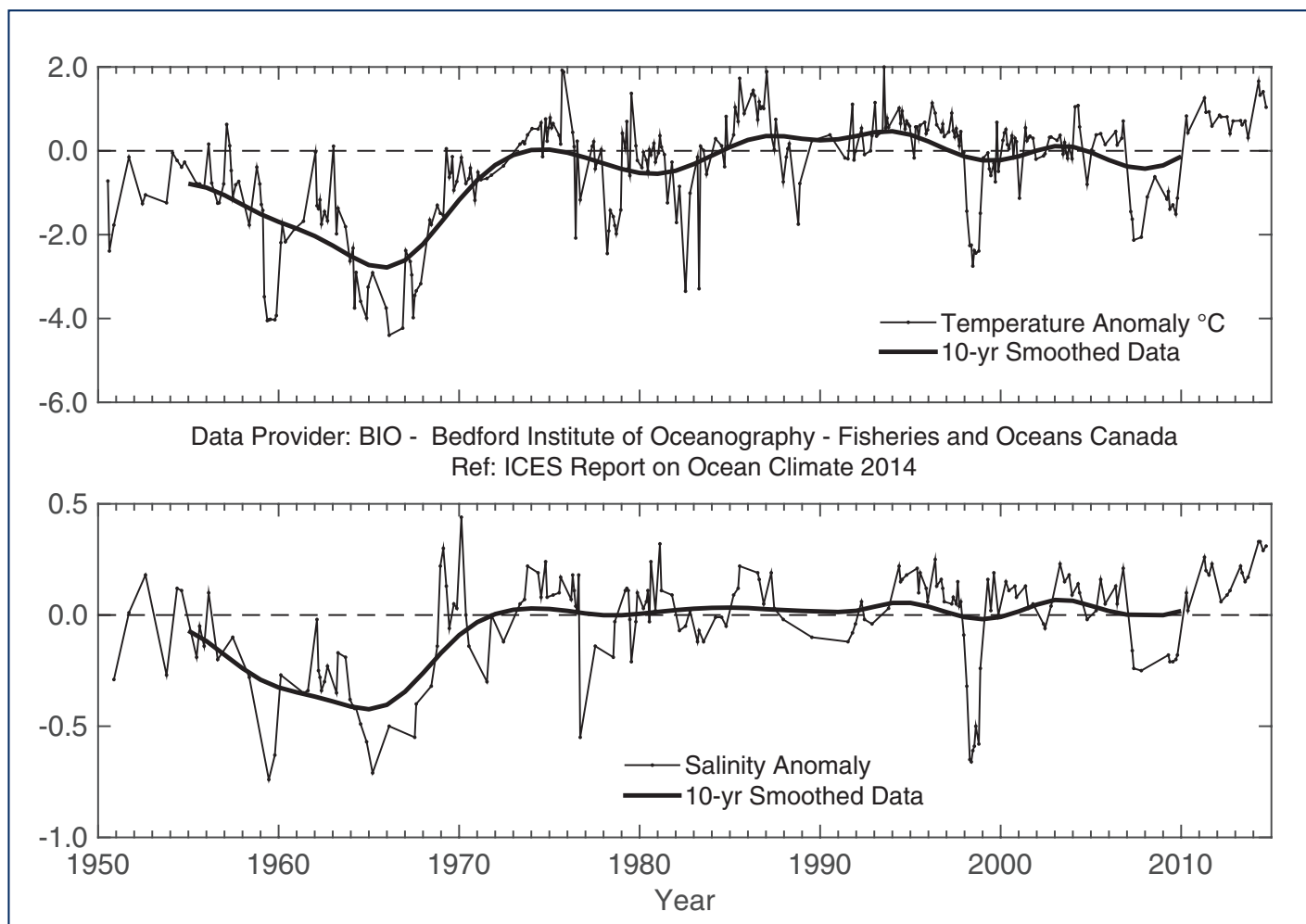
FIGURE 18



Area 2 - Northwest Atlantic: Scotian Shelf. Near-bottom temperature (upper panel) and salinity (lower panel) anomalies at Misaine Bank (100 m).



FIGURE 19



Area 2 - Northwest Atlantic: Scotian Shelf. Near-bottom temperature (upper panel) and salinity (lower panel) anomalies on the central Scotian Shelf (Emerald Basin, 250 m).

NEWFOUNDLAND – LABRADOR SHELF

This region is situated on the western side of the Labrador Sea, stretching from the Hudson Strait to the southern Grand Bank and dominated by shallow banks, cross-shelf channels or saddles, and deep marginal troughs near the coast. Circulation is dominated by the south-flowing Labrador Current, which brings cold freshwater from the north as well as sea ice and icebergs to southern areas of the Grand Banks.

Hydrographic conditions are determined in part by the strength of the winter atmospheric circulation over the Northwest Atlantic Ocean (NAO), advection by the Labrador Current, cross-shelf exchange with warmer continental slope water, and bottom topography. Superimposed are large seasonal and interannual variations in solar heat input, sea-ice cover, and storm-forced mixing. The resulting water mass on the shelf exhibits large annual cycles with strong horizontal and vertical temperature and salinity gradients.

The annual NAO index (Iceland-Azores), a key indicator of climate conditions in the Northwest Atlantic, after being in a negative phase for three of the past four years, returned to a strong positive phase at 1.3 s.d. above normal in 2014. As a result, Arctic air outflow to the Northwest Atlantic increased in most areas during winter 2014.

Annual air temperatures over Labrador decreased from 0.7°C (0.6 s.d) above normal at Cartwright in 2013 to near-normal values in 2014. Farther south at St. John's, air temperature anomalies remained above normal at +0.3°C (0.4 s.d.), but decreased from 0.7°C (0.8 s.d) in 2013. The winter sea ice extent on the Newfoundland-Labrador (NL) Shelf remained below normal (1.5 s.d.) in 2013, but increased substantially during winter 2014, with the first positive anomaly (0.4 s.d. higher than normal) observed in 16 years. As a result of these and other factors, local water temperatures on the NL Shelf in 2014 decreased significantly over 2013 values.



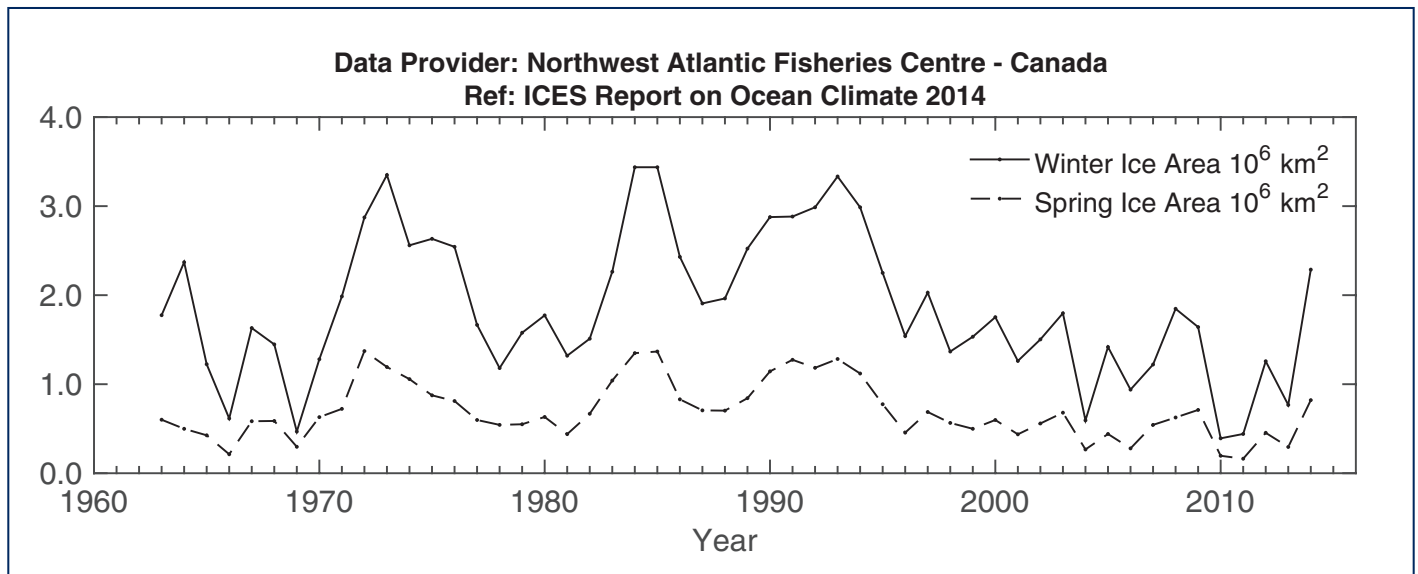
At the standard monitoring site off eastern Newfoundland (Station 27), the depth-averaged annual water temperature has experienced a decreasing trend during the past three years from the record high in 2011 when it was +1.1°C (2.8 s.d.) above normal. In 2014, it had decreased to near-normal values at -0.1°C (0.2 s.d.) down from 0.4°C (1.1 s.d.) above normal in 2013.

A robust index of ocean climate conditions in eastern Canadian waters is the extent of the cold intermediate layer (CIL) of $< 0^{\circ}\text{C}$ water overlying the continental shelf. This winter-cooled water remains isolated between the seasonally heated upper layer and the warmer shelf-slope water throughout summer and early autumn. During the 1960s, when the NAO was well below normal and had the lowest value ever in the 20th century, the volume of CIL water was at a minimum (warmer-than-normal conditions), and during the high NAO years of the early 1990s, the CIL volume reached near-record high values (colder-than-normal conditions). Since the late 1990s, as ocean temperatures have increased, the area of CIL water has experienced a downward trend that lasted until 2011. Since then, however, the CIL area has trended upward and reached its highest level since 1985 in 2014 on the Grand Bank (2.0 s.d. above normal) during spring and the highest since 1991 off eastern Newfoundland during summer (1.0 s.d. above normal).

THE AREA OF COLD INTERMEDIATE LAYER (CIL) WATER DURING SPRING 2014 WAS AT ITS HIGHEST LEVEL SINCE 1985 ON THE GRAND BANKS OF NEWFOUNDLAND.



FIGURE 20



Area 2 - Northwest Atlantic: Newfoundland-Labrador Shelf. Winter and spring sea-ice areas off Newfoundland-Labrador between 45° and 55°N (upper panel). Annual air temperature anomalies at Cartwright on the Labrador Coast (lower panel).

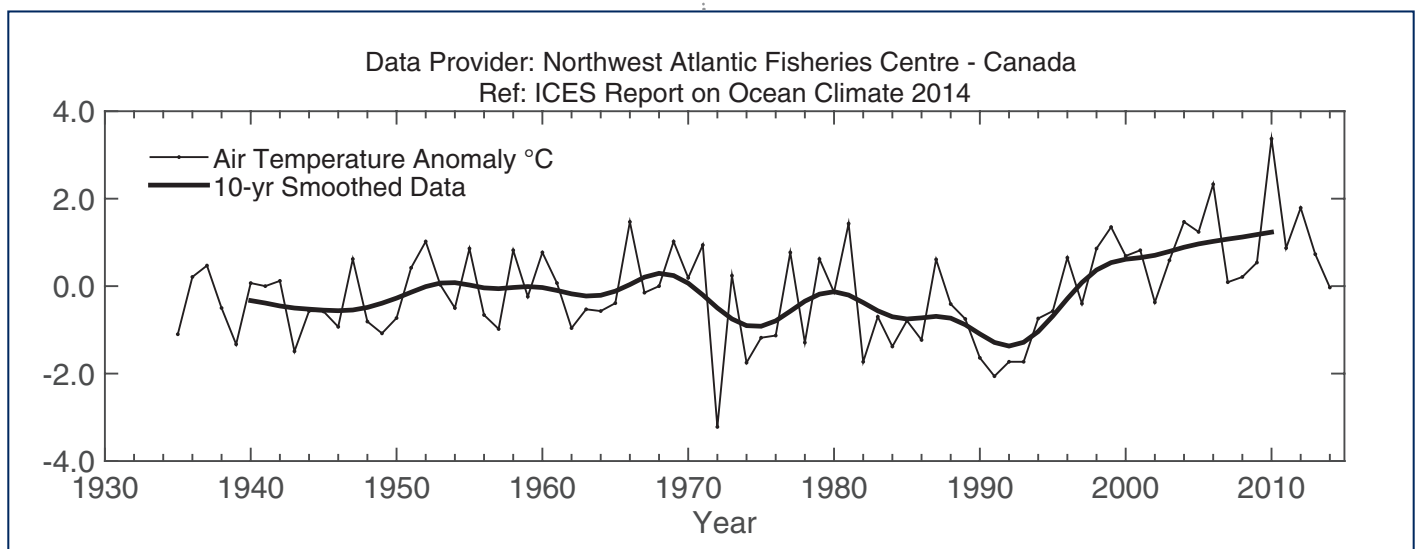
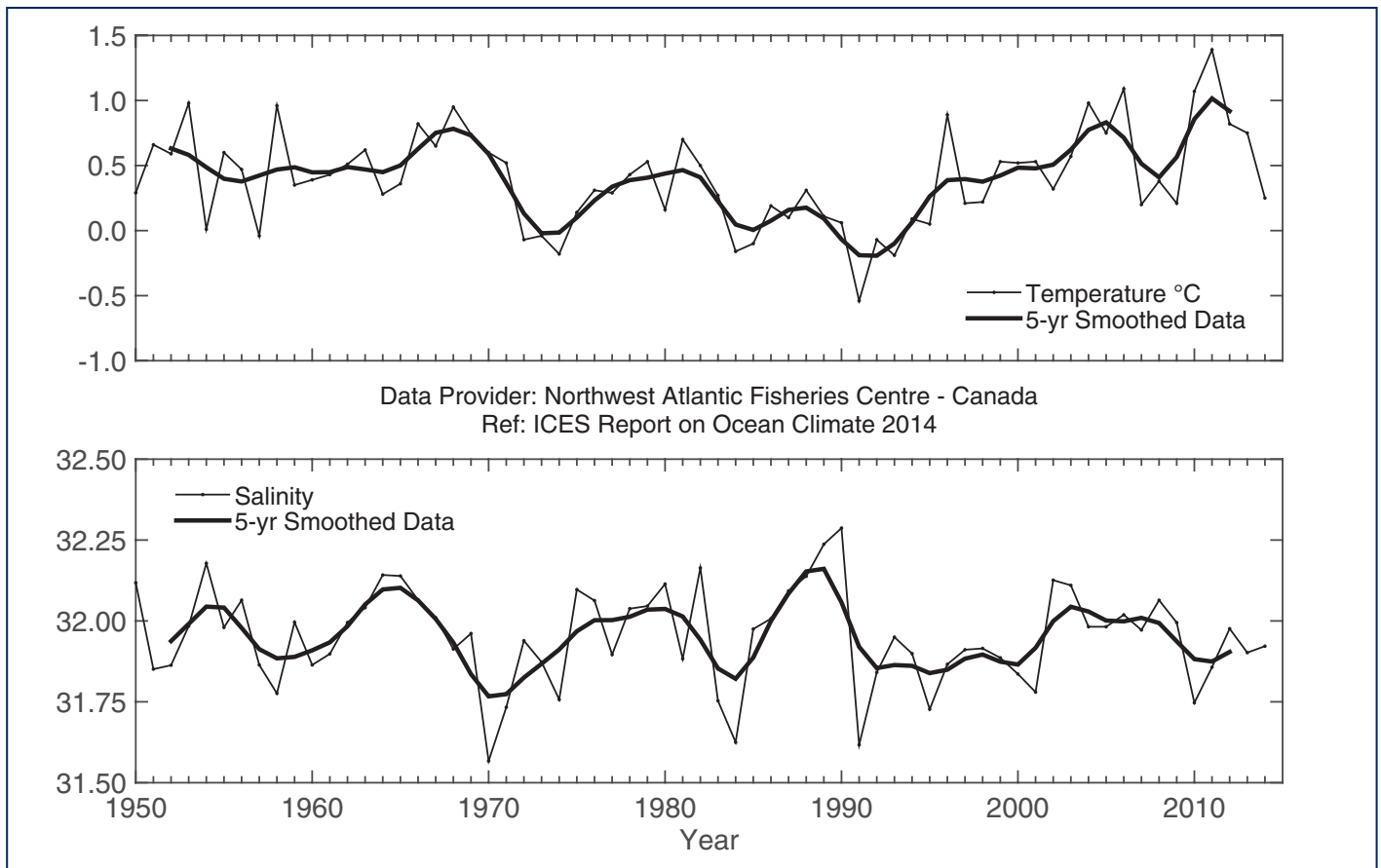
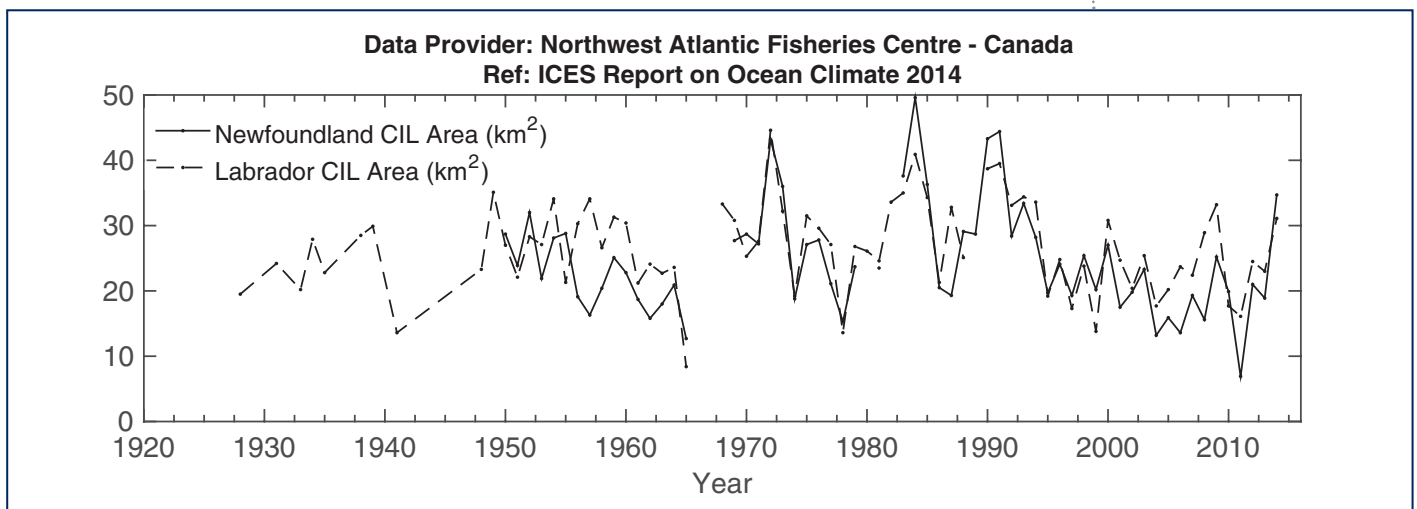


FIGURE 21



Area 2 - Northwest Atlantic: Newfoundland-Labrador Shelf. Annual depth-averaged Newfoundland Shelf temperature (top panel) and salinity (middle panel) anomalies at Station 27 (47.55°N 52.59°W), and spatial extent of cold intermediate layer (CIL; bottom panel).



4.4 AREA 2B - LABRADOR SEA

The Labrador Sea is located between Greenland and the Labrador coast of eastern Canada. Cold, low-salinity waters of polar origin circle the Labrador Sea in an anticlockwise current system that includes both the north-flowing West Greenland Current on the eastern side and the south-flowing Labrador Current on the western side. Warm and saline Atlantic waters originating in the subtropics flow north into the Labrador Sea on the Greenland side and become colder and fresher as they circulate.

Changes in Labrador Sea hydrographical conditions on interannual time-scales depend on the variable influences of heat loss to the atmosphere, heat and salt gain from Atlantic water, and freshwater gain from Arctic outflow, melting sea ice, precipitation, and run-off. A sequence of severe winters in the early 1990s led to deep convection, peaking in 1993-1994, that filled the upper 2 km of the water column with cold freshwater. Conditions have generally been milder since the mid-1990s. The upper levels of the Labrador Sea have become warmer and more saline as heat losses to the atmosphere have decreased and Atlantic waters have become increasingly dominant.

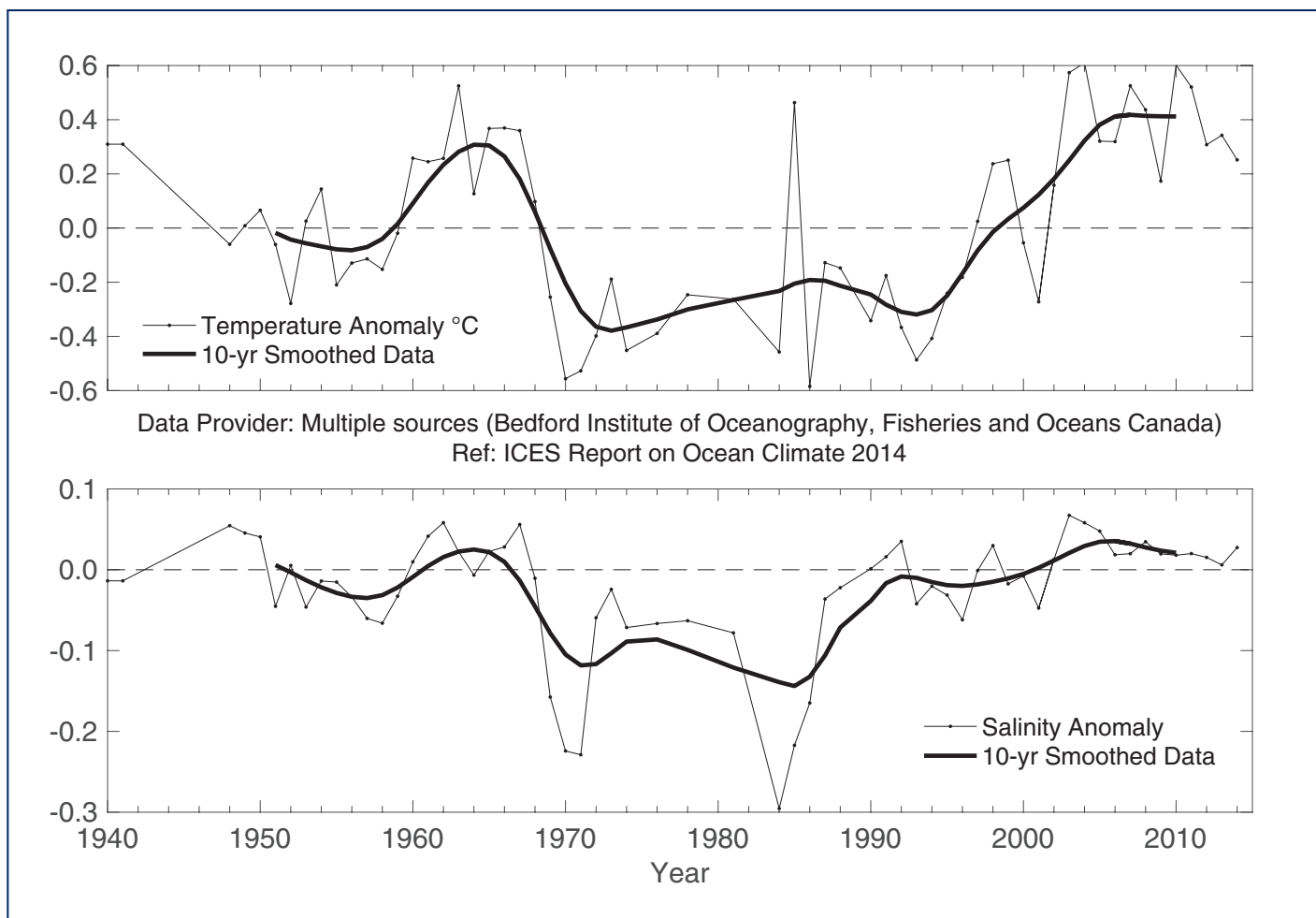
The 25th annual survey of the AR7W Line in the Labrador Sea (presently the core part of AZOMP - Atlantic Zone Off-Shelf Monitoring Program) took place on CCGS "Hudson" during 2-26 May 2014.

The National Centers for Environmental Prediction (NCEP) reanalysis of the surface air temperature indicates above-normal conditions, with an anomaly ranging between 1 and 3°C over the Labrador Sea during winter, interrupted by significant drops in temperature, while ca. -1°C below normal for most of Labrador Sea during spring, ca. 1°C above normal for summer, and with an anomaly of 0-2°C during autumn. Except in winter, sea surface temperature (SST) anomalies in the Labrador Sea mainly followed the patterns observed in air temperature: mixed SST anomalies (positive and negative) were present in winter, while positive anomalies were dominant in other seasons. Ice concentration over most of the Labrador Shelf was above normal during winter 2014 (reference period: 1979-2000). In the northern Labrador Sea, the sea ice concentration was ca. 25% below normal in January, but, interestingly, ca. 25% above normal in March.

The surface freshening observed in 2012-2013 in the central Labrador Sea was reduced and reversed in 2014. However, low-salinity anomalies were still present over the Labrador shelf and slope. The upper intermediate waters (200-1000 m) experienced significant cooling and freshening, measuring the coldest and freshest since the end of 2009 and, basin-wide, the freshest in the century.

Oceanic heat lost in winter, as shown by the NCEP and ERA-interim net heat flux anomaly over the Northwest Atlantic led to winter convection in 2014 that reached 1800 m, significantly deeper than the 1000 m observed in 2013. The deeper part of the intermediate layer, 1800-2500 m, of the central Labrador Sea has been gradually warming since the mid-1990s.

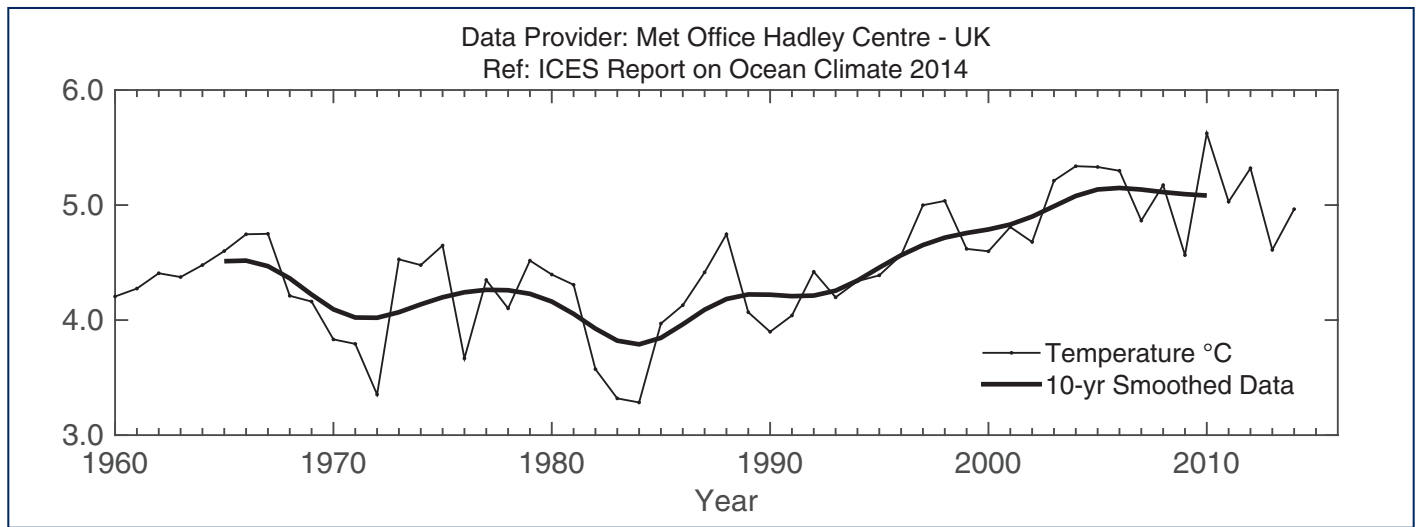
FIGURE 22



Area 2b - Labrador Sea. Potential temperature (upper panel) and salinity (lower panel) anomalies at 50–200 m from CTD and Argo data in the west-central Labrador Sea (centred at 56.7°N 52.5°W). Estimates of seasonal cycle (derived from all data in the time-series) have been removed from the observations.

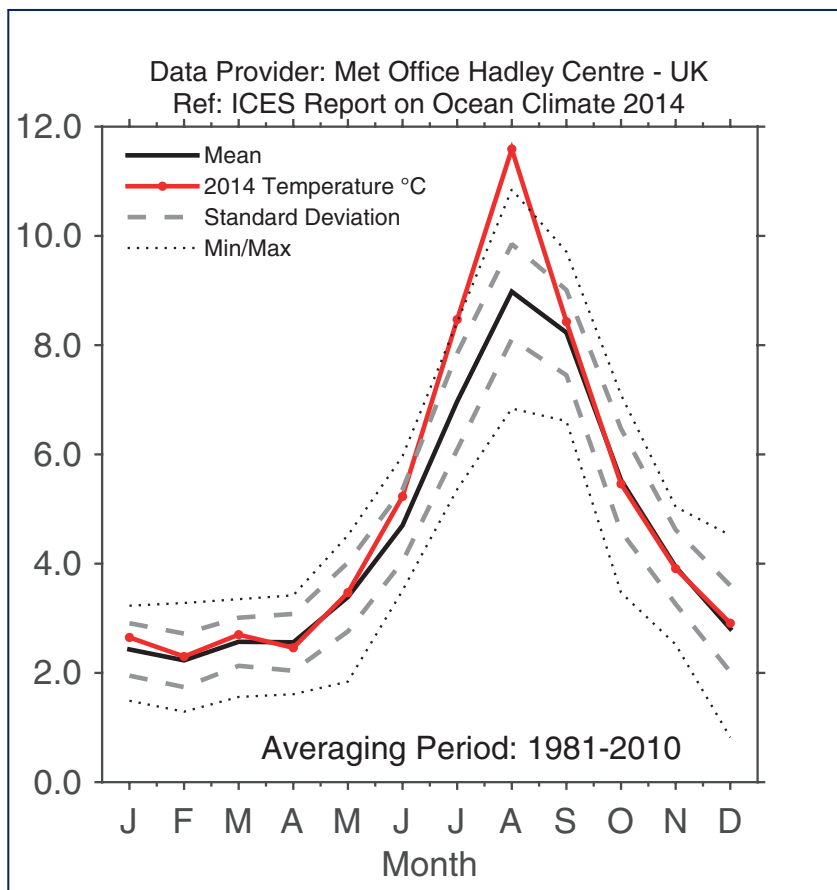


FIGURE 23



Area 2b - Labrador Sea. Annual mean sea surface temperature data from the west-central Labrador Sea (56.5°N 52.5°W). Data obtained from the HadISST1.1 sea ice and sea surface temperature dataset, UK Meteorological Office, Hadley Centre.

FIGURE 24



Area 2b - Labrador Sea. Monthly average (1971-2000) seasonal cycle with 2014 monthly sea surface temperature from the west-central Labrador Sea (3° × 3° area centred on 56.5°N 52.5°W). Data obtained from the HadISST1.1 sea ice and sea surface temperature dataset, UK Meteorological Office, Hadley Centre.

4.5 AREA 2C – MID-ATLANTIC BIGHT

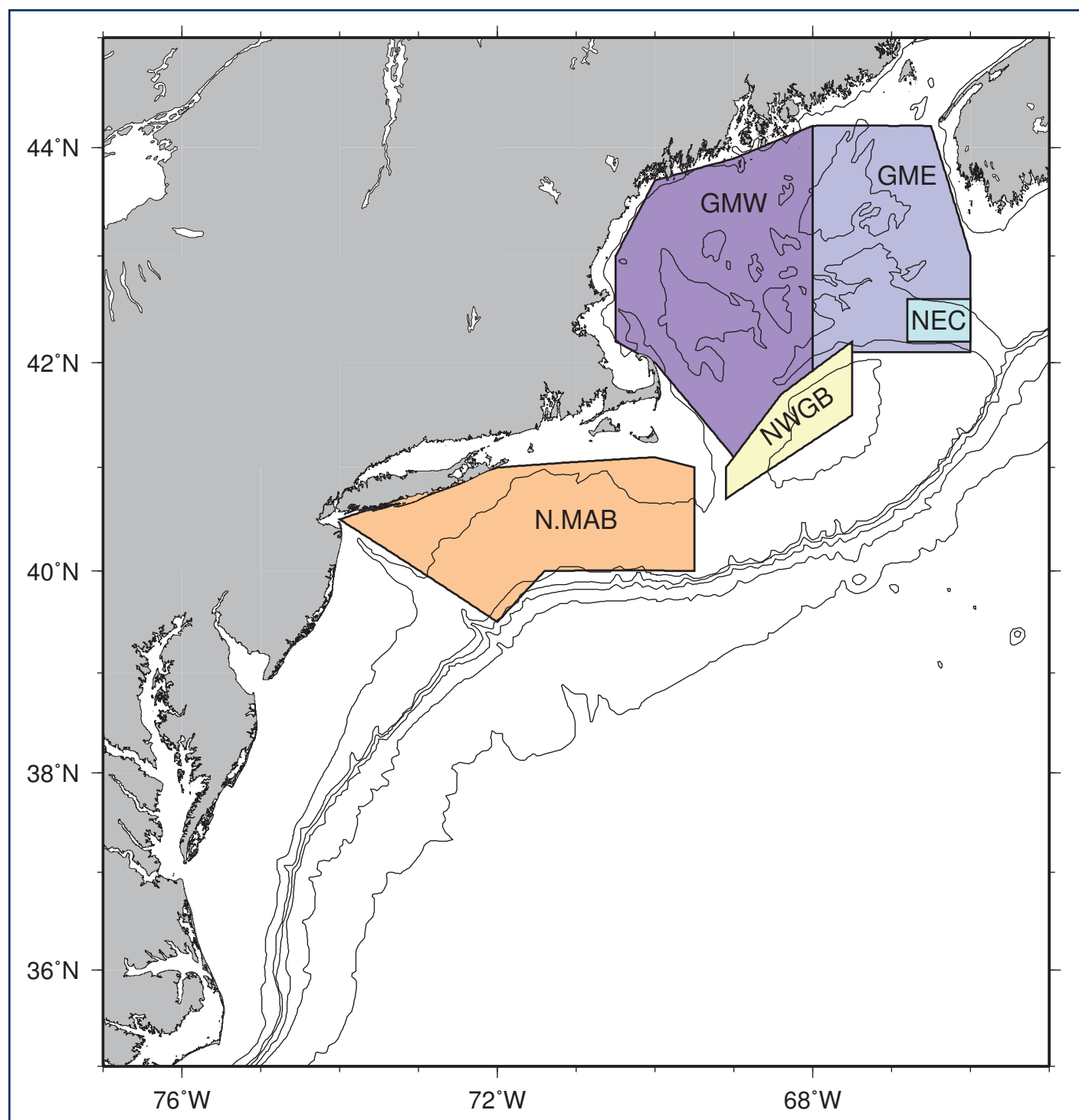
Hydrographic conditions in the western North Atlantic slope sea, the Mid-Atlantic Bight, and the Gulf of Maine depend on the supply of water from the Labrador Sea, along the shelf and continental slope, as well as the Gulf Stream offshore. Shelf-wide hydrographic conditions have been monitored annually since 1977 as part of quarterly ecosystem monitoring and twice-yearly bottom-trawl surveys conducted by the US National Marine Fisheries Service, Northeast Fisheries Science Center. The surveys extend from Cape Hatteras into the Gulf of Maine, including Georges Bank and the Northeast Channel. Until 2014, commercial vessels were instrumented and used to regularly monitor temperature and surface salinity along two repeat cross-shelf transects: one crossing the Gulf Stream east of New York City and the other crossing the Gulf of Maine. This is the first year since 1961 that temperature data from these sections were not available due to programmatic budget cuts.

Observations indicate that the entire Northeast US shelf was warmer and more saline in 2014 than the mean for the period 1981–2010. Annually, temperatures at depths 0–30 m were ca. 1°C warmer than normal everywhere, with the largest anomalies observed in the eastern Gulf of Maine. Seasonally, warming was most pronounced during late summer to early autumn. Upper-level (0–30 m) water was anomalously salty, with the largest annual anomalies observed in the Mid-Atlantic Bight. Extreme temperature anomalies observed during summer/autumn coincided with extremes in salinity as well, particularly in the Mid-Atlantic Bight. Extreme conditions observed during summer/autumn were caused by a procession of Gulf Stream warm-core rings, whose interaction with the topography at the shelf break drove an incursion of slope water onto the inner shelf between spring and autumn 2014.

Temperature and salinity anomalies derived from hydrographic observations collected within the deep layer (150–200 m) in the Northeast Channel indicate that deep inflow to the Gulf of Maine remained warmer and saltier in 2014 than the long-term mean. These deep waters are uninfluenced by seasonal atmospheric forcing and represent deep inflow conditions for one of the dominant water mass sources to the Gulf of Maine (the slope waters).

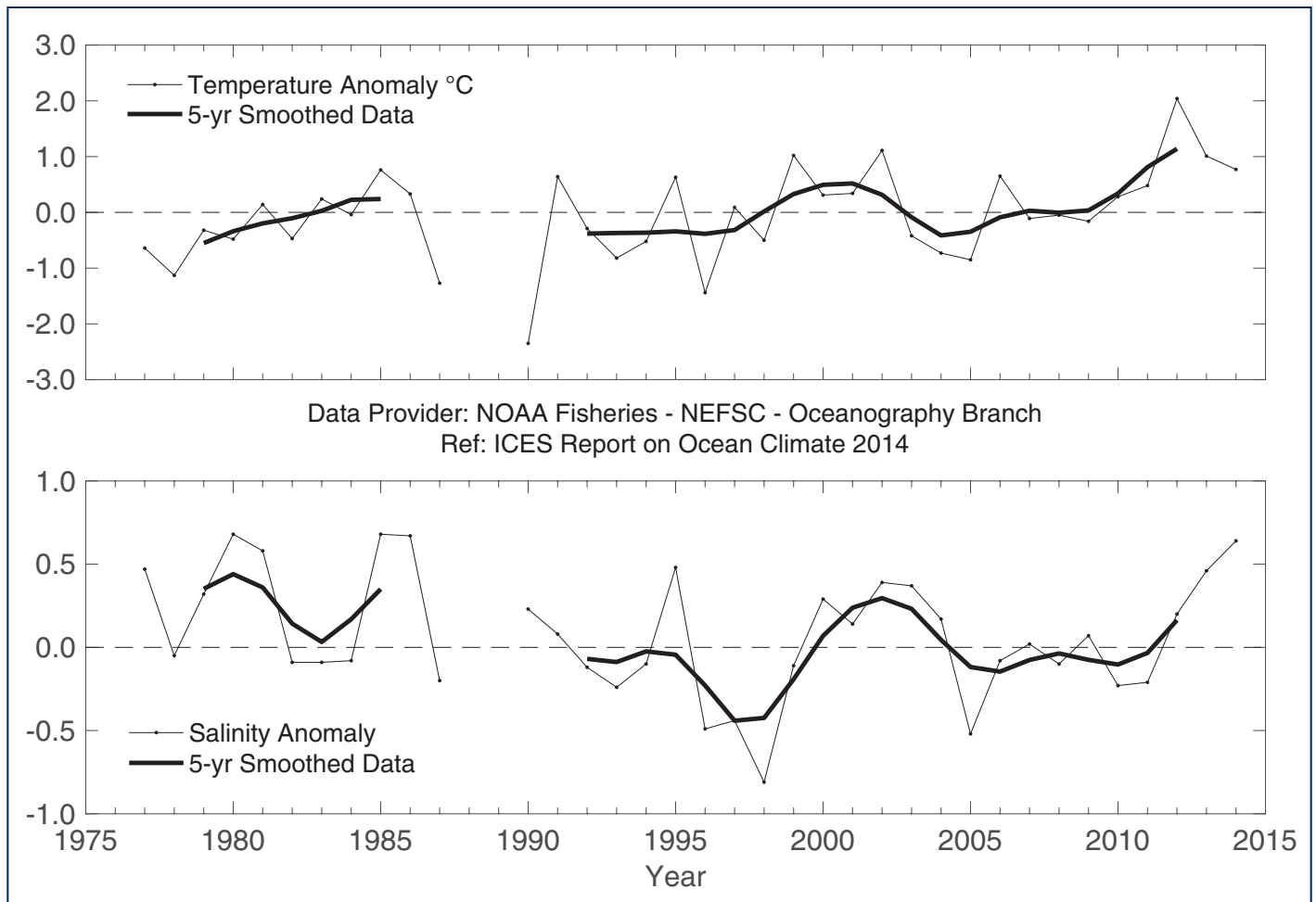


FIGURE 25



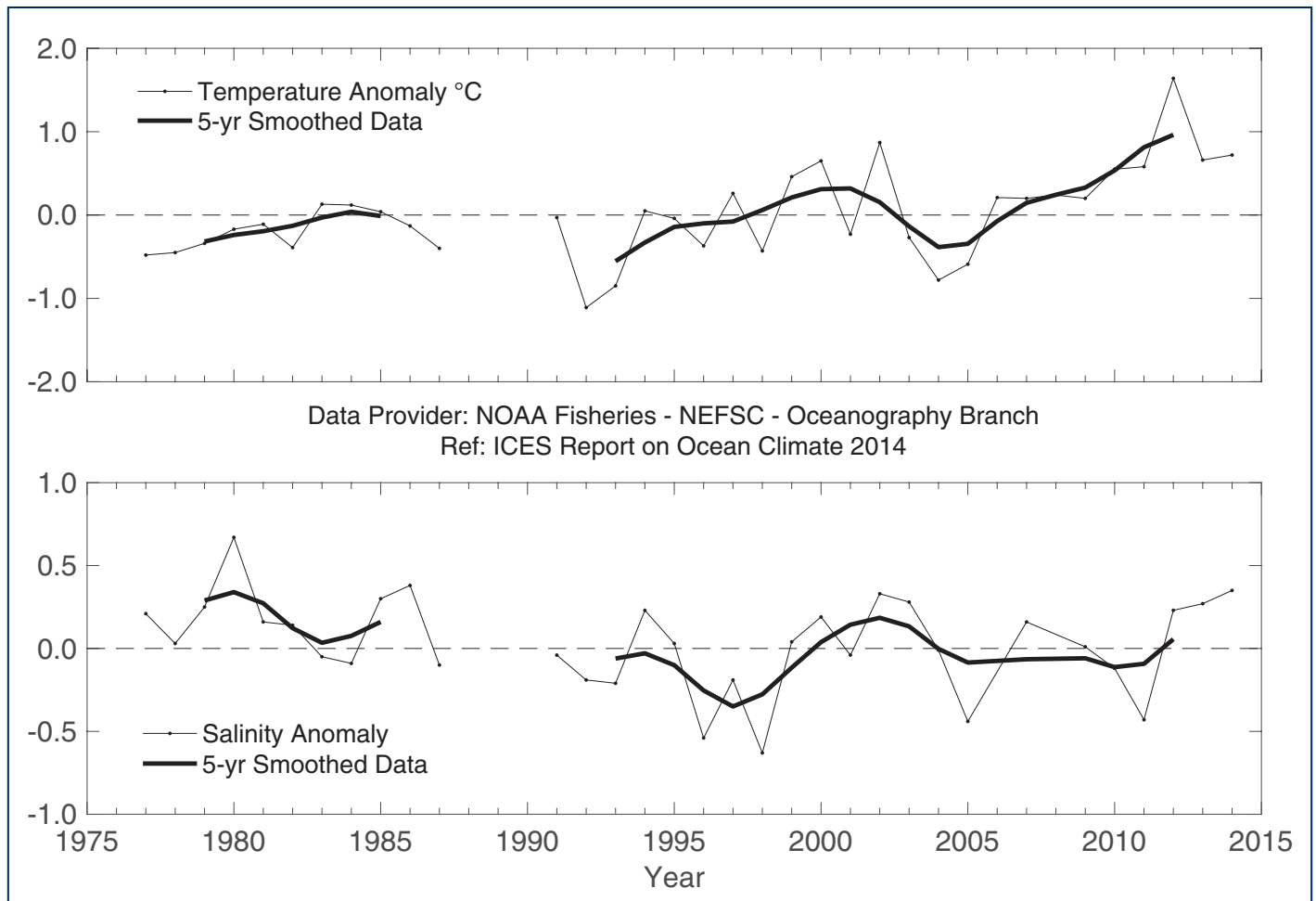
Area 2c - Mid-Atlantic Bight (MAB). The five regions within which CTD observations are used to compute regional average time-series: eastern and western GM = Gulf of Maine; northern MAB; NEC = Northeast Channel; NWGB = Northwest Georges Bank. The 50, 100, 500, 1000, 2000, and 3000 m isobaths are also shown.

FIGURE 26



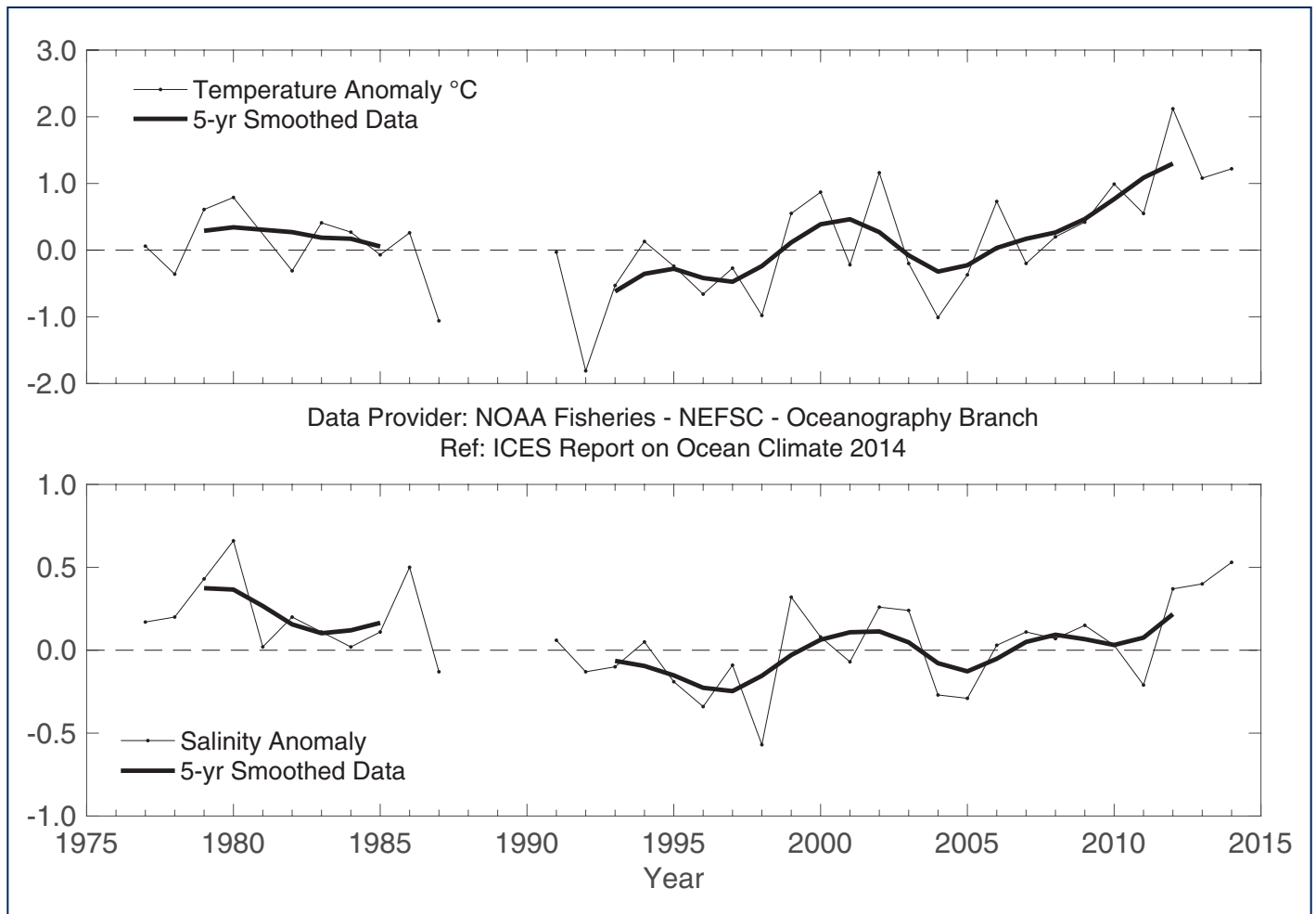
Area 2c - Mid-Atlantic Bight. Time-series plots of 0-30 m averaged temperature anomaly (upper panel) and salinity anomaly (lower panel) in the region between Hudson Canyon and Cape Cod, Massachusetts. Anomalies are calculated relative to 1981-2010, using hydrographic data from shelf-wide surveys.

FIGURE 27



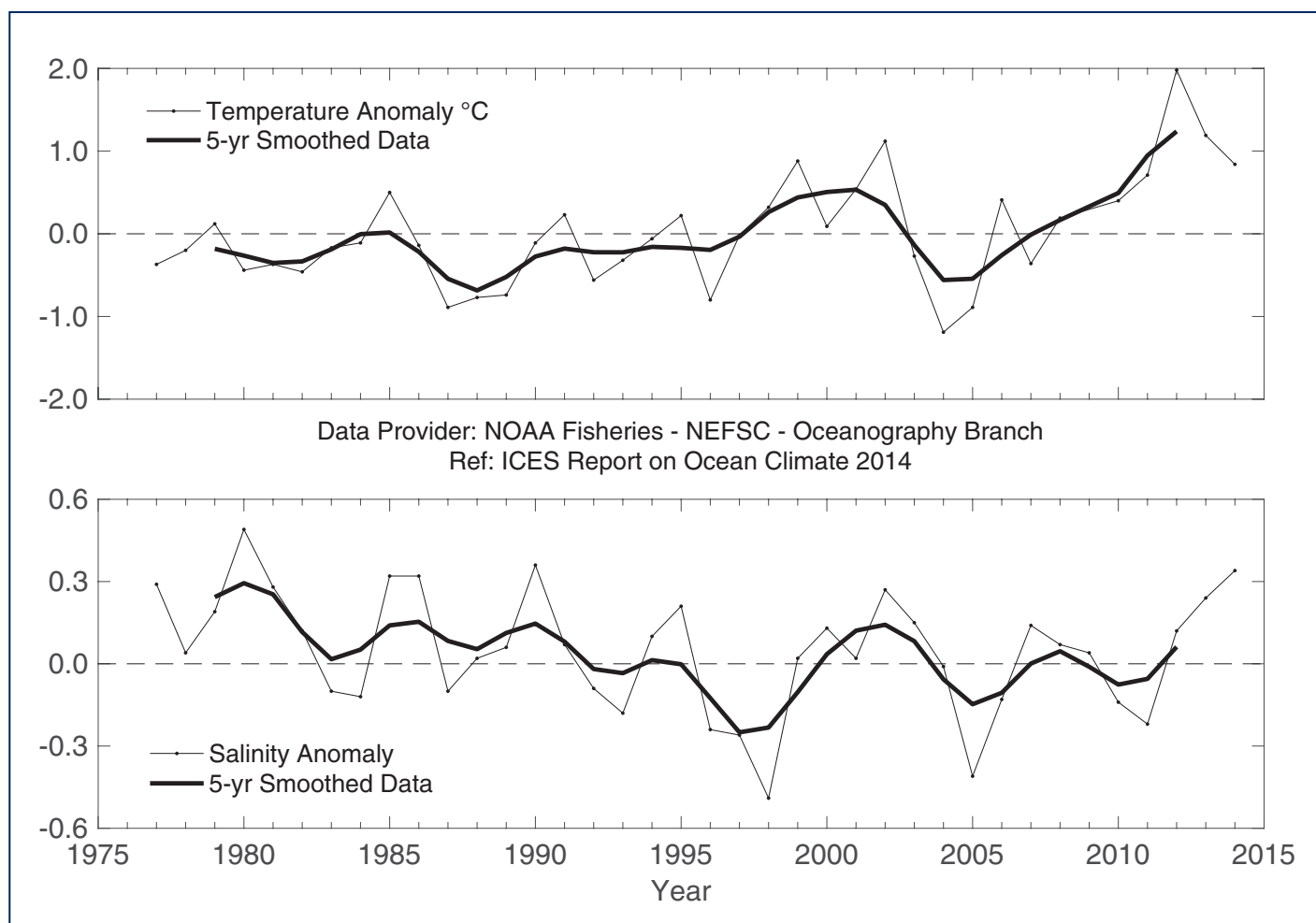
Area 2c - Mid-Atlantic Bight. Time-series plots of 0-30 m averaged temperature anomaly (upper panel) and salinity anomaly (lower panel) in the western Gulf of Maine. Anomalies are calculated relative to 1981-2010, using hydrographic data from shelf-wide surveys.

FIGURE 28



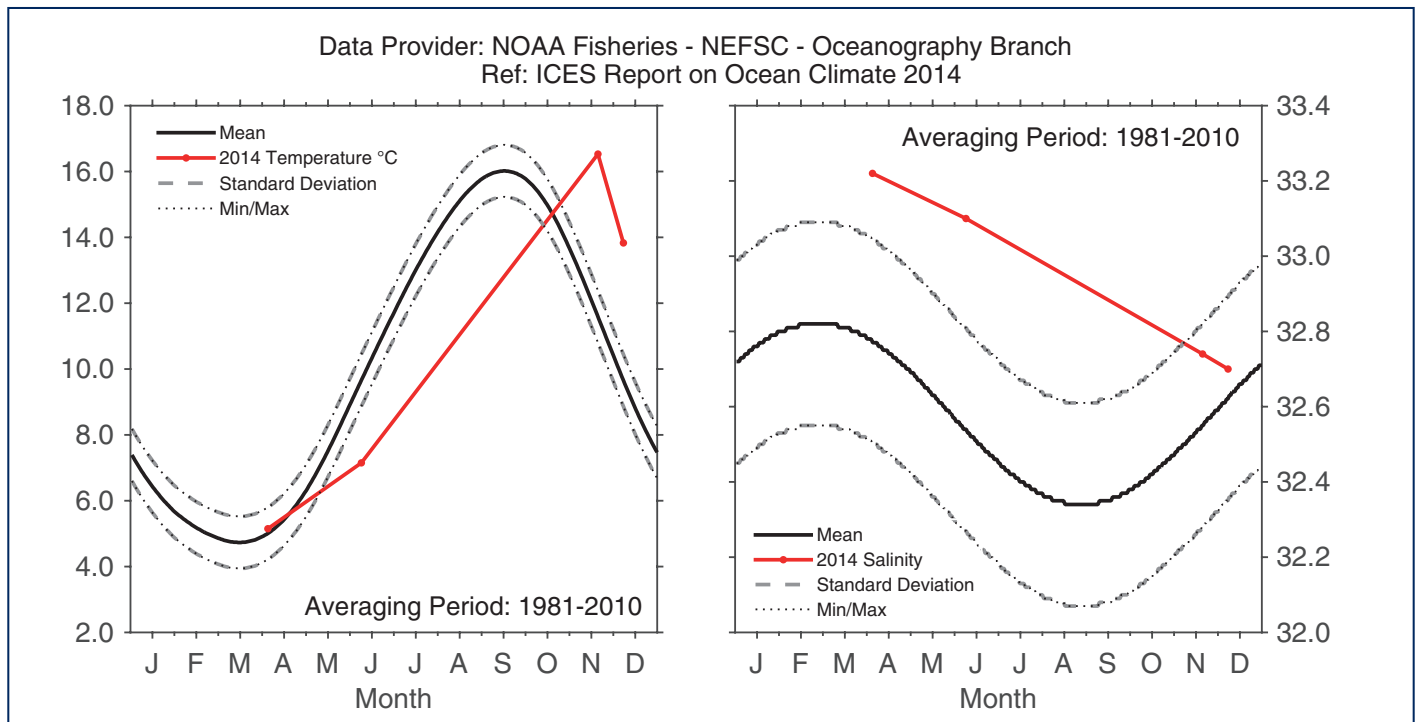
Area 2c - Mid-Atlantic Bight. Time-series plots of 0-30 m averaged temperature anomaly (upper panel) and salinity anomaly (lower panel) in the eastern Gulf of Maine. Anomalies are calculated relative to 1981-2010, using hydrographic data from shelf-wide surveys.

FIGURE 29



Area 2c - Mid-Atlantic Bight. Time-series plots of 0–30 m averaged temperature anomaly (upper panel) and salinity anomaly (lower panel) on the northwestern Georges Bank. Anomalies are calculated relative to 1981–2010, using hydrographic data from shelf-wide surveys.

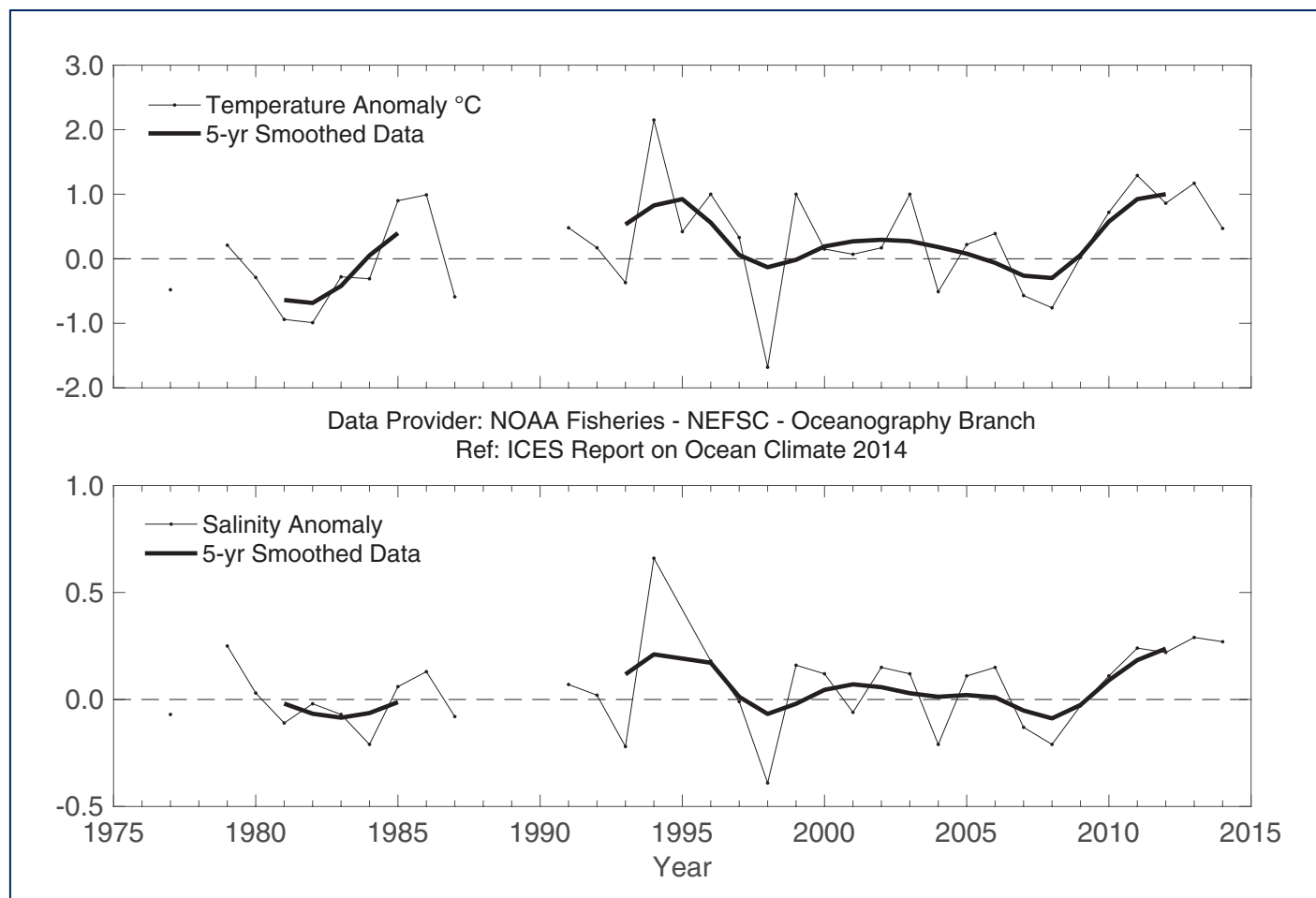
FIGURE 30



Area 2c - Mid-Atlantic Bight. 2014 temperature (left) and salinity (right) averaged over 0-30 m on the northwestern Georges Bank, relative to the annual cycle calculated for 1981-2010. The envelope corresponding to the monthly range and 1 s.d. are shown.



FIGURE 31



Area 2c - Mid-Atlantic Bight. Time-series plots of 150-200 m averaged temperature anomaly (upper panel) and salinity anomaly (lower panel) in the Northeast Channel. Anomalies are calculated relative to 1981-2010, using hydrographic data from shelf-wide surveys.

4.6 AREA 3 – ICELANDIC WATERS

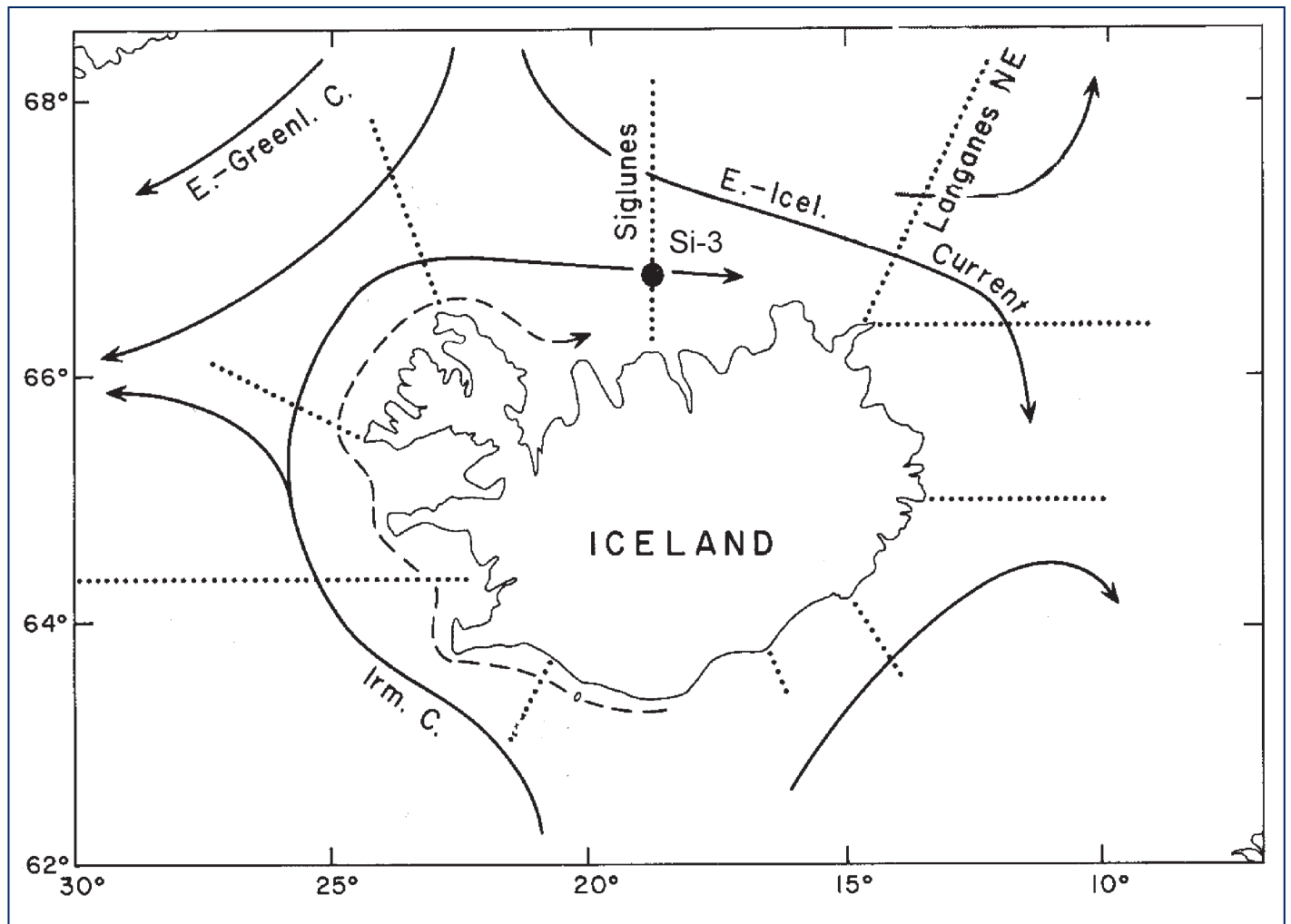
Iceland is at the meeting place of warm and cold currents which converge in an area of submarine ridges (Greenland-Scotland Ridge, Reykjanes Ridge, Kolbeinsey Ridge) that form natural barriers to the main ocean currents. The warm Irminger Current (6–8°C), a branch of the North Atlantic Current, flows from the south, and the cold East Greenland and East Icelandic currents (–1° to 2°C) flow from the north. Deep and bottom currents in the seas around Iceland are principally the overflow of cold water from the Nordic seas and the Arctic Ocean over the submarine ridges into the North Atlantic.

Hydrographic conditions in Icelandic waters are generally closely related to atmospheric or climatic conditions in and over the country and the surrounding seas, mainly through the Icelandic low-pressure and Greenland high-pressure systems. These conditions in the atmosphere and the surrounding seas affect biological conditions, expressed through the oceanic food chain, including recruitment and abundance of commercially important fish stocks.

In 2013, mean air temperatures in the south (Reykjavik) and north (Akureyri) were slightly above the long-term average, but in 2014, both were well above. Temperature in the Atlantic water from the south was lower than previous years, whilst above the long-term mean; salinity was lower in 2013 and 2014 than in the previous fifteen years. Salinity and temperature in the East Icelandic Current in spring 2013 and 2014 were both above average. North of Iceland in 2013, upper-layer temperatures were near the long-term mean, and in spring and summer 2014, temperatures were among the highest observed in the last 40 years. Salinity was slightly above the long-term mean in 2013 and further increased in 2014.

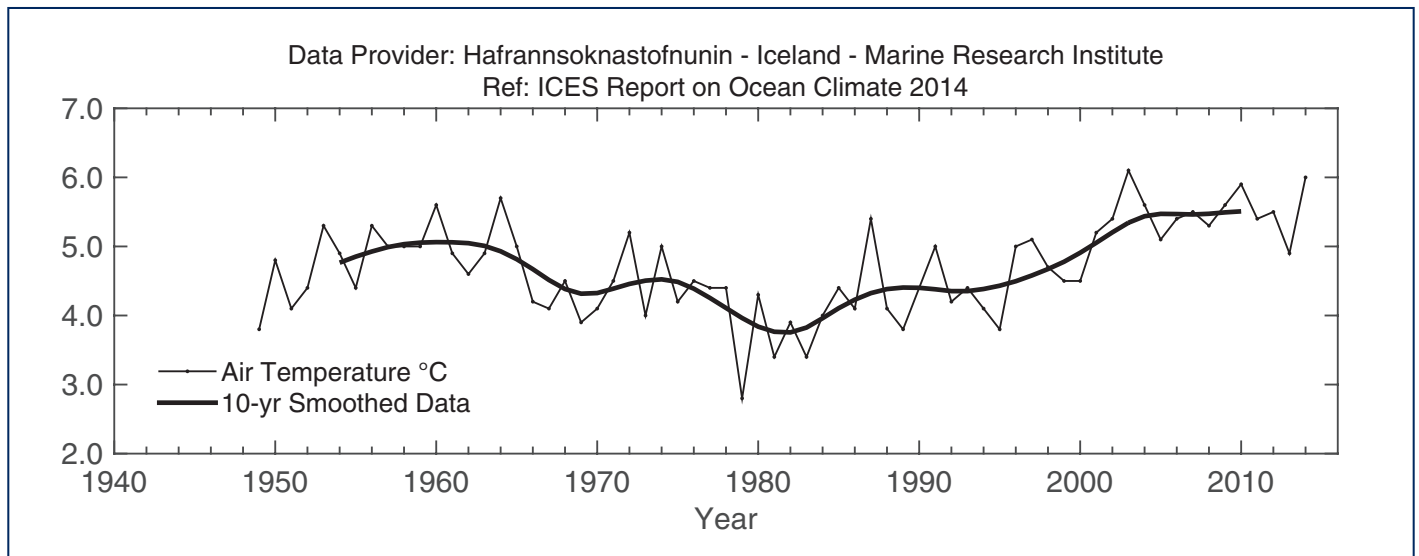


FIGURE 32



Area 3 - Icelandic waters. Main currents and location of standard sections.

FIGURE 33



Area 3 - Icelandic waters. Mean annual air temperature at Reykjavík (upper panel) and Akureyri (lower panel).

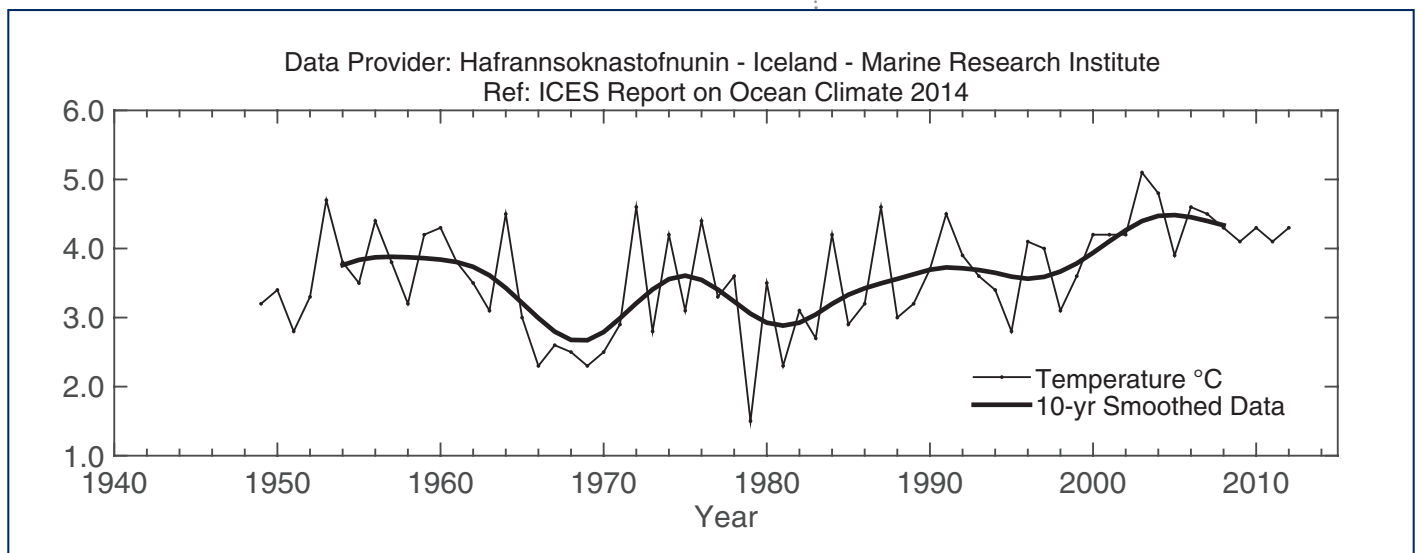
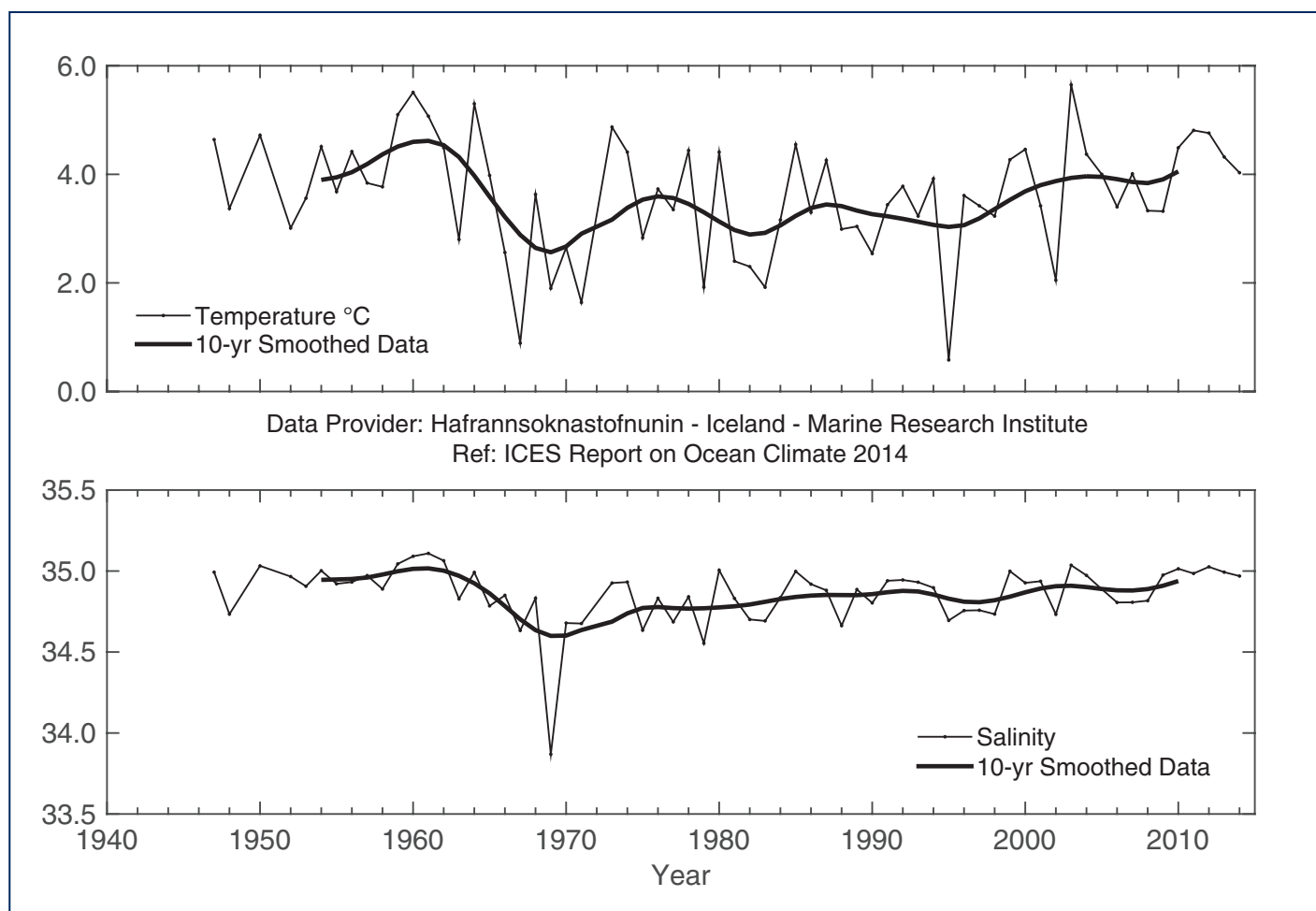
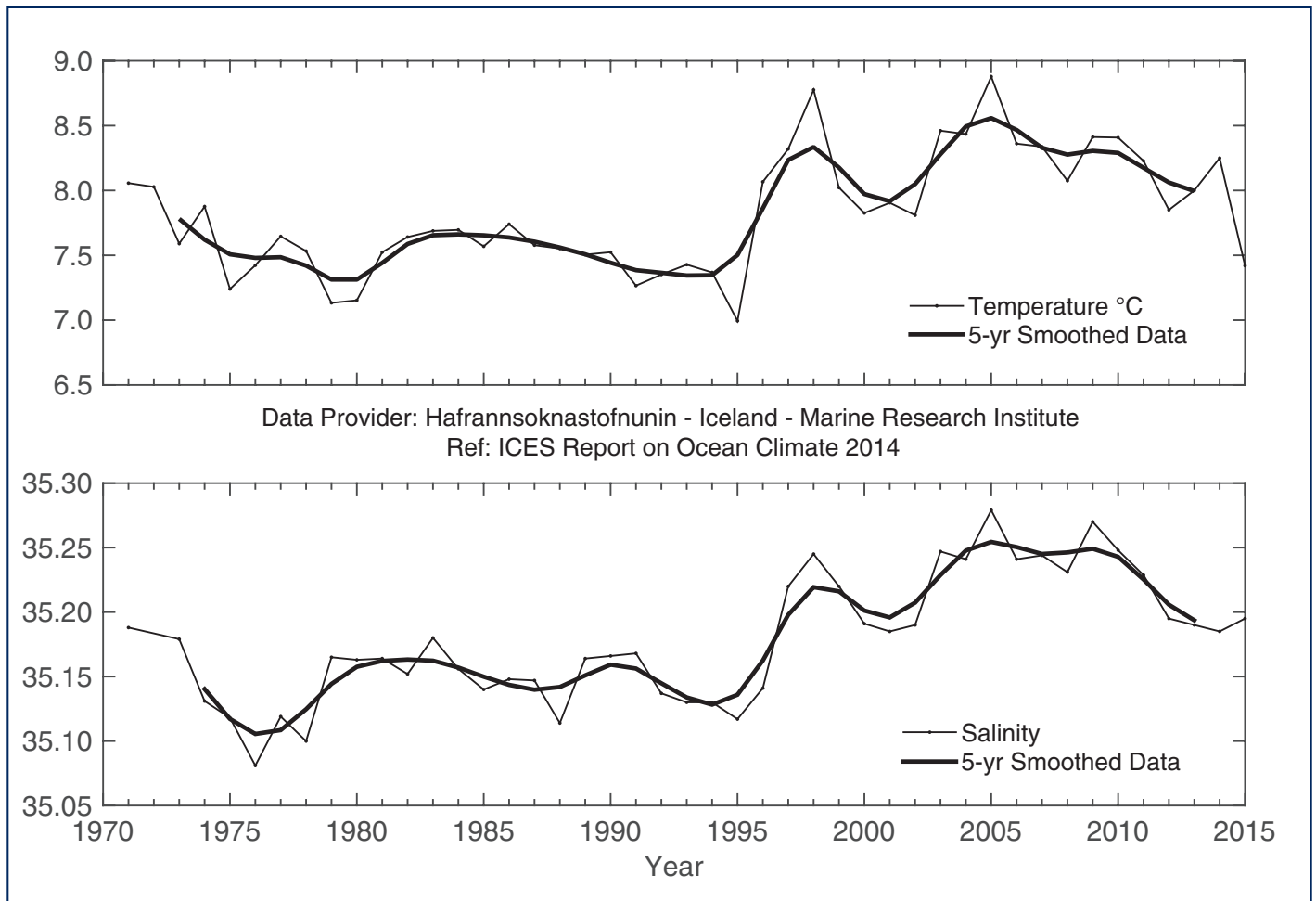


FIGURE 34



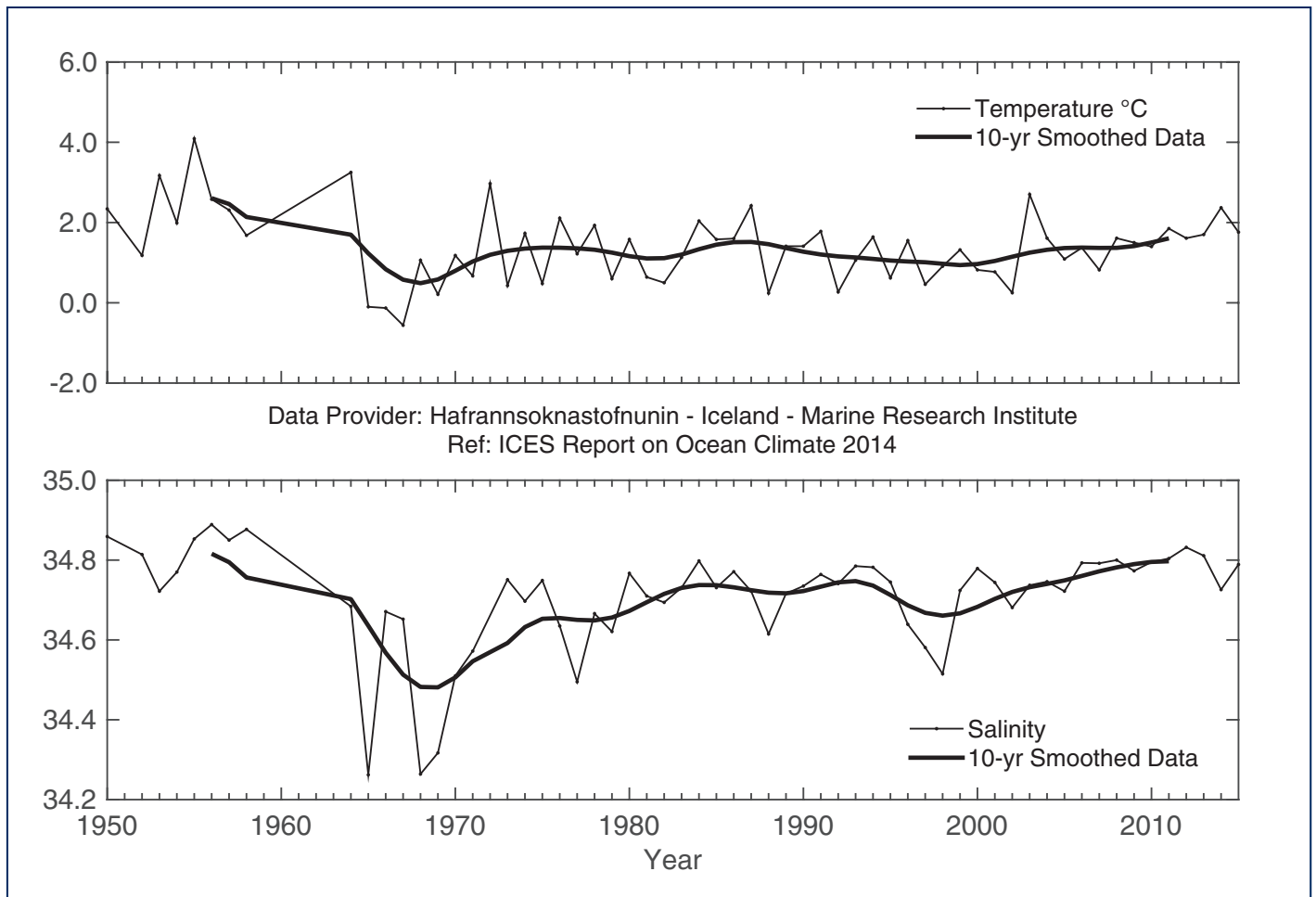
Area 3 - Icelandic waters. Temperature (upper panel) and salinity (lower panel) at 50-150 m at Siglunes Stations 2-4 in North Icelandic waters.

FIGURE 35



Area 3 - Icelandic waters. Temperature (upper panel) and salinity (lower panel) at 0-200 m at Selvogsbanki Station 5 in South Icelandic waters.

FIGURE 36



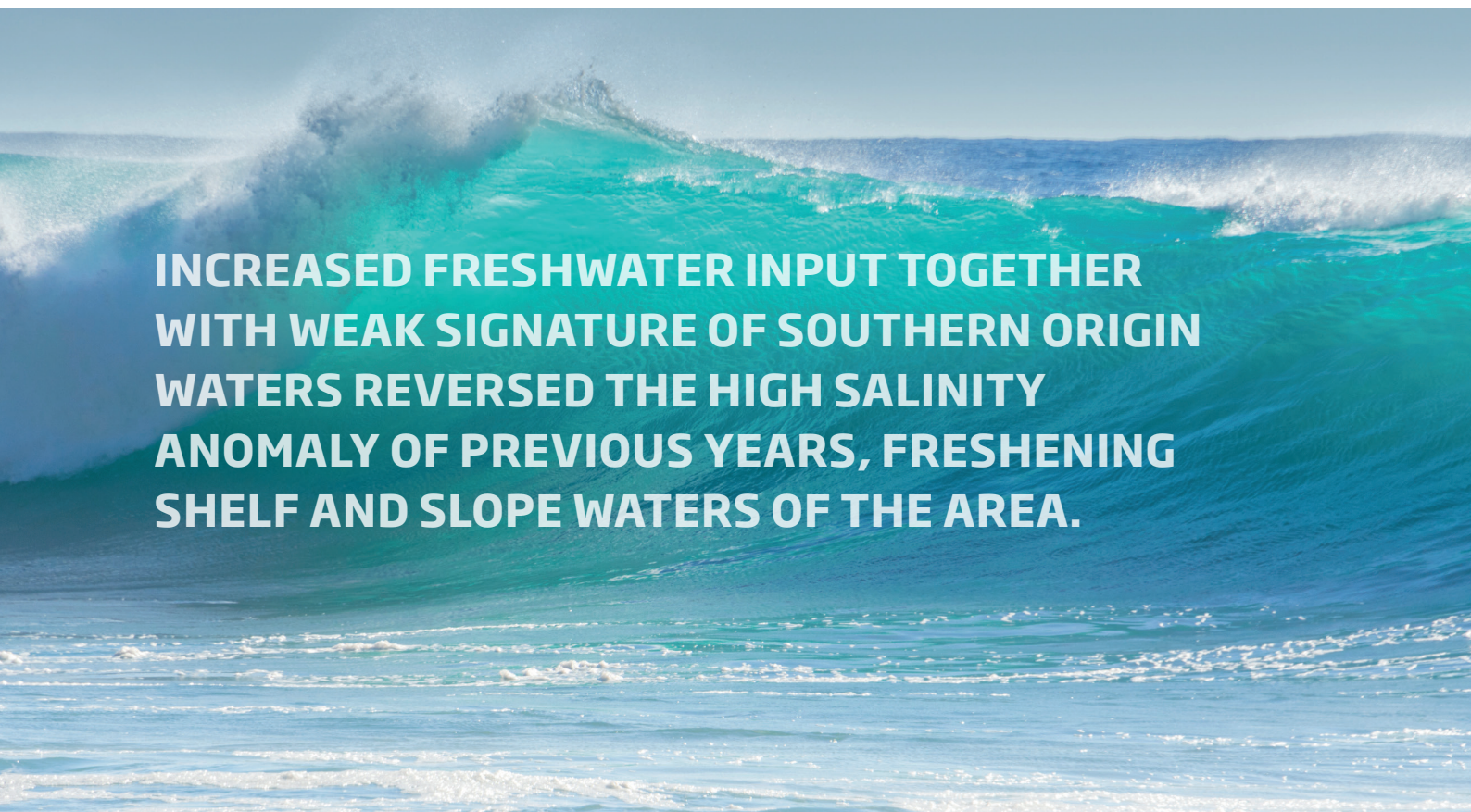
Area 3 - Icelandic waters. Temperature (upper panel) and salinity (lower panel) at 0-50 m in the East Icelandic Current (Langanes Stations 2-6).

4.7 AREA 4 – BAY OF BISCAY AND EASTERN NORTH ATLANTIC

The Bay of Biscay, located in the eastern North Atlantic at the northeast edge of the subtropical anti-cyclonic gyre, is almost an adjacent sea, with relatively weak anticyclonic circulation. Shelf and slope currents are important in the system, characterized by coastal upwelling events in spring–summer and the dominance of a geostrophic balanced poleward flow (known as the Iberian Poleward Current) in autumn and winter.

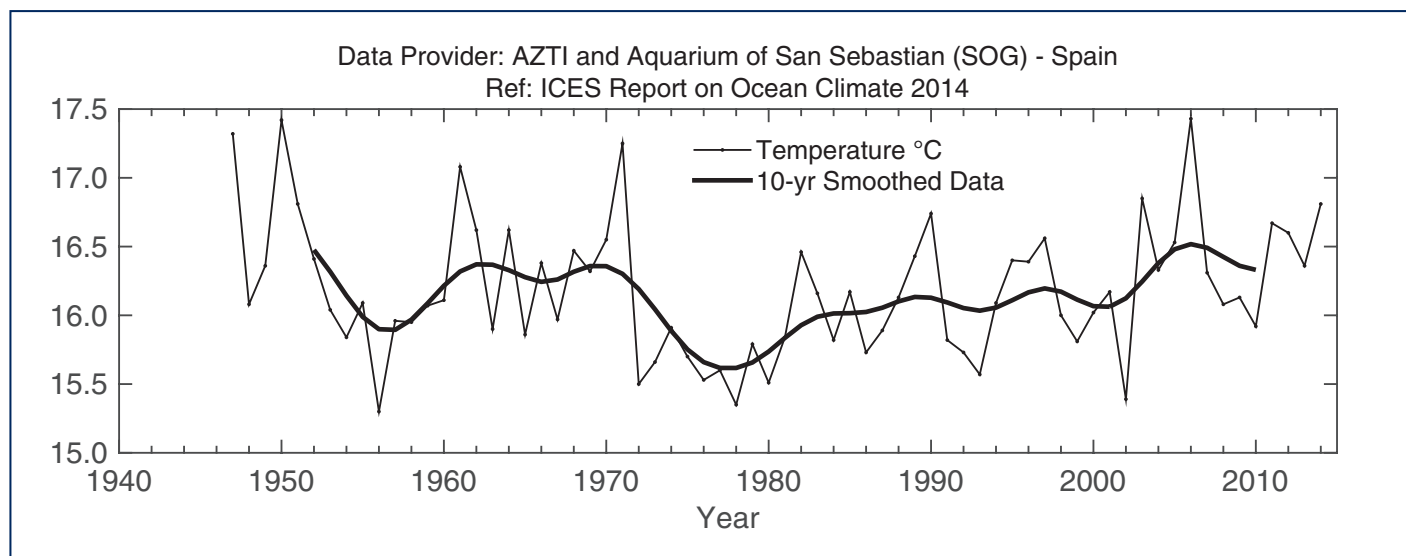
From an atmospheric point of view, 2014 can be considered very warm with respect to the long-term mean at the Iberian Peninsula and southern Bay of Biscay. Overall, average temperature exceeded 0.9°C with respect to 1981–2010. The year also stands as one of the warmest of the present century, with positive anomalies comparable to those recorded in 2003 and 2011. The seasonal cycle pattern showed a strong anomalous character, with very warm winter and autumn and warm spring and summer seasons. Sea surface temperature responded to the atmospheric temperature, yielding warmer-than-normal values year-round, especially in autumn. On average, sea surface temperature exceeded 0.65°C with respect to 1981–2010. 2014 can also be considered a wet year concerning the precipitation regime. The seasonal cycle is characterized by wet winter and autumn seasons, while spring and summer can be classified from normal to dry.

The subsurface structure of the water column was related to a combination of mild atmospheric conditions, increased precipitation and river runoff, and the prevalence of strong turbulence and downwelling conditions in winter. Subsurface waters were also conditioned by lack of a strong signature of southern origin waters. The combination of those factors reversed the high salinity anomaly developed in 2011–2012, with 2014 slightly fresher than 2013. Thus, increased freshwater inputs in 2014 enhanced the decreasing salinity trend.



INCREASED FRESHWATER INPUT TOGETHER WITH WEAK SIGNATURE OF SOUTHERN ORIGIN WATERS REVERSED THE HIGH SALINITY ANOMALY OF PREVIOUS YEARS, FRESHENING SHELF AND SLOPE WATERS OF THE AREA.

FIGURE 37



Area 4 - Bay of Biscay and eastern Atlantic. Sea surface temperature (upper panel) and air temperature (lower panel) at San Sebastian (43°18.5'N 02°2.37'W).

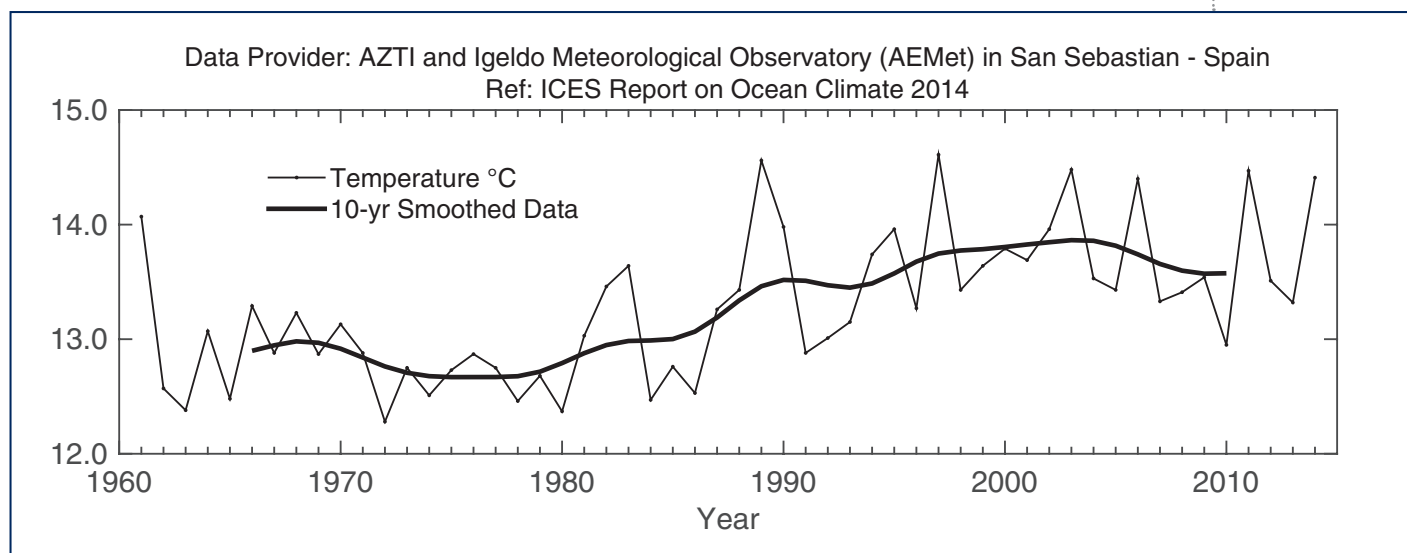
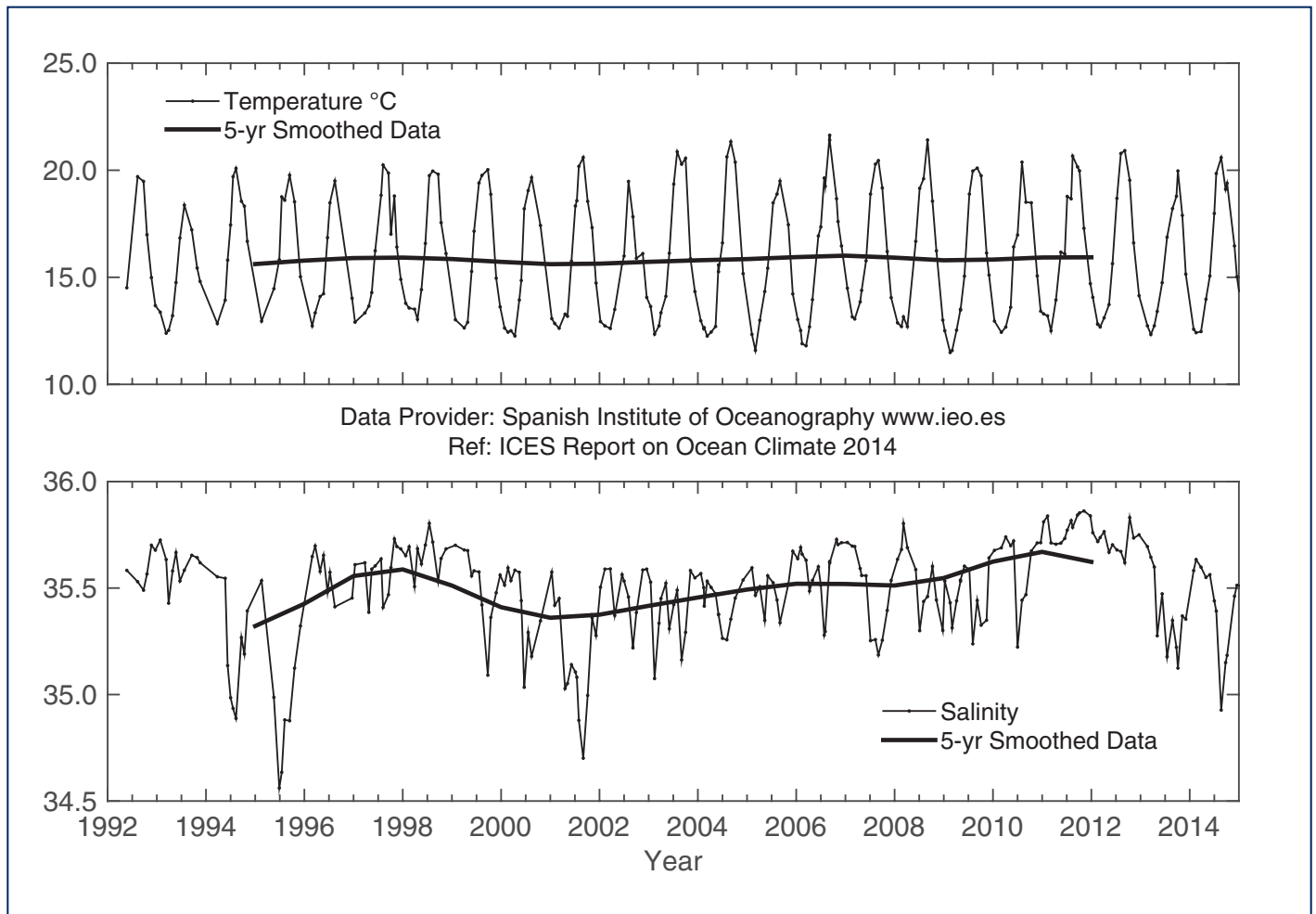
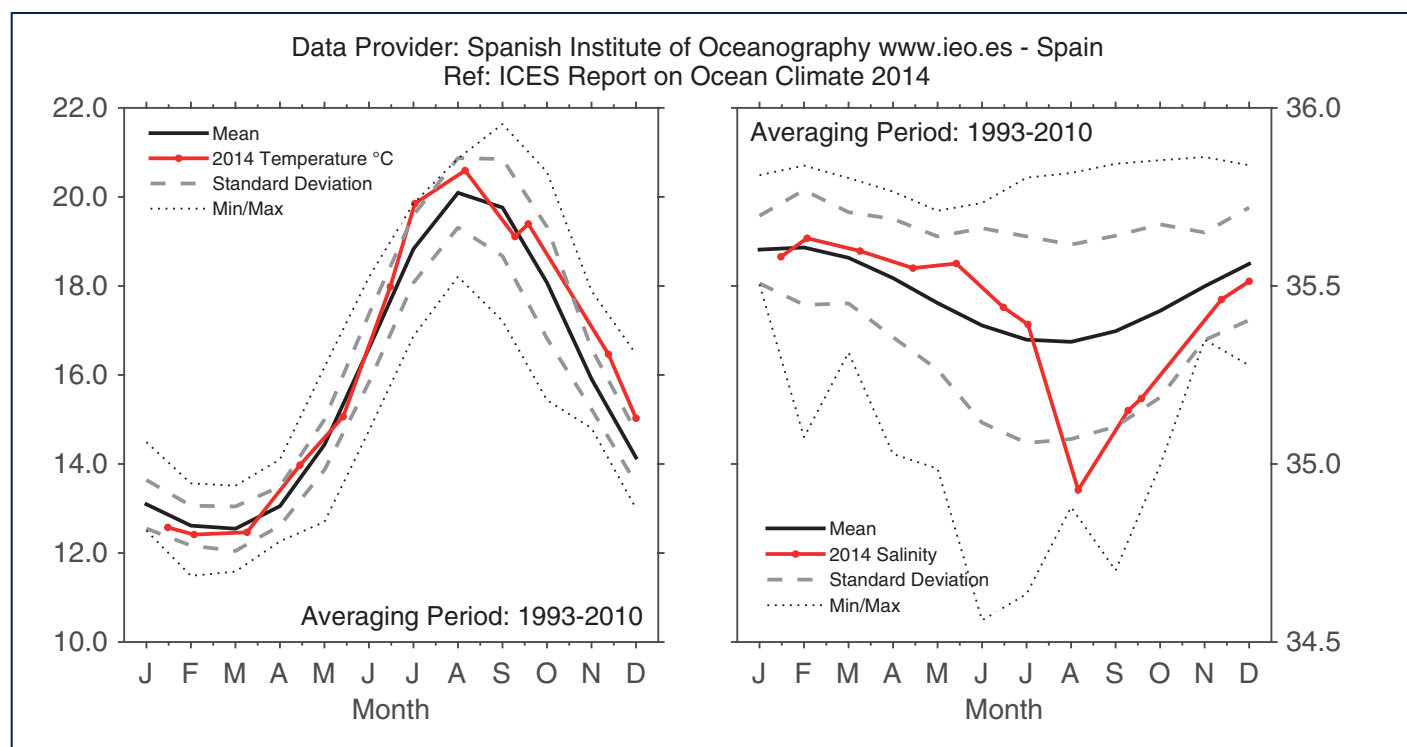


FIGURE 38



Area 4 - Bay of Biscay and eastern North Atlantic. Potential temperature (upper panel) and salinity (lower panel) at Santander Station 6 (5-300 m).

FIGURE 39



Area 4 - Bay of Biscay and eastern North Atlantic. 2012 monthly temperature (left panel) and salinity (right panel) at Santander Station 6 (5-300 m).



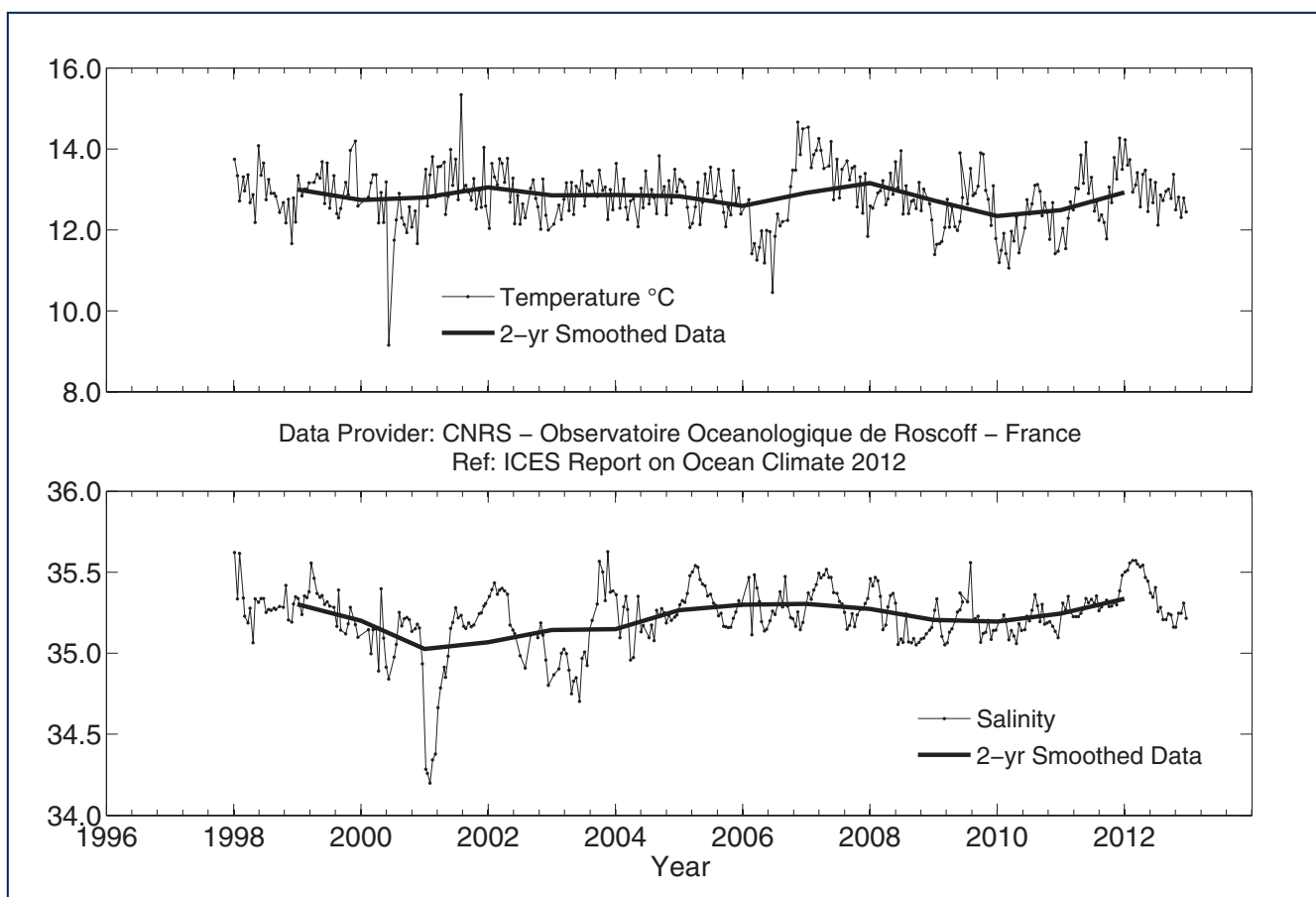
4.8 AREA 4B – NORTHWEST EUROPEAN CONTINENTAL SHELF

NORTHERN COAST OF BRITTANY

Measurements are collected twice monthly at a coastal station on the northern coast of Brittany, France. The Astan site (48.77°N 3.94°W) is located 3.5 km offshore, and measurements began in 2000. Properties at this site are typical of western Channel waters. Bottom depth is ca. 60 m, and the water column is well mixed for most of the surveys.

No update available for 2013/2014.

FIGURE 40



Area 4b - Northwest European continental shelf. Temperature (upper panel) and salinity (lower panel) anomalies of surface water at the Astan station (48.77°N 3.94°W) base period 1998-2010 (data to 2012).

WESTERN ENGLISH CHANNEL

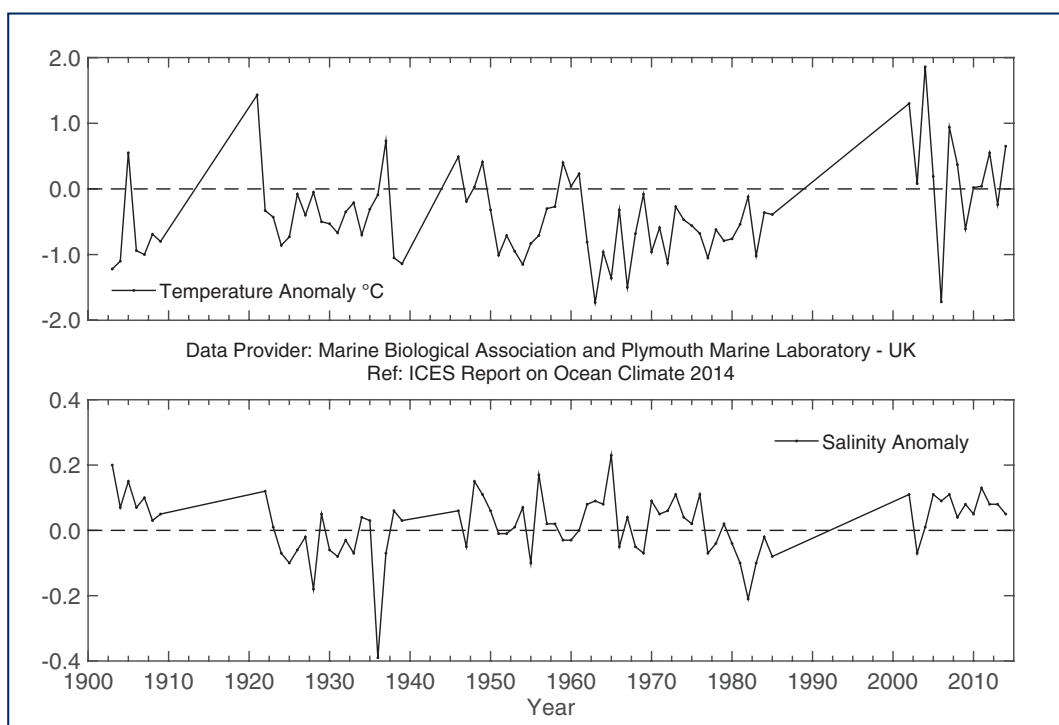
Station E1 (50.03°N 4.37°W) is situated in the western English Channel and is mainly influenced by North Atlantic water. Water depth is 75 m, and the station is tidally influenced by a 1.1-knot maximum surface stream at mean spring tide. The seabed is mainly sand, resulting in a low bottom stress ($1-2 \text{ ergs cm}^{-2} \text{ s}^{-1}$). The station may be described as oceanic, with development of a seasonal thermocline; stratification typically starts in early April, persists throughout summer, and disappears by the end of October. Typical depth of the summer thermocline is ca. 20 m. The station is greatly affected by ambient weather.

Measurements have been taken at this station since the end of the 19th century, with data currently available since 1903. The series is unbroken, apart from the gaps for the two world wars and a hiatus in funding between 1985 and 2002. Data are in the form of vertical profiles of temperature and salinity. Early measurements were taken with reversing mercury-in-glass thermometers and discrete salinity bottles. More recently, electronic equipment (Seabird CTD) has been utilized.

The time-series demonstrates considerable interannual variability in temperature. In 2013, annual average temperature was below the long-term mean, but in 2014, temperature increased and was close to the 2012 value. Through 2014, average temperature of the upper 40 m of the water column was warmer than average in all months except August.

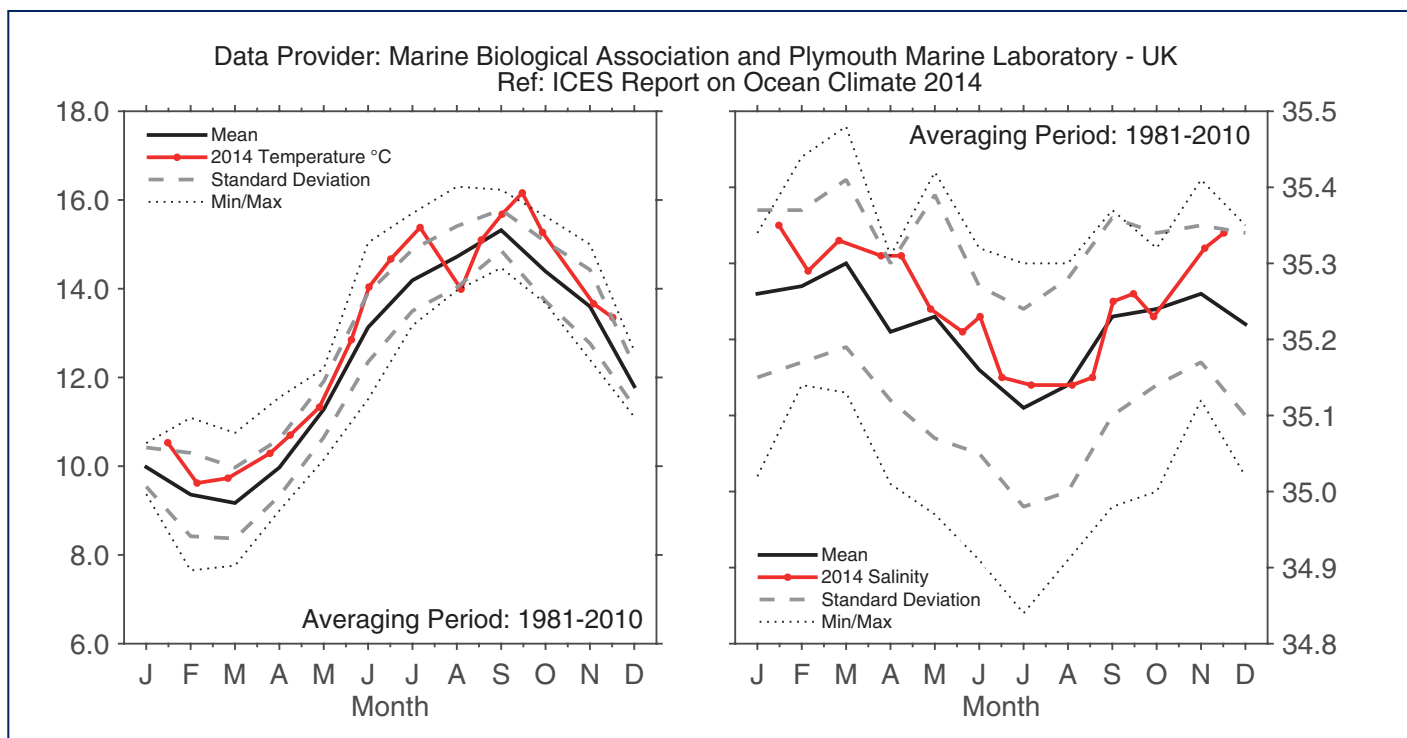
Salinity recorded in 2014 was generally higher than the long-term mean, particularly at the end of the year.

FIGURE 41



Area 4b - Northwest European continental shelf. Temperature (upper panel) and salinity (lower panel) anomalies of surface (0-40 m) water at Station E1 in the western English Channel (50.03°N 4.37°W).

FIGURE 42



Area 4b - Northwest European continental shelf. Monthly average seasonal cycle with 2014 temperature (left panel) and salinity (right panel) observations of surface water (0-40 m) at Station E1 in the western English Channel (50.03°N 4.37°W).

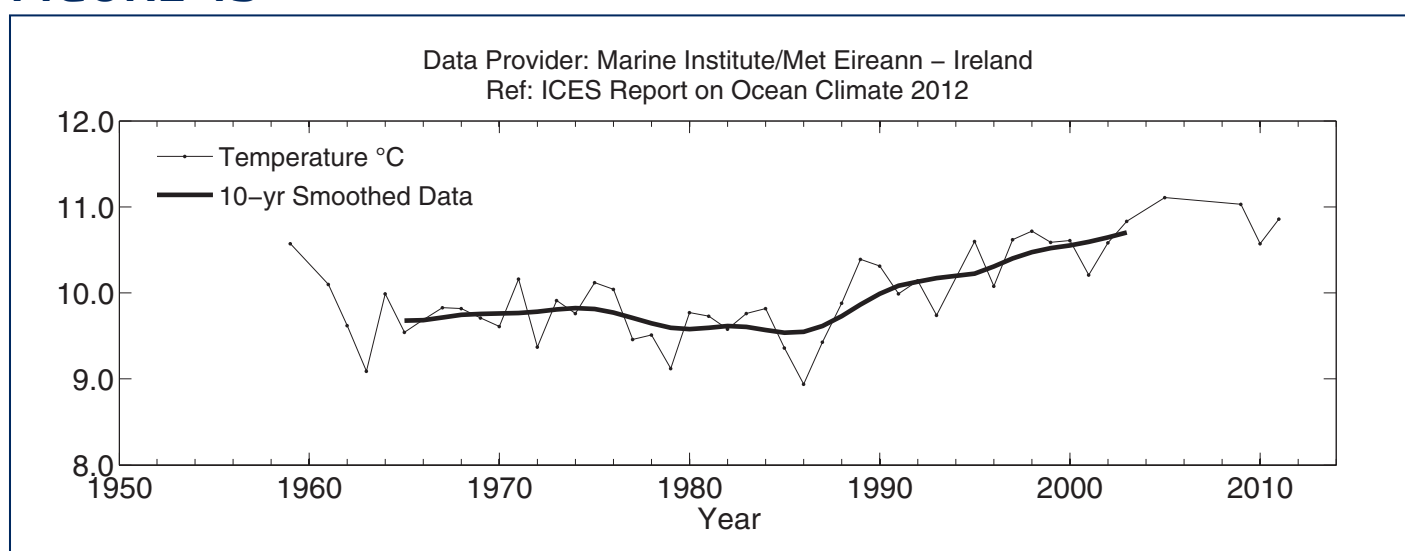


NORTH AND SOUTHWEST OF IRELAND

The time-series of surface observations at the Malin Head coastal station (the most northerly point of Ireland) is inshore of coastal currents and influenced by run-off. The early part of the record between 1959 and 2006 used bucket measurements, while the post-2007 period has used a SBE 39 temperature sensor. An offshore weather buoy has been maintained at 51.22°N 10.55°W off the southwest coast of Ireland since mid-2002, where sea surface temperature data are collected hourly.

No update available for 2013/2014.

FIGURE 43



Area 4b - Northwest European continental shelf. Temperature at the Malin Head coastal station (55.39°N 7.38°W) (data to 2012).



4.9 AREA 5 – ROCKALL TROUGH TO ICELAND

ROCKALL TROUGH

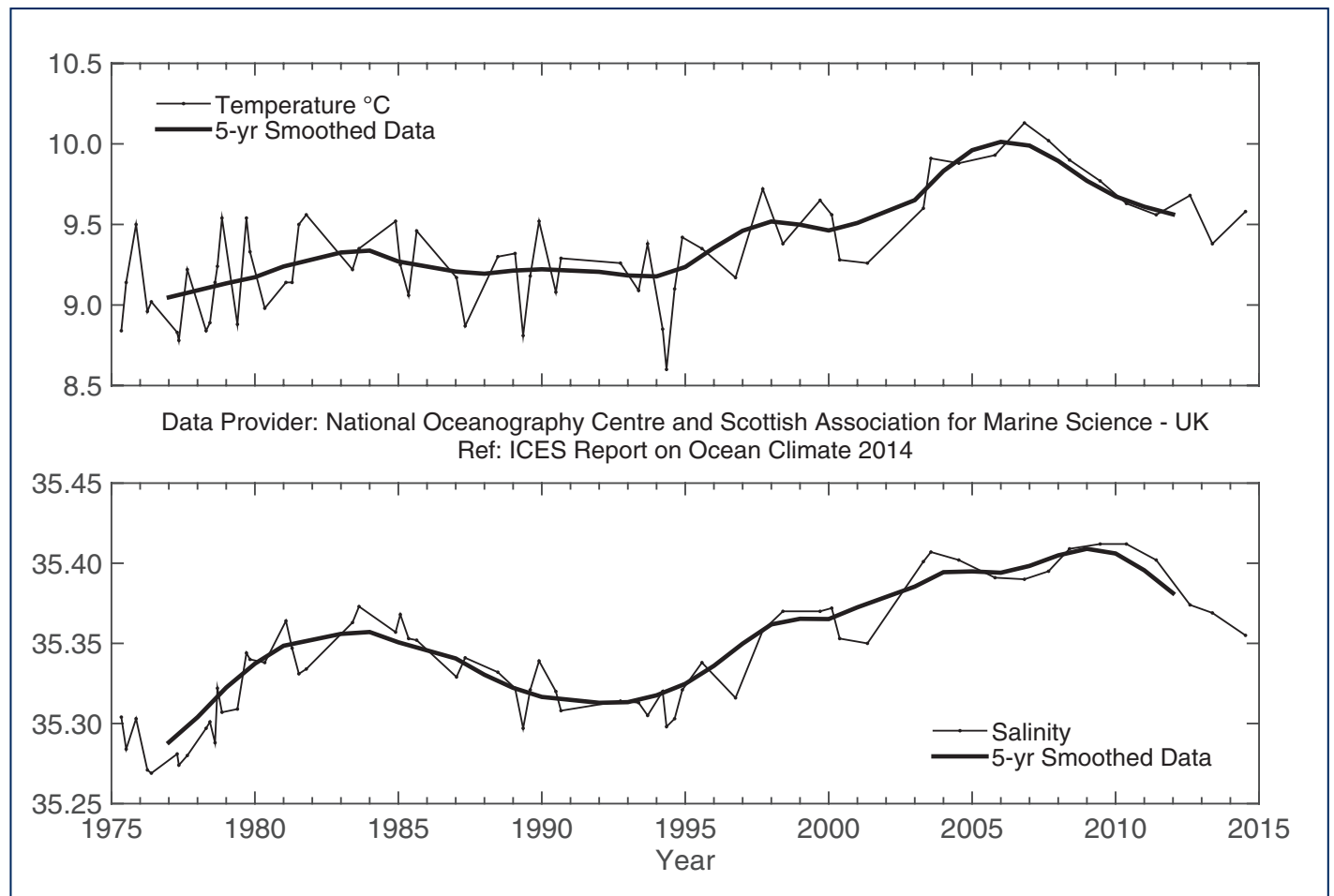
Rockall Trough is situated west of Britain and Ireland and is separated from the Iceland Basin by Hatton and Rockall banks and from the Nordic seas by the shallow (500 m) Wyville-Thomson Ridge. It allows warm North Atlantic upper water to reach the Norwegian Sea, where it is converted into cold, dense overflow water as part of the thermohaline overturning in the North Atlantic. The upper water column is characterized by poleward-moving eastern North Atlantic water, which is warmer and more saline than waters of the Iceland Basin, which also contribute to the Nordic sea inflow.

The potential temperature of the upper 800 m remains higher than the long-term mean. The upper ocean has been steadily cooling from the peak of $>10.0^{\circ}\text{C}$ in 2006, although 2014 was marginally warmer than 2013. Salinity of the upper 800 m has sharply decreased since the end of the 2000s, and in 2014 returned to close to the long-term mean.

**ROCKALL TROUGH UPPER OCEAN
SALINITY HAS FRESHENED TO
THE LONG-TERM MEAN.**



FIGURE 44



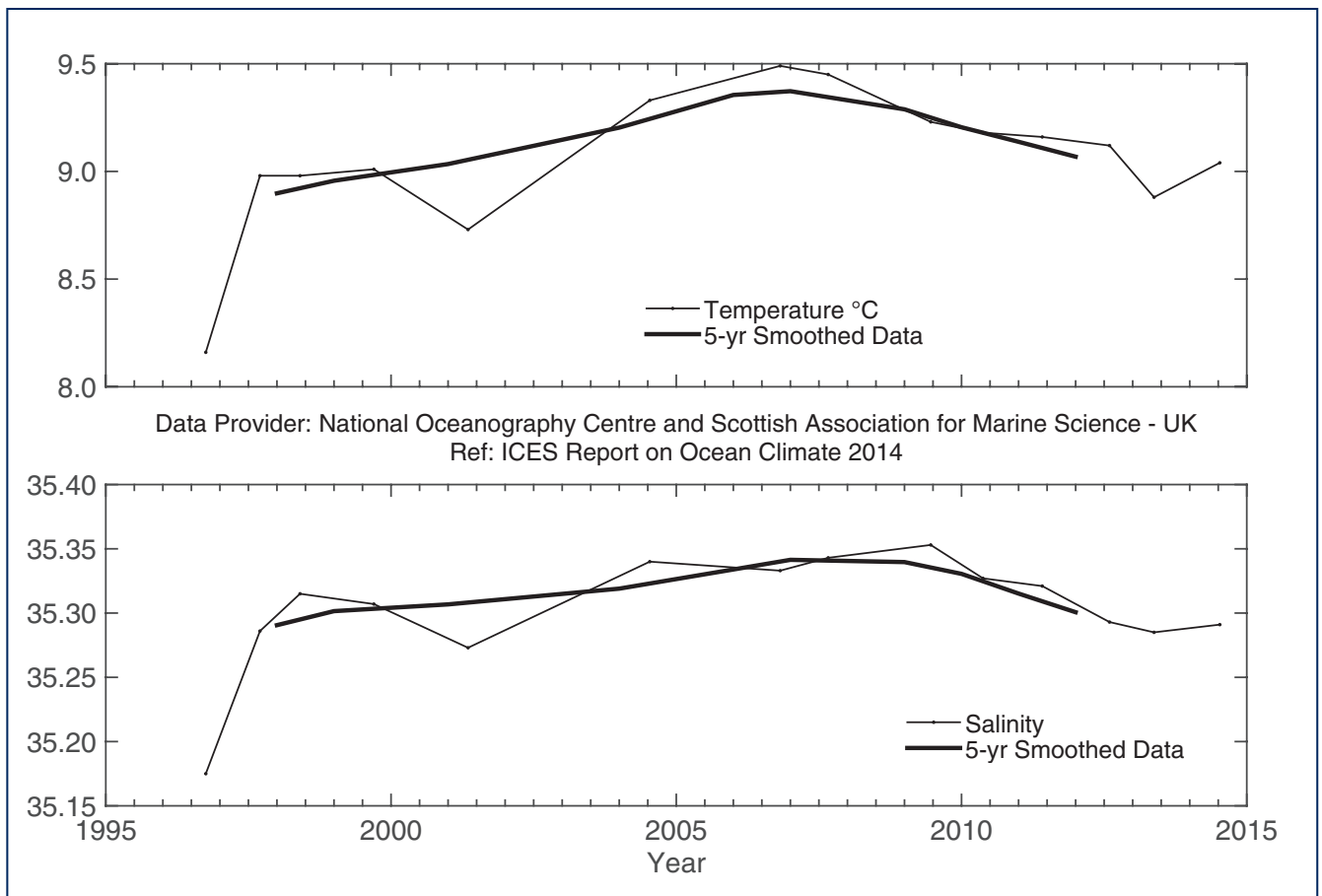
Area 5 - Rockall Trough. Temperature (upper panel) and salinity (lower panel) for the upper ocean (0-800 m).

HATTON – ROCKALL BASIN

This shallow basin (1000 m) lies between the Iceland Basin to the west and Rockall Trough to the east, bounded by the Hatton and Rockall banks. The basin is filled with well-mixed subpolar-mode water moving northward as part of the North Atlantic Current (NAC) complex. Winter mixing reaches 800–1000 m here. Temperature and salinity vary considerably depending on the type of North Atlantic Current water that enters the basin; the region lies in the transition zone between cold, fresh central subpolar water and warm, saline eastern subpolar water. When the NAC fronts shift westward, the basin becomes warmer and more saline.

The range of basin-mean temperature and salinity in the upper 1000 m is 1°C and >0.1, respectively, rather higher than the Iceland Basin to the west and Rockall Trough to the east. The lowest values were seen in 1996, followed by a steady rise to maximum values in the late 2000s. Since 2010, there has been a decrease in temperature and salinity; in 2014, properties were similar to those observed in 1997.

FIGURE 45



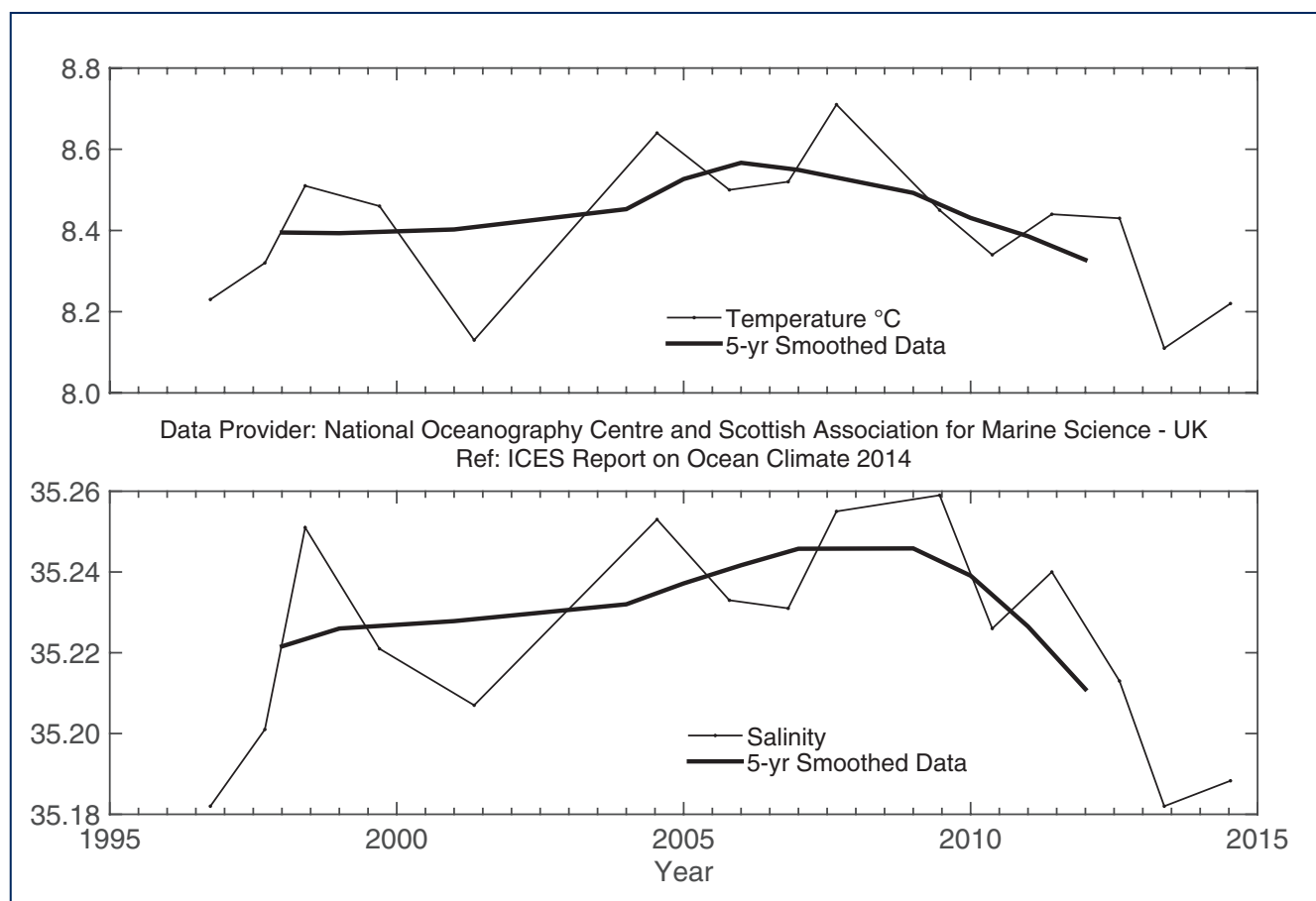
Area 5 - Hatton-Rockall Basin. Temperature (upper panel) and salinity (lower panel) for the upper ocean (potential density 27.20-27.50, representing the top 600 m and excluding the seasonally warmed surface layer).

ICELAND BASIN

A major part of the North Atlantic Current (NAC) flows into the Iceland Basin adjacent to the shallow Hatton Bank on the southeast side of the basin. The NAC typically consists of one or two fronts between warmer and more saline water in the east and colder, fresher water to the north and west. The region is rich in eddy activity, and water properties are extremely variable in time and space. Most of the water entering the Iceland Basin from the south flows through into the Nordic seas over the Iceland–Scotland ridge. A smaller fraction of the NAC water recirculates south of Iceland in the boundary currents of the main anticlockwise circulation of the Subpolar Gyre.

Temperature and salinity of the upper ocean (ca. the top 500–600 m) varies from year to year, but also show multi-year changes. From 1996 to the late 2000s, both temperature and salinity were increasing, but since then, there has been an overall decrease. In 2014, the physical properties were close to those recorded in 1996. This change implies that the basin is receiving more water originating in the west and central subpolar region and less warm, saline water from the eastern intergyre regions.

FIGURE 46



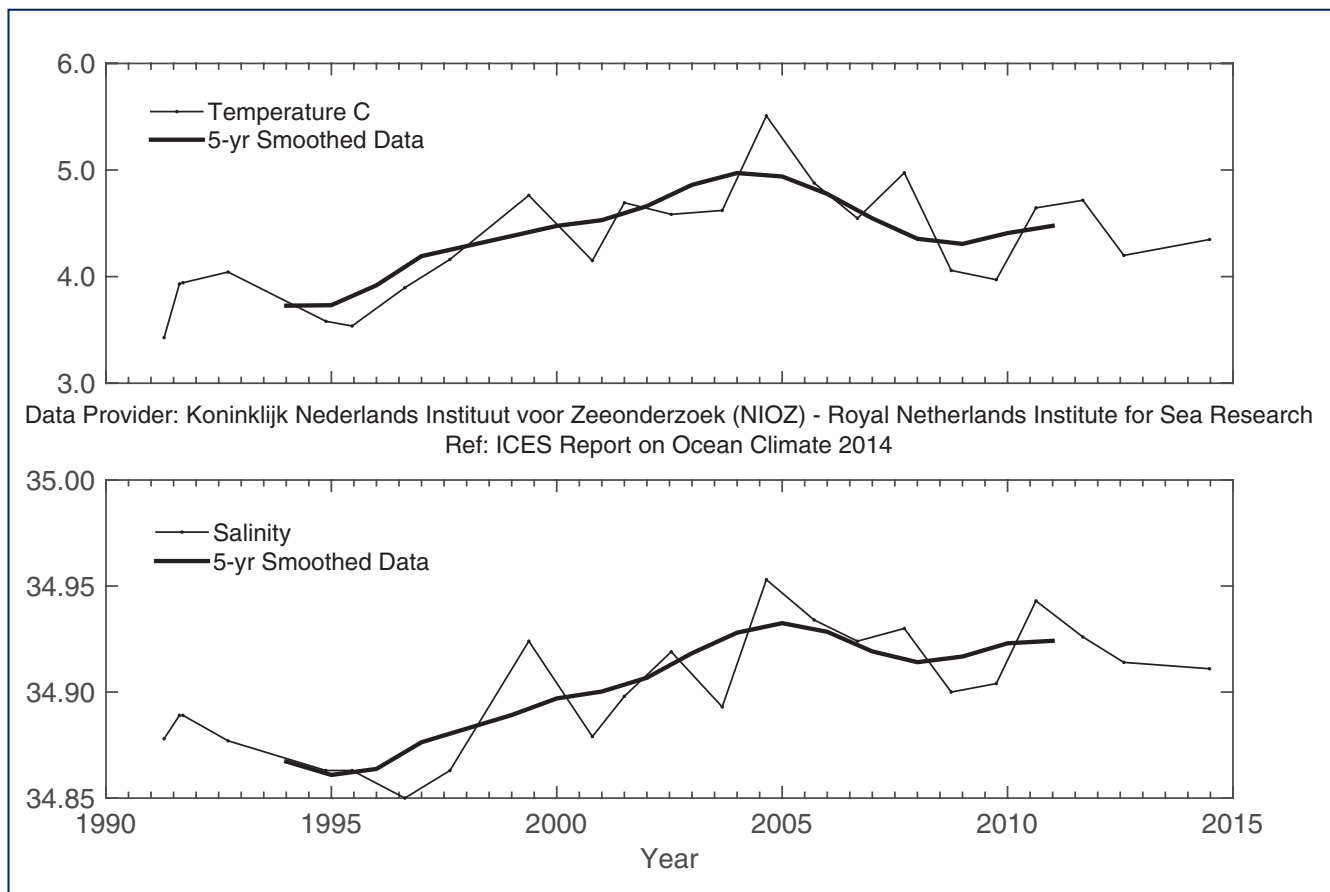
Area 5 - Iceland Basin. Temperature (upper panel) and salinity (lower panel) for the upper ocean (potential density 27.20–27.50, representing the top 500 m and excluding the seasonally warmed surface layer).

4.10 AREA 5B – IRMINGER SEA

The Irminger Sea is the ocean basin between southern Greenland, the Reykjanes Ridge, and Iceland. This area forms part of the North Atlantic subarctic cyclonic gyre. Due to this gyre, the exchange of water between the Irminger and Labrador seas proceeds relatively fast. In the bottom layers of the Irminger Sea, cold water originating from the (sub)Arctic seas flows from Denmark Strait southwards over the continental slope of Greenland.

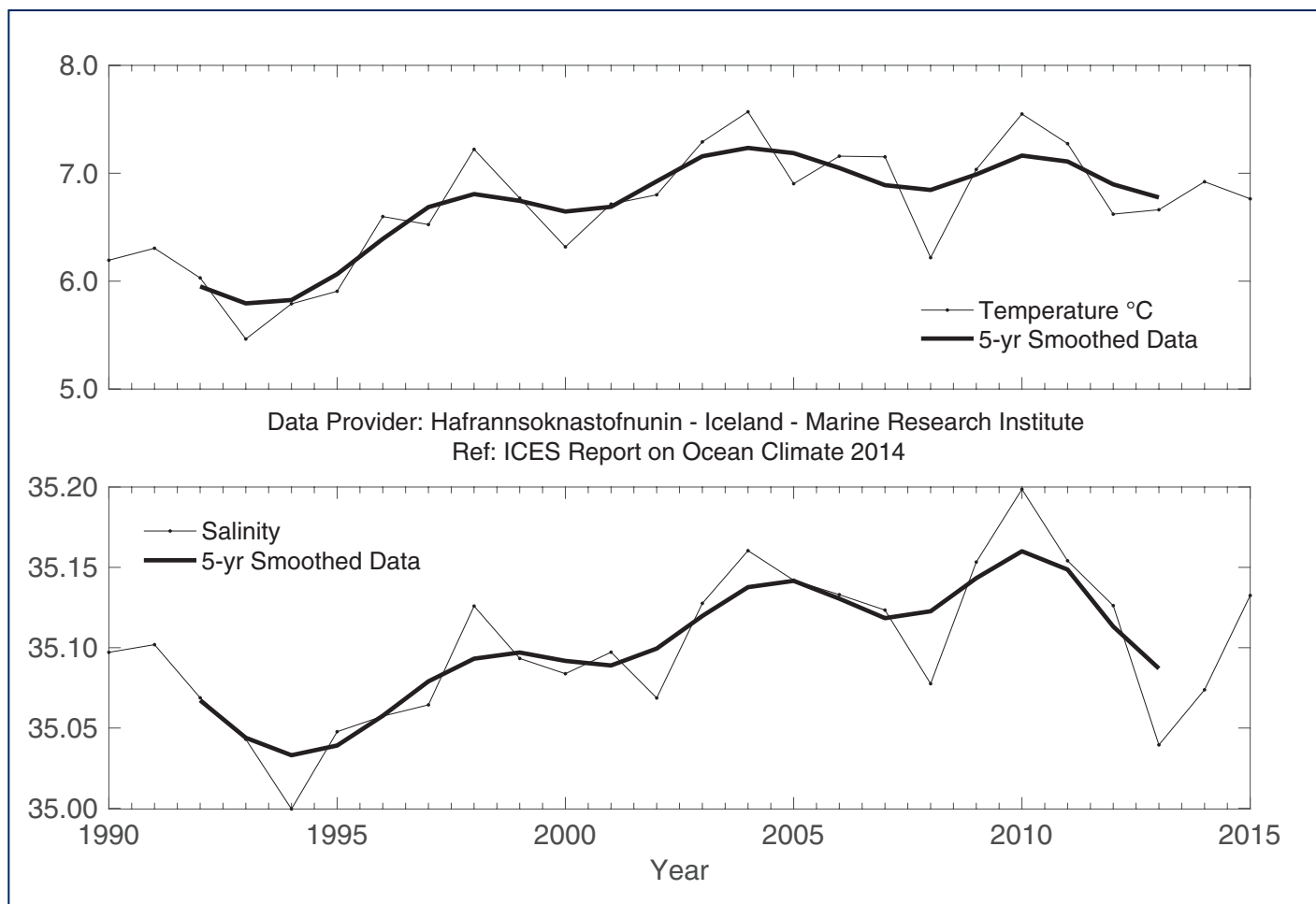
In 2004, subpolar mode water (SPMW) in the centre of the Irminger Sea in the pressure interval 200–400 dbar reached its highest temperature and salinity since 1991. Since then, temperature has exhibited well-correlated interannual variations, without a clear long-term trend, suggesting that variations in wind-driven circulation are the main cause of this hydrographic variability. In 2014, temperature and salinity of SPMW in the central Irminger Sea were 0.046°C and 0.012°C above the long-term mean. There were, unfortunately, no data available in 2013.

FIGURE 47



Area 5b - Irminger Sea. Temperature (upper panel) and salinity (lower panel) of subpolar mode water in the central Irminger Sea (averaged over 200–400 m).

FIGURE 48



Area 5b - Irminger Sea. Temperature (upper panel) and salinity (lower panel) of subpolar mode water in the northern Irminger Sea (Station FX9, 64.33°N 28°W), from winter observations averaged over 200-500 m).

4.11 AREA 6 AND 7 – FAROESE WATERS AND FAROE – SHETLAND CHANNEL

One branch of the North Atlantic Current crosses the Greenland–Scotland Ridge, flowing on either side of the Faroes. Its properties are sampled by the Faroe Bank Channel before it crosses the ridge, and by the Faroe Current after it crosses the ridge. Some of this water recirculates and is sampled within the Faroe–Shetland Channel as modified North Atlantic water (MNAW).

Farther east, the continental slope current flows along the edge of the Northwest European Continental Shelf; originating in the southern Rockall Trough, it carries warm, saline Atlantic water (AW) into the Faroe–Shetland Channel. A proportion of this AW crosses onto the shelf itself and enters the North Sea, where it is diluted with coastal water and eventually leaves in the Norwegian Coastal Current. The remainder enters the Norwegian Sea and joins water coming from north of the Faroes to become the Norwegian Atlantic water.

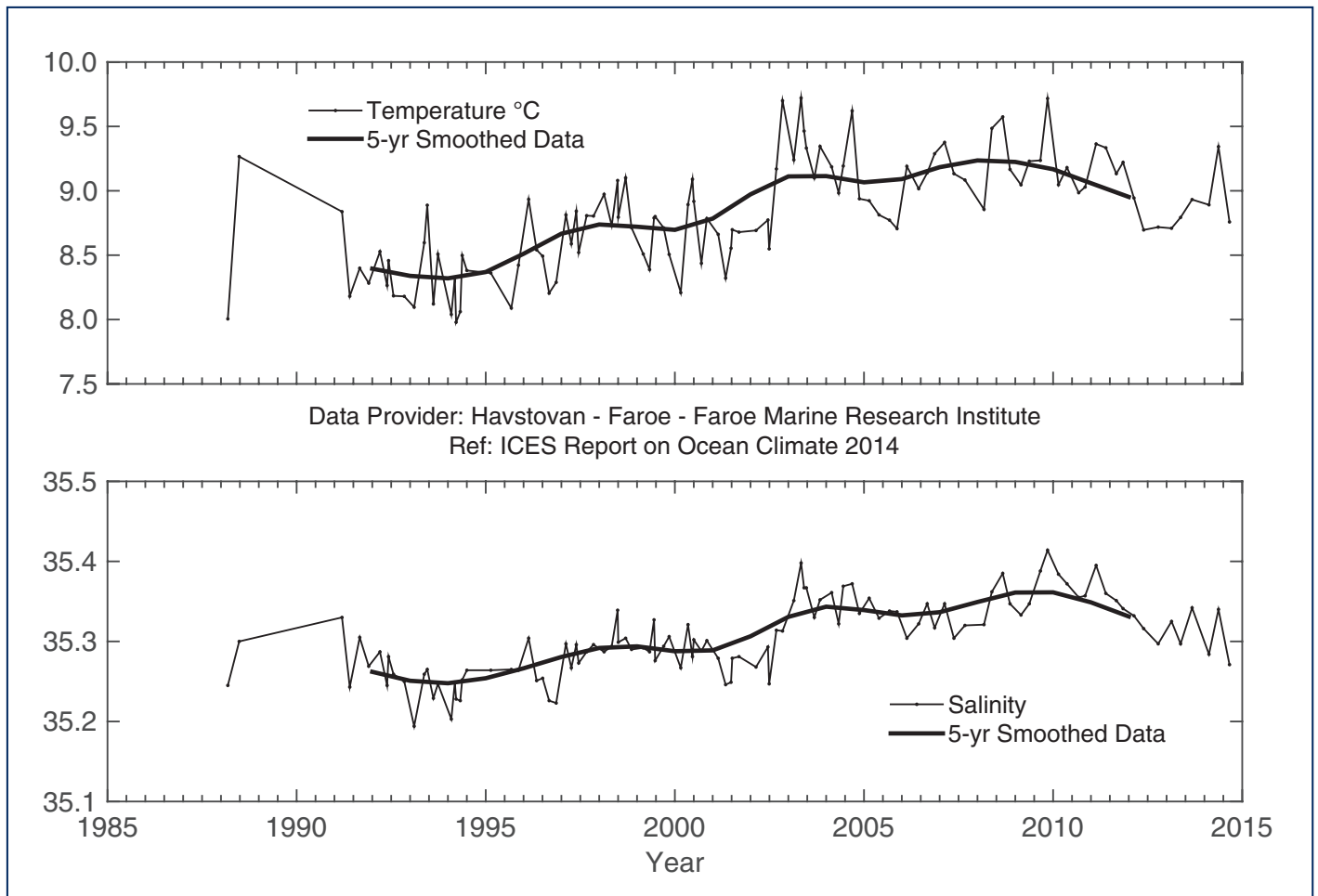
Generally, both temperature and salinity in all upper-layer waters around Faroe and the Faroe–Shetland Channel increased markedly during the 1990s and 2000s. Both temperature and salinity decreased slightly in the beginning of the 2010s.

After the record-high salinities observed in the Faroe Bank Channel and the Faroe Current in November 2009, salinities have decreased, but levelled off somewhat in 2013–2014. Temperatures in the Faroe Bank Channel decreased in 2012 and remained at this lower level during 2013, but recovered in 2014. The properties of the Faroe Current usually lag behind the properties of the Faroe Bank Channel, so in the Faroe Current, salinities continued to decrease in 2014, while temperatures partly recovered. On the Faroe Shelf, annual average temperature increased in 2013–2014 compared to 2012. Conditions, therefore, still remain warm and saline in the century-long perspective given by the Faroe coastal temperature time-series, although, like all coastal and shelf time-series, this is affected by atmospheric and terrestrial effects.

Temperature and salinity of the surface waters of the Faroe–Shetland Channel have generally increased over the past two decades. Water on the western slopes of the Channel, known as modified North Atlantic water, reached record-high temperature and salinity values in 2010. Temperature and salinity of Atlantic water masses on both sides of the Faroe–Shetland Channel have decreased slightly since then; values are now near the long-term mean. Water temperatures in 2014, however, were slightly higher than observed in 2013.

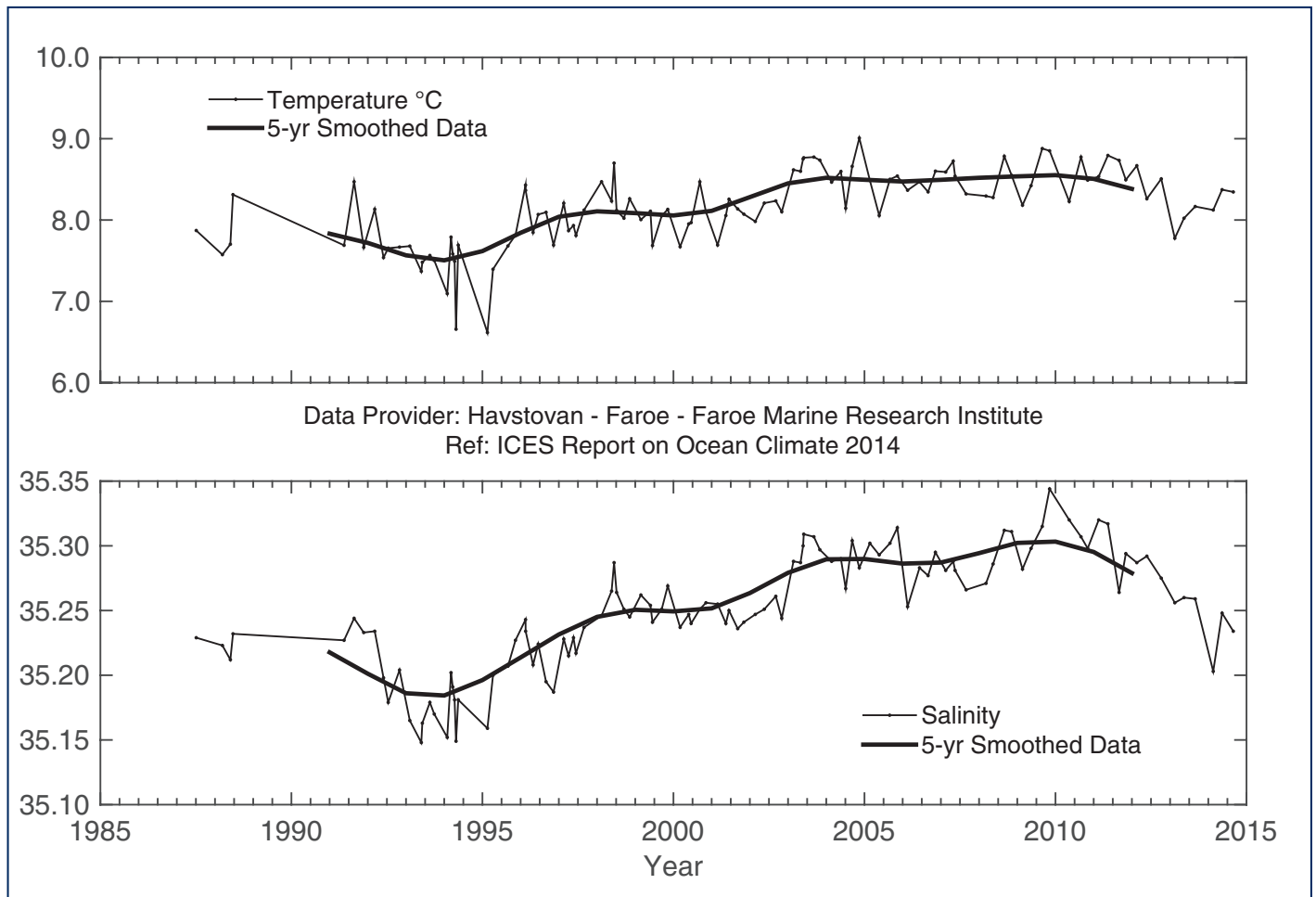


FIGURE 49



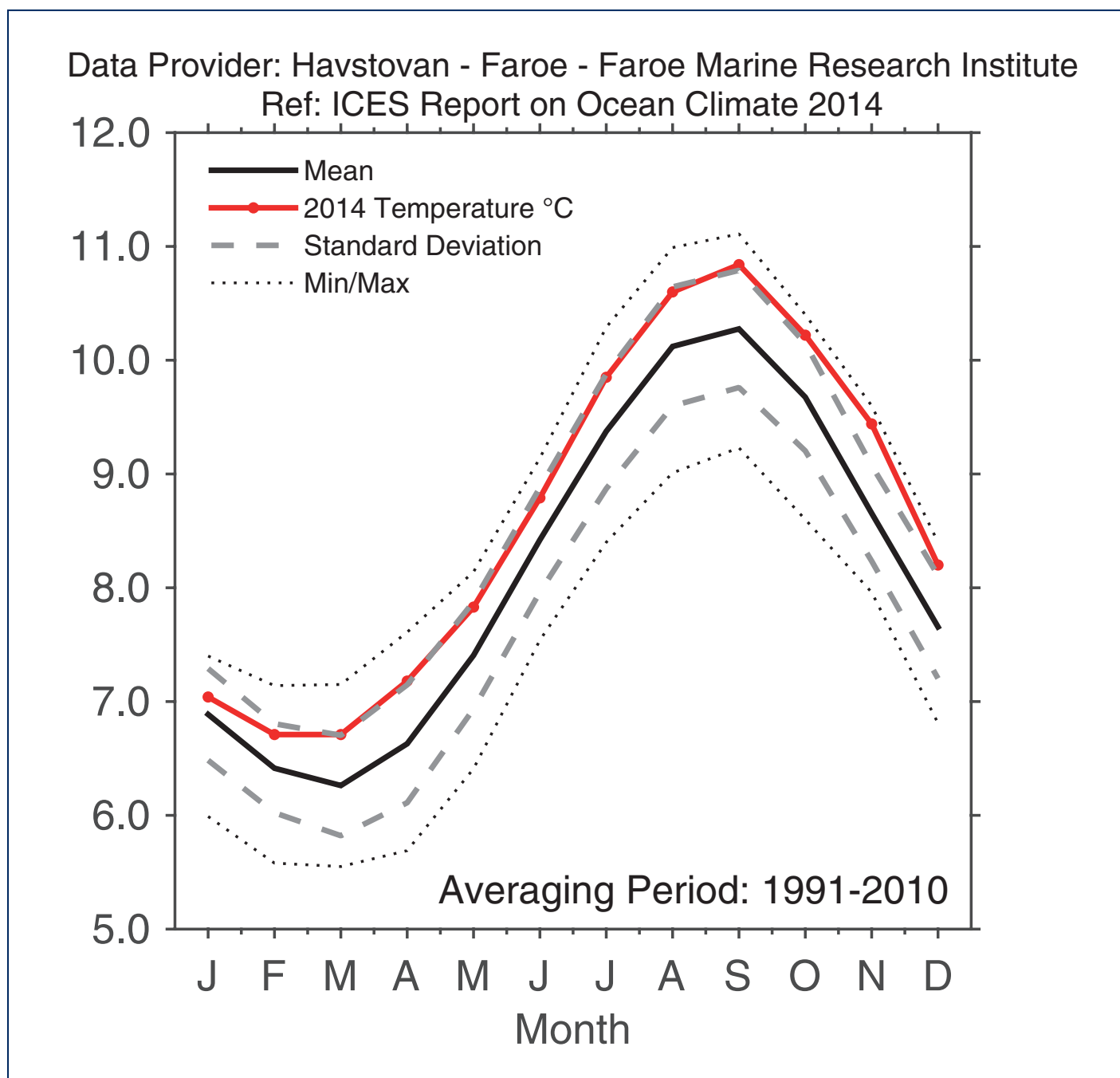
Areas 6 and 7 - Faroe Bank Channel. Temperature (upper panel) and salinity (lower panel) in the high salinity core of the Atlantic water over the Faroe Bank Channel (maximum salinity averaged over a 50 m deep layer).

FIGURE 50



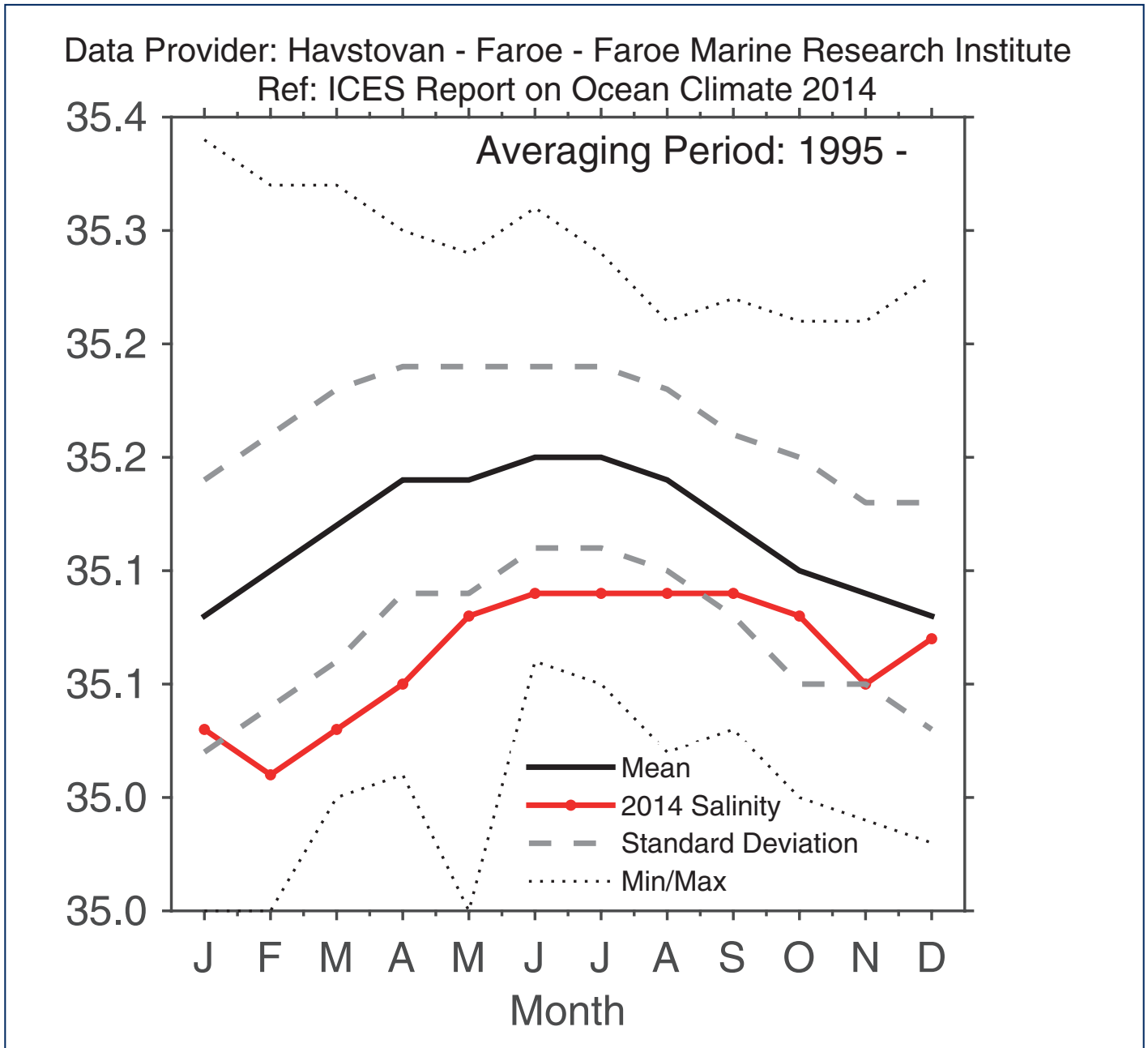
Areas 6 and 7 - Faroe Current. Temperature (upper panel) and salinity (lower panel) in the high salinity core of the Faroe Current north of the Faroes (maximum salinity averaged over a 50 m deep layer).

FIGURE 51a



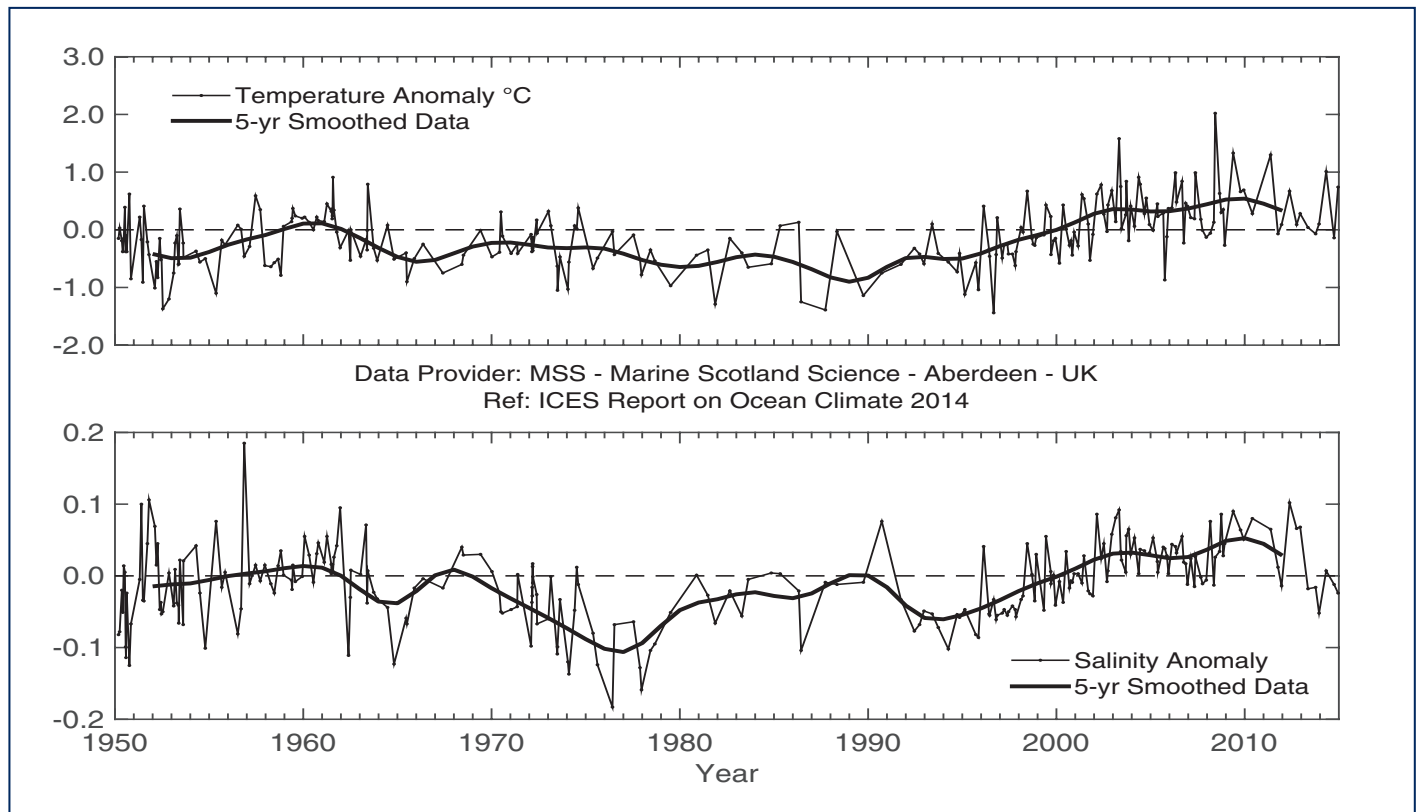
Areas 6 and 7 - Faroe Shelf. 2014 monthly temperature from the Faroe coastal station at Oyrargjogv (62.12°N 7.17°W). Note that the temperature averaging period has been changed and is now based on data from Oyrargjogv in 1991-2010.

FIGURE 51b



Areas 6 and 7 - Faroe Shelf. 2014 monthly salinity from the Faroe coastal station at Skopun (61.91°N 6.88°W). Salinity averaging period is 1995-2014.

FIGURE 52



Areas 6 and 7 - Faroe-Shetland Channel. Temperature anomaly (upper panel) and salinity anomaly (lower panel) in the modified Atlantic water entering the Faroe-Shetland Channel from the north after circulating around the Faroes.

IN 2013 AND 2014, TEMPERATURES IN BOTH AREAS DECREASED SLIGHTLY. SINCE THE RECORD-HIGH VALUES IN 2009, SALINITIES CONTINUED TO DECREASE AND ARE NOW CLOSE TO THE LONG-TERM MEAN.

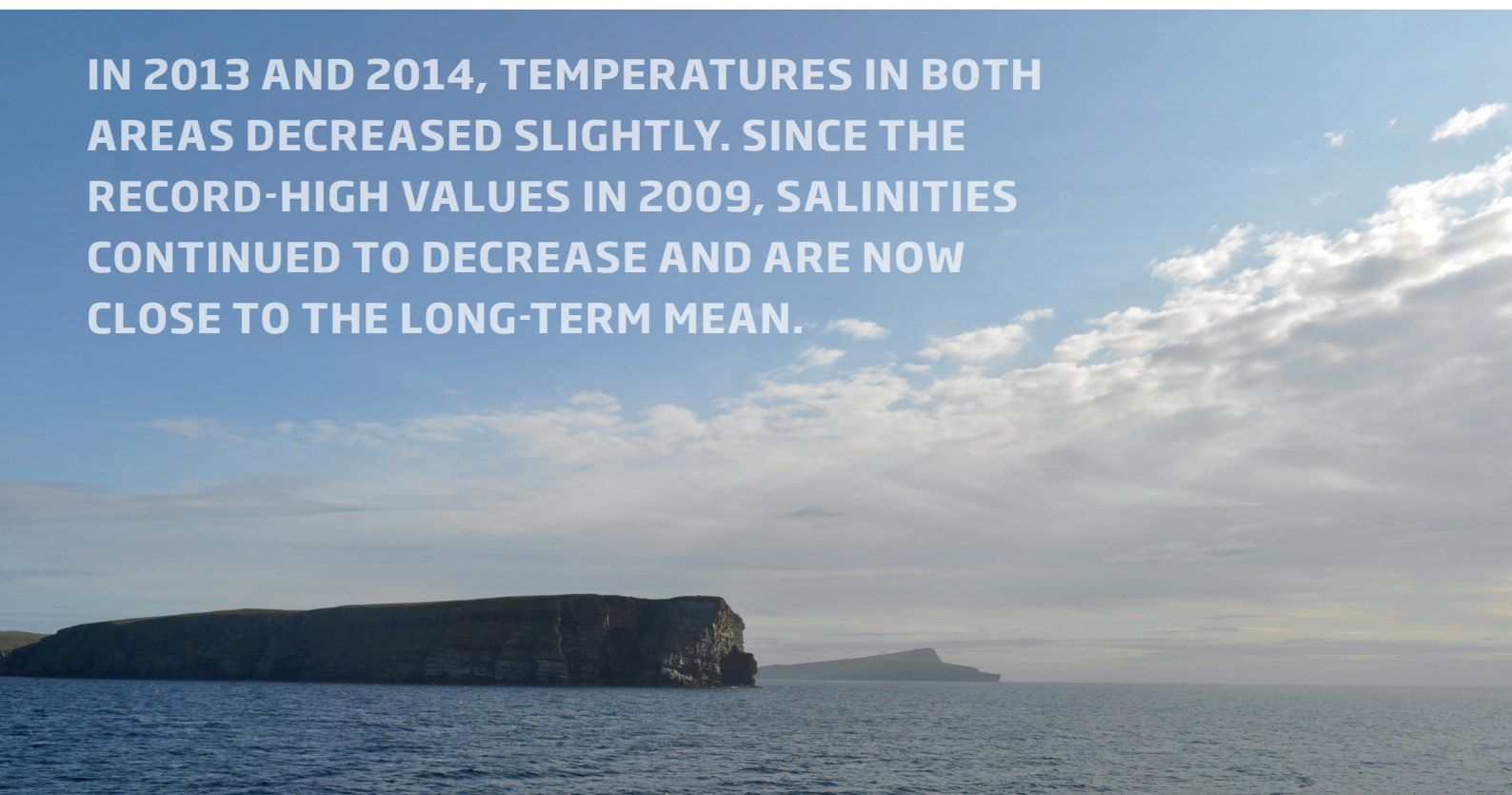
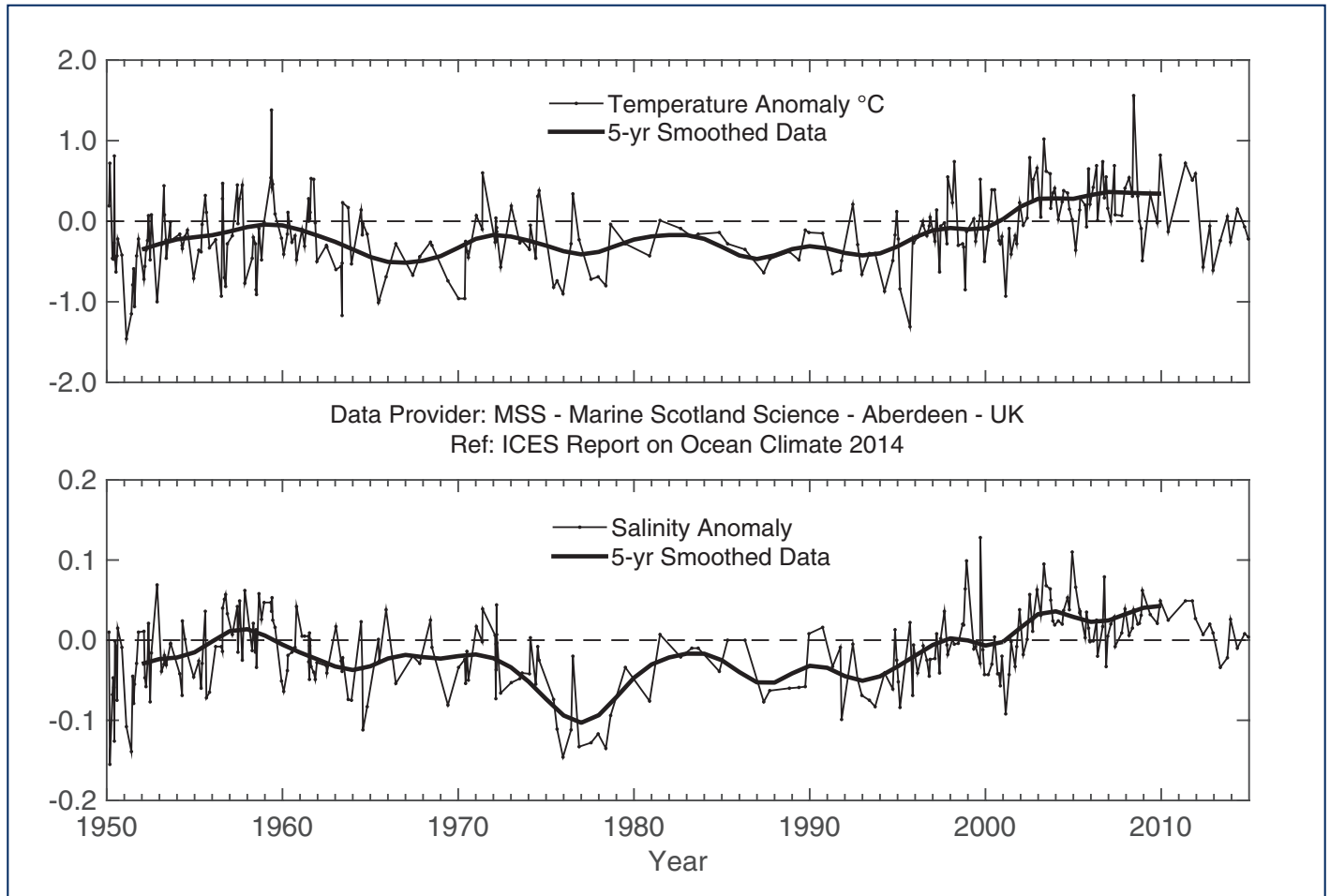


FIGURE 53



Areas 6 and 7 - Faroe-Shetland Channel. Temperature anomaly (upper panel) and salinity anomaly (lower panel) in the Atlantic water in the Slope Current.

4.12 AREAS 8 AND 9 – NORTHERN AND SOUTHERN NORTH SEA

North Sea oceanographic conditions are determined by the inflow of saline Atlantic water (AW) and the ocean-atmosphere heat exchange. Inflow through the northern entrances (and, to a lesser degree, through the English Channel) can be strongly influenced by the NAO. Numerical model simulations also demonstrate strong differences in North Sea circulation, depending on the state of the NAO. The AW mixes with river run-off and lower salinity Baltic Outflow along the Norwegian coast. A balance of tidal mixing and local heating forces the development of a seasonal stratification from April/May to September in most parts of the North Sea.

In 2014, all monthly area-averaged North Sea SST means exceeded the climatological means. Additionally, the July and November means also exceeded the maxima of the reference period 1981–2010. The anomalies of June and July were about 1.9 K. During the second week of August, a big mixing event was caused by the passage of the tropical ex-hurricane “Bertha” which dropped the North Sea SST about 1.5 K within a few days. This is also the reason for the relative low August mean. The annual SST mean is the warmest since the beginning of the record in 1969, with an anomaly of +1.2 K. Besides the inflow of warmer Atlantic water at the northern boundary and through the English Channel, much of the SST variability is caused by the local ocean-atmosphere heat flux.

In 2014, the large-scale horizontal summer temperature distribution in the surface layer differed significantly from the 10-year average (2000–2010, but without 2002). The southern part was much warmer, with anomalies up to +3 K, while the area north of 58°N was much colder, with negative anomalies up to -3 K at the southern tip of Norway. In the bottom layer, the pattern was different, with negative anomalies around the Shetlands and in the eastern part of the North Sea and with a local maximum northwestward off the northern tip of Jutland. In both areas, the negative anomalies reached values of -3 K. Positive anomalies up to +2 K in the bottom layer were observed along the Danish, German, and Dutch coasts. In the central North Sea, the maximum difference between surface and bottom temperature exceeded 10 K, which is, with the exception of 2013, ca. 2 K more than in previous years. The maximum vertical temperature gradient was about 3 K m^{-1} in the southern North Sea and weakened towards the north. The depth of the thermocline varied between 13 and 31 m.

Compared to 2013, the total heat content increased to $1.740 \times 10^{21} \text{ J}$ and exceeded the reference mean of $1.631 \times 10^{21} \text{ J}$ by 1.3 s.d.



During summer, the tongue of Atlantic water >35 psu intruding from the north reached southward to 60°N at the surface and to ca. 56°N at the bottom. Generally, there is a positive anomaly relative to the 10-year average (2000–2010, but without 2002) in the eastern North Sea, with a maximum >2 psu at the surface and a negative anomaly in the western North Sea. The area covered by Atlantic water >35 psu at the surface is much smaller compared to previous years. This is possibly the result of two storms passing the North Sea on 10–11 and 18–19 August, both causing strong vertical mixing in the surface layer. Vertical zonal sections show that AW penetrated into the central North Sea southward until 57°N ; small lenses of AW were also visible in the eastern part of the 56°N section. Compared to 2013, total salt content increased to 1.137×10^{12} t, which is slightly above the 10-year average.

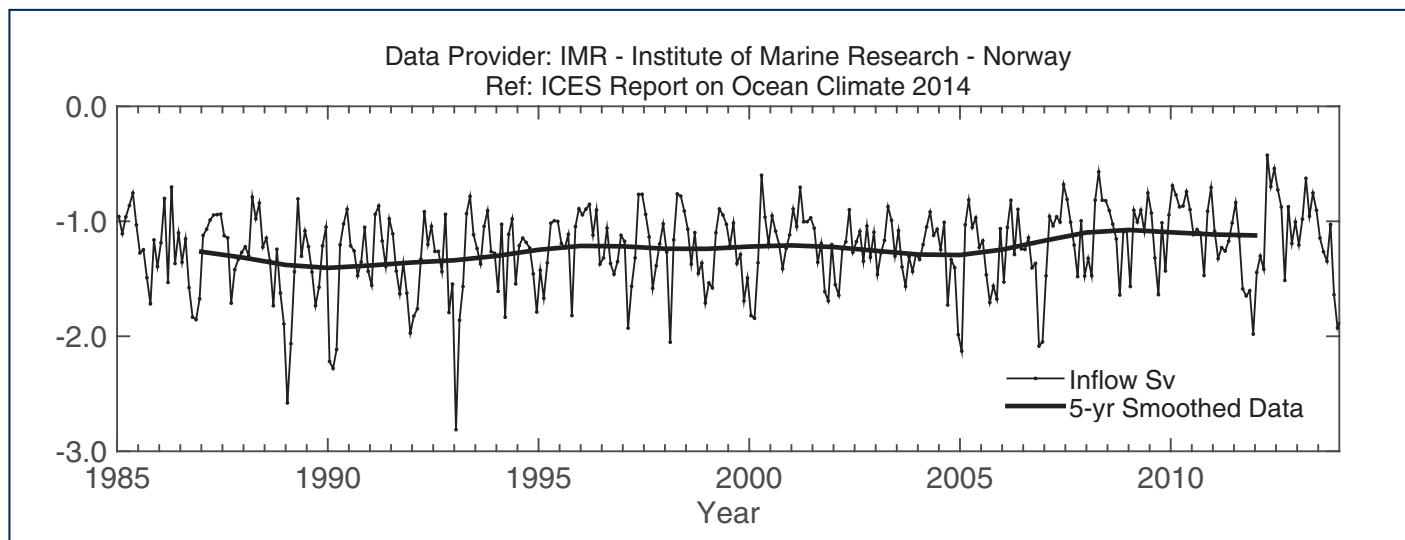
Until May, the monthly run-off volumes were below the reference period 1971–2000; volumes in the remaining months were close to the reference period. Therefore, the annual run-off volume of $15 \text{ km}^3 \text{ yr}^{-1}$ was below the long-term mean ($22 \text{ km}^3 \text{ yr}^{-1}$), but still within the 95% band.

Temperature and salinity at two positions in the northern North Sea illustrate conditions in the Atlantic inflow (Figure 54). The first (Location A) is at the near-bottom in the northwest part of the North Sea, and the second (Location B) is in the core of the AW at the western shelf edge of the Norwegian Trench. Measurements were taken during summer and represent the previous winter's conditions. Average temperature at Location A was $1\text{--}2^{\circ}\text{C}$ lower than at Location B, and salinity was also slightly lower. In both locations, there were above-average temperatures and salinities in 2009, and there has been an increase in both salinities and temperatures since 2008.

IN 2014, ALL MONTHLY AREA-AVERAGED NORTH SEA SST MEANS EXCEEDED THE CLIMATOLOGICAL MEANS. THE ANNUAL SST MEAN IS THE WARMEST SINCE THE BEGINNING OF THE RECORD IN 1969, WITH AN ANOMALY OF $+1.2 \text{ K}$.



FIGURE 54



Area 8 - Northern North Sea. Modelled monthly mean volume transport of Atlantic water (AW) into the northern and central North Sea southwards between the Orkney Islands and Utsira, Norway (top panel). Temperature (middle panel) and salinity (bottom panel) near the seabed in the northwest part of the North Sea (Location A) and in the core of AW at the western shelf edge of the Norwegian Trench (Location B) during summers 1970-2014.

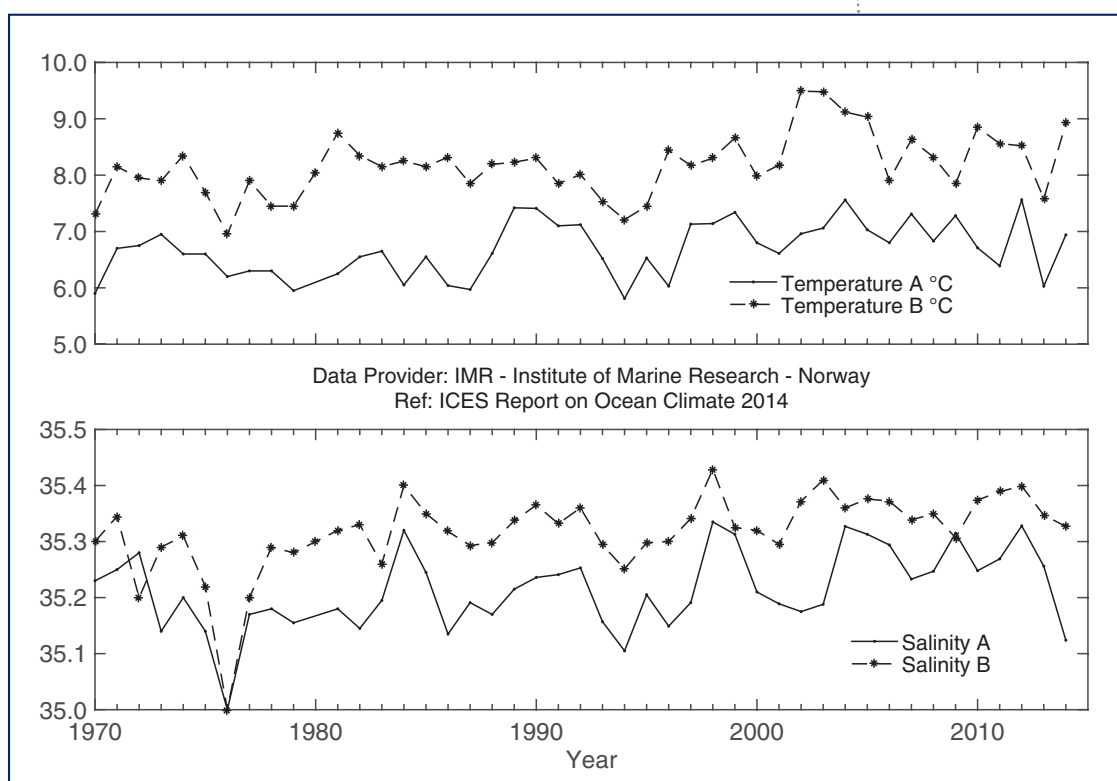
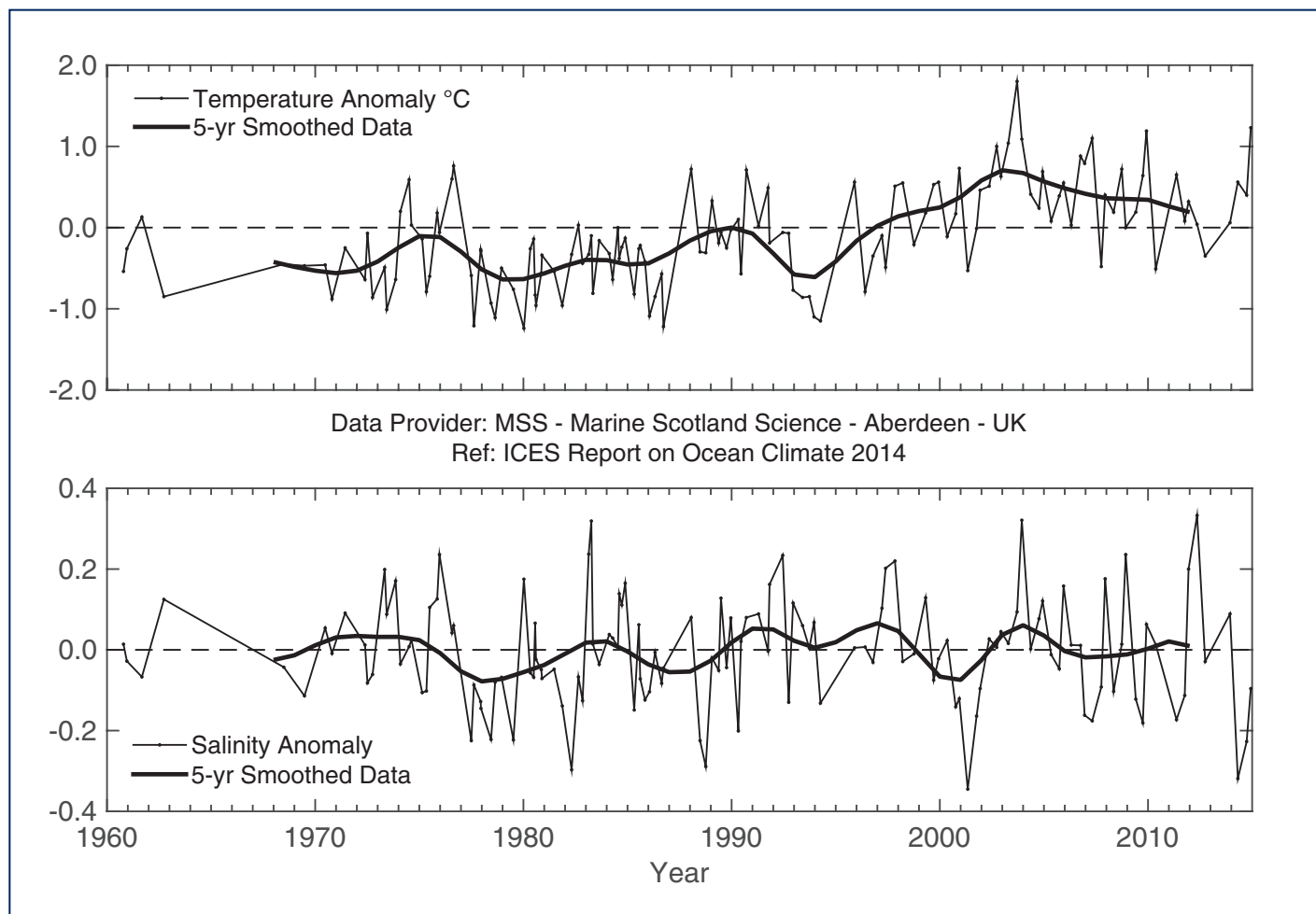
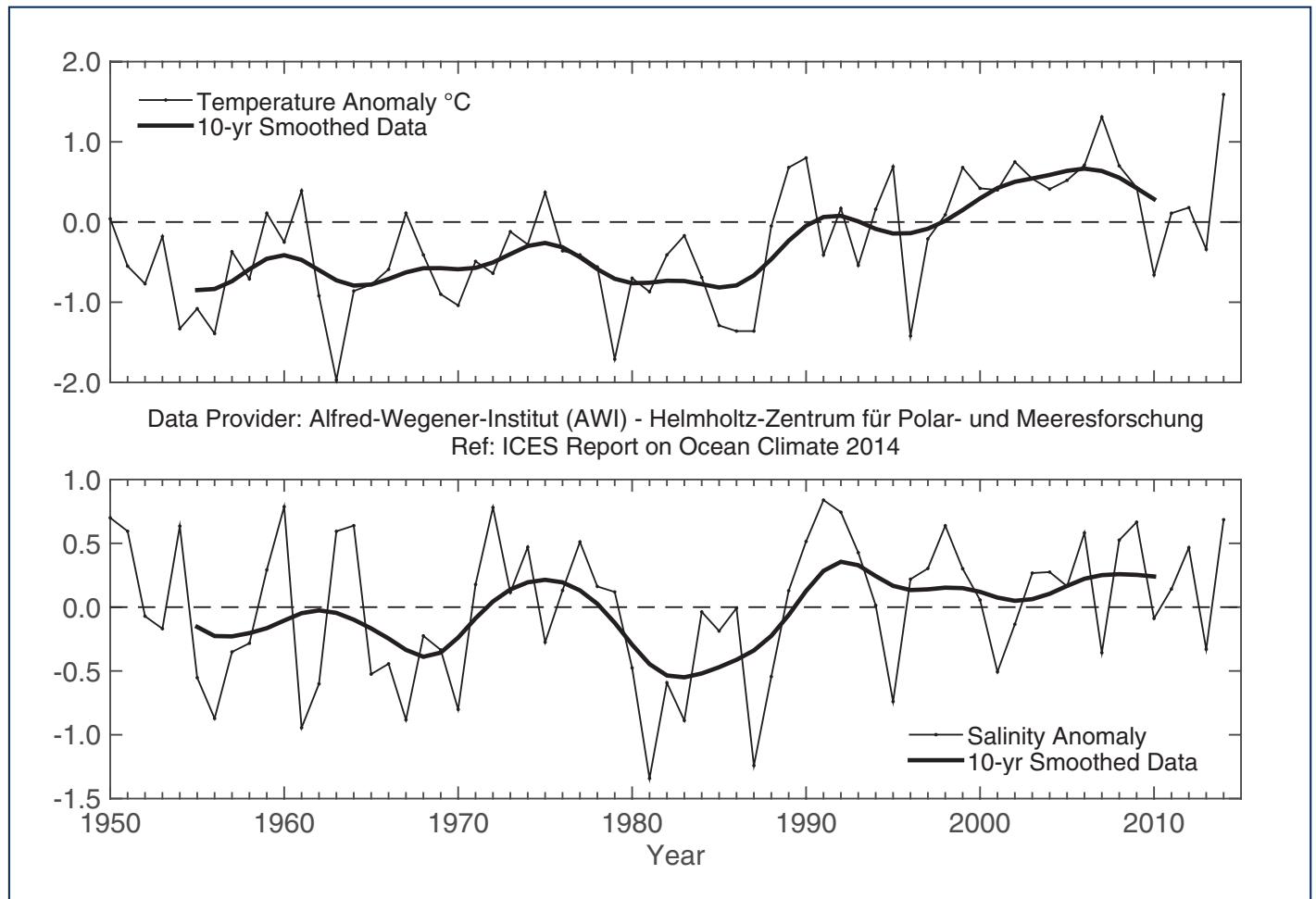


FIGURE 55



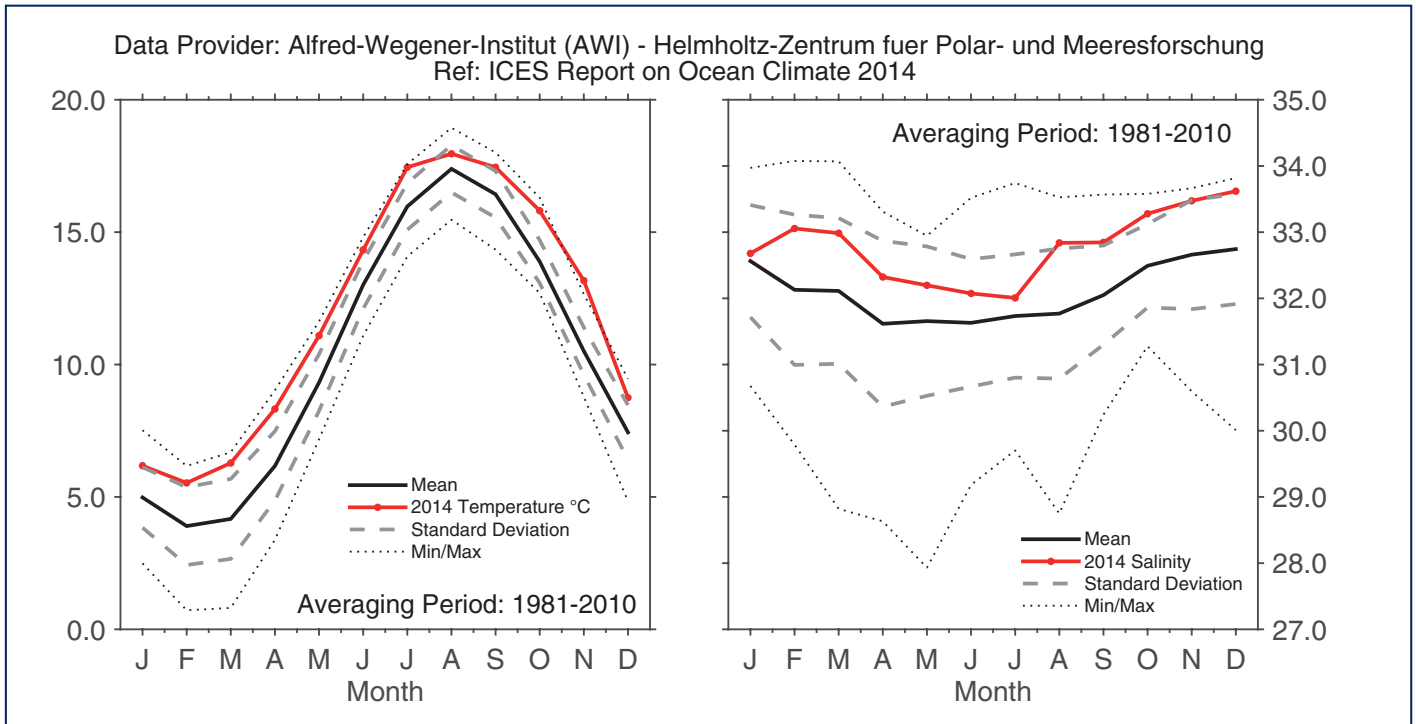
Area 8 - Northern North Sea. Temperature anomaly (upper panel) and salinity anomaly (lower panel) in the Fair Isle Current entering the North Sea from the North Atlantic.

FIGURE 56



Area 9 - Southern North Sea. Annual mean surface temperature anomaly (upper panel) and salinity anomaly (lower panel) at Station Helgoland Roads.

FIGURE 57



Area 9 - Southern North Sea. 2009 monthly surface temperature (left panel) and salinity (right panel) at Station Helgoland Roads.

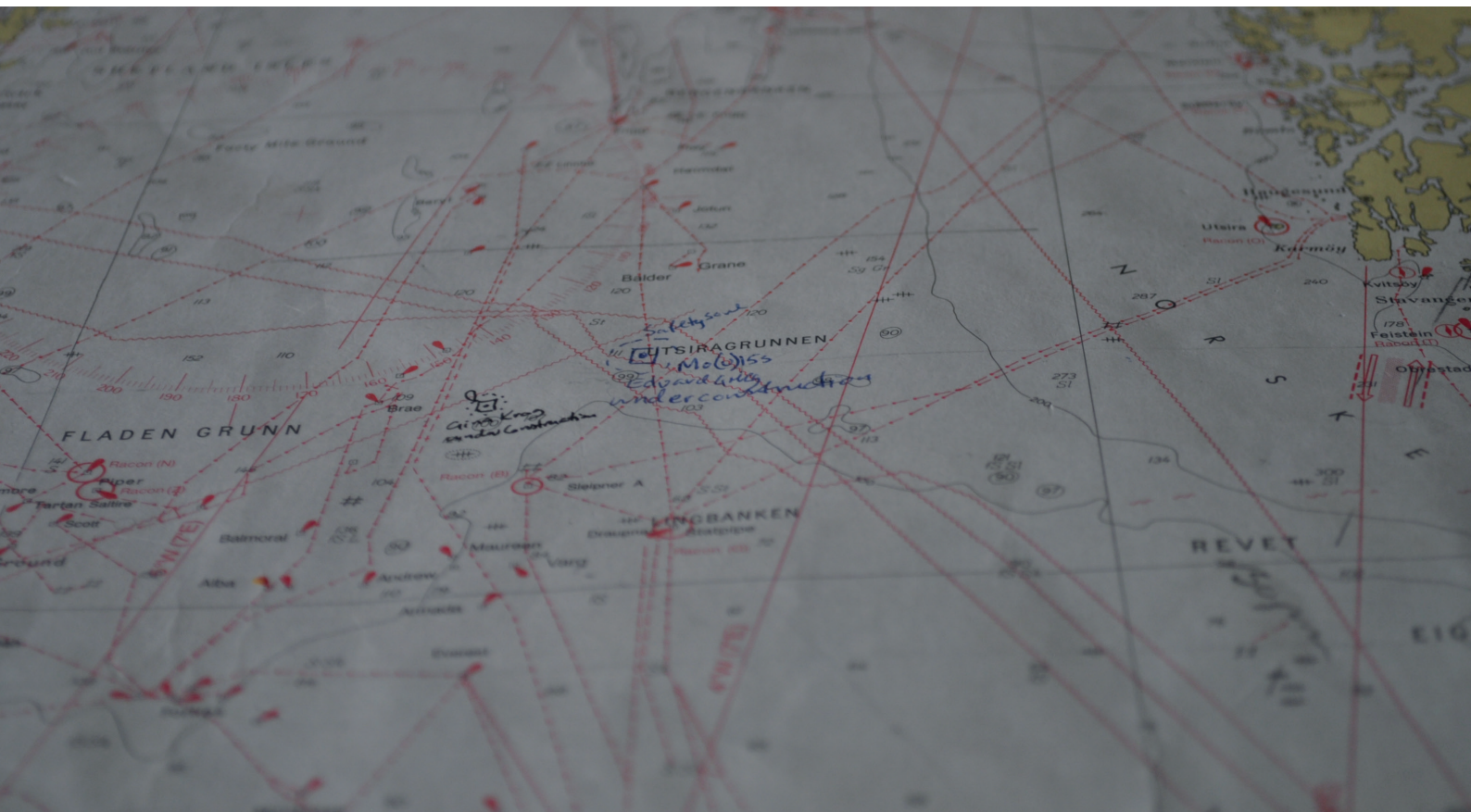
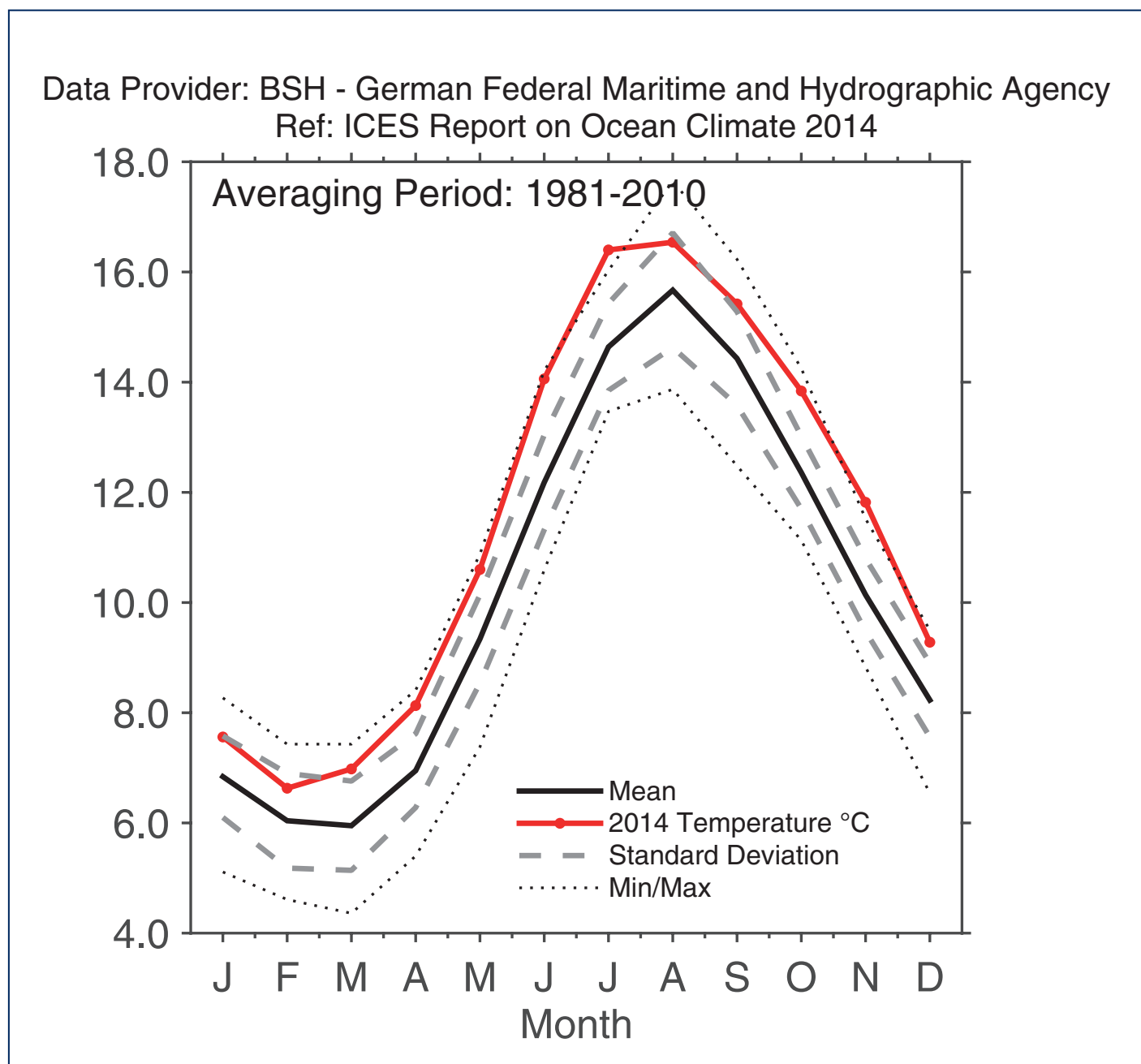


FIGURE 58



Areas 8 and 9 - Northern and southern North Sea. North Sea area-averaged sea surface temperature (SST) annual cycle; 2014 monthly means based on operational weekly North Sea SST maps.

4.13 AREA 9B – SKAGERRAK, KATTEGAT, AND THE BALTIC

The seas in Area 9b are characterized by large salinity variations. In the Skagerrak, water masses from different parts of the North Sea are present. The Kattegat is a transition area between the Baltic and the Skagerrak. The water is strongly stratified, with a permanent halocline (sharp change in salinity at depth). The deep water in the Baltic proper, which enters through the Belts and the Sound, can be stagnant for long periods in the inner basins. In the relatively shallow area in the southern Baltic, smaller inflows pass relatively quickly, and the conditions in the deep water are extremely variable. Surface salinity is very low in the Baltic proper and its gulfs. The Gulf of Bothnia and the Gulf of Finland are ice-covered during winter.

Owing to its central location relative to the Skagerrak, Kattegat, and Baltic, the weather in Sweden can be taken as representative of the area. The yearly mean temperature in 2014 was the highest recorded since 1860 when the time-series started. In February, the anomaly in the northernmost parts of Sweden almost reached 11°C. June was the only month when most of the country had temperatures below normal. For the whole year, precipitation was somewhat higher than normal in the south and lower than normal in the north, i.e. quite the opposite of the previous year. The number of sun hours was above normal.



Sea surface temperatures were above normal for most of the year in the whole area. The only exception was at the beginning of the year when low temperatures were found in Skagerrak and Kattegat due to large outflows of cooler Baltic Sea water. The effect of the outflows was also seen in the surface salinity which was unusually low in Skagerrak and Kattegat during January and February. For the rest of the year, salinity exhibited normal variations for this region. In the southern part of the Baltic proper, surface salinities were normal. The freshening of surface water in the eastern parts of the Gotland Basin that was noted last year prevailed for the entire year. Although observations in this paragraph are limited to surface values, it is worth noting that temperature in the upper 100 m in Skagerrak in November was 1–4 °C above normal.

In autumn, high-pressure conditions, with an associated longer period of outflows, lowered the sea level in the Baltic to about 40 cm below normal, resulting in the right preconditions for a major inflow. In December, several low-pressure systems with southwesterly winds forced saline water into the Baltic. During this period, an inflow volume of approximately 70 km³ entered through Öresund, with an additional inflow of 30 km³ at the beginning of 2015. (About one-third of the total inflow to the Baltic is transported through Öresund, while two-thirds enters through the Danish Straits.) The last major inflow was in 2003. The effects of the inflow on oxygen conditions in the Baltic Sea will be followed closely in the coming year.

The ice season 2013/2014 was mild, with a maximum ice extent of 93 000 km² achieved on 7 February. The ice began to form in mid-November, but because of the mild and windy start of winter, it was not until late January that the Bothnian Bay was ice covered. Mild weather conditions in February and subsequent months shortened the ice season somewhat, and the Bothnian Bay was ice-free around 14 May.

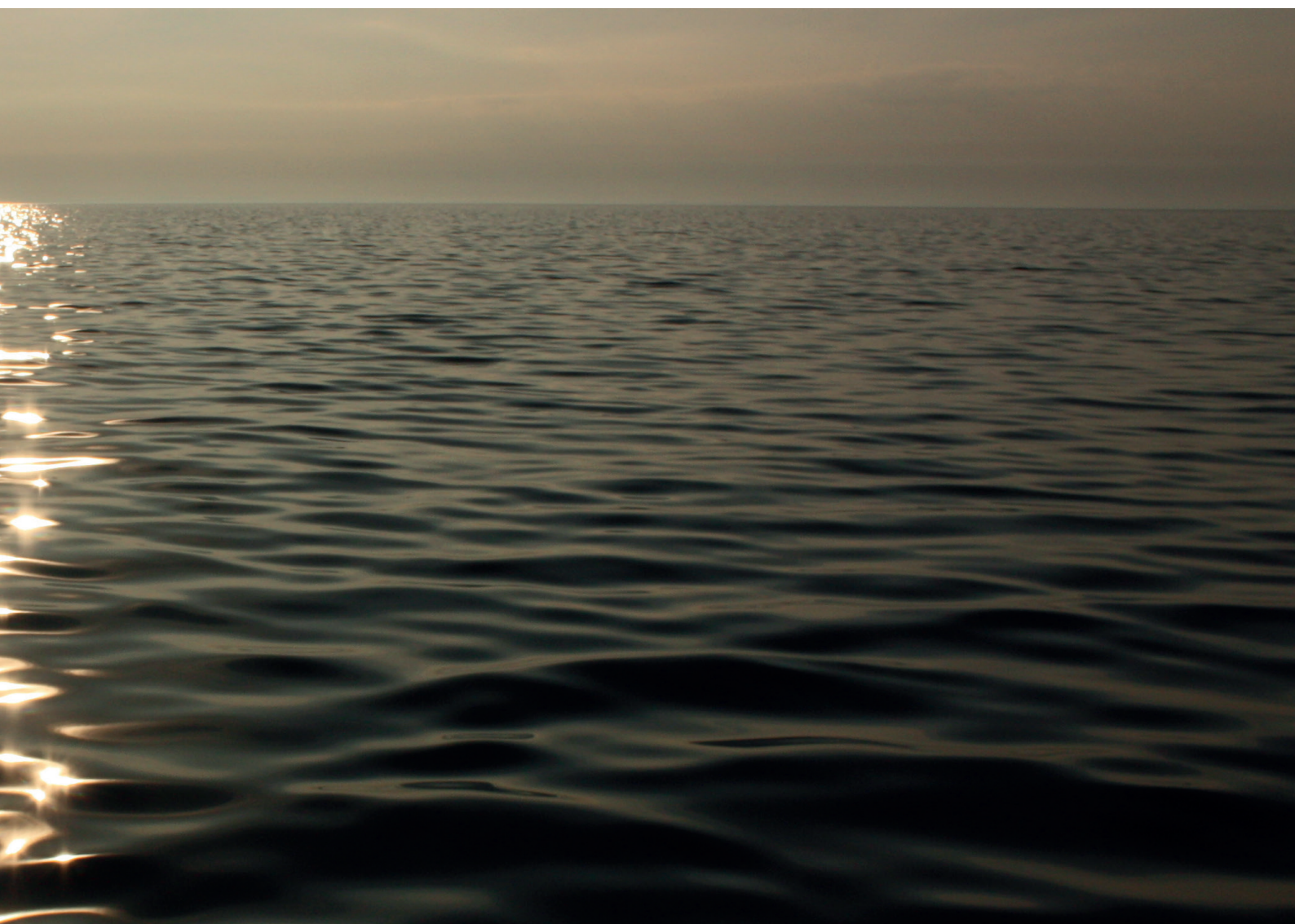
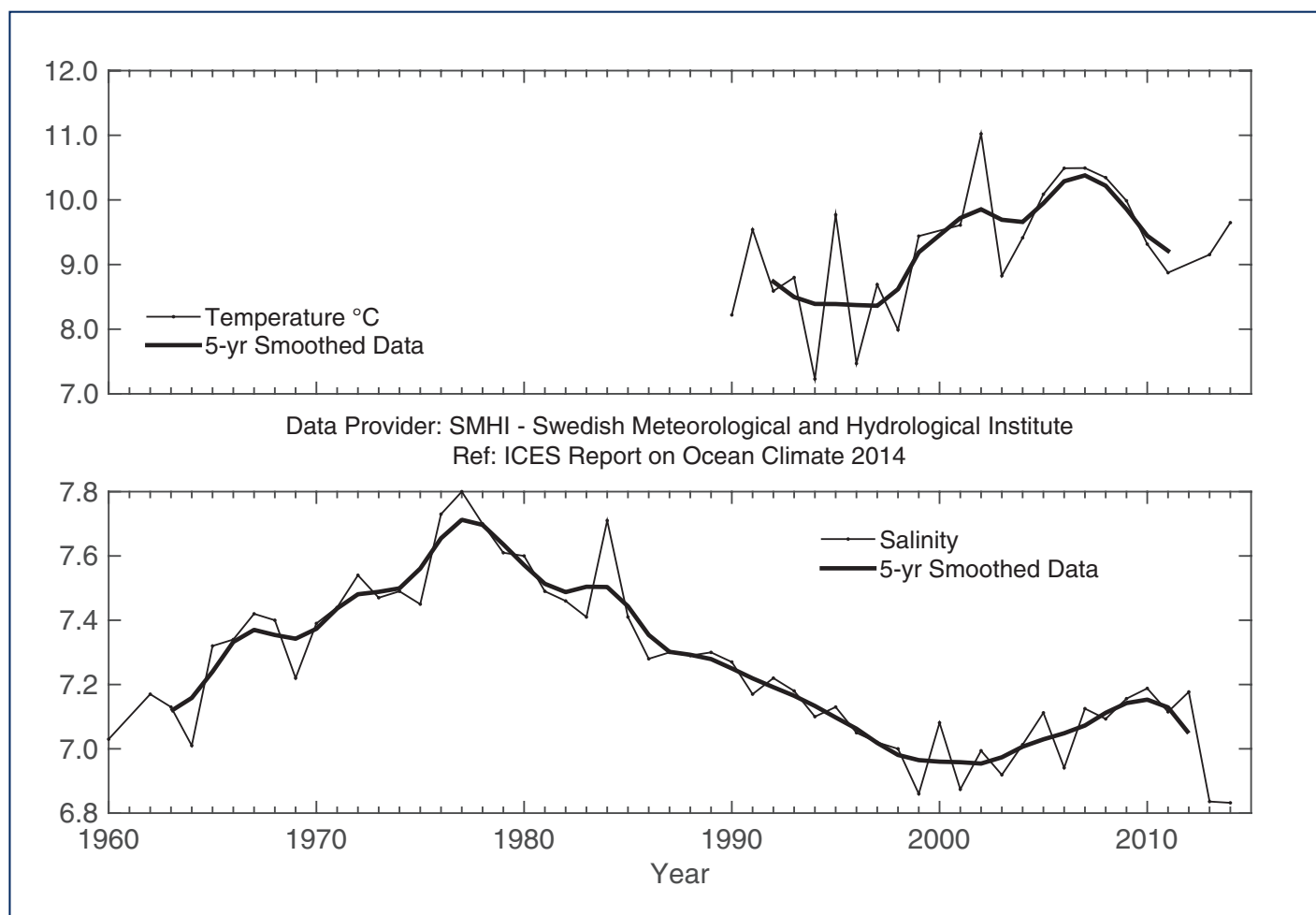
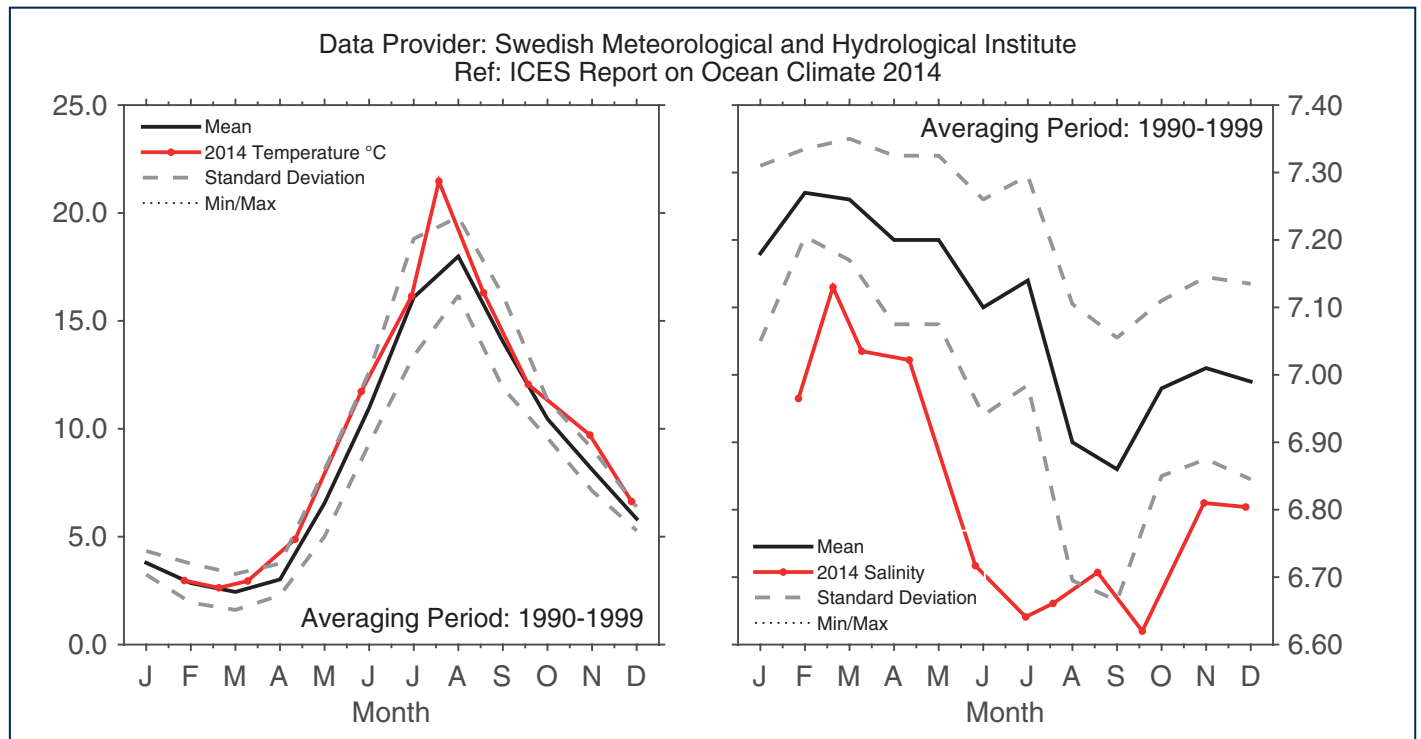


FIGURE 59



Area 9b - Skagerrak, Kattegat, and the Baltic. Surface temperature, yearly mean (upper panel) and surface salinity, yearly mean (lower panel) at Station BY15 (east of Gotland) in the Baltic proper.

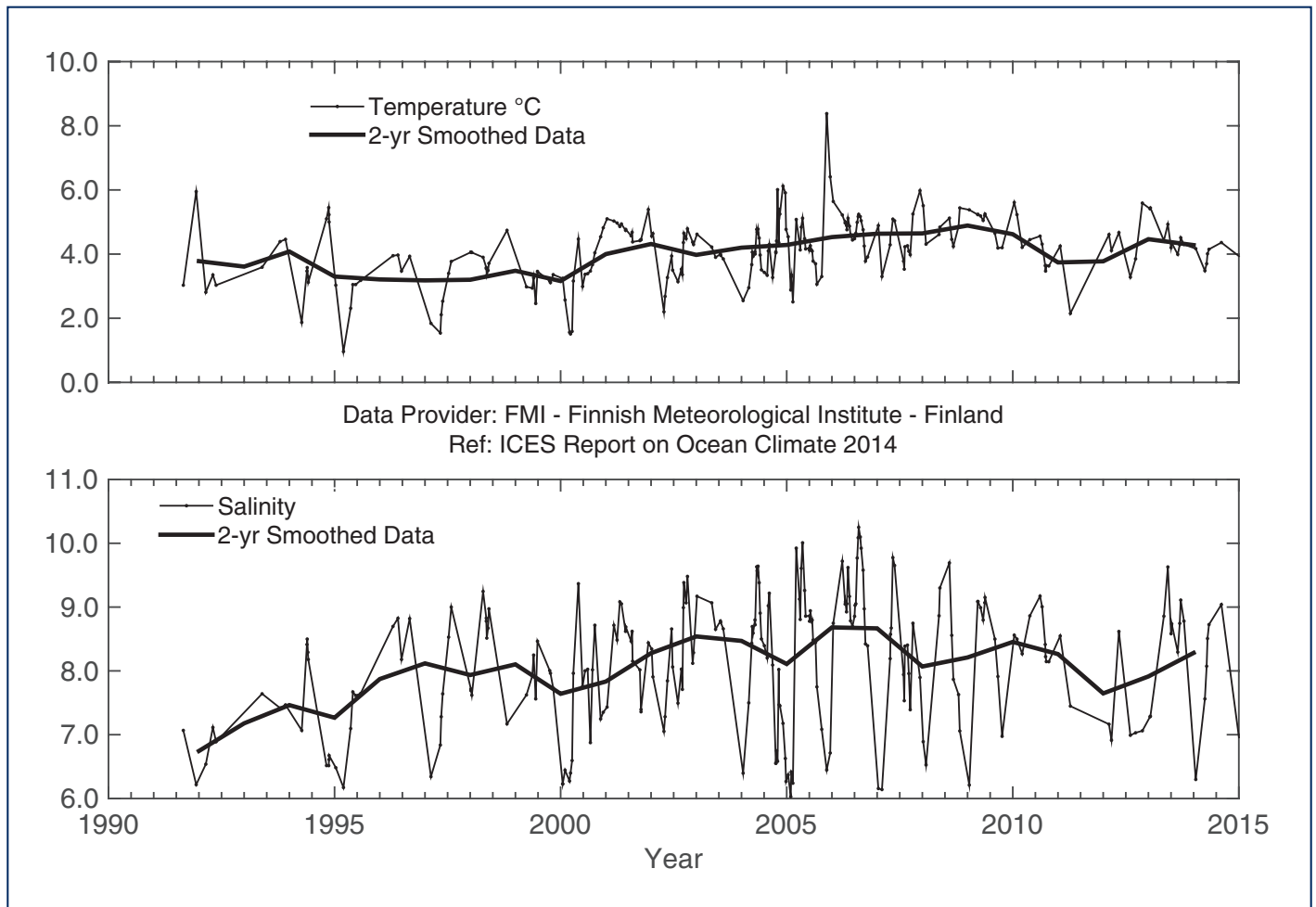
FIGURE 60



Area 9b - Skagerrak, Kattegat, and the Baltic. Monthly surface temperature (left panel) and salinity (right panel) at Station BY15 (east of Gotland) in the Baltic proper.

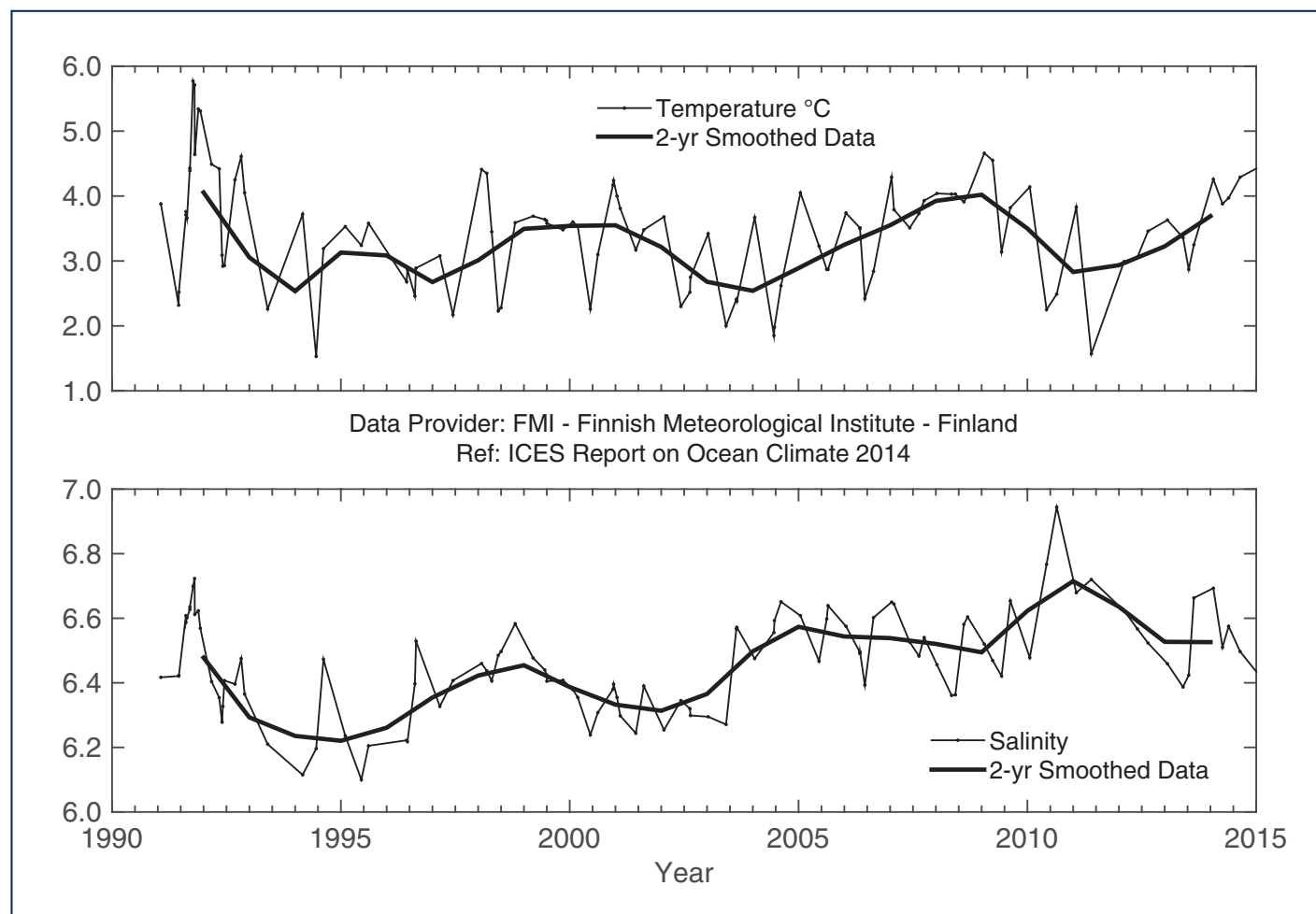
A MAJOR INFLOW TO THE BALTIC SEA TOOK PLACE AT THE END OF 2014 AND SEA SURFACE TEMPERATURES WERE HIGHER THAN NORMAL FOR MOST OF THE YEAR.

FIGURE 61



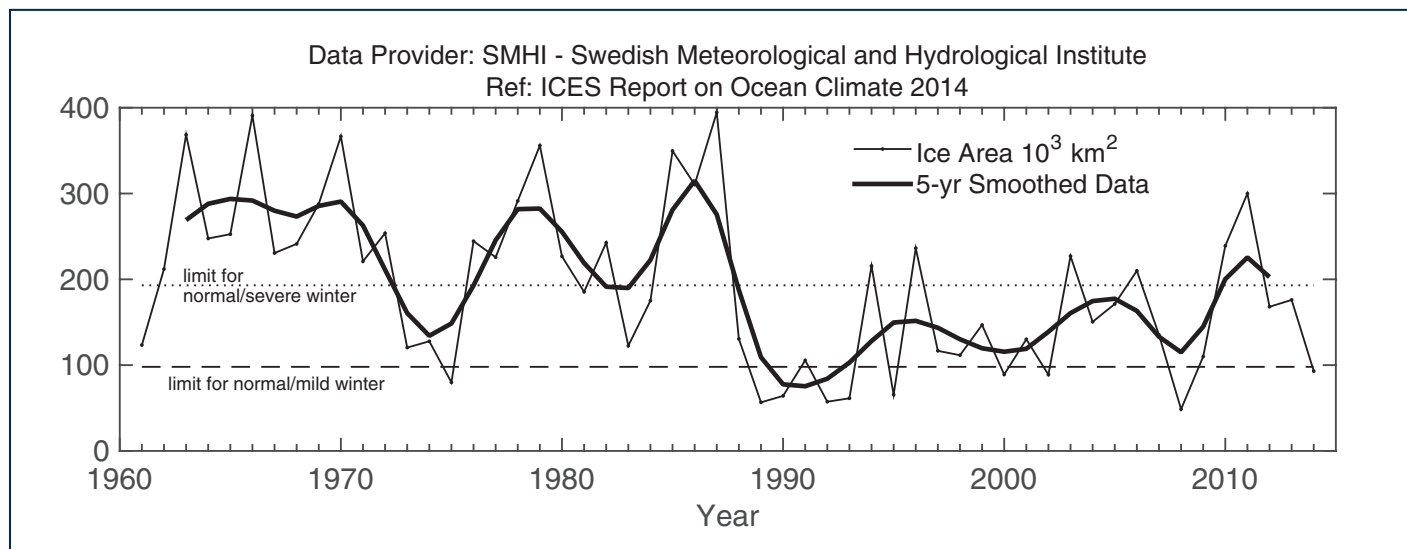
Area 9b - Skagerrak, Kattegat, and the Baltic. Temperature (upper panel) and salinity (lower panel) at Station LL7 in the Gulf of Finland.

FIGURE 62



Area 9b - Skagerrak, Kattegat, and the Baltic. Temperature (upper panel) and salinity (lower panel) at Station SR5 in the Bothnian Sea.

FIGURE 63



Area 9b - Skagerrak, Kattegat, and the Baltic. The maximum ice extent in the Baltic starting from 1961.



4.14 AREA 10 – NORWEGIAN SEA

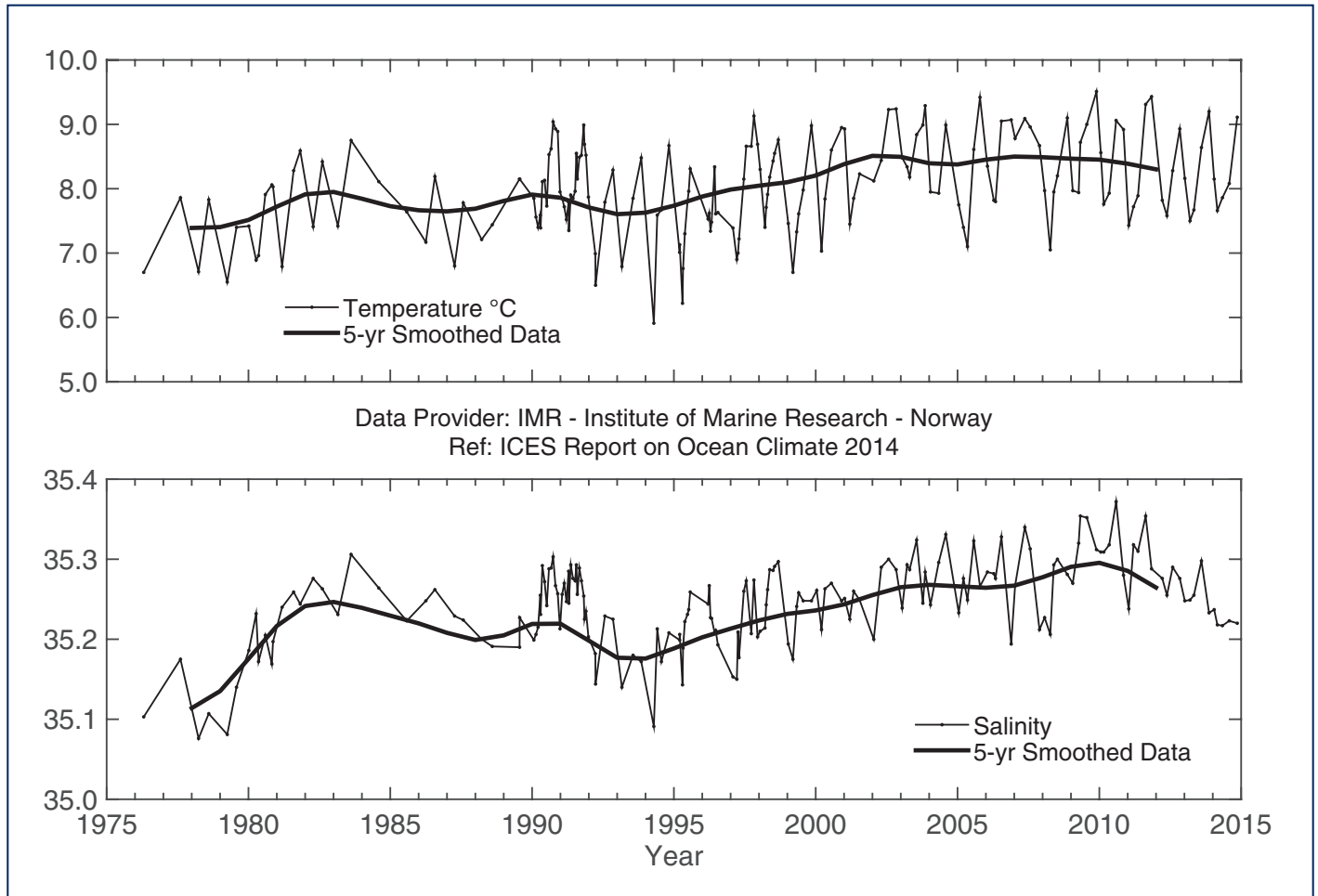
The Norwegian Sea is characterized by warm Atlantic water on the eastern side and cold Arctic water on the western side, separated by the Arctic front. Atlantic water enters the Norwegian Sea through the Faroe-Shetland Channel and between the Faroes and Iceland via the Faroe Front. A smaller branch, the North Icelandic Irminger Current, enters the Nordic seas on the western side of Iceland. Atlantic water flows north as the Norwegian Atlantic Current, which splits when it reaches northern Norway; some enters the Barents Sea, whereas the rest continues north into the Arctic Ocean as the West Spitsbergen Current.

Three sections from south to north in the eastern Norwegian Sea demonstrate the development of temperature and salinity in the core of the Atlantic water (AW) at Svinøy-NW, Gimsøy-NW, and Sørkapp-W. In general, there has been an increase in temperature and salinity in all three sections since the mid-1990s, except for the most recent years when both temperature and salinity declined. In 2014, salinity was close to normal in the two southernmost sections and still above the long-term mean in the northernmost section. Temperature was close to the long-term averages in all three sections. Annual temperature averages in 2014 were 0.2°C above the long-term means at the Svinøy and Gimsøy sections, and 0.3°C above the long-term mean in the Sørkapp section. Salinity averages in 2014 were 0.01 below the long-term mean in the Svinøy section, and 0.01 and 0.05 above the long-term means in the Gimsøy and Sørkapp sections, respectively.

ABOUT AVERAGE TEMPERATURE AND SALINITY IN THE NORWEGIAN SEA IN 2014.

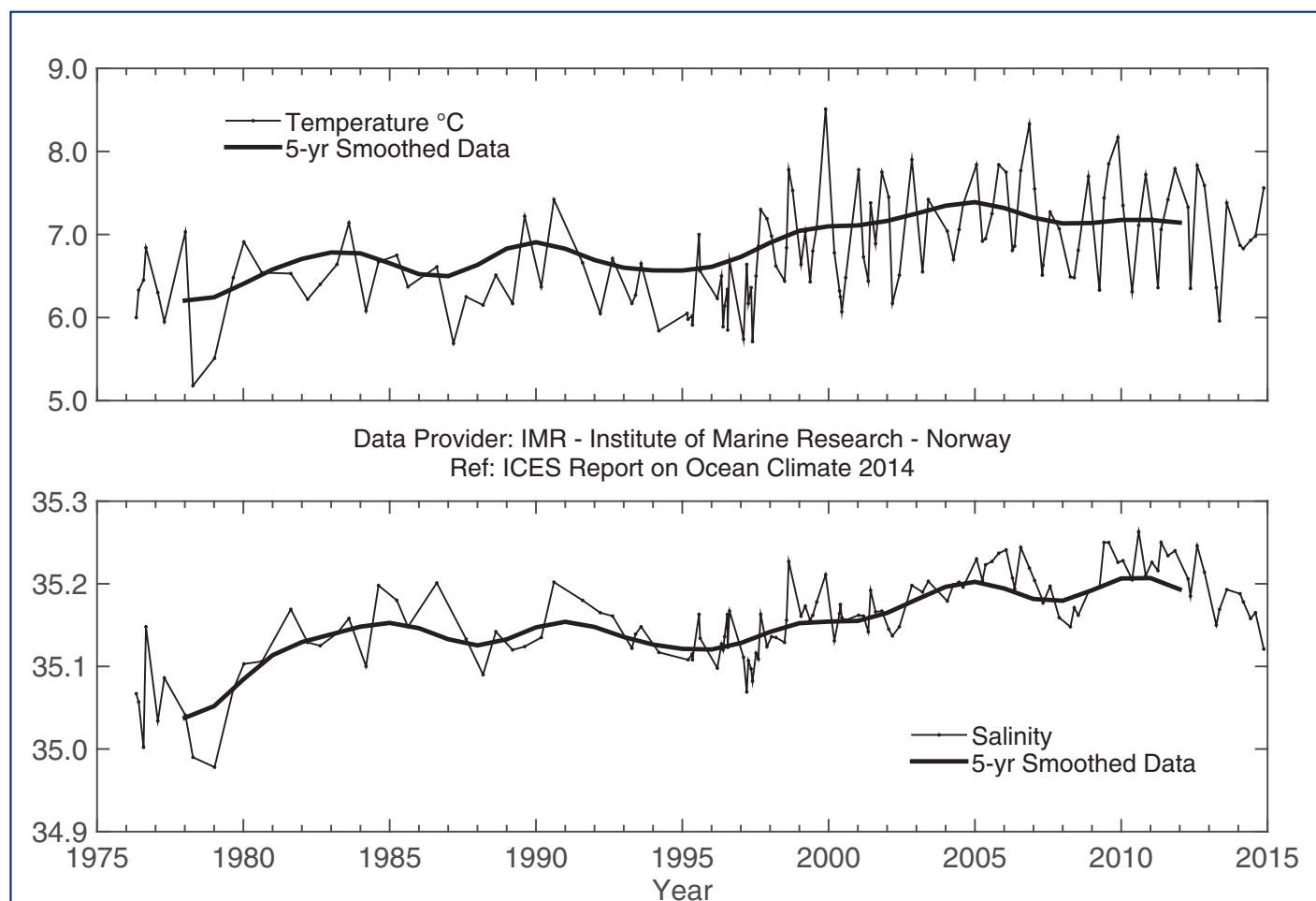


FIGURE 64



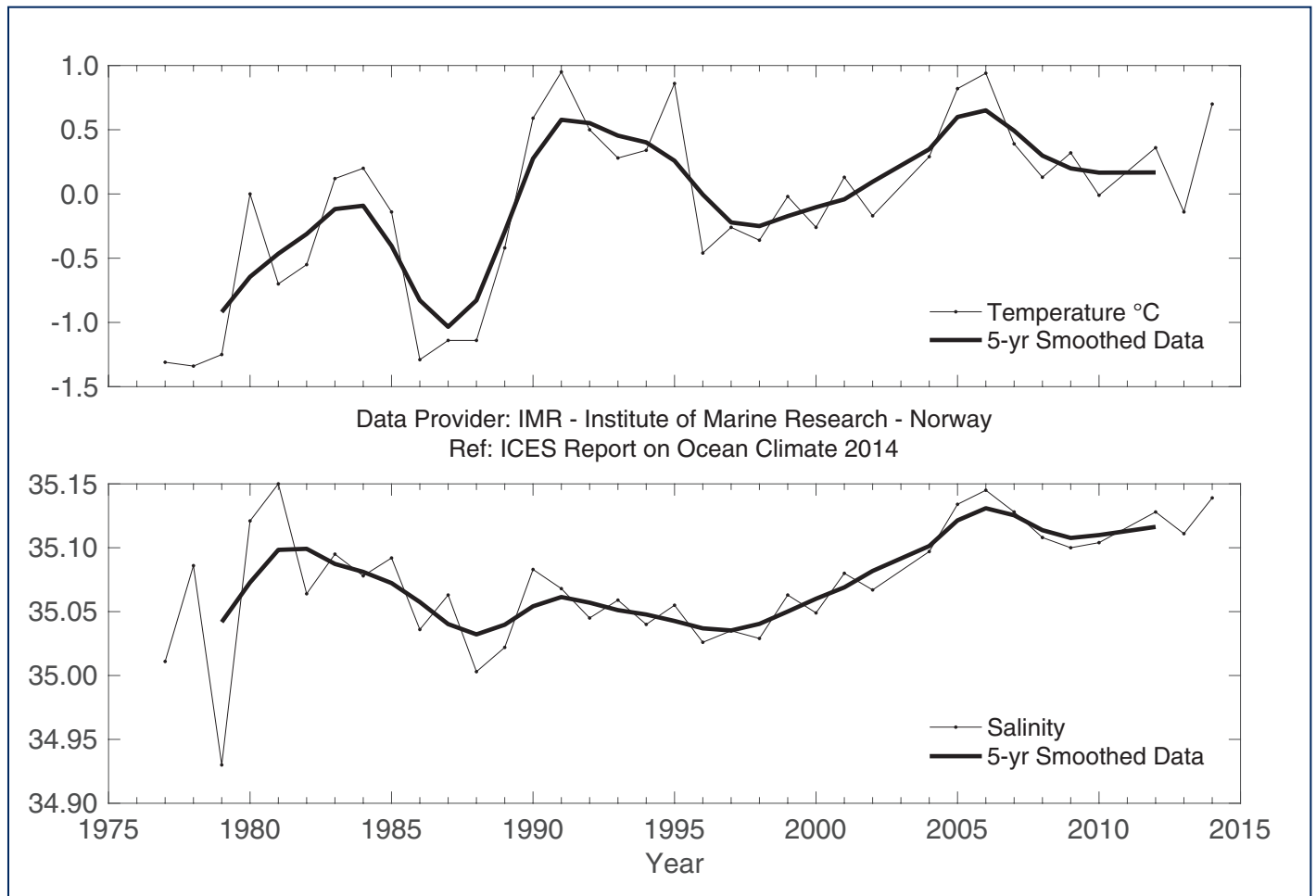
Area 10 - Norwegian Sea. Temperature (upper panel) and salinity (lower panel) above the slope at the Svinøy Section (63°N).

FIGURE 65



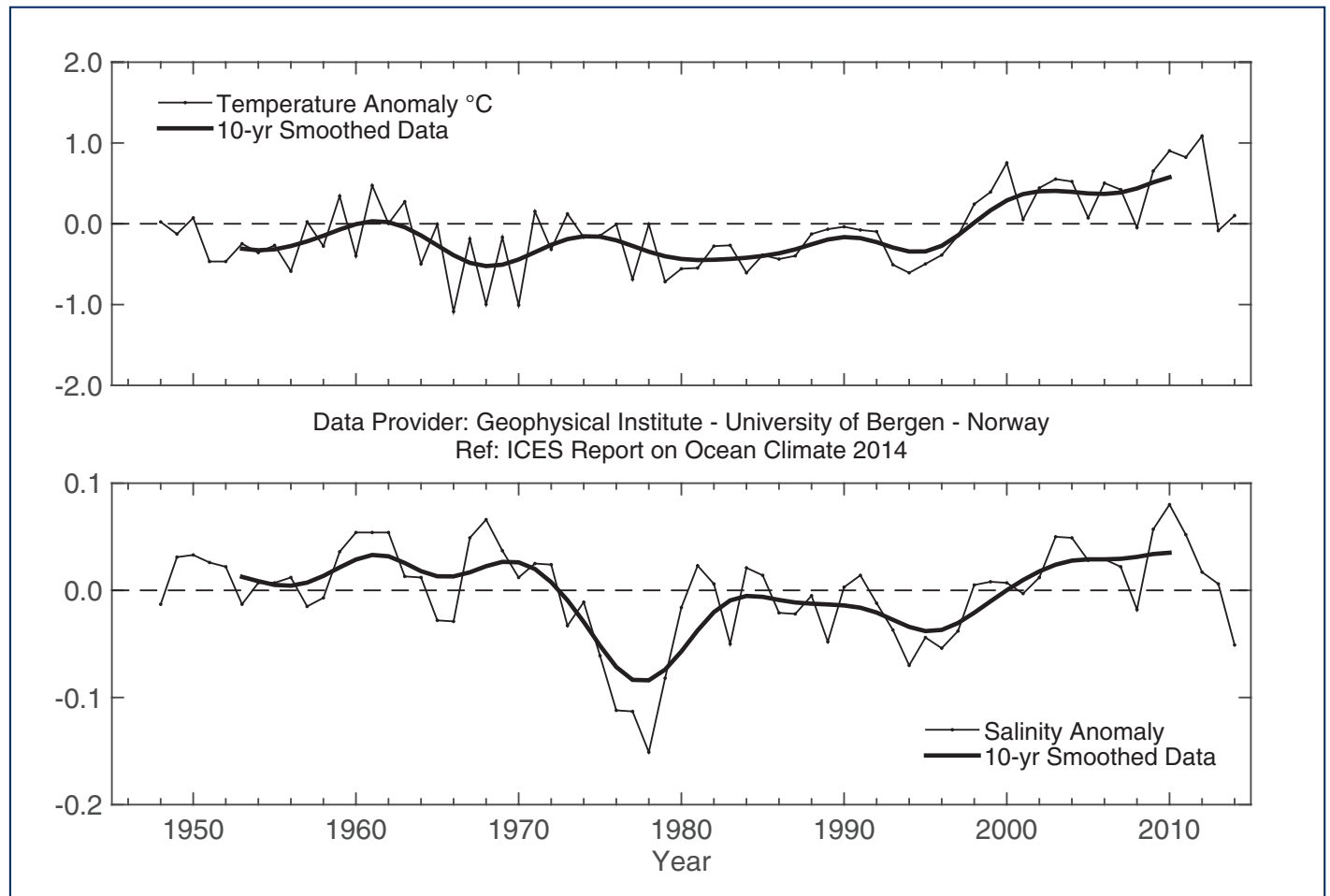
Area 10 - Norwegian Sea. Temperature (upper panel) and salinity (lower panel) above the slope at the Gimsøy Section (69°N).

FIGURE 66



Area 10 - Norwegian Sea. Temperature (upper panel) and salinity (lower panel) above the slope at the Sørkapp Section (76°N).

FIGURE 67



Area 10 - Norwegian Sea. Temperature anomaly (upper panel) and salinity anomaly (lower panel) at 50 m at Ocean Weather Station "M" (66°N 2°E).

4.15 AREA 11 – BARENTS SEA

The Barents Sea is a shelf sea, receiving an inflow of warm Atlantic water from the west. The inflow demonstrates considerable seasonal and interannual fluctuations in volume and water mass properties, causing high variability in heat content and ice coverage of the region.

In 1996 and 1997, after a period with high temperatures in the first half of the 1990s, temperatures in the Barents Sea dropped to values slightly below the long-term average. From March 1998, temperature in the western Barents Sea increased to just above average, whereas temperature in the eastern part remained below average during 1998. From the beginning of 1999, there was a rapid temperature increase in the western Barents Sea that also spread to the eastern part. Since then, temperature has remained above average.

During 2013 and 2014, temperatures in the Barents Sea were still higher than normal by up to 1.6°C in 2013 and by up to 1.3°C in 2014, which was typical of warm and anomalously warm years. In 2013, surface waters were extremely warm from July to October; the 0-50 m layer temperature in the Kola Section was the highest since 1951 because of enhanced seasonal warming. The deeper layers in 2013 were also warmer than normal, but colder than in 2012. In the first half of 2014, Atlantic water in the Kola Section (0-200 m) was 0.6-0.8°C warmer than normal. From June to November 2014, temperature anomalies decreased down to 0.1°C, but then increased again to 0.5°C by the end of the year. Annual mean temperature of Atlantic water in the Kola Section was 5.4°C in 2012, 4.9°C in 2013, and 4.7°C in 2014, which was well above normal (4.2°C). Annual mean salinity of Atlantic water in the Kola Section was close to normal (34.77) in 2012 (34.79), 2013 (34.77), and 2014 (34.78).

In August-September 2013, surface waters in most of the Barents Sea were much warmer than average (by 2.0-3.3°C) and warmer than in 2012 (by 1.3-2.7°C). Surface temperatures were the highest since 1951 in about 50% of the Barents Sea. Temperatures below 100 m were mostly 0.5-1.2°C higher than average, but 0.5-1.2°C lower than in 2012. In August-September 2014, surface waters were 0.5-1.3°C warmer and 0.2-0.6 saltier than average, but fresher and much colder



than in 2013 in most of the Barents Sea. Negative temperature anomalies were found only in the northeastern part of the sea. Negative salinity anomalies were observed south of 73°N and in the northern part of the sea near the ice edge. All over the Barents Sea deeper and bottom waters were 0.5–1.1°C warmer and slightly saltier (by up to 0.1) than average. The area occupied by water with temperatures below zero was much larger in autumn 2013 than in 2012, and decreased slightly in 2014.

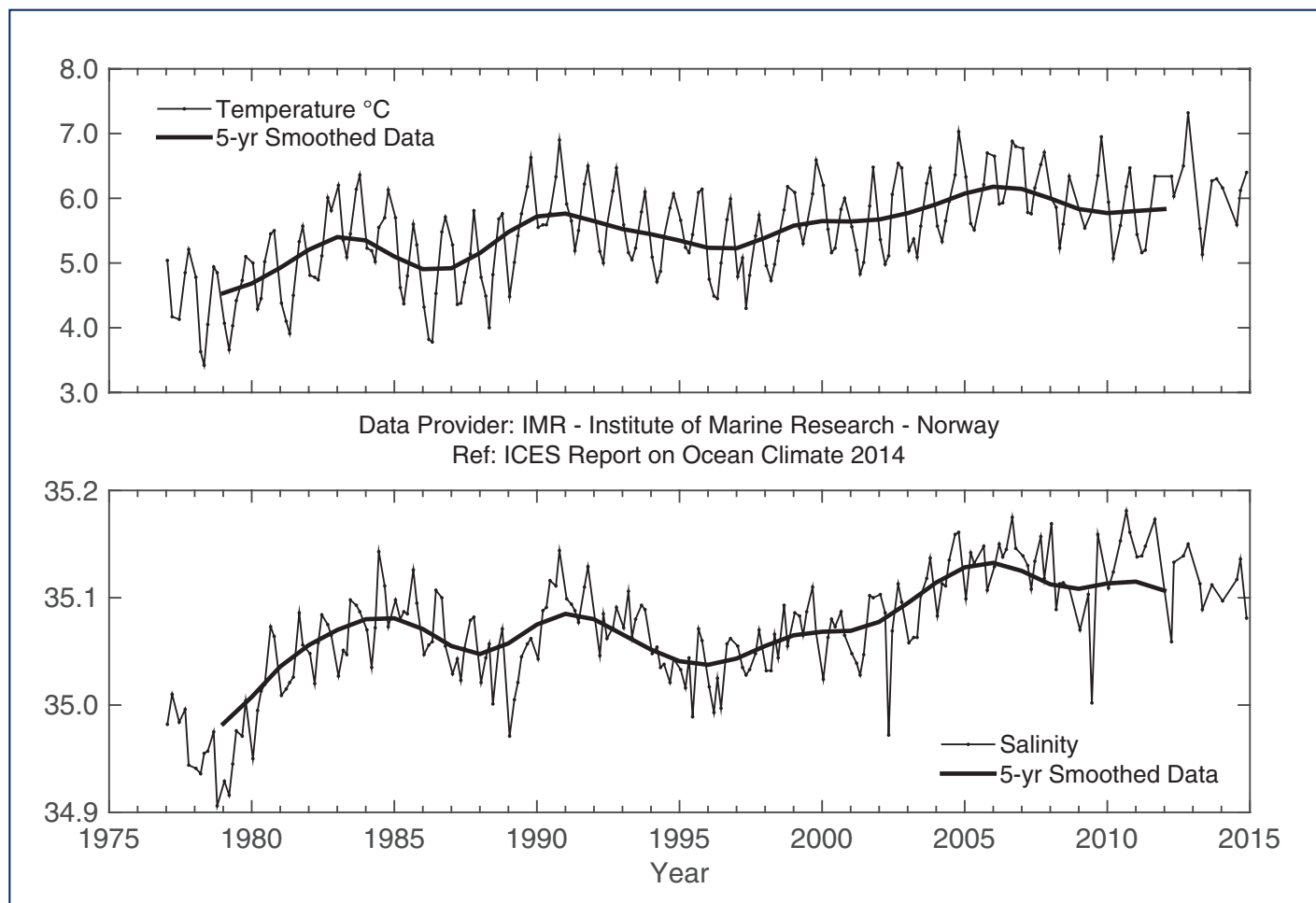
Throughout 2013, ice coverage of the Barents Sea was still lower than average, but higher than in 2012. In August and September 2013, there was no ice in the Barents Sea; the ice edge was located much farther north than usual – at ca. 84°N. In winter 2014, ice coverage was mainly lower than average. For the first time since 2004, ice coverage in 2014 was close to or above average for five consecutive months. In September 2014, ice coverage was the highest for this month in the last 20 years.

The volume flux into the Barents Sea varies by periods of several years and was significantly lower in 1997–2002 than in 2003–2006. In 2006, the volume flux was at a maximum during winter and very low during autumn. Since 2006, inflow has been relatively low. During autumn 2011 and winter 2012, inflow was particularly low, but thereafter increased during spring 2013. During autumn 2013, inflow was close to average. At the start of 2014, inflow was low, but increased somewhat during late winter and early spring 2014. The present data series stops in spring 2014; thus no information about autumn and early winter 2014 is available.

STILL LOWER-THAN-NORMAL ICE COVERAGE AND ABOVE-NORMAL TEMPERATURES IN THE BARENTS SEA IN 2013 AND 2014.

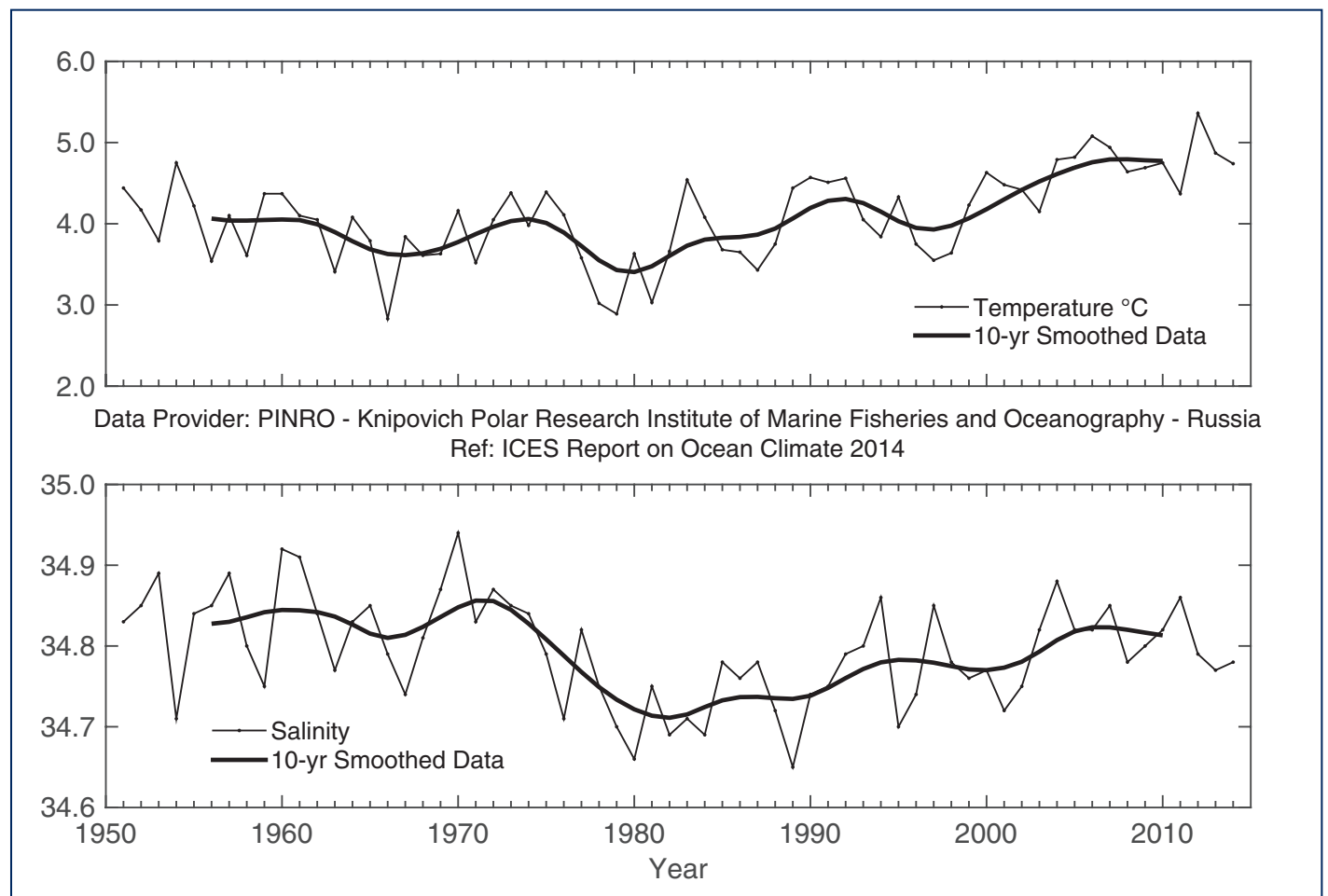


FIGURE 68



Area 11 - Barents Sea. Temperature (upper panel) and salinity (lower panel) in the Fugløya-Bear Island Section.

FIGURE 69



Area 11 - Barents Sea. Temperature (upper panel) and salinity (lower panel) in the Kola Section (0-200 m).

4.16 AREA 12 – GREENLAND SEA AND FRAM STRAIT

Fram Strait is the northern border of the Nordic seas. It is the deepest passage connecting the Arctic to the rest of the world's ocean and one of the main routes whereby Atlantic water (AW) enters the Arctic (the other is the Barents Sea). The AW is carried northwards by the West Spitsbergen Current, and volume and heat fluxes exhibit strong seasonal and interannual variations. A significant part of the AW also recirculates within Fram Strait and returns southward (return Atlantic water). Polar water from the Arctic Ocean flows south in the East Greenland Current and affects water masses in the Nordic seas.

The Greenland Sea section at 75°N has not been measured since 2010. The most recent data in 2010 showed that the temperature of Atlantic water (AW) at the eastern rim of the Greenland Sea (along the 75°N section between 10° and 13°E) was similar to that observed in 2008 (no data for 2009) and close to the long-term mean. A significant increase in salinity was observed compared with 2008 and, since 2004, salinity of AW has remained higher than its long-term average. At the western rim of the Greenland Sea, the temperature of return Atlantic water (RAW) was slightly lower in 2010 than in 2009, whereas salinity remained similar to the 2009 value. Both values were close to their long-term means. Temperature and salinity in the upper layer of the central Greenland Basin, within the Greenland Sea Gyre, were modified by the advection of AW and winter convection. The interface with enhanced temperature and salinity gradients has steadily descended (by more than 1000 m) since the beginning of measurements in 1993. After winter 2007/2008, a two-layer structure resulted from a mixed-layer type convection that supplied both salt and heat into the intermediate layers. In winter 2008/2009, almost half of the Greenland Sea was shielded from convection because of the unusual western location of the Arctic Front (boundary between Atlantic and Greenland Sea waters).

In recent years, the hydrography in the Greenland Sea has been characterized by the increasing and overwhelming influence of AW inflow. This trend continued in the western half of the Greenland Sea Gyre during 2009, but was interrupted by a freshwater event in the eastern half. Mean salinity in the central Greenland Sea in summer 2010 suggests that the high-salinity intrusion into the gyre centre had already surpassed its maximum. There was a tendency towards fresher waters in the gyre centre, but salinity was still higher than before 2004.

In the southern Fram Strait, a record-high summer temperature for AW was observed in 2006, after which both temperature and salinity decreased rapidly in 2007 and 2008, before increasing again in summer 2009. In summers 2013 and 2014, mean temperature at the standard section along 76.50°N (at the level of 200 dbar, spatially averaged between 9° and 12°E) was 3.22°C and 3.86°C, respectively; thus, a slight decrease in 2013 compared to previous years and a return to the average level in 2014. Similar to temperature, salinity in the southern Fram Strait dropped slightly in 2013 and increased again a year later (35.10 and 35.13, respectively), exceeding the long-term mean of 35.06 in both years. Both temperature and salinity trends for 1996–2014 were positive.

In the northern Fram Strait at the standard section along 78.83°N, three characteristic areas can be distinguished in relation to the main flows: the West Spitsbergen Current (WSC) between the shelf edge and 5°E, the Return Atlantic Current (RAC)

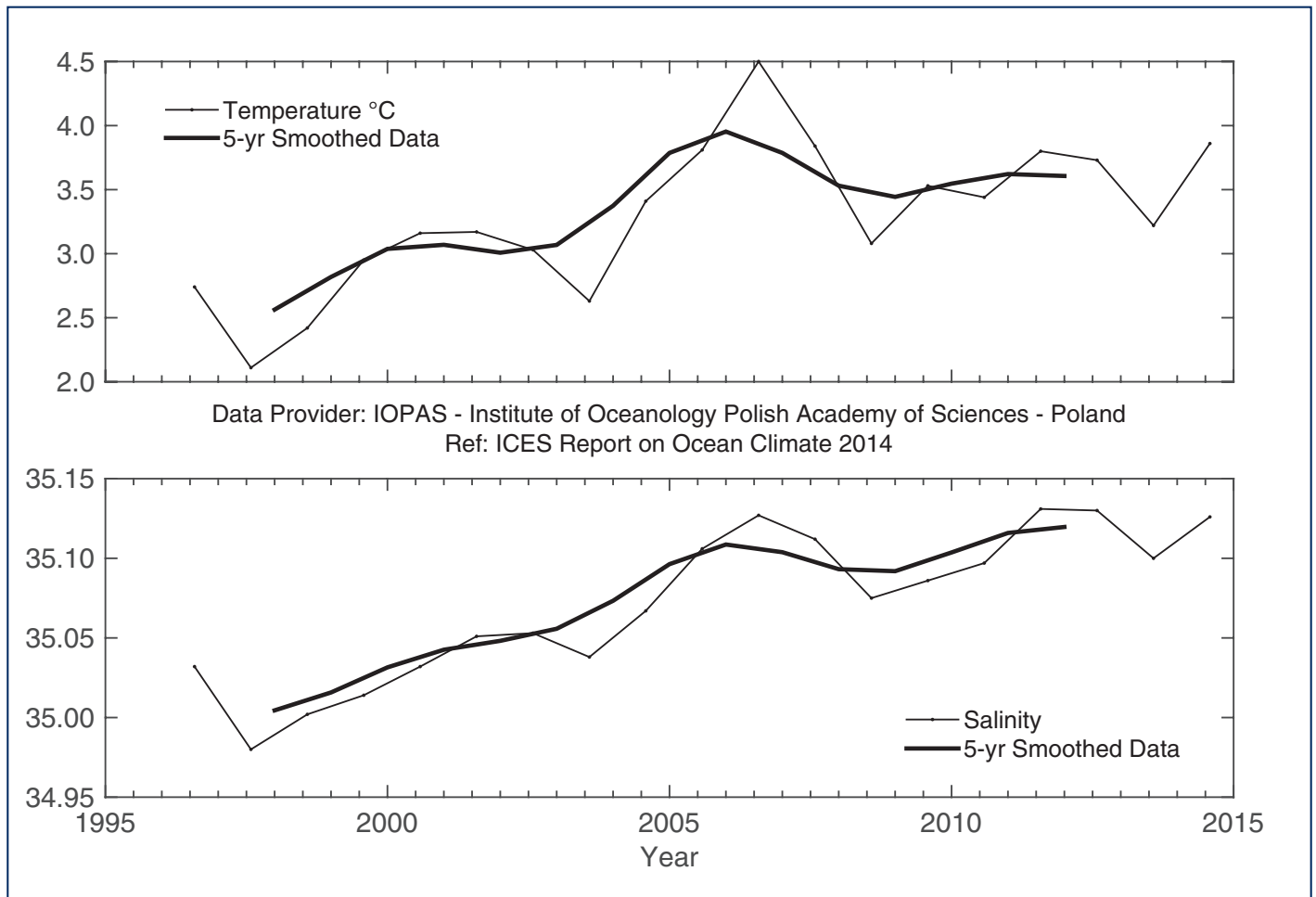
between 3°W and 5°E, and the polar water in the East Greenland Current (EGC) between 3°W and the Greenland Shelf. In 2013 and 2014, the spatially averaged mean temperature of the upper 500 m layer in the WSC increased compared to 2012 to 2.44°C and 3.28°C, respectively. Unlike 2012, this was 0.3–0.7°C warmer than the RAC, which was only minimally warmer than its long-term average. Mean temperature in the EGC domain decreased slightly compared to 2012. Salinity in the upper 500 m in the WSC was slightly lower in 2013 and higher in 2014 than in 2012. Salinity in the RAC in 2013 was 34.83, which was significantly below the long-term mean, but returned to mean in 2014. Salinity in the EGC continued its downward trend, reaching the two lowest values on record of 34.46 (2013) and 34.50 (2014).

In 2013 and 2014, the AW layer in the West Spitsbergen Current was deeper than the previous year. Over the upper shelf slope, the 0°C isotherm was shifted upwards to ca. 800 m (observed at ca. 1000 m in 2011 and ca. 600 m in 2012). The AW temperature in the WSC was warmer in the summers 2013/2014. In both years, water > 5°C was again observed. The AW mean temperature in the WSC (defined after Rudels *et al.* (2005) with $T > 2^{\circ}\text{C}$ and $27.7 < \sigma_{\theta} < 27.97$) was 3.02°C in 2013 and 3.51°C in 2014, respectively, compared to the maximum of 4.88°C observed in 2006. In the western deep part of the strait in the vicinity of the Polar Front, patches of recirculating AW were found, with maximum temperatures less than in 2009–2011 when much warmer water (with temperatures > 5°C and in 2009 even above 6°C) was carried by the Atlantic Return Current west and ultimately south. The position of the Polar Front between the Arctic-derived polar water and Atlantic water at the surface was near 1°W in 2013 and near 1°E in 2014, which was farther east than observed in the preceding years. The thickness of the polar water surface layer observed in 2013/2014 was similar to that in 2012.

In summer 2013, temperature in the core of the WSC was near its long-term mean, but significantly colder in the offshore branch. Conversely, in summer 2014, temperature in the entire WSC (in its core and offshore branch) was near its long-term mean. Salinity values were close to the long-term average. Above the lower continental slope east of Greenland, Arctic Atlantic water subducting below the polar water was also slightly warmer than the long-term average, while over the upper continental slope, weakly negative temperature anomalies were found throughout the water column. Temperature in the deep layer below 1000 m was close to average at the entire section.

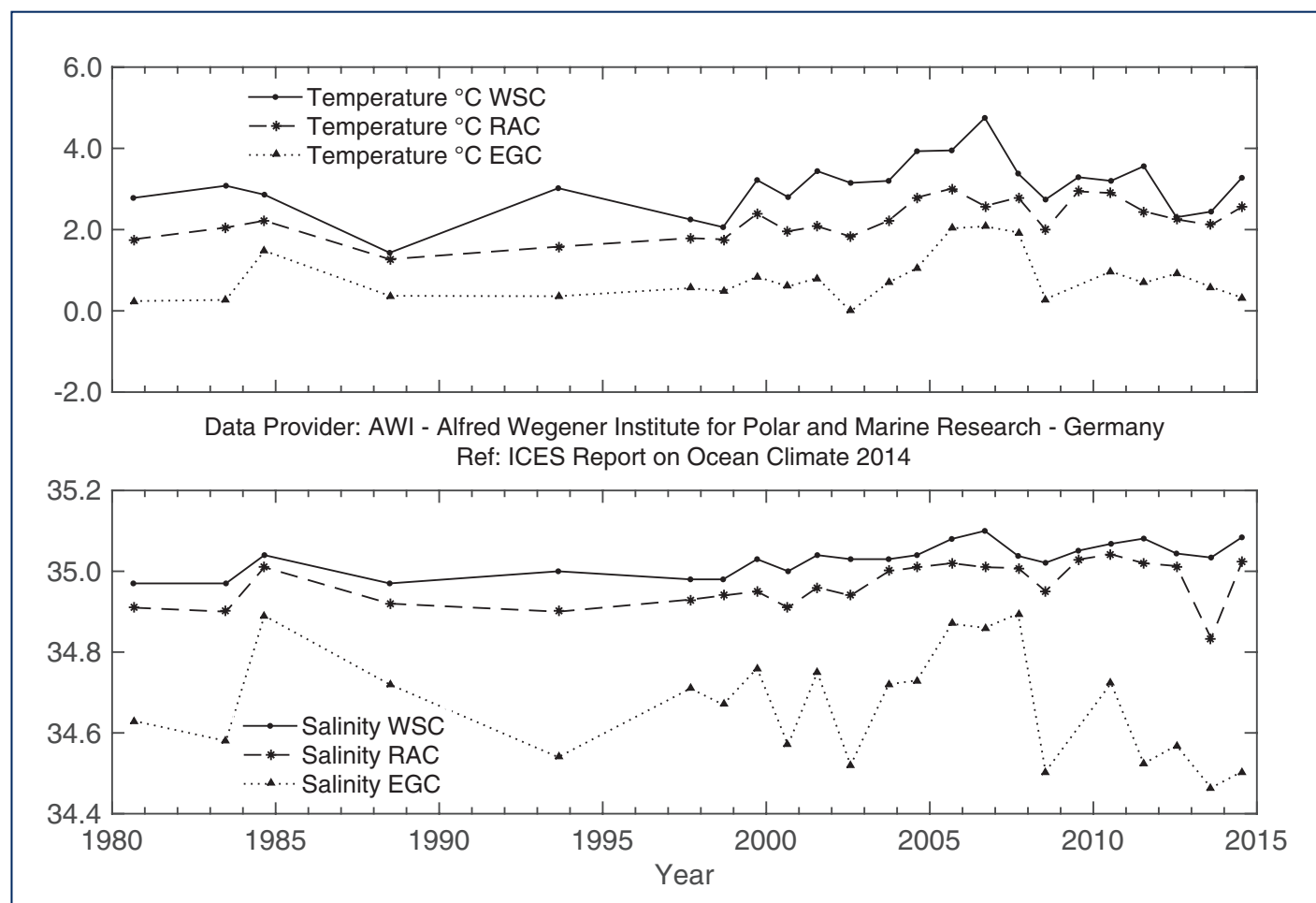
Continuous measurements from moorings along 78°50'N have not been recovered, so the annual temperature evolution cannot yet be updated from 2012 onward. Based on the most recent data, the winter-centred annual mean volume transport in the West Spitsbergen Current was 6.4 Sv in 2011–2012, close to the transport observed in 2010–2011 (6.3 Sv) and slightly higher than the long-term mean of 6 Sv.

FIGURE 70



Area 12 - Greenland Sea and Fram Strait. Temperature (upper panel) and salinity (lower panel) at 200 m in the southern Spitsbergen Section (76.50°N).

FIGURE 71



Area 12 - Greenland Sea and Fram Strait. Temperature (upper panel) and salinity (lower panel) in Fram Strait (78.83°N) at 50-500 m: in the Atlantic water in the West Spitsbergen Current (WSC; between the shelf edge and 5°E), in the Return Atlantic Current (RAC; between 3°W and 5°E), and in the polar water in the East Greenland Current (EGC; between 3°W and the Greenland Shelf).

5. DETAILED AREA DESCRIPTIONS, PART II: THE DEEP OCEAN

5.1 INTRODUCTION

This section focuses on the deeper waters of the Nordic seas and the North Atlantic, typically below 1000 m. The general circulation scheme and dominant water masses are given in Figure 72.

At the northern boundary of the region of interest, the cold and dense outflow from the Arctic Ocean enters Fram Strait along its western side and reaches the Greenland Sea. The outflow is a mixture of Eurasian Basin and Canadian Basin deep waters and upper polar deep water (UPDW). The Eurasian deep water feeds the densest water of all Nordic seas: the Greenland Sea bottom water. The Canadian Basin deep water and UPDW supply the Arctic intermediate water in the Greenland Sea, and the UPDW also includes products of the winter convection. The deep southward outflow from the North Atlantic in the deep western boundary current is fed by the cold and dense overflow waters. The deepest and densest is the Denmark Strait overflow water. This water mass originates in the Arctic intermediate water produced in the Greenland and Iceland seas by winter convection and mixing with surrounding water masses. The Denmark Strait overflow water sinks to the bottom as it passes over the Denmark Strait sill, vigorously entraining ambient water. Downstream, it is overlain by an intermediate water mass, that of Labrador Sea water, formed by deep winter convection in the Labrador Sea. The middle layer of the deep, cold-water export in the deep western boundary current is supplied by the Iceland-Scotland overflow water, originating in water masses formed in the Norwegian Sea (Arctic intermediate water and Norwegian Sea deep water). Passing through the Icelandic Basin, the Iceland-Scotland overflow water also entrains upper ocean water and Labrador Sea water. The deep Antarctic bottom water enters the North Atlantic on the western side, but its signature is also present in eastern Atlantic abyssal basins. At intermediate levels, the Mediterranean water originates from vigorous mixing of Atlantic central waters and Mediterranean outflow waters at the Gulf of Cadiz. This water mass spreads at about 1000 m depth in all directions, with a main vein progressing northward along the European margin. Around the Canaries, the Mediterranean water encounters the northern limit of Antarctic intermediate waters.

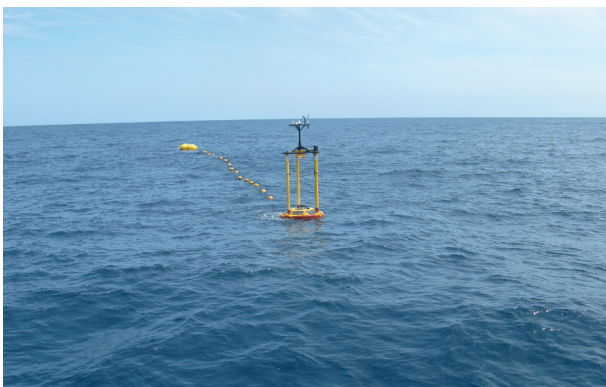
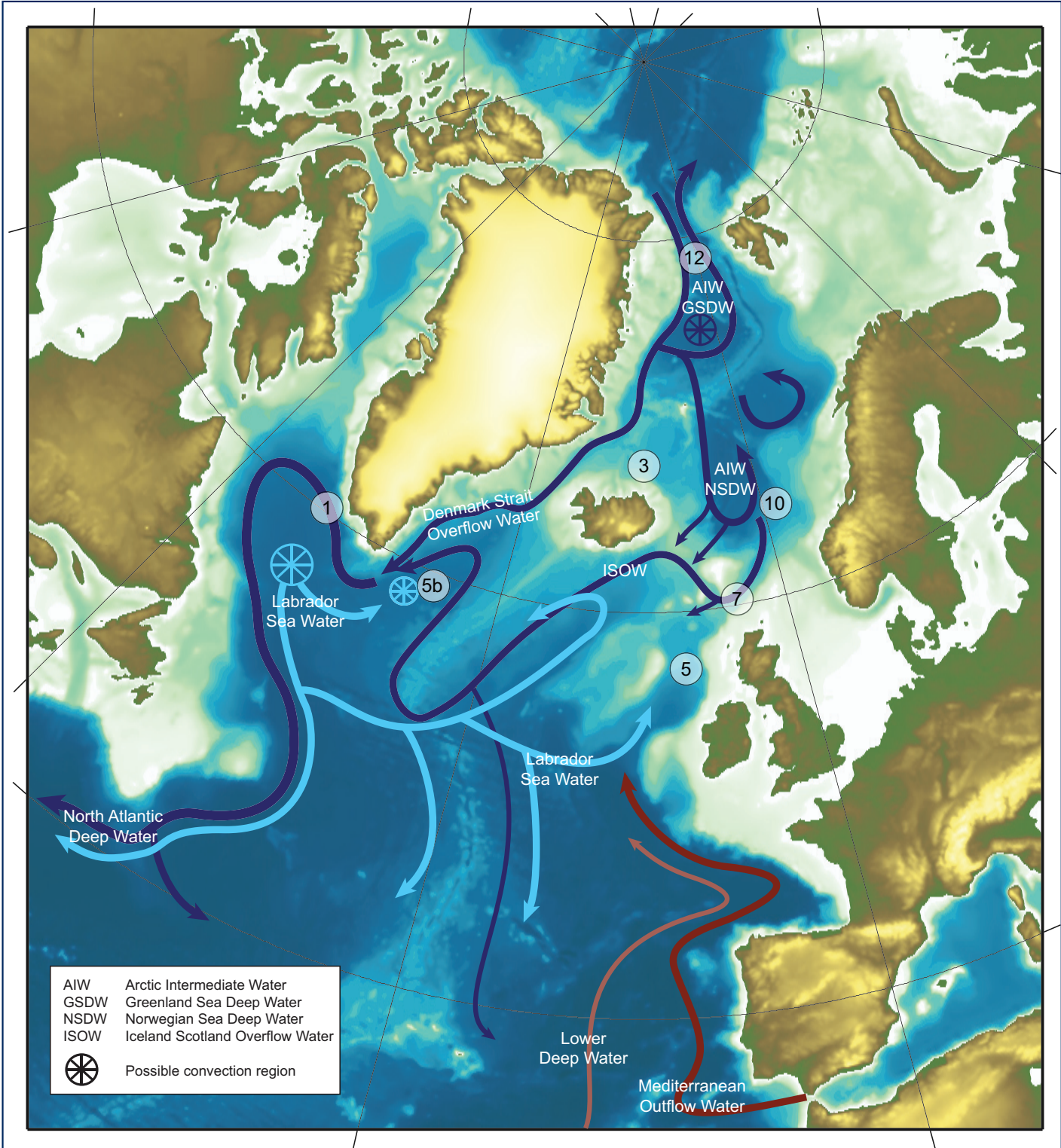


Photo courtesy Alicia Lavin, IEO, Spain.

FIGURE 72



Schematic circulation of the intermediate to deep waters in the Nordic seas and North Atlantic.

5.2 NORDIC SEAS DEEP WATERS

The deep waters of the Greenland, Iceland, and Norwegian seas are all warming. The longest time-series (the Norwegian Sea, Area 10) reveals warming from the mid-1980s; however, a slight decrease in temperature occurred in 2010–2011 and again in 2014. The continuous warming has been observed in the Greenland Sea deep layer at 3000 m (Area 12, no data for 2011–2014), and the temperature increase between 2009 and 2010 was slightly lower (0.01°C) than the increase over the past five years (0.014°C). Warming in the Greenland Sea was accompanied by a year-to-year increase in salinity of 0.001. In the Iceland Sea (Area 3), an increase in temperature at the depth range 1500–1800 m has been observed since the beginning of the time-series (early 1990s), and temperature continued to rise slowly until the end of 2014. The long-term warming rates for the last decade are 0.134°C (Greenland Sea in 2001–2010), 0.06°C (Norwegian Sea), and 0.064°C (Iceland Sea). The source of warming is the deep outflow from the Arctic Ocean, a southward flowing current of the Eurasian and Canadian Basin deep waters and the upper polar deep water found on the western side of Fram Strait at ca. 2000 m depth. The Greenland Sea deep water (GSDW) is warming fastest owing to its direct contact with this Arctic outflow, whereas the Iceland and Norwegian seas are warming more slowly because they are products of the mixing of their own ambient waters with GSDW and Arctic outflow water.

The doming structure in the Greenland Sea Gyre is being replaced by a two-layered water mass arrangement, after a cessation of deep convection. Since measurements began in 1993, the winter convection depth has varied between 700 and 1600 m and has only been significantly deeper in small-scale convective eddies. In winter 2007/2008, the maximum convection depth was estimated to be 1700 m, deeper than the previous year (1200 m) and similar to the maxima observed during 2001/2002 and 2002/2003. The import of warm and saline Atlantic water (AW) to the Greenland Sea is currently not balanced by an import of cool and fresh polar water from the north. The AW, which dominates changes in the upper ocean, took over the role of former ice production as a source of salt and densification in the context of winter convection. The input of AW tends to prevent ice formation and to vertically homogenize waters ventilated by convective processes. The GSDW formerly included a small admixture of surface freshwater through the convective process and, therefore, had lower salinity than the Arctic outflow waters. The observed increase in GSDW salinity may be the result of an adjustment to the Arctic outflow in the continued absence of deep convection and an increased presence of AW in the upper layer.



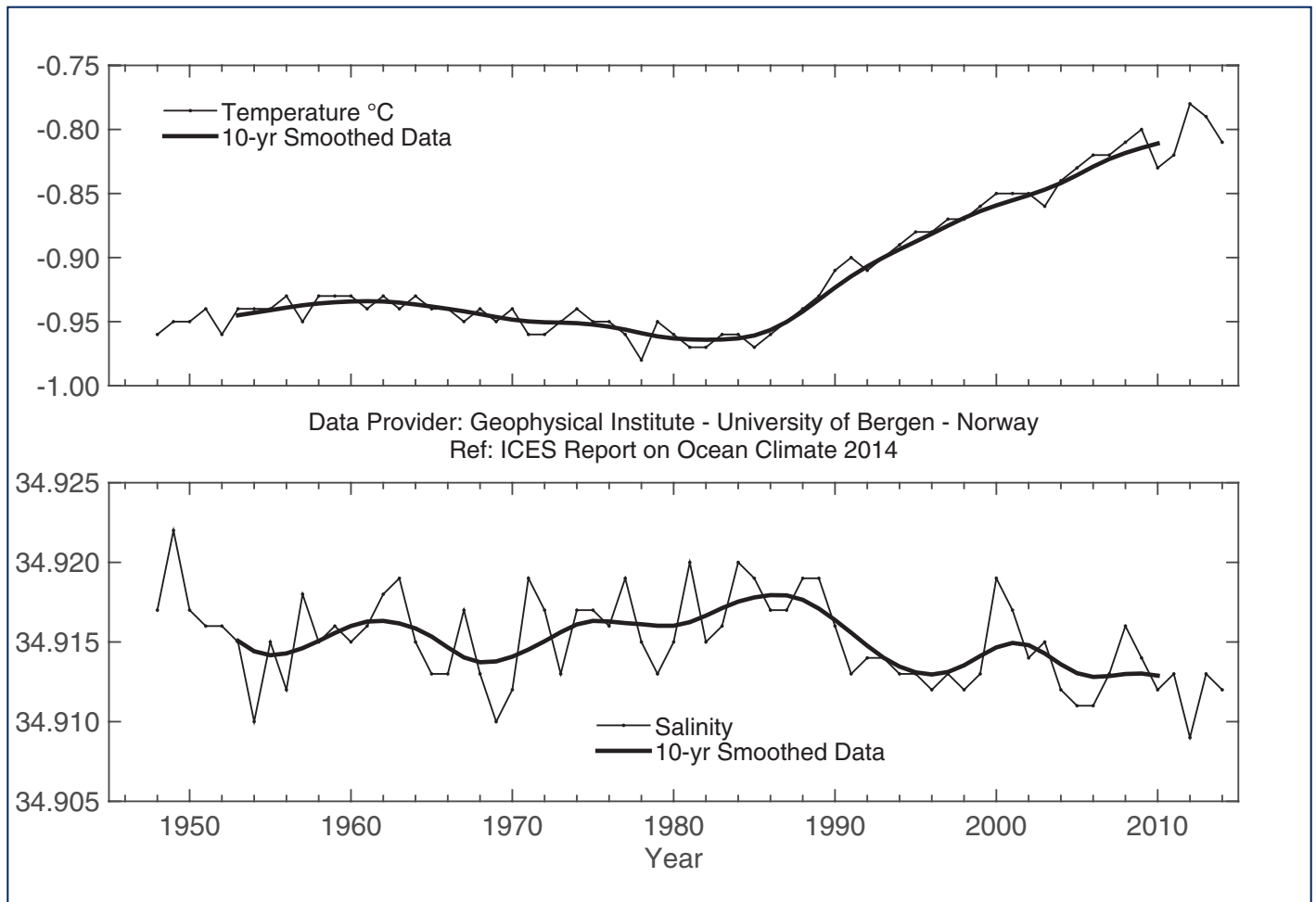
In the Greenland Sea Gyre in summer 2009, the usual relatively homogenous pool, mixed by previous winter convection, was replaced by a bipolar distribution of water masses with higher salinity in the western part of the gyre and fresher waters in its eastern part. This made it difficult to compose a reliable mean profile for the gyre centre and, consequently, because of the lack of a 2009 mean profile for comparison with the 2010 mean profile, it was not possible to provide an unambiguous estimate of the convection depth in winter 2009/2010. Therefore, two possible convection depths were obtained, depending on a choice of the 2009 mean profile. Since 2011, no measurements have been collected in the Greenland Sea deep water, and development of the convection depth in the Greenland Sea Gyre has not been updated.

It is unclear whether there has been any corresponding salinity trend in either the Norwegian or the Iceland Sea deep waters in recent decades. After some decrease in the early 1990s, salinity in Norwegian Sea deep basins has remained relatively stable over the 2000s and until 2014, but with a record low value in 2012. In the Iceland Sea, salinity in the deep layer has also been relatively stable since the end of the 1990s, though with a few pronounced anomalies in 2013.

THE DEEP WATERS OF THE GREENLAND, ICELAND, AND NORWEGIAN SEAS ARE ALL WARMING.

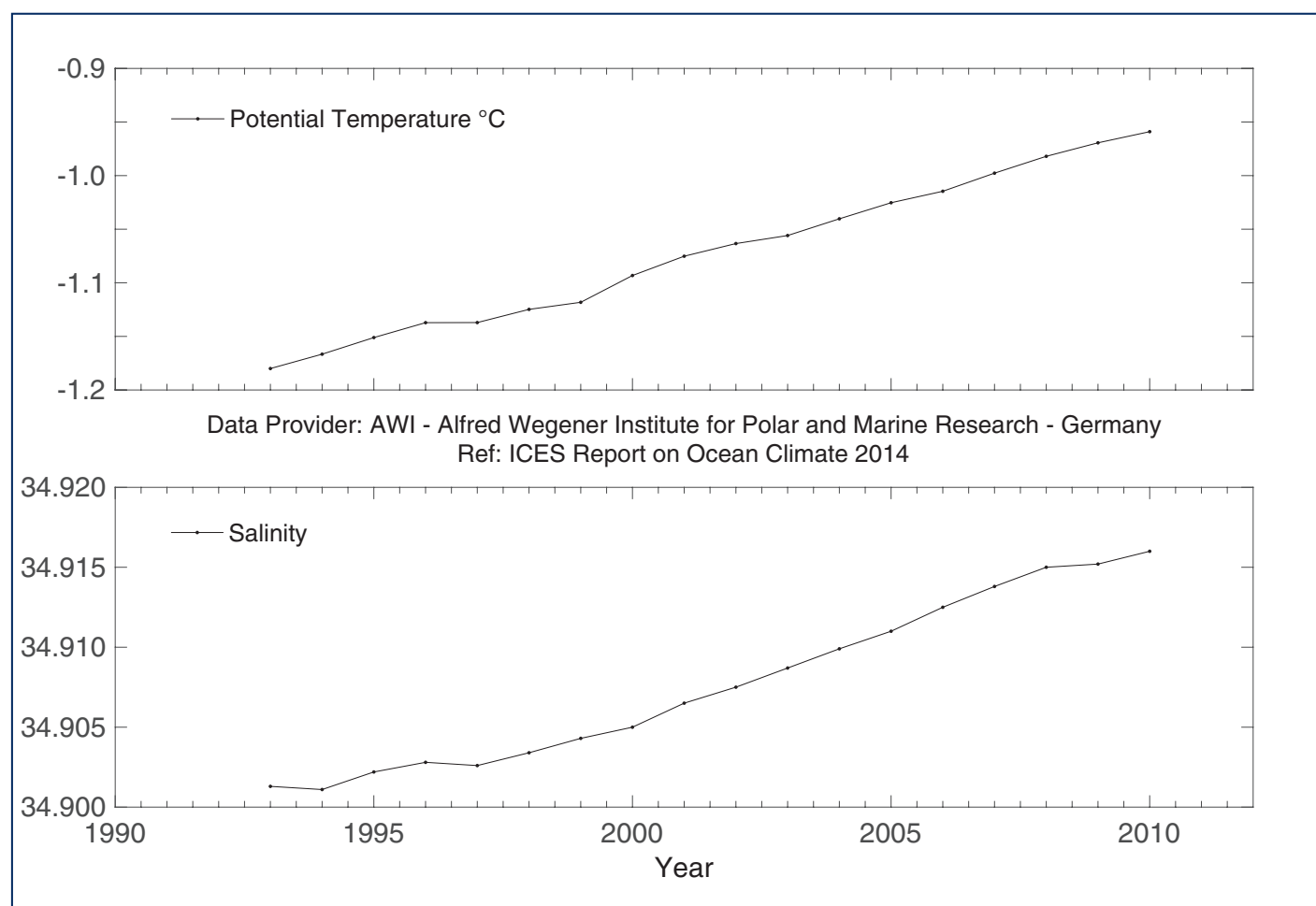


FIGURE 73



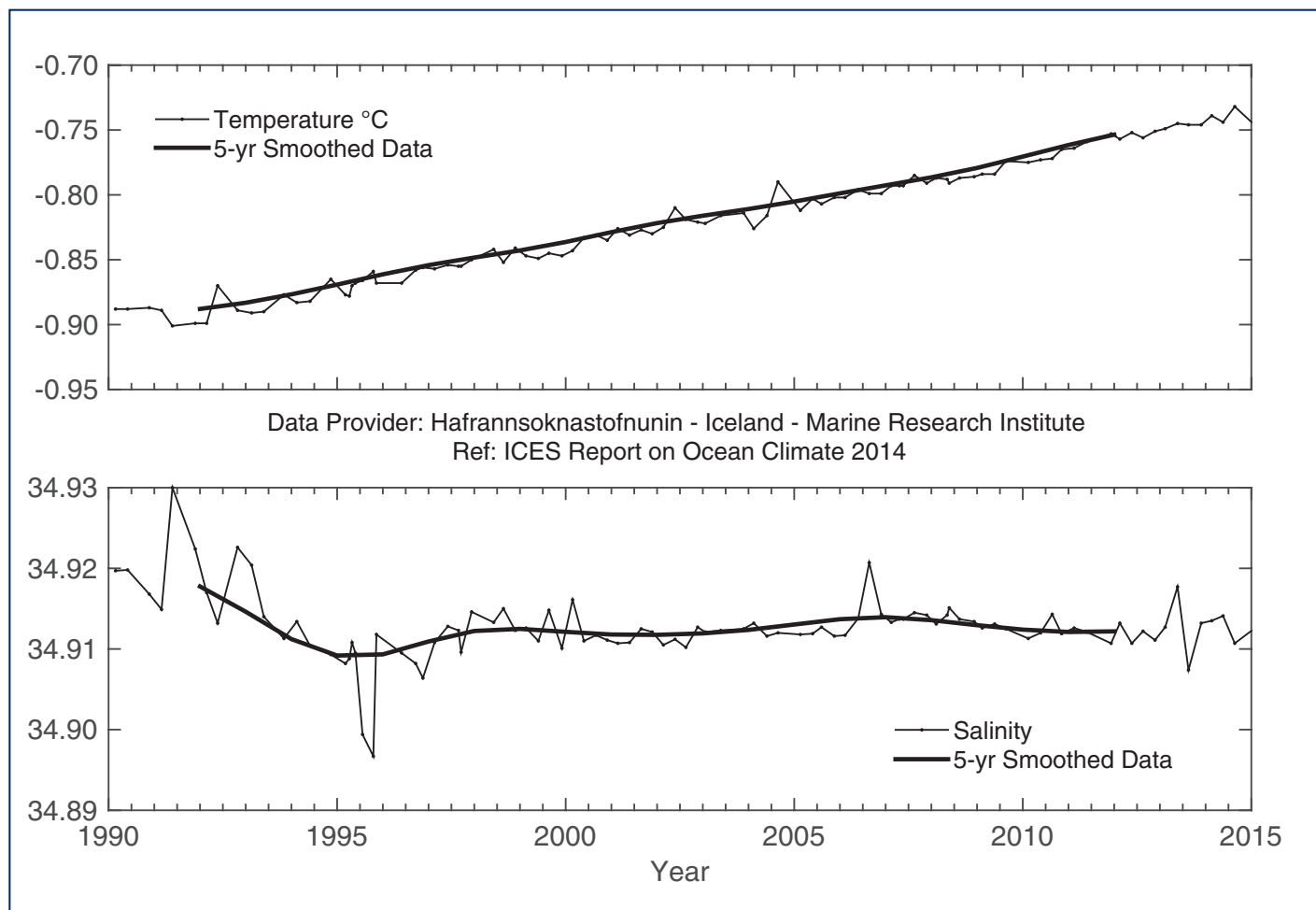
Area 10 - Norwegian Sea. Temperature (upper panel) and salinity (lower panel) at 2000 m at Ocean Weather Station "M" (66°N 2°E).

FIGURE 74



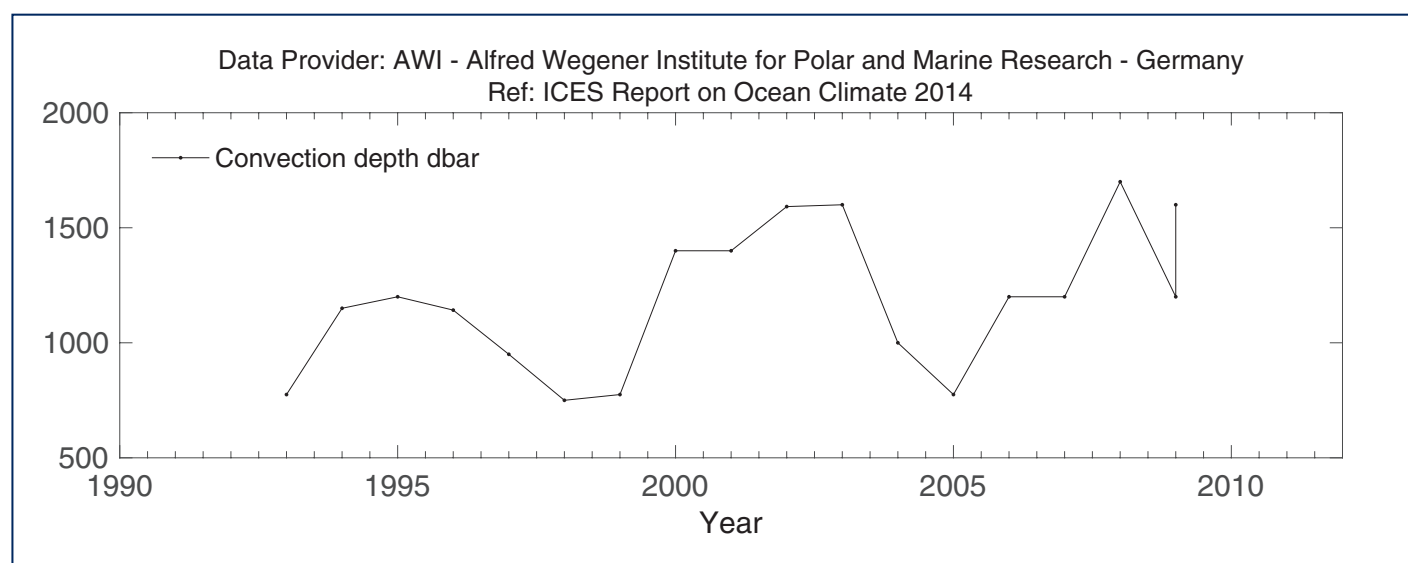
Area 12 - Greenland Sea and Fram Strait. Temperature (upper panel) and salinity (lower panel) at 3000m in the Greenland Sea Section at 75°N (data to 2010).

FIGURE 75



Area 3 - Icelandic waters. Temperature (upper panel) and salinity (lower panel) at 1500-1800 m in the Iceland Sea (68°N 12.67°W).

FIGURE 76



Area 12 - Greenland Sea and Fram Strait. Winter convection depths in the Greenland Sea Section at 75°N (data to 2009; note that due to the ambiguous convection depth in winter 2009/2010, two values are provided for this period).



5.3 NORTH ATLANTIC DEEP WATERS

In the deep layers of the Faroe–Shetland Channel (Area 7), properties at 800 m are the same as those of Norwegian Sea deep water as it passes through the Channel back into the North Atlantic. After a period of decline in the 1990s, temperature has increased since 2000, but still remains lower than the highest temperatures observed in the 1950s, 1960s, and early 1980s. Relatively stable salinity in the first period of measurements (1950 to mid-1970s) was followed by a slow decline through the subsequent 15 years; since 1992, it has stabilized again.

After the Norwegian Sea deep water flows through the Faroe–Shetland Channel and Faroe Bank Channel and into the Iceland Basin (Area 5), it becomes known as Iceland–Scotland overflow water (ISOW). The dense water, supplemented by a small amount of additional flow over the sill between Iceland and the Faroes, mixes rapidly with the upper ocean and intermediate water of the Iceland Basin, entraining the lighter water and increasing the volume of the overflow plume. Properties of the ISOW measured at 20°W in the Iceland Basin, therefore, become a product of the properties of the dense water at the sill and the entrained ambient water. ISOW temperature and salinity vary rather closely with the Labrador Sea water and upper ocean water in the Iceland Basin; since 1996, the water has warmed and increased in salinity, though there has been a slight decrease in both since 2011.

Salinity and potential temperature of the Denmark Strait overflow water (DSOW) near Cape Farewell showed correlated interannual variations between 1991 and 2007 (correlation = 0.7). However, after 2007, changes in temperature and salinity of the DSOW broke this rule; the correlation was reduced to about 0.5. This implies that less than 30% of the variance of the salinity can be explained by the variance of the temperature variability. Density of the DSOW hardly changes on long time-scales. Measurements with moored instrumentation have demonstrated that temperature and density mainly vary at an annual time-scale, possibly forced by wind-driven processes near Denmark Strait. In 2012 and 2014, temperature was 0.14 and 0.11°C, respectively, above the long-term mean, while salinity values were 0.02 and 0.014 above average. There were no data available in 2013.

Properties of the North Atlantic deep water (NADW) in the deep boundary current west of Greenland are monitored at 2000 m depth at Cape Desolation Station 3. Temperature and salinity of this water mass underwent strong interannual variability



Photo by © Crown copyright, Marine Scotland.

during the 1980s. Since the beginning of the 1990s, both characteristics were decreasing and reached their minimum values in 1998 and 1997, respectively. Temperature of the NADW subsequently revealed a positive trend until 2014, whereas salinity rather stagnated between 2007 and 2014. In 2014, temperature increased and salinity decreased and were 0.17°C and 0.01 , respectively, above the long-term mean.

Hydrography and biogeochemistry at Western Iberia and Biscay (Area 4) have been monitored for the whole water column (>5500 m) since 2003 by a repeated section programme which supplements the monthly monitoring of the upper ocean in that area. Cruises were carried out semiannually in 2003–2010 and annually after that. The Finisterre Section, about ca. 400 km, begins west of the Iberian Peninsula ($43^{\circ}\text{N } 9.3^{\circ}\text{W}$) and reaches the centre of the Iberian Abyssal Plain ($43^{\circ}\text{N } 15^{\circ}\text{W}$).

The Finisterre Section provides information about upper, intermediate, and deep waters. Since 2000 m corresponds to the core of LSW and the base of the permanent thermocline, this is considered the limit of intermediate waters. The abyssal waters in this basin are NADW (consisting there of a mixture of all Arctic water masses) and what is known as lower deep water, which presents a signature of waters of Antarctic origin. Interannual variability of these abyssal waters within the monitored period has been weak, with interannual swings below 0.1°C and 0.01 in salinity. No trends have been observed.

Photo by Sarah Hughes. © Crown copyright, Marine Scotland.

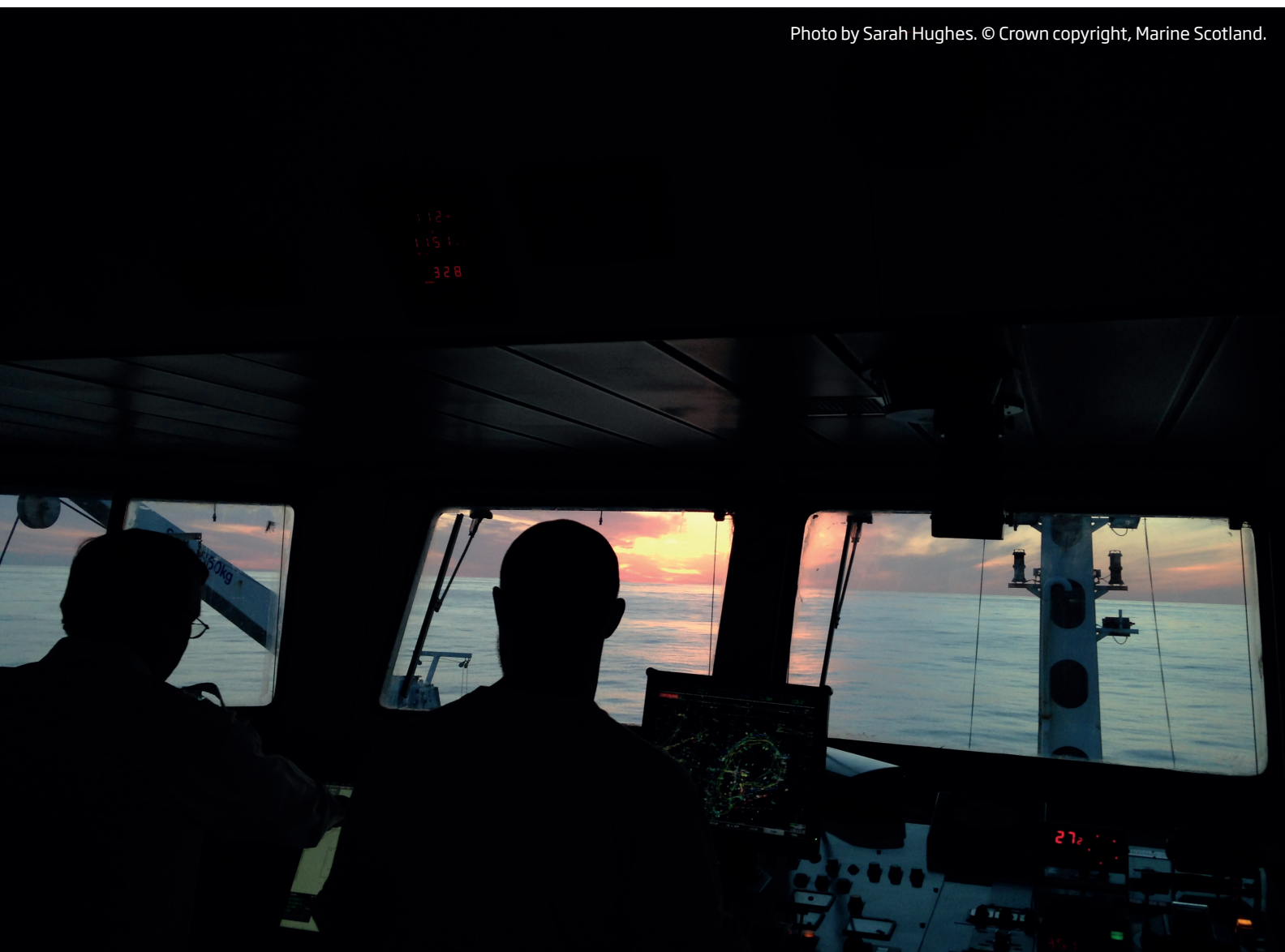
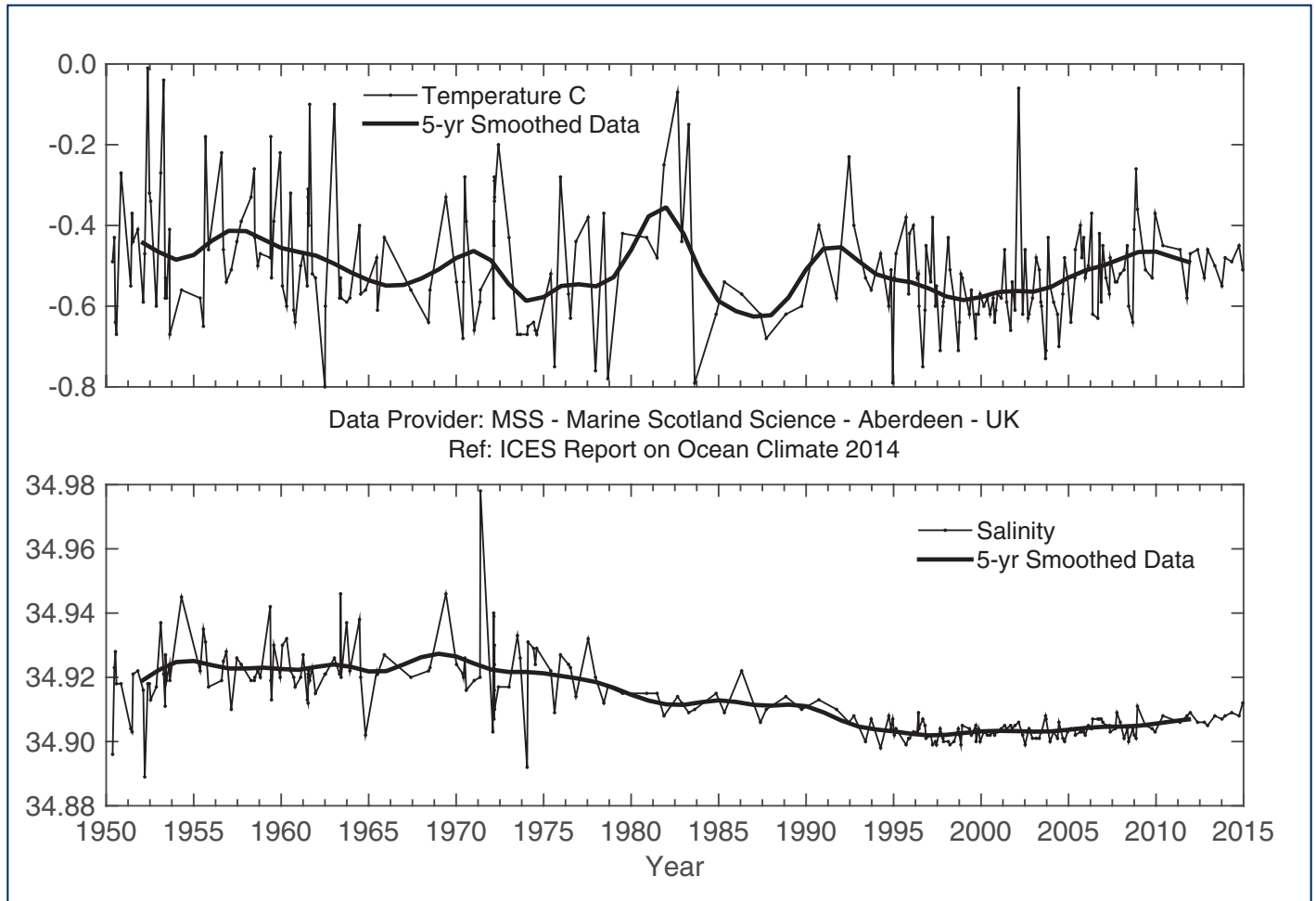
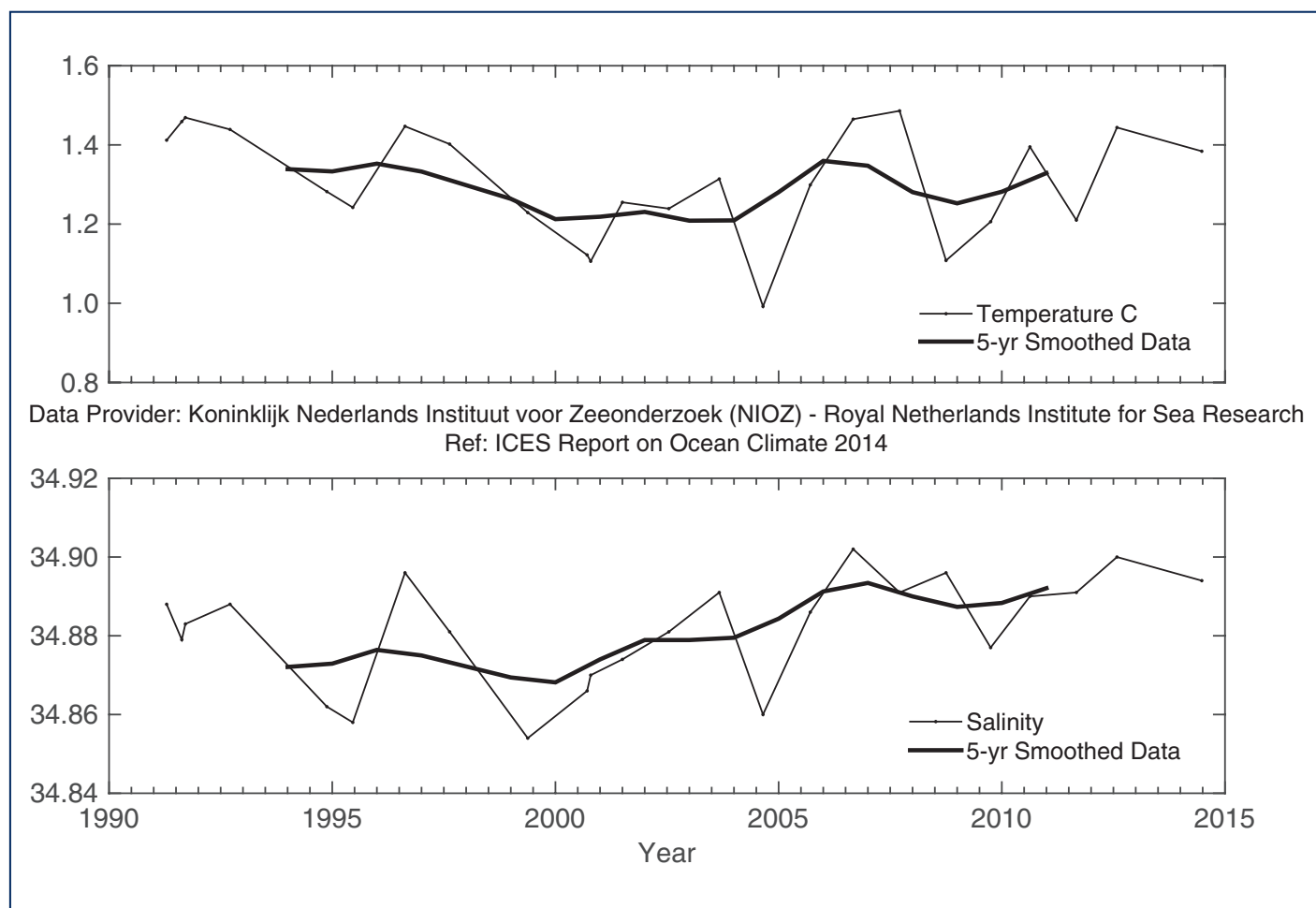


FIGURE 77



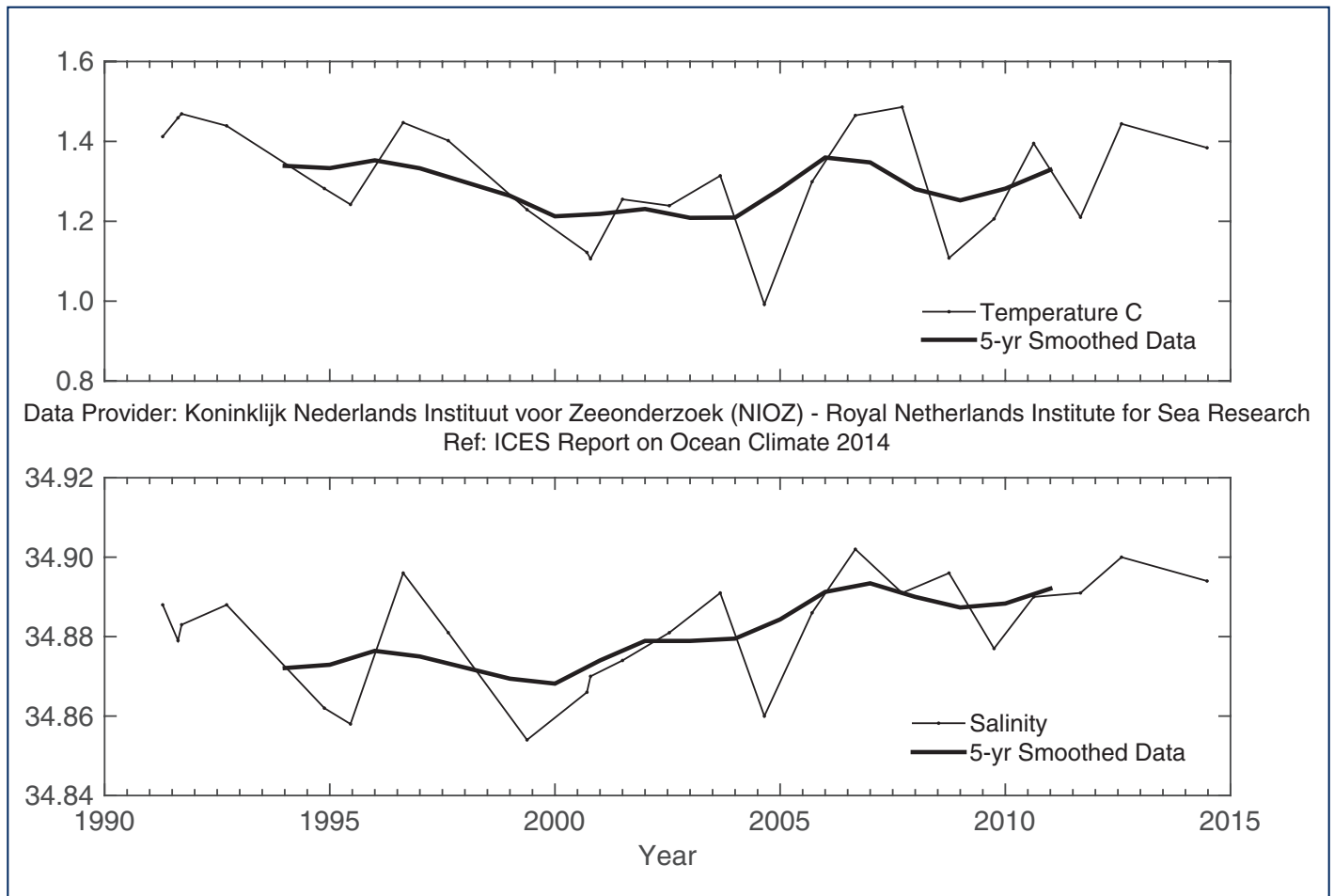
Area 7 - Faroe-Shetland Channel. Temperature (upper panel) and salinity (lower panel) at 800 m.

FIGURE 78



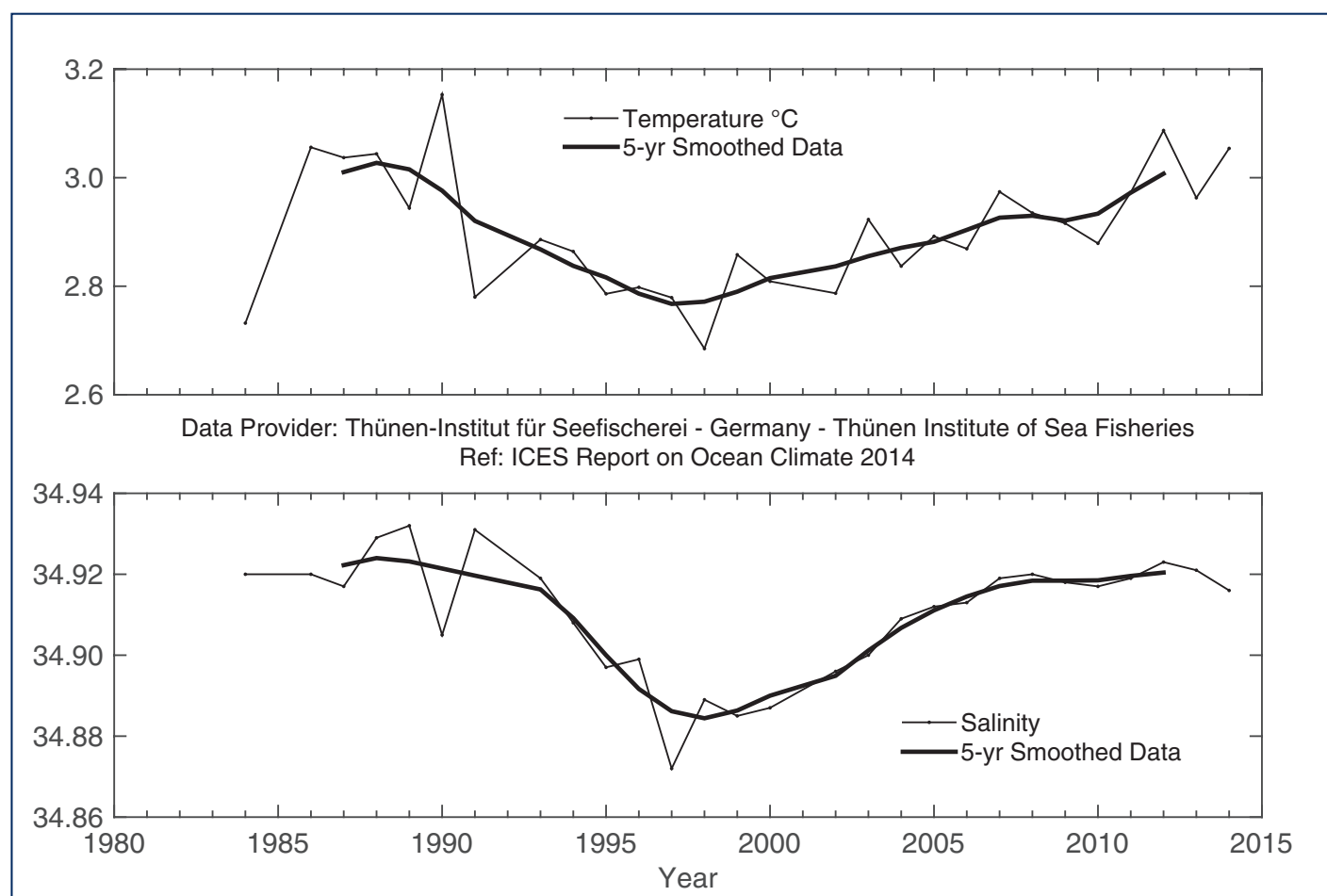
Area 5 - Iceland Basin. Temperature (upper panel) and salinity (lower panel) of Iceland-Scotland overflow water (potential density $>27.85 \text{ kg m}^{-3}$, ca. 2000-2600 m).

FIGURE 79



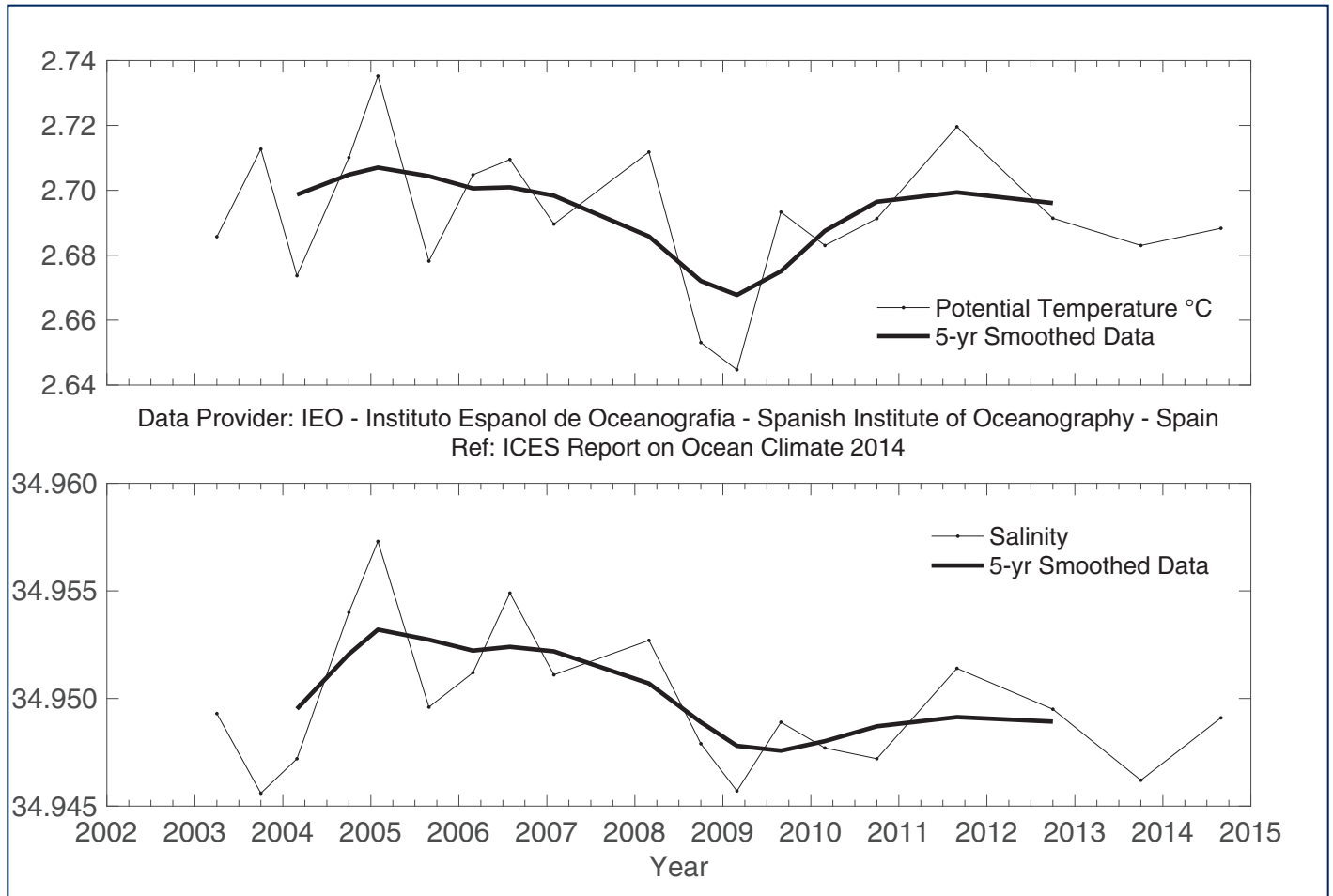
Area 5b - Irminger Sea. Temperature (upper panel) and salinity (lower panel) in Denmark Strait overflow water on the East Greenland Slope.

FIGURE 80



Area 1 - West Greenland. Temperature (upper panel) and salinity (lower panel) at 2000 m water depth at Cape Desolation Station 3 (60.45°N 50°W).

FIGURE 81



Area 4 - Western Iberian Margin. Potential temperature (upper panel) and salinity (lower panel) for the 2000-5500 m layer averaged across the Finsiterre Section.

5.4 NORTH ATLANTIC INTERMEDIATE WATERS

In the Labrador Sea (Area 2b), temperature and salinity, averaged between 1000 and 1800 m, have been continuously increasing since their minima in the early 1990s. In 2011, temperature reached its previous maximum observed in 1970. Salinity was still lower than the record high in 1970, but since 2007, it has remained higher than its long-term average.

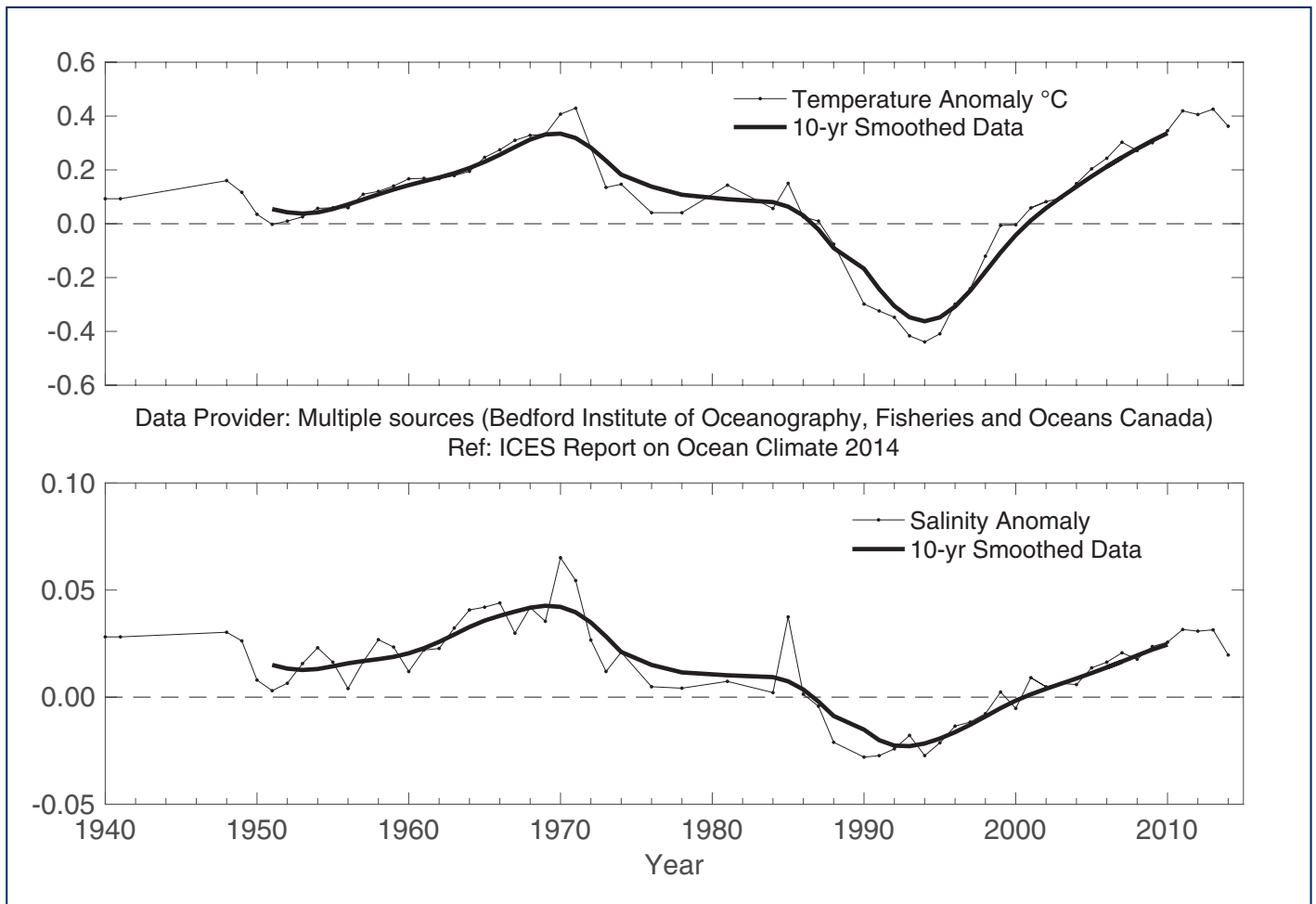
A cold and low-salinity core was observed between 1600 and 2000 m in the central Irminger Sea (Area 5b) during the early 1990s. This was the result of the presence of deep Labrador Sea water (LSW) formed in 1988–1995. Since summer 1996, this LSW core has generally been increasing in temperature and salinity as it mixes with surrounding water masses. In 2012, temperature and salinity were only slightly below the long-term maximum observed in 2011. In 2014, temperature of LSW in the Irminger Sea had continued to decline relative to 2011. Salinity, however, was higher than in 2011 and actually obtained the highest value ever since 1991.

In the Iceland Basin (Area 5), the dominant water mass below about 1000 m is Labrador Sea water (LSW), evident as a large recirculating body of relatively fresh and low-stratified water lying between 1700 and 2000 m. Over the length of the time-series (since 1996), the LSW has become gradually warmer and more saline. In 2014, the LSW was slightly cooler and fresher than the previous year.

In Rockall Trough (Area 5), the dominant water mass below ca. 1500 m is Labrador Sea water (LSW), which usually has its maximum concentration between 1700 and 2000 m. East of the Anton Dohrn Seamount, this peak tends to be characterized by a minimum in salinity and potential vorticity, although its patchy temporal distribution (possibly due to aliasing of mesoscale eddies) results in a noisy year-on-year signal. Over the length of the time-series, a trend of cooling and freshening can be detected. In 2014, the LSW potential temperature (3.38°C) and salinity (34.930) were cooler and fresher than the long-term mean values.

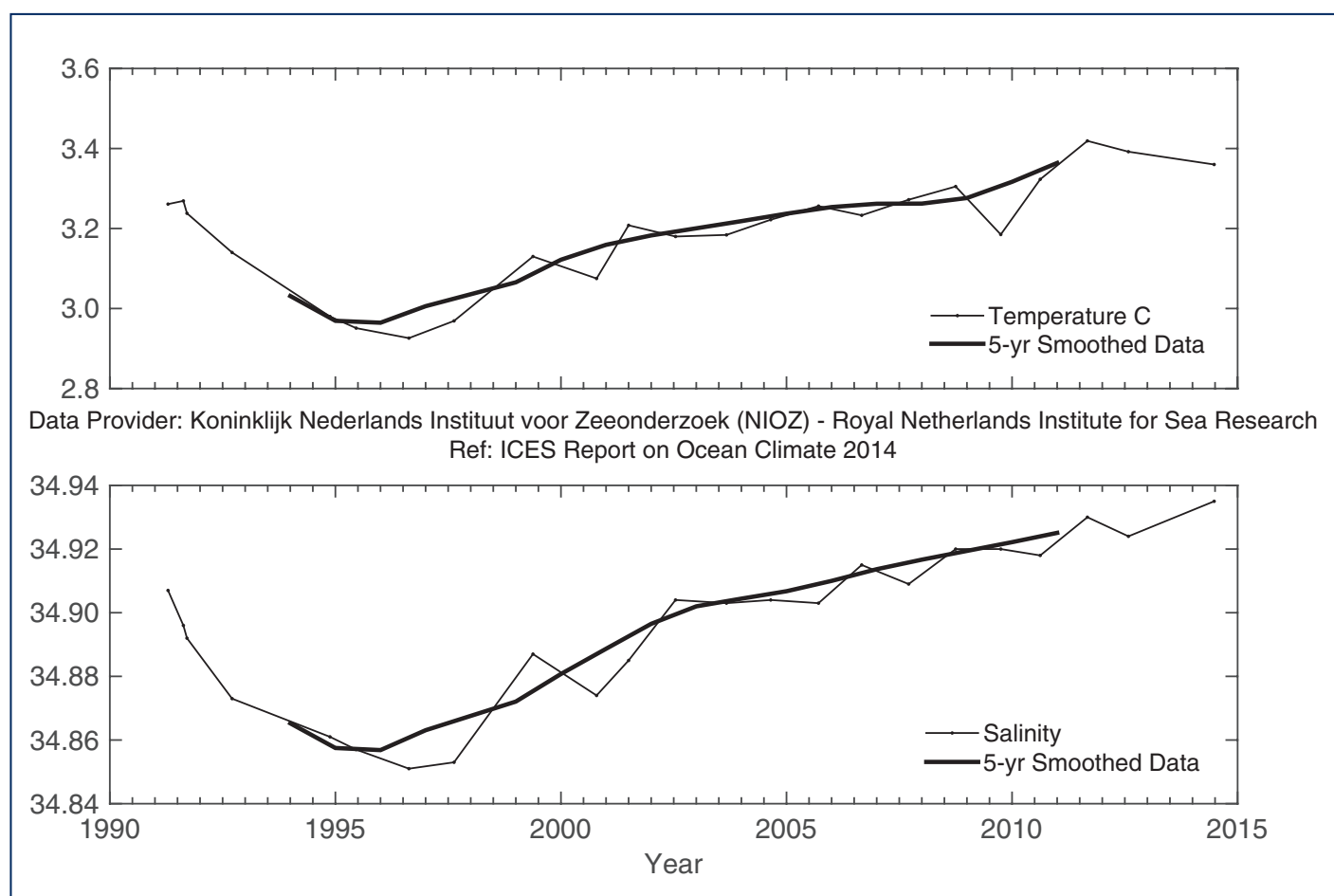
The external stations in Santander (Area 4) have been sampling the entire water column down to 1000 m [core of Mediterranean water (MW)] on a monthly basis since the early 1990s. Overall warming trends are evident at most layers, corresponding to the East North Atlantic central water (ENACW; 200–600 m) and upper MW (600–1000 m). Salinity also shows a notable increase along the whole series, but less smooth than temperature. The water masses evolution is strongly influenced by a strong shift in salinity at lower ENACW (ca. 400 m) in 2005 after the occurrence of very strong winter mixing. In 2014, upper central waters down to 400 m show marked freshening for the first time in about a decade. Below this level, the base of ENACW modal waters continues to be at the highest values of the series. Deeper at the level of the MW, the water masses have remained fairly stable since the mid-2000s, fresher at its core in 2014 after peaking in ca. 2007–2009. Deeper levels than 1000 m have been monitored in the region and at the Western Iberian Margin on a yearly/semi-yearly basis. From the core of MW to the core of LSW (ca. 1900 m), there is a strong gradient and some coherence in variability, indicating the influence of large-scale atmospheric patterns. The main highlight of the series is the passage of a cold and fresh anomaly from 2008 to 2010. The year 2014 was dominated by an upward swing in temperature and salinity in these intermediate waters.

FIGURE 82



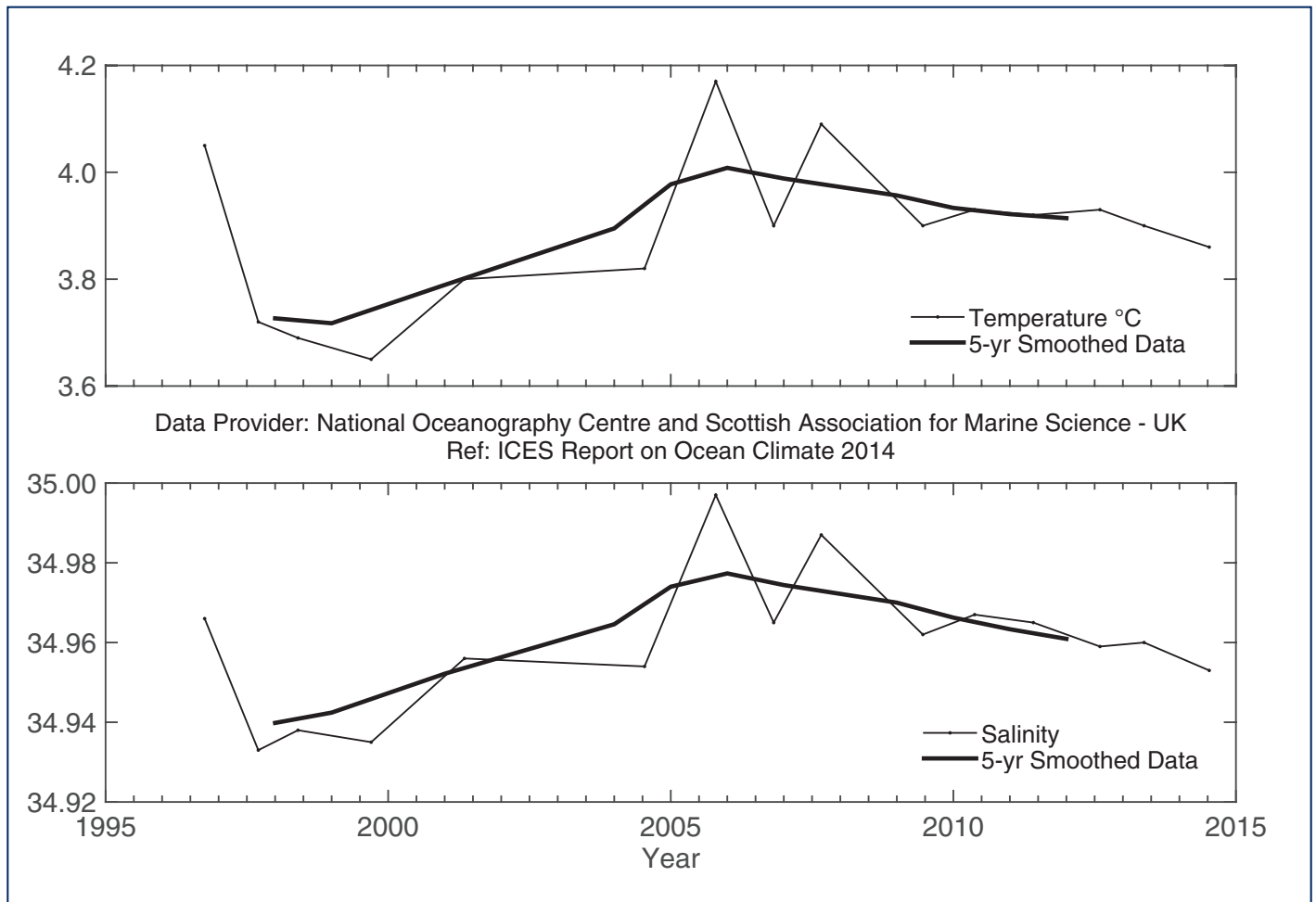
Area 2b - Labrador Sea. Temperature (upper panel) and salinity (lower panel) anomalies of Labrador Sea water (averaged over 1000-1800 m).

FIGURE 83



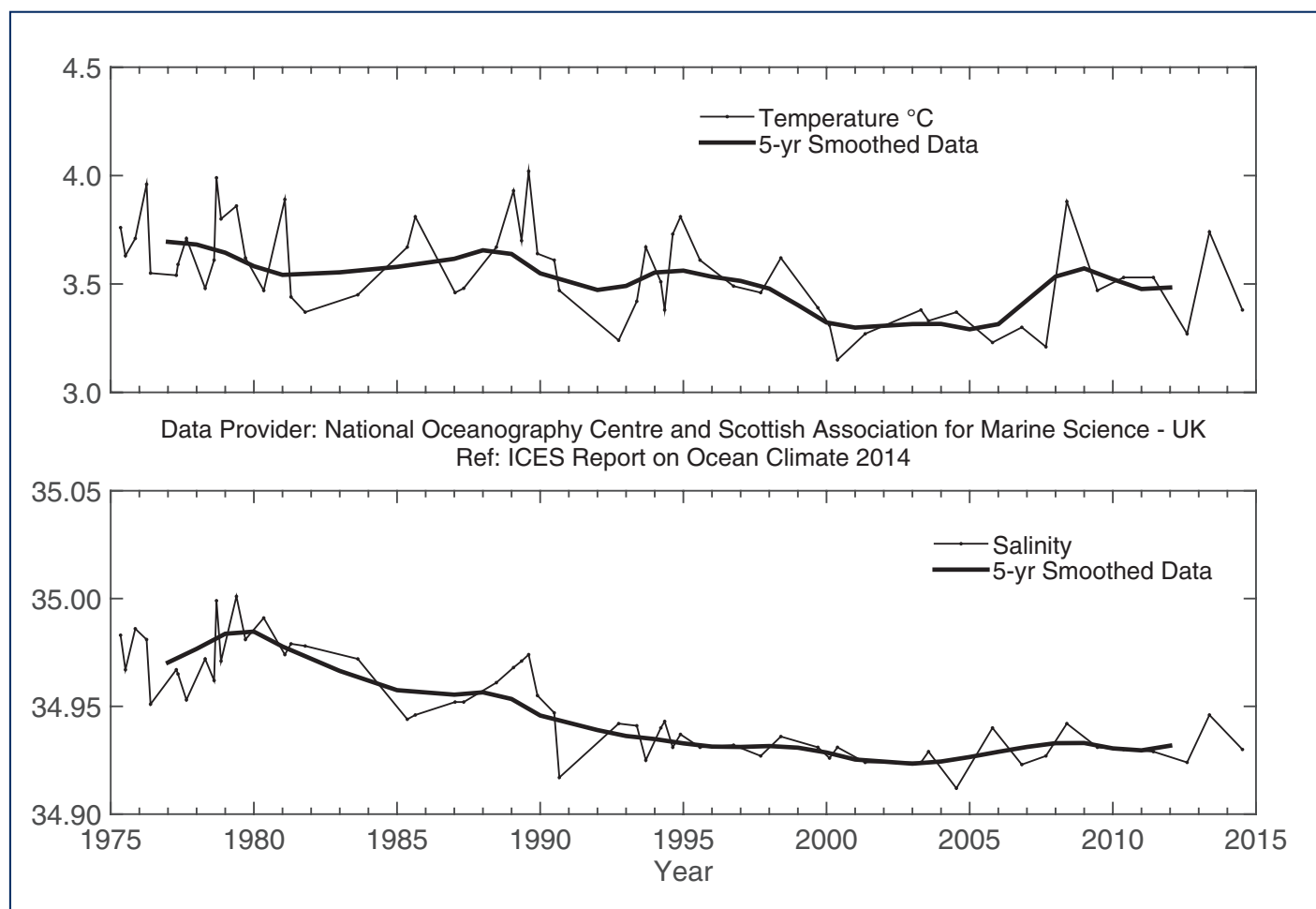
Area 5b - Irminger Sea. Temperature (upper panel) and salinity (lower panel) of Labrador Sea water (averaged over 1600-2000 m).

FIGURE 84



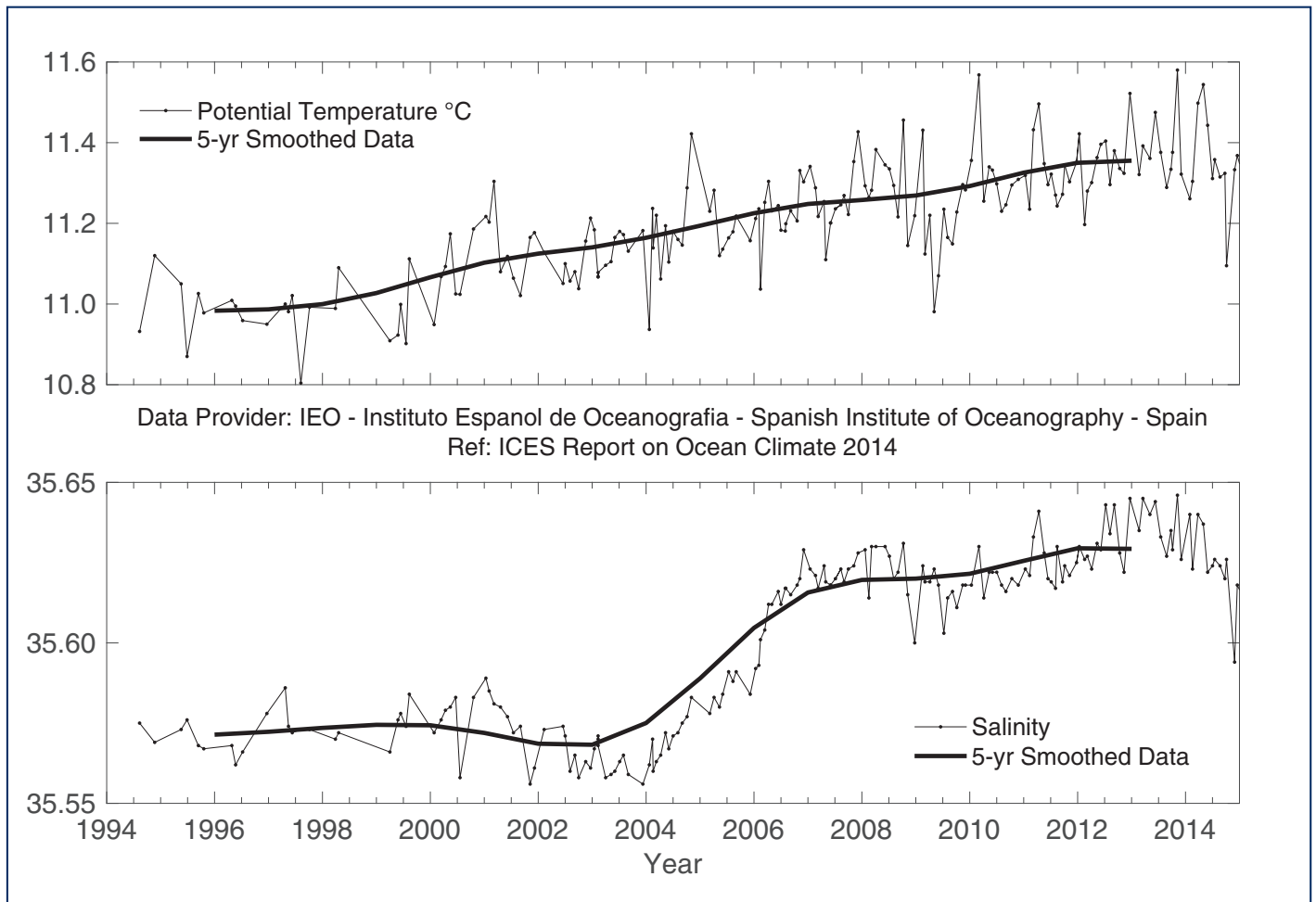
Area 5 - Iceland Basin. Temperature (upper panel) and salinity (lower panel) of Labrador Sea water (potential density range 27.70-27.85 kg m⁻³, ca. 1200-2000 m).

FIGURE 85



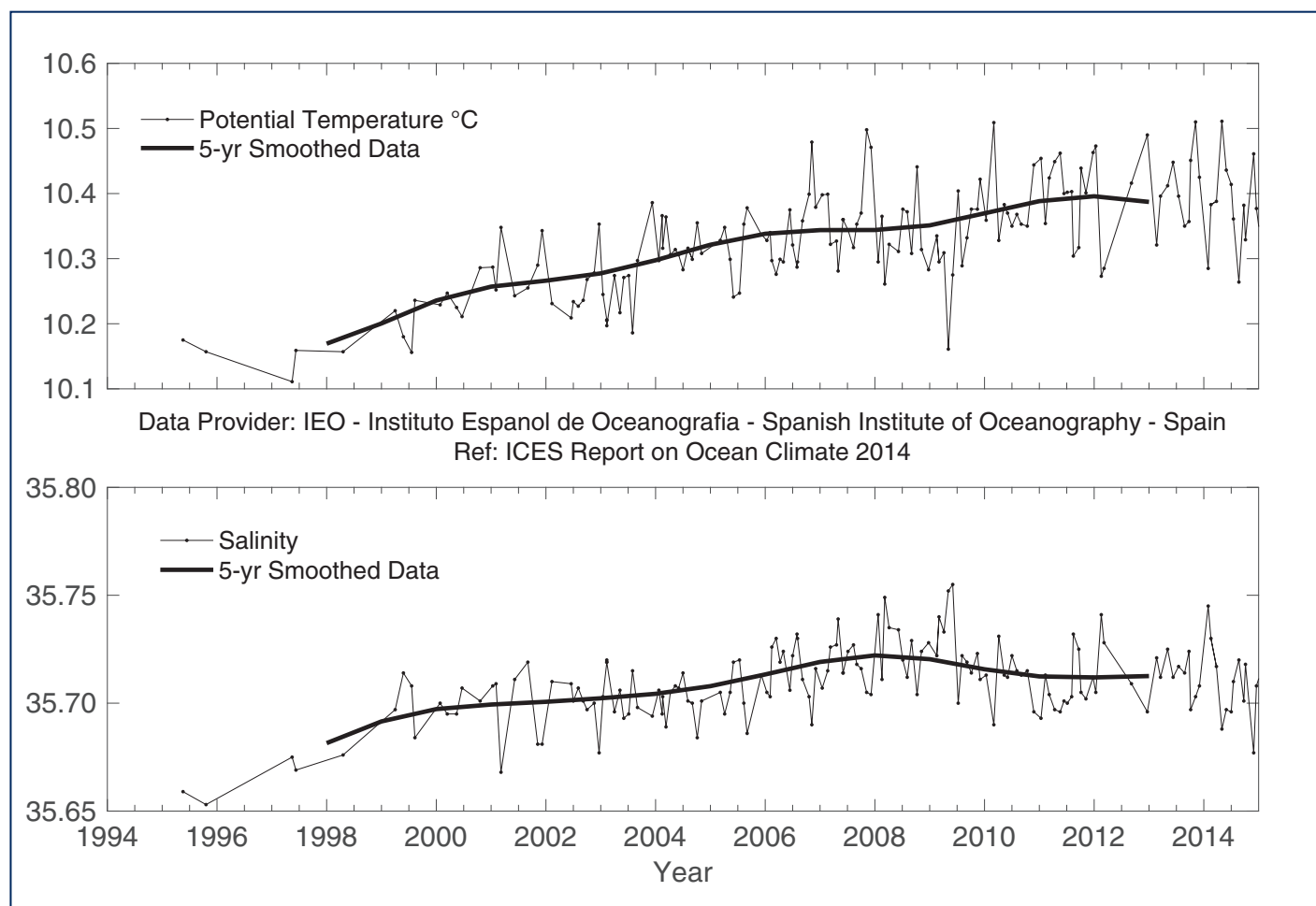
Area 5 - Rockall Trough. Temperature (upper panel) and salinity (lower panel) of Labrador Sea water (1800 m).

FIGURE 86



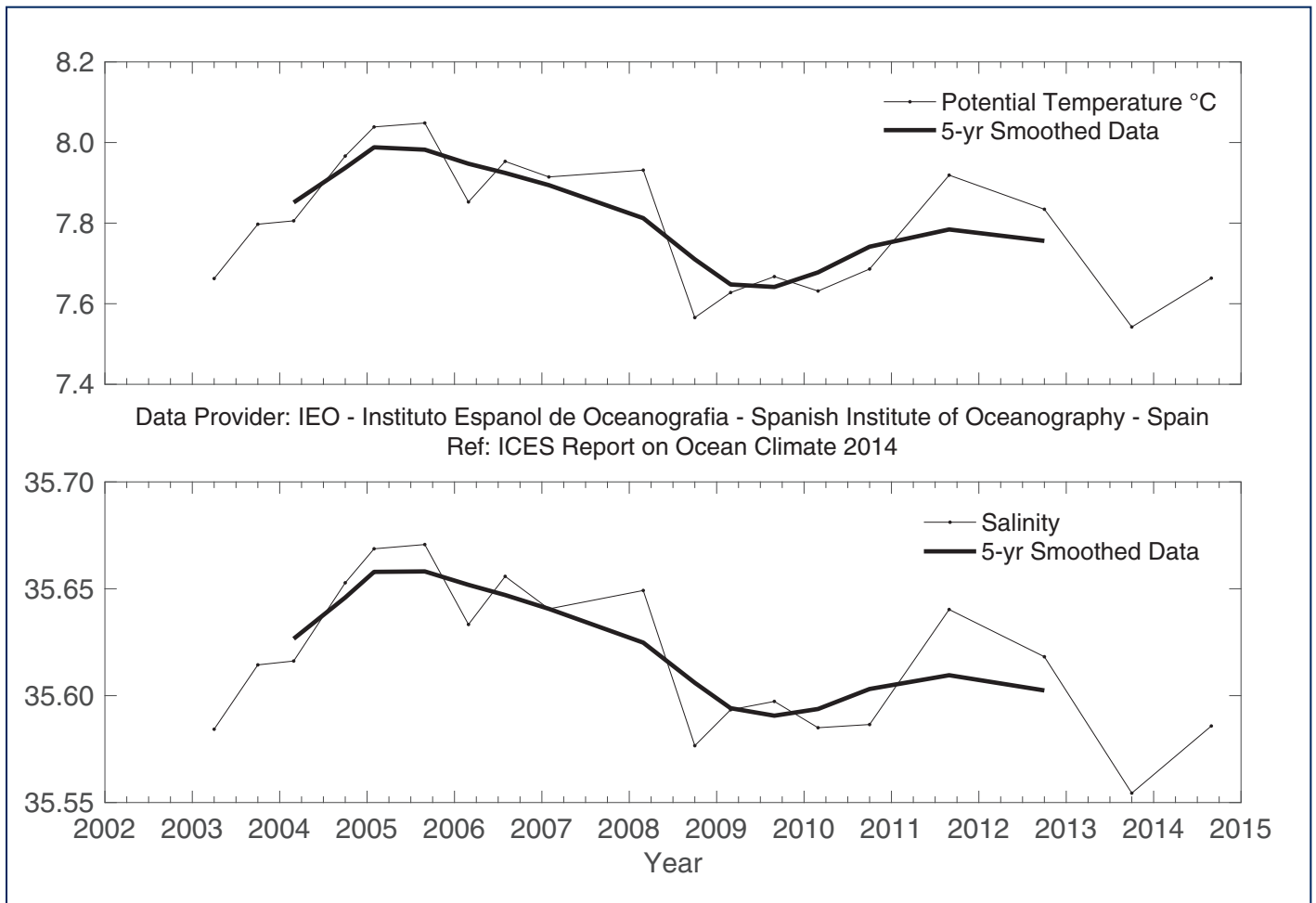
Area 4 - Bay of Biscay. Potential temperature (upper panel) and salinity (lower panel) for the 200-600 m layer at Santander Station 7.

FIGURE 87

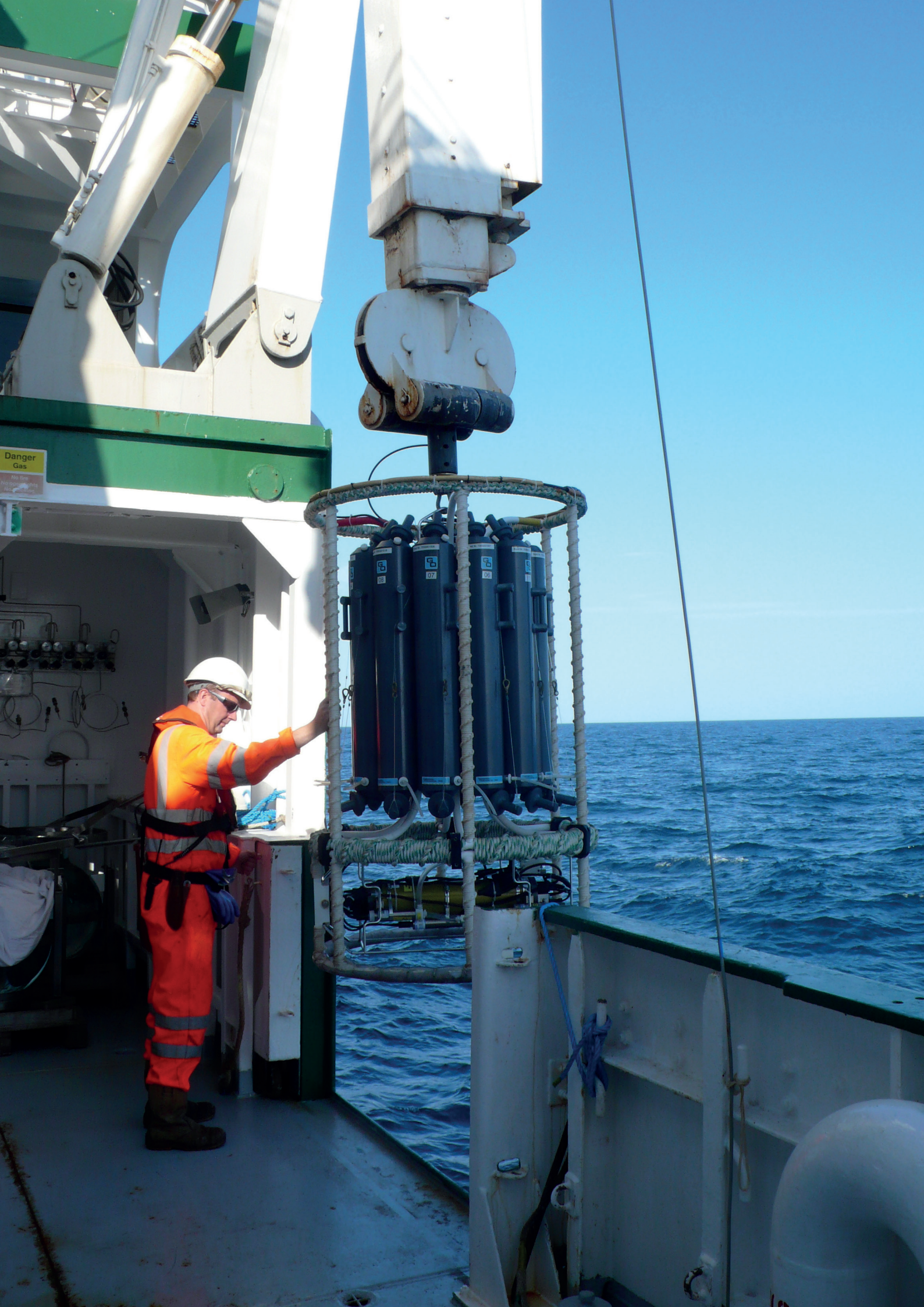


Area 4 - Bay of Biscay. Potential temperature (upper panel) and salinity (lower panel) for the 600-1000 m layer at Santander Station 7.

FIGURE 88



Area 4 - Western Iberian Margin. Potential temperature (upper panel) and salinity (lower panel) for the 800-2000 m layer averaged across the Finisterre Section.



Danger
Gas
No fire
No smoking
No open flames

CONTACT INFORMATION

AREA	AREA NAME	FIGURES	TIME-SERIES	Contact	INSTITUTE
1	West Greenland	14	Nuuk - air temperature	Boris Cisewski (boris.cisewski@vti.bund.de)	Danish Meteorological Institute, Copenhagen, Denmark, and Seewetteramt, Hamburg, Germany
1	West Greenland	15, 16, 80	Fylla Section and Cape Desolation Section	Boris Cisewski (boris.cisewski@vti.bund.de)	Institut für Seefischerei (Institute for Sea Fisheries), Germany
2	Northwest Atlantic	17, 18, 19	Sable Island air temperature, Cabot Strait sea ice, Misaine Bank, Emerald Bank	David Hebert (David.Hebert@dfo-mpo.gc.ca)	BIO (Bedford Institute of Oceanography), Department of Fisheries and Oceans, Canada
2	Northwest Atlantic	20, 21	Newfoundland and Labrador sea ice, Cartwright air temperature, Station 27 CIL	Eugene Colbourne (eugene.colbourne@dfo-mpo.gc.ca)	Northwest Atlantic Fisheries Centre, Canada
2b	Labrador Sea	22, 23, 24, 82	Section AR7W	Igor Yashayaev (Igor.Yashayaev@dfo-mpo.gc.ca)	BIO (Bedford Institute of Oceanography), Department of Fisheries and Oceans, Canada
2c	Mid-Atlantic Bight	26, 27, 28, 29, 30, 31	Central MAB and Gulf of Maine, Georges Bank	Paula Fratantoni (paula.fratantoni@noaa.gov)	NOAA Fisheries, NEFSC, Oceanography Branch, USA
3	Icelandic waters	32, 33, 34, 35, 36, 48, 75	Reykjavik and Akureyri air temperature, Siglunes stations 2-4, Selvogsbanki Station 5, Langanes stations 2-6, Faxafloi Station 9, Icelandic Deep Water (1800 m)	Hedinn Valdimarsson (hv@hafro.is)	Hafrannsóknastofnun (Marine Research Institute), Iceland
4	Bay of Biscay	37	San Sebastian air and water temperature	Victor Valencia (vvalencia@azti.es)	AZTI, Aquarium of San Sebastian (SOG) and Igeldo Meteorological Observatory (INM) in San Sebastian, Spain
4	Bay of Biscay and Western Iberian Margin	38, 39, 81, 86, 87, 88	Santander and Finisterre sections	Cesar Pola (cesar.pola@gi.ieo.es)	Instituto Español de Oceanografía (IEO, Spanish Institute of Oceanography), Spain
4b	NW European Continental Shelf	40	Astan Section, Point 33	Pascal Morin (pmorin@sb-roscoff.fr)	CNRS, Observatoire Oceanologique de Roscoff and IFREMER, France

AREA	AREA NAME	FIGURES	TIME-SERIES	Contact	
4b	NW European Continental Shelf	41, 42	Western Channel Observatory, Station E1	Tim J. Smyth (tjsm@pml.ac.uk)	Marine Biological Association and Plymouth Marine Laboratory, UK
4b	NW European Continental Shelf	43	Malin Head Weather Station	Glenn Nolan (Glenn.Nolan@marine.ie)	Marine Institute/Met Eireann, Ireland
5	Rockall Trough	44, 45, 46, 78, 84, 85	Ellett Line	N. Penny Holliday (nph@noc.soton.ac.uk)	National Oceanography Centre Southampton and Scottish Association for Marine Science, UK
5b	Irminger Sea	47, 79, 83	Central Irminger Sea, East Greenland Slope	Laura de Steur (Laura.de.Steur@nioz.nl)	Koninklijk Nederlands Instituut voor Zeeonderzoek (NIOZ, Royal Netherlands Institute for Sea Research), Netherlands
6	Faroe Bank Channel	49, 50, 51	Faroe Bank Channel - West Faroe Islands, Faroe Current - North Faroe Islands, Faroe Shelf	Karin Margretha H. Larsen (KarinL@hav.fo)	Havstovan (Faroe Marine Research Institute), Faroe Islands
7	Faroe-Shetland Channel	52, 53, 77	Faroe-Shetland Channel - Faroe Shelf and Shetland Shelf, deep waters (800 m)	Sarah Hughes (s.hughes@marlab.ac.uk)	Fisheries Research Services (FRS, Aberdeen), UK
8&9	North Sea	54	North Sea Utsira, Modelled North Sea Inflow	Jon Albretsen (jon.albretsen@imr.no) Solfrid Hjollo (solfrids@imr.no)	Institute of Marine Research (IMR), Norway
8&9	North Sea	55	Fair Isle Current Water	Sarah Hughes (s.hughes@marlab.ac.uk)	Fisheries Research Services (FRS, Aberdeen), UK
8&9	North Sea	56, 57	Helgoland Roads - coastal waters - German Bight, North Sea	Karen Wiltshire (Karen.Wiltshire@awi.de)	Alfred Wegener Institute for Polar and Marine Research (AWI)/Biologische Anstalt Helgoland (BAH), Germany
8&9	North Sea	58	Felixstowe-Rotterdam Section average (52°N)	Stephen Dye (stephen.dye@cefas.co.uk)	Centre for Environment, Fisheries and Aquaculture Science (CEFAS), UK
9b	Baltic Sea	59, 60, 63	Station BY15, Baltic Proper, east of Gotland, and observed ice extent	Karin Borenas (karin.borenas@smhi.se)	Swedish Meteorological and Hydrological Institute (SMHI), Sweden

AREA	AREA NAME	FIGURES	TIME-SERIES	Contact	INSTITUTE
9b	Baltic Sea	61, 62	Stations LL7 and SR5	Pekka Alenius (pekka.alenius@fimr.fi)	Finnish Institute of Marine Research (FIMR), Finland
10	Norwegian Sea	64, 65, 66	Svinøy, Gimsøy, and Sørkapp sections	Kjell Arne Mork (kjell.arne.mork@imr.no)	Institute of Marine Research (IMR), Norway
10	Norwegian Sea	67, 73	Ocean Weather Station Mike	Svein Østerhus (Svein.Osterhus@gfi.uib.no)	Geophysical Institute, University of Bergen, Norway
11	Barents Sea	68	Fugløya-Bear Island Section, Western Barents Sea	Randi Ingvaldsen (randi.ingvaldsen@imr.no)	Institute of Marine Research (IMR), Norway
11	Barents Sea	69	Kola Section, Eastern Barents Sea	Oleg V. Titov (titov@pinro.ru)	Knipovich Polar Research Institute of Marine Fisheries and Oceanography (PINRO), Russia
12	Greenland Sea and Fram Strait	70	Greenland Sea Section N, west of Spitsbergen (76.5°N)	Waldemar Walczowski (walczows@iopan.gda.pl)	Institute of Oceanology, Polish Academy of Sciences (IOPAN), Poland
12	Greenland Sea and Fram Strait	74, 76	Greenland Sea Section 75°N, Greenland Sea Gyre convection depth and deep waters (3000 m)	Gereon Budeus (Gereon.Budeus@awi.de)	Alfred Wegener Institute, Helmholtz Centre for Polar and Marine Research (AWI), Germany
12	Greenland Sea and Fram Strait	71	Fram Strait (78.83°N): West Spitsbergen Current, and East Greenland Current	Wilken-Jon von Appen (Wilken-Jon.von.Appen@awi.de)	Alfred Wegener Institute, Helmholtz Centre for Polar and Marine Research (AWI), Germany



REFERENCES

Antonov, J. I., Locarnini, R. A., Boyer, T. P., Mishonov, A. V., and Garcia, H. E. 2006. World Ocean Atlas 2005, Volume 2: Salinity. S. Levitus, Ed. NOAA Atlas NESDIS 62, U.S. Government Printing Office, Washington, D.C., USA. 182 pp.

Cappelen, J. (Ed). 2013. The Greenland-DMI Historical Climate Data Collection 1873-2012 - with Danish abstracts. DMI Technical Report, 13-04. Copenhagen.

Gaillard, F. 2015. ISAS-13 temperature and salinity gridded fields. Pôle Océan. <http://doi.org/z77>.

Hurrell, J., and National Center for Atmospheric Research Staff (Eds). Last modified 28 October 2015. The Climate Data Guide: Hurrell North Atlantic Oscillation (NAO) Index (station-based). Retrieved from <https://climatedataguide.ucar.edu/climate-data/hurrell-north-atlantic-oscillation-nao-index-station-based>. - See more at: <https://climatedataguide.ucar.edu/climate-data/hurrell-north-atlantic-oscillation-nao-index-station-based#sthash.BoMuELly.dpuf>.

Locarnini, R. A., Mishonov, A. V., Antonov, J. I., Boyer, T. P., and Garcia, H. E. 2006. World Ocean Atlas 2005, Volume 1: Temperature. S. Levitus, Ed. NOAA Atlas NESDIS 61, U.S. Government Printing Office, Washington, D.C., USA. 182 pp.

Rudels, B., Bjork, G., Nilsson, J., Winsor, P., Lake, I., and Nohr, C. 2005. The interaction between waters from the Arctic Ocean and the Nordic Seas north of Fram Strait and along the East Greenland Current: Results from the Arctic Ocean-02 Oden expedition. *Journal of Marine Systems*, 55: 1-30.



ICES REPORT ON OCEAN CLIMATE 2014



ICES

CIEM